

# **EVALUATION OF THE MECHANISMS OF NEUROTOXICITY USING METABOLOMIC STRATEGIES**

---

**A thesis presented by**

**Ibrahim M. Alanazi**

**A thesis submitted in fulfilment of the degree of  
Doctor of Philosophy**

**Biomedical Engineering  
University of Strathclyde  
Glasgow, UK**

**© 2019**

# Author's declaration

'This thesis is the result of the author's original research. It has been composed by the author and has not been previously submitted for examination which has led to the award of a degree.'

'The copy of this thesis belongs to the author under the terms of the United Kingdom Copyright Acts as qualified by University of Strathclyde Regulation 3.50. Due acknowledgement must always be made of the use of any material contained in, or derived from, this thesis.'

Signed:  \_\_\_\_\_

Date: 27-3-2019 \_\_\_\_\_

# Acknowledgement

Firstly, I would like to thank my lord (Allah) for his blessings and the strength he gave to me to complete this work.

Secondly, I would like to express my appreciation and sincere gratitude to my supervisor, Prof, M. Helen Grant for her continuous support and guidance through my research. I will always remember that I was very fortunate to have such a great supervisor. I would also like to extend my appreciation to my second supervisor Dr, David Watson who was extremely supportive and was always present when I needed him. I will always be thankful to have this great opportunity to work with such a kind and intelligent doctor. Special thanks are extended to Dr Rothwelle Tate for his genuine support and sincere advice. It was an honour to learn from you and to receive your guidance.

I will always be thankful to the noble Mrs Catherine Henderson for her support and advise throughout my experiments. It was a life lesson just to work with such a generous intelligent person. My deep thanks go to my friends, Bader Almaamari and Mohammad Alrofaiidi whom I met here, for your support during these years. Special thanks to my colleagues Laura Beattie, Dr. Sarunya Laovithayangoon and Sara Gomez for their support and the times we shared in the lab, you were the best colleagues one can have.

Finally, I would like to thank my wife and children for their support and patience during my studies.

# Abstract

There are many neurotoxic substances that affect humans. Cobalt and mephedrone are examples of neurotoxic compounds with little known about their mode of action. Cobalt neurotoxicity was investigated in human astrocytoma and neuroblastoma cells using proliferation assays coupled with LC-MS based metabolomics and transcriptomics techniques. Cells were treated with a range of cobalt concentrations between 0 and 200  $\mu\text{M}$ . The metabolism of mephedrone at 100  $\mu\text{M}$  was first studied in primary rat hepatocytes and then the neurotoxicity of mephedrone at 100  $\mu\text{M}$  was assessed in human neuroblastoma and astrocytoma cells using proliferation assays coupled with LC-MS based metabolomics.

The 3-(4,5-dimethylthiazol-2-yl)-2,5-diphenyltetrazolium bromide (MTT) assay revealed that cobalt was cytotoxic and decreased cell metabolism and its effect was dose and time dependent in both cell lines. Metabolomic analysis revealed several altered metabolites particularly those related to DNA deamination and methylation pathways. One of the increased metabolites was uracil which can be generated from DNA deamination or from fragmentation of RNA. To investigate the origin of uracil genomic DNA was isolated and analysed by LC-MS. Interestingly, the source of uracil, which is uridine was increased significantly in the DNA of both cell lines. Additionally, the results of the qRT-PCR showed an increase in the production of five genes Mlh1, Sirt2, MeCP2, UNG and TDG in both cell lines. These genes are related to DNA strand breakage, hypoxia, methylation and base excision repair.

Cultured primary hepatocytes were able to metabolise mephedrone and produce many of the metabolites produced by previous research on freshly isolated hepatocytes. However, metabolic capacity was impaired in the cultured hepatocytes with lower quantities of metabolites being produced in comparison with freshly isolated hepatocytes.

MTT and neutral red (NR) assays results showed no negative effect on cells metabolism or growth. There was an increase in cell metabolism at 100  $\mu\text{M}$  of mephedrone. This concentration of mephedrone was used in the metabolomic

experiments to further investigate metabolomics changes associated with this concentration. The metabolomic analysis of neuroblastoma revealed no strong pattern of effect of mephedrone on the cells. However, the analysis of the metabolome of astrocytoma revealed a marked effect after treatment with mephedrone. The predominant change was on lipids particularly ether lipids that play an important role in controlling membrane fluidity.

Overall, metabolomic analysis was helpful in revealing the changes that both cobalt and mephedrone could induce in human neuronal derived cell lines. These findings could help in understanding the effect of these cytotoxic compounds on human brain.

# Table of Contents

<b>Author's declaration</b> .....	<b>i</b>
<b>Acknowledgement</b> .....	<b>ii</b>
<b>Abstract</b> .....	<b>iii</b>
<b>Table of Contents</b> .....	<b>v</b>
<b>List of Figures</b> .....	<b>viii</b>
<b>List of Tables</b> .....	<b>x</b>
<b>List of Equations</b> .....	<b>xi</b>
<b>List of Abbreviations</b> .....	<b>xii</b>
<b>Published Work</b> .....	<b>xiii</b>
<b>Chapter 1 INTRODUCTION</b> .....	<b>1</b>
<b>1.1 Cobalt</b> .....	<b>3</b>
1.1.1 Metals and their effect on humans .....	3
1.1.2 Cobalt forms and its use in clinical and environmental fields .....	5
1.1.3 Cobalt effect on patients with metal on metal (MoM) hip implants .....	6
1.1.4 Cobalt toxicity studies.....	8
1.1.5 Fatalities associated with cobalt consumption .....	13
1.1.6 Mechanism of cobalt toxicity.....	14
<b>1.2 Mephedrone</b> .....	<b>16</b>
1.2.1 Mephedrone and related compounds .....	16
1.2.2 Mephedrone toxicity, incidence and mortality.....	19
1.2.3 Mechanism of mephedrone effect on the CNS, and other adverse reactions....	27
1.2.4 Experimental investigations into toxicity and metabolism .....	29
<b>1.3 <i>In vitro</i> cell culture models and advantages</b> .....	<b>34</b>
1.3.1 2 Dimension (2D) cell culture.....	34
1.3.2 Three dimensional (3D) cell culture .....	35
<b>1.4 Mass spectrometry based metabolomics</b> .....	<b>35</b>
1.4.1 Metabolomics.....	35
1.4.2 Liquid chromatography-mass spectrometry (LC-MS).....	37
<b>1.5 Quantitative real-time polymerase chain reaction (qRT-PCR)</b> .....	<b>40</b>
<b>1.6 Reason for the choice of mephedrone and cobalt for analysis</b> .....	<b>43</b>
<b>1.7 The aims of the project</b> .....	<b>43</b>
<b>Chapter 2 MATERIALS AND METHODS</b> .....	<b>44</b>
<b>2.1 Culture of cells</b> .....	<b>45</b>
2.1.1 Standard stock solutions and preparation methods .....	45
2.1.2 Cell lines and primary cells .....	46
<b>2.2 MTT, NR, LDH and morphology assays</b> .....	<b>48</b>
2.2.1 Neutral red (NR) assay .....	48
2.2.2 Dimethylthiazolyl diphenyltetrazolium bromide (MTT) assay .....	49
2.2.3 Lactate dehydrogenase (LDH) assay.....	50
2.2.4 Morphology.....	50
<b>2.3 Reactive oxygen species (ROS)</b> .....	<b>51</b>
<b>2.4 Lowry and western blotting</b> .....	<b>52</b>
2.4.1 Sample preparation.....	52

2.4.2 Total protein measurement (Lowry assay) .....	52
2.4.3 Western blotting (WB) .....	54
<b>2.5 DNA and RNA isolation .....</b>	<b>59</b>
<b>2.6 DNA digestion .....</b>	<b>60</b>
<b>2.7 Metabolomics and Metabolism.....</b>	<b>60</b>
<b>2.8 Quantitative Real-time PCR (qRT-PCR).....</b>	<b>62</b>
2.8.1 Materials.....	62
2.8.2 Method .....	63
<b>2.9 Statistical methods.....</b>	<b>68</b>
<b>Chapter 3 THE EFFECT OF COBALT ON HUMAN NEUROBLASTOMA AND ASTROCYTOMA .....</b>	<b>69</b>
<b>3.1 Abstract .....</b>	<b>70</b>
<b>3.2 Introduction .....</b>	<b>71</b>
3.2.1 Cobalt .....	71
3.2.2 Oxidative stress .....	71
3.2.3 DNA methylation .....	73
3.2.2 DNA deamination .....	73
<b>3.3 Methods and materials.....</b>	<b>76</b>
<b>3.4 Results and discussion.....</b>	<b>77</b>
3.4.1 Measurement of MTT reduction in neuroblastoma cells in the presence of cobalt .....	77
3.4.2 Measurement of MTT reduction in astrocytoma cells in the presence of cobalt .	81
3.4.3 ROS detection .....	84
3.4.4 Western blotting (Gels).....	90
3.4.5 Real-time PCR.....	95
3.4.6 Metabolomics.....	108
<b>3.6 Summary of findings .....</b>	<b>140</b>
<b>Chapter 4 MEPHEDRONE METABOLISM IN NEURONAL CELL LINES, HEPATOCYTOMA AND PRIMARY RAT HEPATOCYTES, AND THE COMPARISON OF MEPHEDRONE METABOLISM IN FRESHLY ISOLATED HEPATOCYTES WITH CULTURED HEPATOCYTES.....</b>	<b>142</b>
<b>4.1 Abstract .....</b>	<b>143</b>
<b>4.2 Introduction .....</b>	<b>144</b>
4.2.1 Mephedrone.....	144
4.2.2 The use of cell lines and primary hepatocytes in metabolism studies.....	148
<b>4.3 Aims and objectives.....</b>	<b>149</b>
<b>4.4 Materials and methods.....</b>	<b>150</b>
4.4.1 Materials.....	150
4.4.2 Methods.....	151
<b>4.5 Results and discussion.....</b>	<b>152</b>
4.5.1 Comparison of mephedrone metabolism in freshly isolated hepatocyte with cultured hepatocytes.....	152
4.5.2 Metabolism of mephedrone in neuroblastoma, astrocytoma and hepatocytoma	156
<b>4.6 Conclusion .....</b>	<b>158</b>
<b>Chapter 5 MEPHEDRONE EFFECTS ON HUMAN NEUROBLASTOMA AND ASTROCYTOMA CELLS.....</b>	<b>160</b>
<b>5.1 Abstract .....</b>	<b>161</b>
<b>5.2 Introduction .....</b>	<b>162</b>
5.2.1 Mephedrone effect on CNS.....	162
5.2.2 Mephedrone stability.....	162

<b>5.3 Aims and objectives .....</b>	<b>163</b>
<b>5.4 Materials and methods .....</b>	<b>163</b>
<b>5.5 Results and discussion .....</b>	<b>164</b>
5.5.1 The effects of mephedrone on viability measured by MTT, NR and LDH viability assays.....	164
5.5.2 Metabolomics in all cell types in-vitro.....	168
<b>5.6 Conclusion .....</b>	<b>186</b>
<b>Chapter 6 SUMMARY AND FUTURE WORK.....</b>	<b>187</b>
<b>6.1 Summary of results of the cobalt study .....</b>	<b>188</b>
6.1.1 Assessment of the toxicity of cobalt.....	188
6.1.2 Summary of the western blotting results for specific enzymes .....	189
6.1.3 Summary of the results of real-time polymerase chain reaction experiment .....	189
6.1.4 Evaluation of cobalt effect on neuronal cells by metabolomic analysis.....	190
6.2.5 Suggestions for future work on cobalt .....	191
<b>6.1 Summary of results of the mephedrone study .....</b>	<b>192</b>
6.1.1 Metabolism of mephedrone in cultured primary rat hepatocytes .....	192
6.1.2 Assessment of the toxicity of mephedrone.....	193
6.1.3 Evaluation of mephedrone effect on neuronal cells by metabolomic analysis...	194
6.1.4 Suggestions for future work on mephedrone .....	195
<b>7 References .....</b>	<b>197</b>
<b>8 Appendices .....</b>	<b>223</b>

# List of Figures

FIGURE 1. 1 INCIDENCE OF COBALT USE MEASURED BY DEMAND IN SEVERAL INDUSTRIES .....	6
FIGURE 1. 3 MEPHEDRONE CHEMICAL STRUCTURE. ....	16
FIGURE 1. 4 POSSIBLE MEPHEDRONE METABOLISM REACTIONS (PHASE I AND II) IN RAT LIVER. ....	33
FIGURE 1. 5 SCHEME OF THE COMPONENTS OF HPLC SYSTEM WITH DETECTOR. ....	38
FIGURE 1. 6 MASS-SPECTROMETRY SCHEMATIC DIAGRAM SHOWING DIFFERENT PARTS OF THE DETECTOR. ....	39
FIGURE 1. 7 SIMPLE DIAGRAM ILLUSTRATING THE STEPS OF RT-PCR. ....	41
FIGURE 1. 8 THE LINEAR AND LOG PLOTS OF THE MEASURED SYBR-GREEN FLUORESCENCE IN THE RT- PCR PROCESS. ....	42
FIGURE 2. 1 ORDER OF LAYERS FOR MAKING THE GEL/FILTER SANDWICH. ....	57
FIGURE 3. 1 DEAMINATION OF CYTOSINE TO URACIL. ....	74
FIGURE 3. 2 SCHEME OF THE INDUCED CHANGE IN FIRST AND SECOND REPLICATION OF THE DEAMINATED DNA. ....	74
FIGURE 3. 3 SCHEME OF THE PATHWAY OF THYMINE-LESS CELL DEATH. ....	76
FIGURE 3. 4 MTT ASSAY MEASURED IN NEUROBLASTOMA CELLS AT 24 H.....	77
FIGURE 3.5 MTT ASSAY MEASURED IN NEUROBLASTOMA CELLS AT 48 H.....	78
FIGURE 3. 6 MTT ASSAY MEASURED IN NEUROBLASTOMA CELLS AT 72 H.....	79
FIGURE 3. 7 MTT ASSAY MEASURED IN ASTROCYTOMA CELLS AT 24 H.....	81
FIGURE 3. 8 MTT ASSAY MEASURED IN ASTROCYTOMA CELLS AT 48 H.....	82
FIGURE 3. 9 MTT ASSAY MEASURED IN ASTROCYTOMA CELLS AT 72 H.....	83
FIGURE 3. 10 MEASUREMENT OF ROS FLUORESCENCE INTENSITY IN SH-SY5Y CELLS UPON EXPOSURE TO 100, 150, AND 200 $\mu$ M OF COBALT FOR 24H, USING CARBOXY-H2DCFDA TO DETECT ROS AT AN EXCITATION WAVELENGTH OF 495 NM AND EMISSION WAVELENGTH OF 525 NM.....	85
FIGURE 3. 11 IMAGES OF SH-SY5Y NEUROBLASTOMA CELLS WITHOUT COBALT TREATMENT (ON THE TOP LEFT) AND AFTER TREATMENT WITH 100 $\mu$ M OF COBALT (ON THE TOP RIGHT) .....	86
FIGURE 3. 12 MEASUREMENT OF ROS FLUORESCENCE INTENSITY IN U-373 CELLS UPON EXPOSURE TO 100, 150, AND 200 $\mu$ M OF COBALT FOR 24H, USING CARBOXY-H2DCFDA AT AN EXCITATION WAVELENGTH OF 495 NM AND EMISSION WAVELENGTH OF 525 NM FOR DETECTION.....	88
FIGURE 3. 13 IMAGES OF U-373 ASTROCYTOMA CELLS WITHOUT COBALT TREATMENT (ON THE LEFT), AND AFTER TREATMENT WITH 100 $\mu$ M OF COBALT FOR 24 HOURS (ON THE TOP RIGHT AND THE TWO PICTURES BELOW).....	89
FIGURE 3. 14 EXPRESSION OF UNG1, OGG1, TDG, DNMT AND THE HOUSE KEEPING GLYCERALDEHYDE-3-PHOSPHATE DEHYDROGENASE (GAPDH) PROTEINS IN SH-SY5Y CELL LINES AFTER TREATMENT WITH A RANGE OF COBALT CONCENTRATIONS FOR 72 HOURS .....	90
FIGURE 3.15 QUANTIFICATION OF THE LISTED PROTEINS IN SH-SY5Y CELLS AFTER TREATMENT WITH A RANGE OF COBALT CONCENTRATIONS FOR 72 HOURS.....	91
FIGURE 3. 16 EXPRESSION OF UNG1, OGG1, TDG, DNMT AND HOUSE KEEPING (GAPDH) PROTEINS IN U-373 CELLS AFTER TREATMENT WITH A RANGE OF COBALT CONCENTRATIONS FOR 72 HOURS .....	93
FIGURE 3. 17 QUANTIFICATION OF LISTED PROTEINS IN U-373 CELLS AFTER TREATMENT WITH A RANGE OF COBALT CONCENTRATIONS FOR 72 HOURS.....	94
FIGURE 3. 18 MELT CURVE FOR REFERENCE GENE RIBOSOMAL PROTEIN L13A (RPL13A) IN WATER CONTROL SAMPLE ON THE LEFT AND NEGATIVE REVERSE TRANSCRIPTASE CONTROL SAMPLE ON THE RIGHT. ....	96
FIGURE 3. 19 MELT CURVE FOR REFERENCE GENE (RPL13A) ON THE LEFT AND MLH1 GENE ON THE RIGHT IN ALL SAMPLES SHOWING A SINGLE REPRODUCIBLE PEAK FOR EACH SAMPLE.....	97
FIGURE 3. 20 MELT CURVE FOR SIRT2 GENE ON THE LEFT AND MeCP2 GENE ON THE RIGHT IN ALL SAMPLES SHOWING A SINGLE REPRODUCIBLE PEAK FOR EACH SAMPLE. ....	98
FIGURE 3. 21 MELT CURVE FOR UNG1 GENE ON THE LEFT AND TDG GENE ON THE RIGHT IN ALL SAMPLES SHOWING A SINGLE REPRODUCIBLE PEAK FOR EACH SAMPLE. ....	99

FIGURE 3. 22 GENE TRANSCRIPTION IN A NEUROBLASTOMA CELL LINE AFTER TREATMENT WITH A RANGE OF COBALT CONCENTRATION.....	100
FIGURE 3. 23 MELT CURVE FOR REFERENCE GENE (RPL13A) IN WATER CONTROL SAMPLE ON THE LEFT AND NEGATIVE REVERSE TRANSCRIPTASE SAMPLE ON THE RIGHT.....	103
FIGURE 3. 24 MELT CURVE FOR REFERENCE GENE (RPL13A) ON THE LEFT AND MLH1 GENE ON THE RIGHT IN ALL SAMPLES SHOWING A SINGLE REPRODUCIBLE PEAK FOR EACH SAMPLE.....	103
FIGURE 3. 25 MELT CURVE FOR SIRT2 GENE ON THE LEFT AND MeCP2 ON THE RIGHT IN ALL SAMPLES SHOWING A SINGLE REPRODUCIBLE PEAK FOR EACH SAMPLE.....	104
FIGURE 3. 26 MELT CURVE FOR UNG1 GENE ON THE LEFT AND TDG ON THE RIGHT IN ALL SAMPLES SHOWING A SINGLE REPRODUCIBLE PEAK FOR EACH SAMPLE.....	105
FIGURE 3. 27 EXPRESSION OF GENES IN ASTROCYTOMA CELL LINE AFTER TREATMENT WITH A RANGE OF COBALT CONCENTRATION FOR 72 HOURS.....	106
FIGURE 3. 28 A PCA-X SCORE PLOT OF THE SEPARATION BETWEEN CONTROL AND COBALT TREATED U-373 CELLS AFTER 72 HOURS OF INCUBATION.....	109
FIGURE 3. 29 EXTRACTED ION TRACES SHOWING HYDROXYMETHYL THYMIDINE AND A CORRESPONDING EXTRACTED ION TRACE FOR HYDROXYMETHYL URACIL.....	111
FIGURE 3. 30 EXTRACTED ION TRACES SHOWING GUANOSINE AND A CORRESPONDING FRAGMENT FOR GUANINE AND INOSINE AND A CORRESPONDING FRAGMENT FOR HYPOXANTHINE.....	113
FIGURE 3. 31 EXTRACTED ION TRACES SHOWING A WEAK PEAK FOR METHYLCYTIDINE AND A TRACE SHOWING POSSIBLY TRACES OF METHYL CYTOSINE.....	114
FIGURE 3. 32 EXTRACTED ION TRACES FOR INCREASED PENTOSE PHOSPHATE PATHWAY METABOLITES, SEDOHEPTULOSE, RIBOSE PHOSPHATE AND PHOSPHOGLUCONATE.....	117
FIGURE 3. 33 EXTRACTED ION TRACES SHOWING HYDROXYMETHYLDEOXYCYTIDINE, ADENOSINE+DEOXYGUANOSINE, DEOXYADENOSINE, DEOXYCYTIDINE AND METHYLDEOXYCYTIDINE.....	125
FIGURE 3. 34 A PCA-X SCORE PLOT OF THE SEPARATION BETWEEN CONTROL AND COBALT TREATED SH-SY5Y CELLS AFTER 72 HOURS OF INCUBATION.....	126
FIGURE 3. 35 EXTRACTED ION TRACES FOR PE 38:3 ETHER SHOWING EFFECT OF COBALT DOSE ON ITS LEVELS.....	127
FIGURE 3. 36 EXTRACTED ION TRACES SHOWING THE EFFECT OF COBALT DOSE ON THE LEVELS OF PC 38:4.....	128
FIGURE 3. 37 EXTRACTED ION TRACES FOR DECANOIC ACID SHOWING THE EFFECT OF COBALT DOSE ON ITS LEVELS.....	137
FIGURE 3. 38 EXTRACTED ION TRACES FOR HYDROXY DECANOIC ACID SHOWING THE EFFECT OF COBALT DOSE ON ITS LEVELS.....	137
FIGURE 4. 1 POSSIBLE ROUTES FOR THE PHASE I AND II METABOLISM OF (±)-MEPHEDRONE (4-MMC, 3A) IN SPRAGUE-DAWLEY RAT LIVER HEPATOCYTES.....	146
FIGURE 4. 2 RELATIVE AMOUNTS OF METABOLITES OF MEPHEDRONE (4-MMC, 3A) FORMED AFTER INCUBATION WITH CULTURED SPRAGUE-DAWLEY RAT LIVER HEPATOCYTES.....	153
FIGURE 5. 1 MTT ASSAY MEASURED IN (A) SH-SY5Y CELLS AND IN (B) U-373 CELLS AFTER 48 H ..	164
FIGURE 5. 2 NEUTRAL RED ASSAY MEASURED IN (A) SH-SY5Y CELLS AND IN (B) U-373 CELLS AFTER 48 H.....	165
FIGURE 5. 3 MORPHOLOGY OF SH-SY5Y (A AND B) AND U373 (C AND D) CELLS AFTER 6 DAYS INCUBATION WITHOUT MEPHEDRONE TREATMENT (A AND C), AND WITH MEPHEDRONE (B AND D).....	167
FIGURE 5. 4 OPLS-DA SCORE PLOT OF NEUROBLASTOMA (SH-SY5Y) TREATED WITH MEPHEDRONE (BLUE) AND NON-TREATED (GREEN).....	169
FIGURE 5. 5 PERMUTATION ANALYSIS OF THE OPLSDA MODEL FOR MEPHEDRONE TREATED AND NON-TREATED ASTROCYTOMA CELLS.....	170
FIGURE 5. 6 PCA MODEL OF THE CONTROL (BROWN), MEPHEDRONE TREATED (BLUE) ASTROCYTES AND POOLED SAMPLES (GREEN).....	172
FIGURE 5. 7 OPLS-DA SCORE PLOT OF ASTROCYTOMA (U-373) TREATED WITH MEPHEDRONE (BLUE) AND NON-TREATED (GREEN) WITHOUT POOLED SAMPLES. C REPRESENTS THE CONTROL (NON-TREATED) SAMPLES, AND T REPRESENTS THE TEST (TREATED) SAMPLES.....	173

FIGURE 5.8 PERMUTATION ANALYSIS OF THE OPLS-DA MODEL FOR MEPHEDRONE TREATED AND NON-TREATED ASTROCYTOMA CELLS .....	174
FIGURE 5. 9 LIPIDS IN ASTROCYTES SORTED BY ABUNDANCE BEFORE AND AFTER TREATMENT WITH MEPHEDRONE .....	178
FIGURE 5. 10 EXTRACTED ION TRACES SHOWING SIMILAR LEVELS OF ATP IN TREATED AND UNTREATED EXTRACTS BUT A LARGE REDUCTION OF THE AMOUNT OF A MAJOR CELLULAR LIPID (PC 36:2) IN TREATED ASTROCYTOMA CELLS. ....	181

## List of Tables

TABLE 1. 1 NEUROLOGICAL EFFECTS IN RATS AFTER TREATMENT WITH COBALT.....	9
TABLE 2. 1 VOLUMES AND MATERIALS USED TO PREPARE THE STANDARDS FOR PROTEIN DETERMINATION.....	53
TABLE 2. 2 STACKING AND SEPARATING GEL BUFFERS COMPOSITION.....	54
TABLE 2. 3 STACKING AND RESOLVING GELS COMPOSITION. ....	56
TABLE 2. 4 TRANSFER BUFFER COMPOSITION.....	57
TABLE 2.5 GRADIENT PROGRAM FOR ANALYSIS OF EACH SAMPLE SHOWING PERCENTAGES OF A AND B MOBILE PHASES DURING THE TIME OF THE ANALYSIS. ....	62
TABLE 2. 6 PRIMER SETS (FORWARD AND REVERSE) DESIGNED AND USED FOR GENES QUANTIFICATION IN RT-PCR EXPERIMENT. ....	64
TABLE 2. 7 COMPONENTS OF THE 8 <sub>mL</sub> SOLUTION MIXTURE TO BE ADDED TO THE SAMPLE. *FOR THE RT (-) SAMPLES WE ADD 1 <sub>mL</sub> OF RNASE FREE DEPC-TREATED WATER. ....	65
TABLE 2.8 CONTENTS OF EACH SAMPLE IN THE RT-PCR REACTION. ....	66
TABLE 2.9 CONDITIONS OF THE RT-PCR EXPERIMENT. ....	67
TABLE 3. 1 TABLE SUMMARISED THE RESULTS OF CALCULATED LD <sub>50</sub> VALUES DERIVED FROM MTT RESULTS FOR BOTH CELL LINES, SH-SY5Y AND U-373 CELLS. ....	84
TABLE 3. 2 GENE TRANSCRIPTION FOLD CHANGE IN SH-SY5Y CELLS AFTER TREATMENT WITH A RANGE OF COBALT CONCENTRATION.....	100
TABLE 3. 3 GENE EXPRESSION EXHIBITED AS FOLD CHANGES IN U-373 CELLS AFTER TREATMENT WITH A RANGE OF COBALT CONCENTRATIONS .....	106
TABLE 3. 4 METABOLOMIC DATA DERIVED FROM LC-MS OF THE NUCLEAR DNA AFTER SEPARATION FROM NEUROBLASTOMA TREATED (25, 50 AND 100 <sub>mM</sub> ) AND NON-TREATED WITH COBALT FOR 72 HOURS. ....	138
TABLE 4. 1 RELATIVE AMOUNTS OF METABOLITES OF MEPHEDRONE (4-MMC, 3A) FORMED AFTER INCUBATION WITH SPRAGUE-DAWLEY RAT LIVER HEPATOCYTES. ....	147
TABLE 4. 2 IDENTIFIED METABOLITES IN CULTURED HEPATOCYTES AFTER 100 <sub>mM</sub> MEPHEDRONE TREATMENT FOR 6, 24 AND 48 HOURS .....	152
TABLE 4. 3 METABOLITES IDENTIFIED IN U373 CELLS AFTER 100 <sub>mM</sub> MEPHEDRONE TREATMENT FOR 6 DAYS .....	156
TABLE 4. 4 IDENTIFIED METABOLITES IN SH-SY5Y CELLS AFTER 100 <sub>mM</sub> MEPHEDRONE TREATMENT FOR 6 DAYS.....	157
TABLE 4. 5 METABOLITES IDENTIFIED IN HEP G2 AFTER 100 <sub>mM</sub> MEPHEDRONE TREATMENT FOR 6 DAYS .....	157

TABLE 5. 1 LDH RELEASE 6 DAYS AFTER TREATMENT OF SH-SY5Y AND U-373CELLS WITH 100 <sub>M</sub> M MEPHEDRONE .....	166
TABLE 5. 2 METABOLOMIC RESULTS OF SH-SY5Y CELL LINE AFTER INCUBATION WITH 100 <sub>M</sub> M MEPHEDRONE FOR 6 DAYS .....	168
TABLE 5. 3 CVANOVA STATISTICS FOR THE OPLS-DA MODEL FOR ASTROCYTOMA CELLS TREATED AND NON-TREATED WITH MEPHEDRONE. ....	170
TABLE 5. 4 CVANOVA OF THE OPLS-DA MODEL FOR MEPHEDRONE TREATED AND NON-TREATED ASTROCYTOMA. ....	174
TABLE 5. 5 NON-LIPID METABOLITE CHANGES IN U-373 ASTROCYTES FOLLOWING TREATMENT WITH 100 <sub>M</sub> M MEPHEDRONE FOR 6 DAYS .....	179
TABLE 5.6 MAJOR INTRACELLULAR METABOLITES IN ASTROCYTOMA CELLS THAT ARE NOT AFFECTED BY MEPHEDRONE TREATMENT. ....	180

## List of Equations

EQUATION 2. 1 EQUATION USED TO CALCULATE THE REQUIRED VOLUME OF LAEMLI BUFFER.....	54
EQUATION 2. 2 EQUATION OF THE VOLUME OF LYSIS BUFFER. ....	60
EQUATION 2. 3 EQUATION OF DELTA THRESHOLD CYCLE OF THE CONTROL SAMPLE.....	67
EQUATION 2. 4 EQUATION OF DELTA THRESHOLD CYCLE OF THE TREATED SAMPLE. ....	67
EQUATION 2. 5 EQUATION OF DELTA-DELTA THRESHOLD CYCLE OF THE TREATED SAMPLE. ....	67
EQUATION 2. 6 EQUATION FOR FOLD CHANGE FOR TREATED SAMPLE. ....	67

# List of Abbreviations

AMP	Adenosine monophosphate
ATP	Adenosine triphosphate
cDNA	Complementary DNA
Ct	Cycle threshold
CTP	Cytidine triphosphate
DA	Dopamine
DAT	Dopamine transporter
DNMT1	DNA methyltransferase
dTTP	Deoxythymidine triphosphate
dUTP	Deoxyuridine triphosphate
GSH	Glutathione
GSSG	Glutathione disulfide
HIF-1 $\alpha$	Hypoxia inducible factor-1 $\alpha$
5-HT	Serotonin
4-MMC	Mephedrone
LC-ESI-MS	Liquid chromatography-electrospray-mass spectrometry
LC-MS	Liquid chromatography-mass spectrometry
LC-MS/MS	Liquid chromatography-mass spectrometry/mass spectrometry
LDH	Lactate dehydrogenase
MeCP2	Methyl-CpG Binding Protein 2
Mlh1	MutLgamma 1
MoM	Metal on metal
M/z	Mass to charge ratio
OGG1	8-oxoguanine glycosylase
OPLS-DA	Orthogonal partial least squares-discriminant analysis
PCA	Principal component analysis
PG	Glycerophospholipid
PI	Phosphatidylinositol
PS	Phosphatidylserine
qRT-PCR	Quantitative real time polymerase reaction
ROS	Reactive oxygen species
RPL13A	Ribosomal Protein L13A
SIRT	Sirtuin
SM	Sphingomyelin
SP	Sphingolipids
TCA	Citric acid cycle
TDG	Thymine DNA glycosylase
UNG	Uracil-DNA glycosylases

# Published Work

## Posters:

- I. I Alanazi, DG Watson, MH Grant Comparison of the metabolism of mephedrone in cultured and in freshly isolated primary rat hepatocytes. In Vitro Toxicology Society Meeting, Glasgow 14-15 November 2016; Applied in Vitro Toxicology 2(4), p241.
- II. I Alanazi, DG Watson, MH Grant. The metabolism of mephedrone in cultured and freshly isolated hepatocytes. Scottish Metabolomics Society Meeting, Inverness, Scotland, 16-17 November 2016 (unpublished poster abstract).
- III. Alanazi I, Watson DG, Grant MH. Metabolomics applied to cobalt neurotoxicity in vitro. British Toxicology Society Meeting, Liverpool, 3-5 April 2017.

# **Chapter 1 INTRODUCTION**

---

## 1. Introduction

The study of toxicology is the study of the effects of substances on the body (Gallo and Doull, 1996). The knowledge of toxicology goes back to early humans and the study of natural poisons (Kellett, 1946). The ancient Ebers Papyrus (1500 BC) lists many poisons such as hemlock from Greece, aconite from China, opium and metals (copper, lead and antimony) (Wu, 1984). Modern toxicology has expanded to include the study of biology using toxic compounds (Bae and Lee, 2016).

Since, little is known about the mode of action of mephedrone and cobalt in neuronal cells, the aim of this thesis was to investigate the mode of action of these agents in these cells using multiple toxicology methods in addition to metabolomics analysis. This research will link the experiments in the mechanisms of toxicity, with the study of the metabolomics of two neurotoxic chemicals, cobalt and mephedrone.

Metabolomics has been widely used to investigate mechanisms of toxicology in human cells. The first study to apply metabolomics in the study of toxicology was carried out in 2007 in order to investigate the effect of valproate on human embryonic stem cells (Cezar *et al.*, 2007). Cezar's research was followed by similar studies on the same cells, which led to the identification of 8 marker metabolites (West *et al.*, 2010). A few other studies have followed that to build models and services to best predict the effect of chemical compounds on human cells (Kleinstreuer *et al.*, 2011; Palmer *et al.*, 2013; Palmer *et al.*, 2017). Metabolomics offered a technical way to identify biomarkers of the effect of toxic compounds leading to better prediction of toxicity (Schnackenberg *et al.*, 2009). Metabolomic analysis used in toxicology research aims to measure the full metabolome and illustrate the change in the biochemical pathways after exposure to toxic compounds

(Robertson, 2005). Metabolic profiling has been reported for multiple drugs exhibiting the change in the metabolome and the biochemical pathways as a result of the exposure to these drugs (Morvan and Demidem, 2007).

## **1.1 Cobalt**

### **1.1.1 Metals and their effect on humans**

Metal toxicity in humans has been widely reviewed (Gossel, 1994; Klaassen and Casarett, 2001; Jaishankar *et al.*, 2014). It is dose dependent, at lower concentrations many metals are essential for life, and the same metals are toxic in higher doses. However, often the toxic level of metals is close to the level essential for life in humans. For instance, the essential daily dosage of zinc for human is 12-15 mg, whereas a dosage > 18 mg was found to deplete copper (essential nutrient for the human body) in adults (Festa *et al.*, 1985).

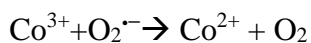
#### **1.1.1.1 Production of reactive oxygen species**

Many studies have reported production of reactive oxygen species, especially hydroxyl radical (HO<sup>•</sup>), as the main toxic mechanism for metals to cause damage to proteins, lipids and DNA in cells (Halliwell and Gutteridge, 1990; Kasprzak, 1996).

Production of the hydroxyl radical in the presence of metal and hydrogen peroxide is governed by the following reaction (the Fenton reaction),



and ending with a cycle of reactions that produce the hydroxyl radical according to the following reactions (Haber-Weiss reaction).



Metals are able to act through Fenton catalysis and this depends on the type and form of the metal. For example,  $\text{Co}^{2+}$ ,  $\text{Fe}^{2+}$ ,  $\text{Ti}^{3+}$  and  $\text{Cu}^+$  can only act by Fenton like catalysis if there are no chelators present (Kasprzak, 1996). Another example is  $\text{Fe}^{2+}$ , its ability for autoxidation is decreased in the presence of deferoxamine or o-phenanthroline, and improved by ethylenediaminetetraacetic acid or nitrilotriacetic acid (Kasprzak, 1996).

#### **1.1.1.2 Metal protein binding and disposition**

Metals bound or unbound to proteins are accumulated in tissues and organs. They can be excreted mainly in faeces and bile, and to a lesser extent in breath, hair, sweat, milk and nails (Apostoli, 1999).

Metals can combine with proteins, such as  $\text{Cu}^{2+}$  with  $\alpha$ -amylase,  $\text{Zn}^{2+}$  with alcohol dehydrogenase,  $\text{Cu}^{2+}$  and  $\text{Zn}^{2+}$  with carbonic anhydrase and  $\text{Fe}^{2+}$  with ferritin. The reactivity of  $\text{Cd}^{2+}$  and  $\text{Hg}^{2+}$  with metallothionein has been extensively studied (Stillman *et al.*, 1992; Szpunar, 2000).

Metals are known to form complexes with peptides, and this plays an important role in catalysis, transport and storage processes in cells. Peptides that contain cysteine (- $\text{CH}_2\text{SH}$ ) or methionine (- $\text{CH}_2\text{CH}_2\text{SCH}_3$ ) bind via the sulphur in their structures to metals such as  $\text{Zn}^{2+}$ ,  $\text{Cd}^{2+}$  and  $\text{Cu}^{2+}$ . Peptides with histidine bind with metals such as  $\text{Zn}^{2+}$  and  $\text{Cu}^{2+}$  after metal deprotonation through the nitrogen in the histidine structure (Romagnoli *et al.*, 1991).

### 1.1.2 Cobalt forms and its use in clinical and environmental fields

Cobalt is an essential metal which is found in cobalamin (vitamin B12) in the human body (Kim *et al.*, 2008).  $\text{Co}^{2+}$  is proposed to produce hydroxyl radicals, to upregulate hypoxia-inducible factors, and to have  $\text{Ca}^{2+}$  and  $\text{Fe}^{2+}$  antagonism properties (Simonsen *et al.*, 2012).

There are over a million workers who deal with and are under the risk of exposure to toxic concentration of cobalt (ATSDR, 2004). Cobalt is used in many industries such as rechargeable battery manufacture, metal alloy production, and in magnetics due to its physical properties (improved conductivity, low corrosiveness, elevated melting point and magnetic function) (see Figure 1.1, data taken from [www.statista.com](http://www.statista.com)). It is also used in steel manufacturing, the diamond industry, dyeing and pigment production (Barceloux, 1999). It is an essential component of cobalt-chromium alloys widely used in the medical devices industry and is particularly important in manufacture of artificial joints. An example of an artificial hip joint is shown on Figure 1.2. There is no doubt that this application of cobalt-chrome alloy exposes many thousands of patients to a significant source of cobalt.

Cobalt powder concentration in the open air was measured and found to be around  $1 \times 10^{-9} \text{ mg/m}^3$  (IARC, 1991). The air safety limit of cobalt in the work place is  $0.1 \text{ mg/m}^3$  (Keegan *et al.*, 2008). Another study measured cobalt concentration in the air of a hard metal producing factory and the levels were about  $14.6$  to  $37 \text{ mg/m}^3$  (Goldoni *et al.*, 2004). Cobalt particles can be inhaled causing several lung diseases, examples are fibrosis, asthma, and pneumonitis (Malard *et al.*, 2007). Safety limits

are set by the European Food Safety Authority (EFSA) to be 0.012 mg daily in the UK (Feed, 2009).

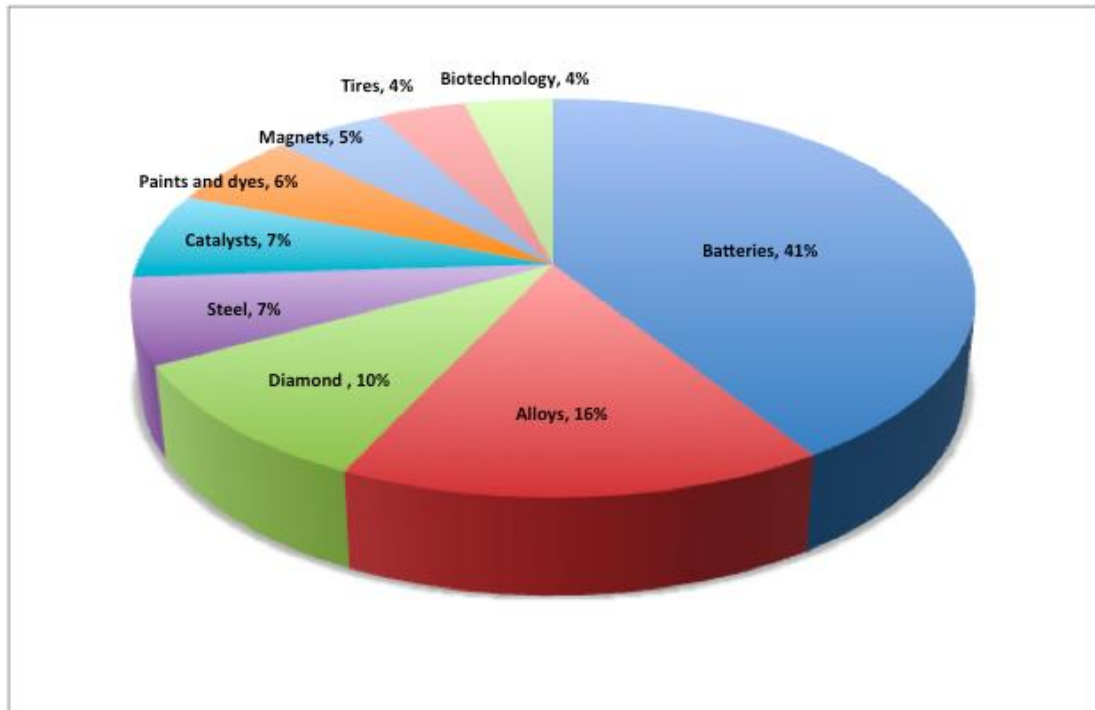


**Figure 1. 1 Incidence of cobalt use measured by demand in several industries. (www.statista.com, 2016).**

### **1.1.3 Cobalt effect on patients with metal on metal (MoM) hip implants**

It is believed that more than a million patients globally have metal on metal (MoM) implants in their bodies (Malard *et al.*, 2007). The discovery of adverse effects accompanying the leakage of cobalt ions from MoM hip implants (see Figure 1.2) has generated alarm about the systemic complications of cobalt. Increases in cobalt ions resulting from friction can trigger acute pathological complications (Lombardi *et al.*, 2012). There appear to be a number of important risk factors, both in terms of the implant and the patient, associated with the risk of systemic cobalt toxicity (Ikeda *et al.*, 2010; Munichor *et al.*, 2003). The safety limit of cobalt concentration resulted

from MoM implant in patient blood recommended by the European Consensus Statement ranged from 2 to 7  $\mu\text{g/L}$  of whole blood (Hannemann *et al.*, 2013). The higher air and food safety limits compared with the MoM Co safety limits can be explained by the fact that the source of cobalt exposure in the MoM is endogenous and not subject to absorption processes as it is the case in food and air exposure.

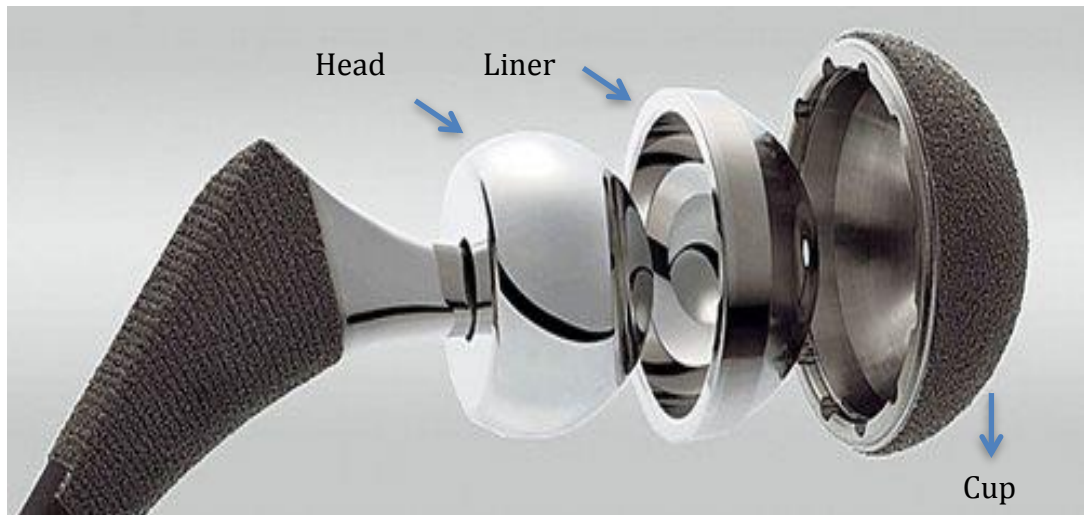


**Figure 1. 2 Picture of metal on metal implant showing the cobalt chromium head, metallic liner and cup. Picture was obtained from [www.good-legal-advice.com](http://www.good-legal-advice.com).**

A genotoxic and carcinogenic action was described in the International Agency for Research on Cancer (IARC) in which Co is classified as group 2A carcinogen (probably carcinogenic to humans) (Wroblewski *et al.*, 2004). Isolated case reports of neurological symptoms after exposure to high doses of Co were also described, following professional exposure, therapeutic ingestion of cobalt chloride ( $\text{CoCl}_2$ ) metal dust and metallic ion release from cobalt–chromium (Co–Cr) alloy in orthopaedic implants (prosthesis) (Humans, 2006; Licht *et al.*, 1972).

## **1.1.4 Cobalt toxicity studies**

### **1.1.4.1 Cobalt neurotoxicity**

People exposed to cobalt through inhalation at work have encountered some effects on their nervous system such as hearing loss, lack in visual ability and memory loss (Gardner, 1953; Licht *et al.*, 1972). When rats and mice inhaled cobalt sulfate (19 mg/m<sup>3</sup>) for 16 days, they developed congestion in their brain blood vessels (Jordan *et al.*, 1990; Meecham and Humphrey, 1991).

Through the oral administration route for Co, to our knowledge, there have been no studies on the effect on human neuronal system. On the other hand, there were many studies performed on rats *in vivo*. Table 1.1 illustrates the different neurological effects related to specific doses of cobalt administered to rats orally.

**Table 1. 1 Neurological effects in rats after treatment with cobalt.**

<b>Dose of cobalt (mg/kg)</b>	<b>Duration</b>	<b>Cobalt form</b>	<b>Effect</b>	<b>Reference</b>
<b>4.25</b>	Single dose	Cobalt chloride	Moderate decrease in reactivity, muscle tendency, touch feeling and breathing.	(Bucher <i>et al.</i> , 1990)
<b>19.4</b>	Single dose	Cobalt sulfate	Mild decrease in the above mentioned effects.	(Singh and Junnarkar, 1991)
<b>4.96</b>	Daily (30 days)	Cobalt chloride	Alteration in sympathetic system contraction ability	(Singh and Junnarkar, 1991)
<b>6.44</b>	Daily (30 days)	Cobalt nitrate	Higher sensitivity, reduced maximal response to drugs that mimic acetylcholine actions (cholinergic agonists).	(Mutafova-Yambolieva <i>et al.</i> , 1994)
<b>20</b>	57 days	Cobalt chloride	Increased avoidance to stress.	(Vassilev <i>et al.</i> , 1993)
<b>20</b>	69 days	Cobalt chloride	Decrease in pedal pushing rate and no change in reactivity to stress.	(Bourg <i>et al.</i> , 1985)
<b>0.5</b>	7 months	Cobalt chloride	Increase in latent response period.	(Nation <i>et al.</i> , 1983)
<b>2.5</b>	7 months	Cobalt chloride	Disruption in conditioned response.	(Krasovskii and Fridlyand, 1971)

Cobalt distribution in blood was investigated and it was found that cobalt binds to albumin and transferrin proteins in serum (Sadler *et al.*, 1994). Other studies specified the N-terminal peptide of albumin at the sequence Asp-Ala-His-Lys as a binding site for cobalt (Bar-Or *et al.*, 2000). Some pathological conditions such as trauma, diabetes, liver and renal diseases, brain ischaemia and scleroderma can affect the ability of albumin to bind to cobalt (Govender *et al.*, 2008). Transferrin protein,

which has a role in iron uptake, can also bind to cobalt. In a study aimed to investigate the stability of cobalt-transferrin complex in the existence of albumin, showed a decrease of 50% of the complex (Smith, 2005).

#### **1.1.4.2 Cobalt effect on other organs**

##### 1.1.4.2.1 Cobalt effect on the lung

In a previous study, 50 patients were observed after consumption of 0.04 mg of cobalt/kg/day in beer, which contained cobalt sulfate stabiliser, for over a year. These patients developed cardiomyopathy (mainly tachycardia and arrhythmia) and led to pulmonary edema (Morin *et al.*, 1971).

In a study conducted on rats, 30.2 mg/kg was administered daily to rats in drinking water. These rats showed an increase in lung weight compared to relevant controls (Domingo *et al.*, 1984).

##### 1.1.4.2.2 Cobalt effect on the heart

People who consumed cobalt-containing beer (0.04 mg/kg) for years developed cardiomyopathy (Alexander, 1969; Bonenfant *et al.*, 1969; Morin *et al.*, 1971; Sullivan *et al.*, 1969). However, an anaemic patient who received cobalt chloride daily for 90 days with larger doses than that found in the beer (0.6-1 mg/kg) did not develop any effect in their heart (Davis and Fields, 1958).

In a study conducted on guinea pigs to mimic circumstances causing cardiomyopathy in cobalt-beer drinkers, pigs drank 20 mg of cobalt/kg daily (cobalt sulfate) alone or mixed with alcohol for five weeks (Mohiuddin *et al.*, 1970). The pigs that consumed cobalt with and without alcohol, developed cardiomyopathy as expected. Rats that

received a single dose of cobalt fluoride (176 mg/kg) and a single dose of cobalt oxide (795 mg/kg), both developed myocardial degeneration (proliferation as a result of interstitial tissue and muscle fibre enlargement) after 10 days of administration (Speijers *et al.*, 1982). Rats exposed daily to 8.4 mg of cobalt sulfate/kg developed left ventricular damage after 24 weeks of exposure (Haga *et al.*, 1996).

#### 1.1.4.2.3 Cobalt effect on the reproductive system

To our knowledge, there are no studies on the effect on the human reproductive system as a result of cobalt ingestion. The consequences for the human reproductive system after exposure to cobalt have been considered in several reviews (Mathur *et al.*, 2010; Paustenbach *et al.*, 2013), but no thorough study has been carried out.

In rats, daily exposure to 19 mg of cobalt sulfate/m<sup>3</sup> for 16 days caused testicular degeneration (Haga *et al.*, 1996). As a consequence of cobalt sulfate treatment to mice for 13 weeks, they developed slower sperm movement at a concentration of 1.14 mg of cobalt sulfate/m<sup>3</sup>, testicular degeneration at a concentration of 11.4 mg of cobalt sulfate/m<sup>3</sup> and longer estrous cycle in females at 11.4 mg/m<sup>3</sup> (Bucher *et al.*, 1990).

#### 1.1.4.2.4 Cobalt effect on the liver

Patients with cardiomyopathy who were exposed to cobalt containing beer developed liver dysfunction diagnosed by necrosis and increased plasma bilirubin and hepatic enzymes (lactate dehydrogenase, glutamic pyruvic transaminase, glutamic oxaloacetic transaminase, creatine phosphokinase and isocitric dehydrogenase) activities (Alexander, 1972). However, the liver effect observed here could have been caused as a complication from cardiomyopathy or as a result of alcohol

consumption.

#### **1.1.4.3 Cobalt genotoxicity**

Genotoxicity of a compound means the ability of this compound to harm genetic material such as chromosomes, DNA, RNA and other genetic materials.

The major causes for cobalt induced genotoxicity are thought to be the generation of reactive oxygen species and the reduction of the base excision repair ability (Murdock, 1959). Cobalt, in both soluble and insoluble forms, caused genotoxicity *in vitro*. Blood cells, after being exposed to soluble cobalt chloride, showed abnormalities in chromosome numbers. Insoluble cobalt sulfide caused breakage in the DNA strands in Chinese hamster ovary cells (Lison *et al.*, 2001). Cobalt, in the presence of hydrogen peroxide was found to generate reactive oxygen species causing damage to DNA in human lymphocytes (Robison *et al.*, 1982)..

In addition, cobalt chloride inhibited base excision repair *in vitro* after UV irradiation of human fibroblasts (Anard *et al.*, 1997). Repair of base excision is important for the stability of DNA and its inhibition can lead to mutation or carcinogenicity (Hartwig *et al.*, 1991). This effect of cobalt was explained by its competition with  $Mg^{+2}$  ions and its substitution with zinc in transcription factor (YY1) fingers (Kasten *et al.*, 1997).

#### **1.1.4.4 Cobalt carcinogenicity**

In a study conducted on rats and mice, it was found that inhaling sprays of cobalt sulfate for a long period caused lung cancer (Hamilton-KochSnyder and Lavelle, 1986). Cobalt, in the forms of cobalt sulfate, cobalt salts and cobalt metal alone and in mixtures, was found to be carcinogenic in animals but there is limited evidence for

carcinogenicity in humans (Bucher *et al.*, 1999).

In humans there were discrepancies in results regarding the carcinogenicity of cobalt leading to the conclusion of limited evidence for its carcinogenicity in human. Moulin *et al.* (1993) found no increase in cancer among workers exposed to cobalt in a cobalt producing electrochemical factory (Humans, 2006). In contrast, other studies investigated cancer cases in workers in hard metal plant factories producing cobalt and tungsten carbide mixture particles, and found an increase in cancer cases (Moulin *et al.*, 1993). This discrepancy can be explained by the increased genotoxicity of cobalt when combined with tungsten carbide (Hogstedt and Alexandersson, 1987; Lasfargues *et al.*, 1994; Wild *et al.*, 2000).

However, recent cohort study that reviewed cancer incidence among cobalt production workers in the period from 1961 to 2013, has concluded that there is no evidence of an association between cobalt exposure and the increase in lung cancer cases among cobalt production workers (Sauni *et al.*, 2017). Previous research concluded that cobalt concentration less than 300  $\mu\text{g/L}$  are probably non carcinogenic (Unice *et al.*, 2012). Additionally, it was reported that chronic exposure to reasonable level of cobalt are not expected to cause cancer (Tvermoes *et al.*, 2015).

#### **1.1.5 Fatalities associated with cobalt consumption**

Some cohort studies on humans have concluded that there is no increase in fatality among workers who are exposed to cobalt (Lison *et al.*, 2001). Other studies showed an increased fatality as a result of lung cancer caused by the exposure to cobalt as metal alloy (mixture of cobalt and tungsten carbide) or as cobalt salts (Moulin *et al.*, 1993). Some mortality as a result of lung hard metal disease (Mur *et al.*, 1987;

Lasfargues *et al.*, 1994; Moulin *et al.*, 1998) and cardiomyopathy (Ruokonen *et al.*, 1996) have also been related to cobalt exposure.

In a study investigating the effect of cobalt sulfate containing beer, death cases were reported among consumers as a result of cardiomyopathy (Barborik and Dusek, 1972). It was found that daily consumption of a beer containing up to 0.14 mg of cobalt sulfate/kg for years would cause death (Alexander, 1969; Morin and Daniel, 1967; Bonenfant *et al.*, 1969). In contrast, anaemic women (pregnant and non pregnant) who daily consumed higher doses (1 mg of cobalt/kg) than that in cobalt sulfated beers, did not suffer fatality (Alexander, 1972).

With regard to the oral route of exposure to cobalt in animals, the LD<sub>50</sub> was calculated in many studies in rats and the results and ranged from 42.4 to 317 mg/kg for cobalt chloride and cobalt carbonate, respectively (Bucher *et al.*, 1990; Bucher, 1991). Rats in these studies developed liver, kidney, gastrointestinal tract and heart related diseases. Death occurred at a dose of 161 mg of cobalt chloride/kg in force-fed Sprague-Dawley rats (Singh and Junnarkar, 1991; Speijers *et al.*, 1982). Mice have an LD<sub>50</sub> of 89 and 123 mg/kg for cobalt chloride and cobalt sulfate, respectively (Domingo and Llobet, 1984). When Guinea pigs were force-fed with 20 mg of cobalt sulfate/kg alone or in alcohol over 5 weeks, 25% of the guinea pigs died (Singh and Junnarkar, 1991). In this study, alcohol did not increase toxicity of cobalt, as it did in human consumers of cobalt containing beer.

#### **1.1.6 Mechanism of cobalt toxicity**

The exact mechanism of cobalt toxicity to cells is still ambiguous, though, several mechanisms of action have been proposed. Previous studies have concluded that

cobalt hard metal alloy (cobalt combined with tungsten carbide) has higher toxicity compared to either cobalt or tungsten carbide alone. In this study, the higher toxicity of cobalt hard metal was explained by conductivity of tungsten carbide that enhanced the ionisation of cobalt metal to  $\text{Co}^{2+}$  by moving electrons to the oxygen molecule near the tungsten carbide particle (Mohiuddin *et al.*, 1970). This makes cobalt more soluble and generates more reactive oxygen species. The same results were observed *in vitro*, where cobalt hard metal generated reactive oxygen species and caused peroxidation of lipids (Lasfargues *et al.*, 1995; Lison *et al.*, 1995).

Additionally, oxidative stress was increased in rat pneumocytes after cobalt treatment (Hoet *et al.*, 2002). The oxidative stress was measured by a decrease in glutathione (GSH) level combined with an increase in glutathione disulfide (GSSG) and oxidative damage to DNA (Zanetti and Fubini, 1997).

Guinea pigs and rats exposed to cobalt showed an increase in the peroxidation of lipids in their livers and the oxidation of glutathione (Ivancsits *et al.*, 2002). Cobalt had an impact on several proteins associated with oxidation such as erythropoietin, hypoxia inducible factor 1 and catalase (Christova *et al.*, 2002). These mechanisms described earlier by researchers were proposed as leading causes for cellular apoptosis in liver as a result of cobalt intake (Bunn *et al.*, 1998; Hoet *et al.*, 2002).

Regarding the mechanism of action of cobalt in the body, it was found that cobalt intake simulate hypoxic stress by enhancing erythropoietin to preserve cells during hypoxia, increasing the production of hypoxia inducible factor-1 (HIF-1) to decrease oxidative stress, producing growth factor to stimulate angiogenesis, and increasing glycolysis to compensate for ATP loss (Xue *et al.*, 2010). Cobalt was found to

increase protoporphyrins, which has protective and anti-inflammatory effect, in cells (Cao et al., 2012). Furthermore, cobalt can have positive effect by normalising glucose level. Consequently, it can improve conditions such as diabetes mellitus, hypertension and atherosclerosis (L'Abbate *et al.*, 2007).

## 1.2 Mephedrone

### 1.2.1 Mephedrone and related compounds

Mephedrone is a synthetic ring-substituted cathinone, 4-methylmethcathinone (Figure 1.3). It is structurally similar to the phenethylamine family of neuroactive amines, with the only difference being the presence of a keto functional group at the beta carbon (Gibbons and Zloh, 2010).

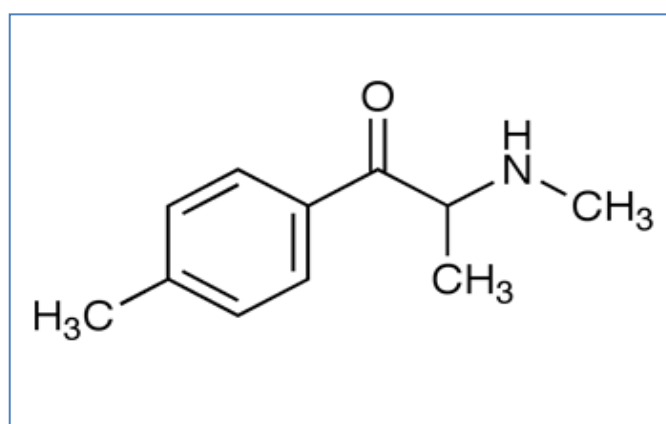


**Figure 1. 3 Mephedrone chemical structure.**

The International Union of Pure and Applied Chemistry (IUPAC) name for mephedrone is (RS)-2-methylamino-1-(4-methylphenyl) propan-1-one (Davey *et al.*, 2010). It has many other chemical names such as *N*-methylephedrone,  $\beta$ -keto-(4,*N*-

dimethylamphetamine), 4,*N*-dimethylcathinone, *p*-methyl-methcathinone and 2-aminomethyl-1-tolyl-propan-1-one (Davey *et al.*, 2010). In this review the compound is referred to as mephedrone or 4-MMC.

Mephedrone is used recreationally. Several other synthetic cathinones were also recorded as drugs of abuse by the Early Warning System at the European Monitoring Centre for Drugs and Drug Addiction (EMCDDA) (Wood *et al.*, 2015).

#### **1.2.1.1 Physical form of mephedrone**

Mephedrone is often distributed as a white crystalline powder with a yellowish tinge (Gibbons and Zloh, 2010). It is soluble in water, thus can be dissolved to use orally, rectally or by injection. Mephedrone is sold as pressed tablets or in encapsulated powder form (Dick and Torrance, 2015). Before mephedrone was classified as an illegal drug under the UK Misuse of Drugs Act, 1971, it was often sold with a label stating ‘not for human consumption’ as a way to bypass legislation for national medicines (Dargan *et al.*, 2011). There is no proof for mephedrone use as a food for plants, a bath salt or as a cosmetic product (Dargan *et al.*, 2010a).

#### **1.2.1.2 Sources of mephedrone**

The data collected from users’ discussion forums and surveys suggested that mephedrone has multiple sources (Dragon and Wood, 2010). Examples of these are street dealers, street marketing outlets, and online suppliers (Dragon and Wood, 2010).

The European Monitoring Centre for Drug Addiction (EMCDDA), using the procedure for snapshot survey, has screened Internet sites marketing mephedrone

and other new psychoactive substances (Dragon and Wood, 2010). One survey carried out in 2010 found that there were 77 websites where a person could purchase mephedrone and the majority of these websites were based in the UK (Wood *et al.*, 2015). This finding showed that the number of websites selling mephedrone had almost doubled compared to the number in 2009. Most of the websites do not state any country that they cannot send to. Remarkably, it was noticed that unlike other drug marketing websites, almost all these Internet sites were selling only mephedrone or mephedrone and other cathinones. After mephedrone was controlled in the UK on 16 April 2010, there was a sharp drop in the number of sites selling mephedrone compared to other legal highs. Investigations have deduced that these websites are in many cases selling a mixture of other cathinones together with mephedrone without stating the composition on the package (Ramsey *et al.*, 2010). Many of the UK Internet sites have moved overseas and continue to send orders by shipments, announcing that shipping orders are compatible with the UK regulations. The fact that it is illegal to possess mephedrone is being neglected.

Reports have also shown that mephedrone was available from street dealers before it was controlled in the UK (Dargan *et al.*, 2010b). This later source has been popular particularly among the young age users (Dargan *et al.*, 2010b). This source of supply is used because young users do not have credit cards to order shipments online, and they live in their family home so they do not have a private address. From the time when mephedrone was classified in the UK in April 2010, street dealing seems to have become the predominant source of mephedrone (Measham *et al.*, 2013). A study that used surveys from 150 mephedrone users found that 63% continued using the drug for two months following its classification; and 55% of them said that they

are going to continue to purchase the same quantity (Winstock *et al.*, 2010). There was, in fact, a rise of about 16% in purchasing from street dealers after mephedrone was classified.

## **1.2.2 Mephedrone toxicity, incidence and mortality**

### **1.2.2.1 Toxicological effects and cases of mephedrone toxicity**

As mephedrone is chemically similar to amphetamines, it would be expected to increase dopamine (DA) and serotonin (5-HT) concentrations in brain in a similar way to which amphetamines affect these compounds (Baumann *et al.*, 2012). Previous studies conducted on rat brain synaptosomes found that mephedrone prevents serotonin uptake in cortical and striatal synaptosomal preparations to a greater extent than it does dopamine (DA) uptake, and it has the role of a substrate for the cell membrane monoamine transporters (Baumann *et al.*, 2012; López-Arnau *et al.*, 2012). Previous results of a similar study conducted on these tissues proposed that vesicles are essential in understanding the chemical effects of mephedrone on the neurons (López-Arnau *et al.*, 2012). Other similar studies using rat brain synaptosomes have deduced that mephedrone acts in a selective way to release 5-HT more than DA (Hadlock *et al.*, 2011). Mephedrone intake increases extracellular 5-HT and DA with an increase of 5-HT 2–3 times greater than that of DA in rat brain synaptosomes (Baumann *et al.*, 2012).

### **1.2.2.2 Acute toxicity**

The mephedrone acute *in vivo* toxicity information is collected from sources such as

data obtained from reports to poisons information centers; reports from Emergency Department cases and case series; and user reports on Internet based discussions and user questionnaires (Brunt *et al.*, 2011; James *et al.*, 2011; Nicholson *et al.*, 2010; Sammler *et al.*, 2010). There is a limitation to the reports collected from self-reported mephedrone use in that there may be misconceptions about using mephedrone or other drugs since no samples were analysed in these reports (Brandt *et al.*, 2010; Ramsey *et al.*, 2010). Additionally, there is a potential that other drugs are present with mephedrone, and consequently the described effects could refer to the co-administered drug, or an interaction between drugs. Thus, when using these data it is important to consider these limitations in order to develop a more accurate understanding of mephedrone acute toxicity.

### **1.2.2.3 Chronic toxicity**

According to mephedrone pharmacology, physical dependency and withdrawal reactions are not expected after long term use (Dargan *et al.*, 2011). Nevertheless, psychological dependency can be developed. Mephedrone has only been available and thus abused since 2008 (Dargan *et al.*, 2011).

Previous reports suggested users could acquire a strong desire for mephedrone (Dargan *et al.*, 2010a; Measham *et al.*, 2013). A survey conducted on Scottish schools chose around 200 students who had used mephedrone in the past, and revealed that 17% of them mentioned that they experienced addiction or dependency (Dargan *et al.*, 2010a). Hundreds of the UK clubbers compared the addictive effect of mephedrone to cocaine or even stronger drugs (Winstock *et al.*, 2011b). Furthermore, addiction was found to be described more by insufflation route users.

The threat of developing the strong desire for using mephedrone is related to its chronic use (Measham *et al.*, 2013). This acquired desire was mentioned by users as an important issue with the use of mephedrone (Dragon and Wood, 2010). It is believed that this desire developed as a result of the fast onset and short time of euphoria occurring after mephedrone use. This has encouraged users to intake multiple doses in one time session (Winstock *et al.*, 2011b).

#### **1.2.2.4 Mephedrone-related Fatalities**

Throughout the year 2010, there was large concern in the UK media and many other countries, concerning fatalities related to mephedrone use. Even though it was stated in the media that mephedrone was consumed, in many cases in the UK, mephedrone was not detected or there was no request by the Coroner to investigate mephedrone as a cause of death (Dargan and Wood, 2011). Thus these media reports of fatality are not accurate.

The first mortality case of resulting from mephedrone intake alone was an 18 year old Swedish girl (Gustavsson and Escher, 2009). The girl had survived a previous cardiac arrest following mephedrone and cannabis use. On this occasion, hospital examinations resulted in low sodium in blood (120 mM) compared to the normal level (135 to 145 mM), brain swelling and increased acidity. Even after surviving the cardiac arrest, she died 36 hours after reaching the emergency department as a result of brain failure in intensive care. The toxicological analysis of her blood and urine detected only mephedrone although the level was not indicated. No other drugs were discovered.

Many other death reports published in previous studies stated that mephedrone was

present in the biological samples of the deceased (Wood *et al.*, 2010; Torrance and Cooper, 2010; Dickson *et al.*, 2010). In Scotland, a study detected the presence of mephedrone in four mortality cases in the post-mortem samples (Torrance and Cooper, 2010). All cases had undergone toxicological analysis of post-mortem samples (hair in one case, urine in three, and blood in all). However, there was an absence of clinical data in these cases, and there were other medicinal and illicit drugs present in addition to mephedrone in three of these cases. Consequently, it is not possible to significantly rely on the findings of this study. However, in two of the cases mephedrone abuse was reported as the cause of death.

Mephedrone related death was also reported on a sample collected before death of a 29-year-old male who was found collapsed and unwell in a nightclub (Wood *et al.*, 2010). Toxicology analysis of the white powder found in his possession revealed that it was mephedrone. Comparable to the Swedish girl's death case, cerebral oedema and a low blood sodium level (125 mM) were detected. Though, the osmolality measurement in blood and urine proposed that this was due to intoxication by water overload. After having a general convulsion in the Emergency Department, the CT scan for the head revealed he suffered from cerebral herniation (high pressure within the skull). Qualitative toxicological analysis of his blood sample confirmed that mephedrone was present. Additionally, no other drugs of abuse were present in the powder and in his blood samples before death. The cause of death was identified as brain failure after a brain swelling and water overload as a result of psychoactive drug intake.

In another case, a male in his twenties in Maryland, USA, was found dead.

Toxicology analysis of urine detected a group of drugs of abuse including acetylmorphine, codeine, morphine and doxylamine in addition to mephedrone at a concentration of 198 mg/L. The concentration in blood was 0.5 mg/L. The cause of death was identified as poisoning with a drug mixture. Thus it was difficult to estimate the mephedrone contribution to this mortality case (Dickson *et al.*, 2010).

Lastly, the UK National Programme on Substance Abuse Deaths provides data collected on drugs of abuse suspected of causing deaths from multiple sources in the UK. In a previous annual report, issued in October 2010, it reported 45 cases of death cases where death has been linked to mephedrone in England (Ghodse *et al.*, 2013). Recently, 4 cases of mephedrone (3-methylmethcathinone) related deaths were reported (Ameline *et al.*, 2018).

In the European Monitoring Centre for Drugs and Drug Addiction information was collected in July 2010 on deaths related to mephedrone as a mephedrone risk assessment (Dargan and Wood, 2011). According to the data provided, the cases specified as mephedrone related only referred to deaths that took place in the UK and Sweden. Moreover, in the UK, there were cases where mephedrone was present and was associated with death even if it was administered with other drugs, and other cases where mephedrone was confirmed by analysis but was not thought to be connected to death. In other European countries there were no reports of cases of death associated with mephedrone intoxication, however, in many cases mephedrone was not considered in the analysis suggesting that it would have been missed.

#### **1.2.2.5 Animal models studies for mephedrone effects and toxicity**

Many studies have used animals to study mephedrone pharmacology and toxicity

(Baumann *et al.*, 2012; Hadlock *et al.*, 2011). Rat synaptosomes were isolated to study how mephedrone affects the uptake of serotonin (5-HT) and dopamine (DA) (Martínez-Clemente *et al.*, 2012). Generally, these investigations found that the uptake of both serotonin and dopamine was inhibited by mephedrone at half maximal inhibitory concentration (IC<sub>50</sub>) value  $0.31 \pm 0.08 \mu\text{M}$  and at an IC<sub>50</sub> value  $0.97 \pm 0.05 \mu\text{M}$ , respectively. Mephedrone also was found to have high affinity for the membrane receptors and transporters of both serotonin (5-HT<sub>2</sub>) and dopamine (D<sub>2</sub>) receptors. This finding correlates the effect of mephedrone with that of amphetamines. In a microdialysis experiment performed on the nucleus accumbens of rats, mephedrone intake was found to increase both serotonin and dopamine concentrations with a higher effect on serotonin (Baumann *et al.*, 2012). Chronic use of mephedrone has been found to induce hyperthermia similar to MDMA chronic use, but it was discovered with mephedrone that the monoamine (5-HT<sub>2</sub> and D<sub>2</sub>) levels did not change in striatum and cortex, which was the case in MDMA chronic use. A similar study, showed that both mephedrone and amphetamine raised dopamine levels in rat nucleus accumbens by 496% and 412% respectively, while MDMA raised it by only 235%. In the same study, mephedrone and MDMA caused a greater increase in the level of serotonin (941% and 911% respectively) while the effect of amphetamine was much less (165% increase) (Kehr *et al.*, 2011).

Mephedrone (four injections of 20 mg/kg with a 2-h interval between each injection) was given to mice, which resulted in elevated body temperature and stimulated motion. Though, unexpectedly and unlike other amphetamines it did not reduce the activity of tyrosine hydroxylase, striatal dopamine content or dopamine transport. Another rat study revealed that mephedrone administration increased locomotion and

reduced social choice (Motbey *et al.*, 2012). Rat brain histological analysis revealed that the activation pattern of the brain by mephedrone was similar to that for combined administration of methamphetamine and MDMA. This research has suggested that mephedrone has similar effects to both MDMA and methamphetamine combined. There have also been *in vitro* and *in vivo* studies conducted to investigate the effect of mephedrone effect on the cardiovascular system (Meng *et al.*, 2012). In *in vitro* guinea pig cardiac myocytes ion transport was measured to investigate if mephedrone can cause cardiac arrhythmia, which would then result in sudden death, but it did not have a significant effect on the transport of ions ( $K^+$ ,  $Na^+$ , and  $Ca^{2+}$ ) in cardiomyocytes. Nevertheless, there were observed *in vivo* effects following a 1.0 mg/kg dose of mephedrone which included increased heart rate, cardiac output, and stroke volume when administered intravenously or subcutaneously to guinea pigs.

These animal *in vitro* and *in vivo* studies aid our understanding of the effect of mephedrone and its acute toxicity. Generally, the pharmacodynamics of mephedrone were consistent with those for coadministration of amphetamine and MDMA regarding elevation of serotonin and dopamine levels. Likewise, the effect of mephedrone on neuro-behaviour and the cardiovascular system are similar to those that resulted after administering the combination of amphetamine and MDMA.

#### **1.2.2.6 Incidence of mephedrone availability**

Previous studies indicated that both the legal status and the low purity for drugs such as MDMA and methamphetamine (Brunt *et al.*, 2011; Winstock *et al.*, 2011a) have led to the illegal production of new illicit drugs identified as “new psychoactive

substances” or “legal highs”. Structurally, they are beta-ketoamphetamines. One example is mephedrone, which is primarily used by immature adults and teenagers (Schifano *et al.*, 2011) and has been easily accessible for legitimate purchase both on the web and in shops. A considerable number of users found that mephedrone has more desirable effects than cocaine and MDMA (Vardakou *et al.*, 2011).

Since mephedrone has similar effects to MDMA, methamphetamine and cocaine, its use spread quickly, initially in the homosexual community and in clubbers, and lately among teenagers and immature adults (Schifano *et al.*, 2015).

European countries started to collect information of mephedrone prevalence of use, when UK crime centres began to question the use of mephedrone in 2010 (Gibbons and Zloh, 2010). Generally, similar to MDMA in the year 2011, the prevalence of use was 1.4% in the age group from 16–59 years old. Similar to cocaine, mephedrone use increased to 4.4% in young people (16–24 years old), while it was only 0.6% in the age group 25–59 years.

Two studies were conducted on school and university students (Dargan *et al.*, 2010a; Dargan *et al.*, 2011). In one of these two studies a sample of 1006 Scottish students were selected (preceding the mephedrone restriction in the UK), and it was found that 205 students stated that they had administered mephedrone previously (Dragon and Wood, 2010). Irregular use, which was described as more than one time, but not more than one use weekly, increased within older age group. 4.4% of students who have used mephedrone indicated that they administered it routinely on daily basis, though the maximum level of daily use was recorded in the younger aged students (under 21 years old). Another study conducted in Northern Ireland in 2010 surveyed

154 students in the age group 14–15 years old following the restriction of mephedrone in the UK, and concluded that 62 of those questioned had previously administered mephedrone one time or more (Dargan *et al.*, 2010a). There were no surveys after 2010, which was the year when mephedrone was classified as controlled drug.

### **1.2.3 Mechanism of mephedrone effect on the CNS, and other adverse reactions**

According to the aforementioned information derived from the user reviews it is believed that mephedrone has a similar CNS effect to other psychoactive drugs (MDMA and cocaine in particular) (Winstock *et al.*, 2011a). The effects reported by users are summarised as follows: mood boosting, sexual stimulation, excitement, general stimulus effect, decreased aggression, and enhanced cerebral activity (Winstock *et al.*, 2010). 60% of UK clubbers who used mephedrone indicated that mephedrone slightly raised their sexual desire, with 8% insisting that it was a regular effect of mephedrone (Winstock *et al.*, 2011b).

In a comparison survey in the UK, clubbers who used mephedrone and cocaine were asked about the difference between the effect of both drugs (Winstock *et al.*, 2011b). More than 50% indicated that mephedrone has a more pronounced euphoria effect than cocaine and more than 60% said that the euphoria of mephedrone lasted longer than that of cocaine. However, it was noticed that the users who stated that they experienced longer effect were oral route users but not nasal route users (Winstock *et al.*, 2011b).

Drugs that affect the transporters of monoamines are divided into two groups,

substrates or blockers. The substrates stimulate cells to produce more neurotransmitters inside the cell. Production of more neurotransmitters by the increase of substrates will lead, eventually, to insufficiencies in monoamine neurons, neurotransmitter reduction, and decreased efficiency of transporters. Recent research determined that the cathinones that were blockers of human monoamines were butylone, MDPV, and naphyrone, whereas the substrates were mephedrone, 4-fluoromethcathinone, and methylone. A neurotoxic effect of the substrate group is proposed to act via the inhibition of neurotransmitter uptake (Eshleman *et al.*, 2013). Some previously published papers have studied the potential neurotoxicity of mephedrone. Repetitive mephedrone dosing to mice or rats had no toxic effect to the cortex and striatum DA neural endings, and did not stimulate the striatum microglial cells and astrocytes in mice (Angoa-Pérez *et al.*, 2014). However, mephedrone increased amphetamine (methamphetamine and methyldioxymethamphetamine) neurotoxicity in mouse brain as a mephedrone plus amphetamines mixture decreased serotonin levels more than either of them alone (Angoa - Pérez *et al.*, 2013).

In a recent study conducted on rats (López-Arnau *et al.*, 2015), the authors concluded that when mephedrone is administered in doses mimicking human abuse intake, it decreases weight and causes irregularities of body temperature. The decrease in weight in rats treated with mephedrone can be explained as a result of appetite suppression caused by the drug use, similar to that observed with other amphetamine use (Angoa-Pérez *et al.*, 2014). However, the loss in weight was temporary and the weight was regained in seven days following the last drug administration. Body temperature was significantly and instantly decreased following the first mephedrone dose.

In López-Arnau's experiments, it was found that hyperthermia was detected only after a binge like dosing of mephedrone. The elevated body temperature was related to mephedrone binge dosing at both ambient (Baumann *et al.*, 2012) and high temperature (Hadlock *et al.*, 2011; López-Arnau *et al.*, 2015).

Additionally, mephedrone has a noticeable effect on DA and 5-HT transporters along with causing a decrease of the enzymes responsible for synthesis of DA and 5-HT. As a result of mephedrone intake in rats, DA transporters were decreased only in the frontal cortex, though, 5-HT transporters were reduced in all of the investigated parts of the rat brain (the striatum, the frontal cortex, and the hippocampus) (López-Arnau *et al.*, 2015).

#### **1.2.4 Experimental investigations into toxicity and metabolism**

##### **1.2.4.1 Toxicity experiments**

On site tests for mephedrone detection can be carried out by portable Raman and infrared spectrometers (Dargan *et al.*, 2011). These can measure only pure mephedrone, and do not allow separation of the drug from biological samples. The identification of mephedrone and its metabolites can be achieved reliably using liquid chromatography with tandem mass spectrometry (LC-MS/MS) and gas chromatography-mass spectrometry (GC-MS) (Gibbons and Zloh, 2010; Camilleri *et al.*, 2010; Meyer *et al.*, 2010). However, these methods can only differentiate between the methyl-methcathinone structural isomers if there are standards for reference or through analysis by nuclear magnetic resonance spectroscopy (NMR) (Gibbons and Zloh, 2010; Meyer *et al.*, 2010).

A study conducted by den Hollander in 2014 on human neuroblastoma cells (SH-

SY5Y), found that mephedrone had a toxic effect on cells at 500  $\mu$ M and greater (den Hollander *et al.*, 2014). The study has also demonstrated that mephedrone has redox electron donor reactivity and displays a relationship of this activity to high pH values and this is accompanied by formation of an N-acetylated mephedrone. According to den Hollander, mephedrone decreased mitochondrial respiration. The use of the SH-SY5Y cell line shows that mephedrone yielded cytotoxicity only at high concentrations; while at lower levels it decreased lactate dehydrogenase (LDH) production. It is proposed that oxidative deamination, followed by the oxidative cleavage of mephedrone produces acetic acid, which acetylates mephedrone.

Notably, many *in vivo* studies have found no sign of toxicity of mephedrone (Angoa - Pérez *et al.*, 2012; den Hollander *et al.*, 2013; Motbey *et al.*, 2012). Variable metabolism reactions and/or inability to penetrate brain and blood barriers could result in this negative finding.

It was found that mephedrone acts synergistically to significantly enhance methamphetamine induced DA toxicity (Angoa - Pérez *et al.*, 2013). The same hyperthermia was produced in the treatment of mice with both mephedrone and methamphetamine, and in the treatment of any of the drugs separately. The neurotoxicities of amphetamine and 3,4-methylenedioxymethamphetamine on the nerve endings of DA in mice striatum were also enhanced. As mephedrone increases methamphetamine neurotoxicity, this suggests that it has different interaction with the dopamine transporter (DAT) than that observed with other DAT inhibitors such as amphetamic acid and nomifensine (Pu *et al.*, 1994; Poth *et al.*, 2012). The fact that mephedrone itself has no significant effect on DA nerve endings, could imply a

potential high risk caused by its interaction with other drugs, and could lead to neurotoxic complications (Angoa - Pérez *et al.*, 2013).

In a recent study, it was found that when mephedrone was co-administered with ethanol in mice the neurotoxicity of mephedrone was enhanced (Ciudad-Roberts *et al.*, 2016). This finding was explained by the authors to be a result of increased oxidative stress in the hippocampus, causing decreased learning, memory, and neurogenesis in the mice.

In another drug interaction study, mephedrone was co-administered with nicotine in mice (Budzynska *et al.*, 2015). The co-administration was found to be effective in reducing general antioxidant function, catalase activity, and antioxidant enzyme activities in the brain, and in increasing lipid peroxidation.

#### **1.2.4.2 Metabolism experiments**

The data of another recent study on rat carried out by Khreit and coworkers investigated the metabolic pathways of mephedrone (see Figure. 1.4) in freshly isolated hepatocytes. The study detected glucuronidated Phase II conjugates, but no sulphated ones (Khreit *et al.*, 2013). The main metabolites detected were normephedrone, carboxymethcathinone, hydroxymethyl-methcathinone and methylephedrine in addition to seven other metabolites illustrated in Figure 1.4. The main pathways were acetylation, reduction, demethylation, oxidation, conjugation and aromatic hydroxylation.

A Danish study which was published on 2013, investigated both *in vitro* mephedrone metabolism by cytochrome P450 enzymes and *in vivo* metabolism by analysing

blood and urine samples from four authentic forensic traffic cases (Pedersen *et al.*, 2013). In the *in vitro* experiment, CYP2D6 was found to be the major enzyme responsible for the phase I metabolic pathway of mephedrone metabolism. Mephedrone was detected unchanged together with its metabolites, in urine. The metabolite hydroxytolyl-mephedrone was detected in both *in vivo* and *in vitro* situations, and found to be the most abundant metabolite in the *in vitro* environment. Notably, hydroxytolyl-mephedrone was the major phase I metabolite to be excreted mainly (80%) as the  $\beta$ -glucuronide and arylsulphate in urine. Nor-mephedrone was also identified in both *in vivo* and *in vitro* experiments. On the other hand, dihydro-, 4-carboxy-dihydro-, and 4-carboxy-mephedrone were only detected *in vivo*. Regarding the *in vivo* findings, hydroxytolyl- and 4-carboxy-dihydro-mephedrone were mainly detected in urine, while all other metabolites were detected in both blood and urine samples.

Another metabolic study conducted using both rat and human urine samples (Meyer *et al.*, 2010), concluded there was no difference between the metabolic pathways in the urine samples from either species, and consequently it is applicable to use rats to predict mephedrone metabolism. The detected metabolites were: nor-, nor-dihydro-, hydroxytolyl-, and nor-hydroxytolyl mephedrone in addition to the parent drug (mephedrone). In this experiment, the three suggested phase I metabolic pathways were: reduction of the keto moiety of the respective alcohol, N-demethylation of the primary amine, and oxidation of the tolyl moiety of the corresponding carboxylic acid and alcohol.

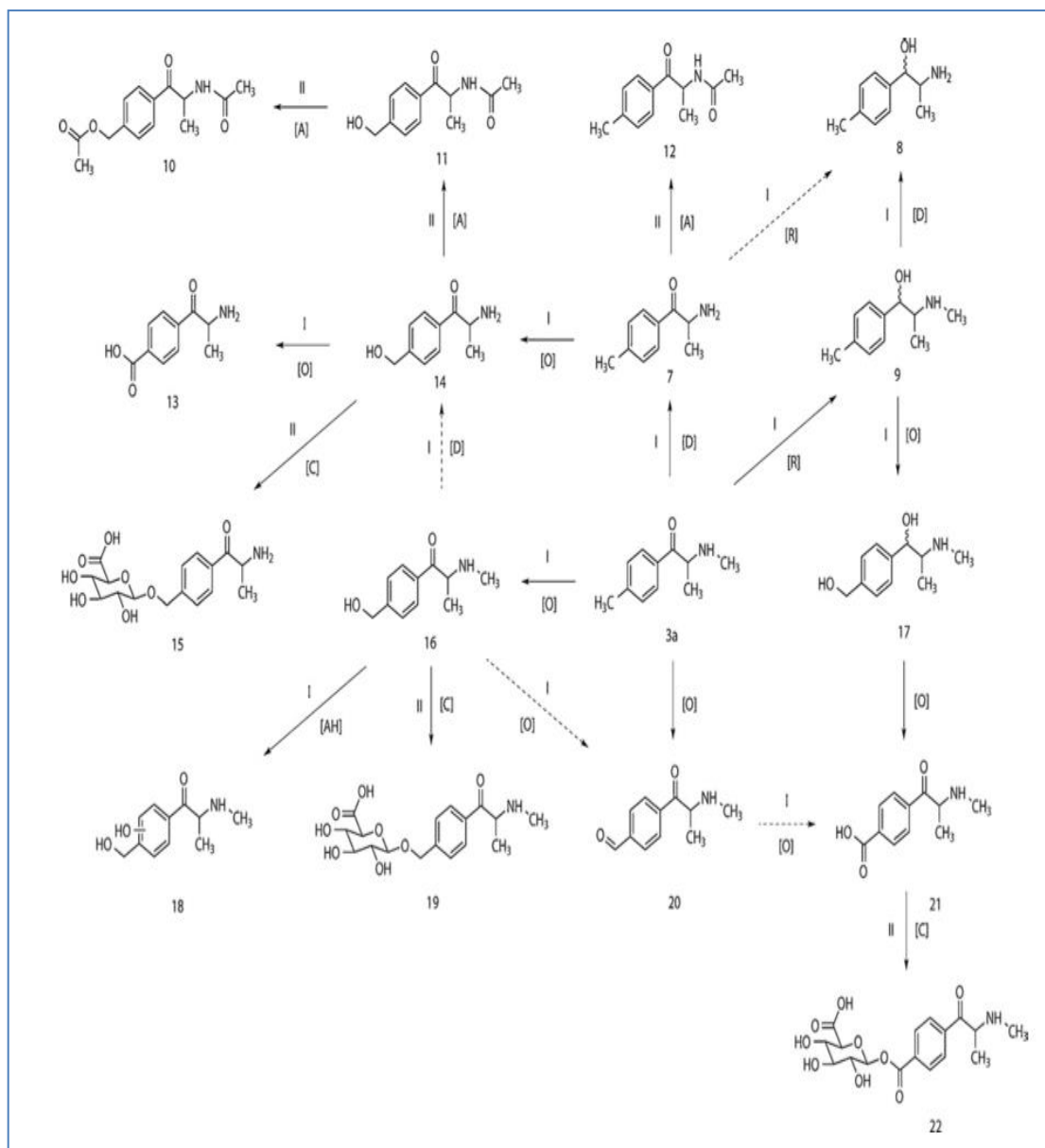


**Figure 1. 4 Possible mephedrone metabolism reactions (phase I and II) in rat liver. [A]=acetylation; [R]=reduction; [D]=demethylation; [O]=oxidation; [C]=conjugation; [AH]=aromatic hydroxylation. From (Khreit *et al.*, 2013).**

In this thesis metabolism and toxicity of mephedrone on the human neuronal cells will be assessed using the application of metabolomics. To our knowledge, this is the first study of mephedrone toxicity using a metabolomics approach.

### **1.3 *In vitro* cell culture models and advantages**

The main aim of any *in vitro* cell culture model is to minimise variation during experiments and to study them under precise and simply evaluated environments. Depending on the precise design of the study and desired outcome, the experiment is likely to simulate the *in vivo* environment. It is, however, not compulsory that every *in vitro* experiment should mimic the *in vivo* environment. The use of *in vitro* procedures has showed that they are efficient for investigating cell biology, pathology and physiology, however, they have many artefacts and limitations, and the results can be deceiving if disconnected from their physiological framework. Complete organs *in vivo* reveal wide interactions between several cell categories that regulate all physiological activities. When selective cells or tissues are cultured *in vitro* this connected system is absent. The cells or organ cultures provide a simplified system separated from the *in vivo* environment, which limits the assumptions that can be deduced from the experiment. It is widely agreed that it is impossible for *in vitro* culture to simulate whole animal studies, however, 2 dimension (2D) and 3 dimension (3D) cell cultures are widely used to study chemical metabolism and toxicity *in vitro*.

#### **1.3.1 2 Dimension (2D) cell culture**

2 Dimension (2D) cell culture systems were first used over 100 years ago (Lasnitzki, 1958; Lasnitzki and Lucy, 1961). Presently, there is an expansion in their use either as primary cells or as cell lines in 2D treated plastic containers. This technique is the main model used to study the biological cell activity and toxicity testing investigations. The wide use of the dissociated cell culture model is a result of the discovery that cells can attach to plastics. However, there are many factors which

made this technique feasible such as; simple cell preservation and management; cost effectiveness; availability of the commercial products needed in the technique; the presence of many new techniques allowing genetical management of cells; protein and gene expression control; possibility of high-throughput screening (HTS); and the low cost of sterilisation.

### **1.3.2 Three dimensional (3D) cell culture**

3D cultures were historically used in research on engineering and regeneration of tissue, but more recently in modeling of disease, toxicology, and molecular studies. Many studies name 3D culture supports as scaffolds, and culture systems as bioreactors (Elliott and Yuan, 2011; Justice *et al.*, 2009; Badylak *et al.*, 2009).

Scaffolds can be very different in their nature: synthetic polymers, natural products, both of which may have or may not have adhesive additives or cellular proteins within them, and a range in the size of their pores. They can be mechanically tailored, and be solid, spongy, or gels. Synthetic scaffolds are precisely made, have manageable properties and are reproducible, though on the other hand they may need special additives to allow intracellular interactions. Scaffolds that contain naturally obtained proteins (e.g., collagen) have integral cellular receptors. Cells may be obtained for example from cell lines, or from primary cells obtained from tissues by enzymatic dispersion or by mechanical dissociation (Pampaloni *et al.*, 2007).

## **1.4 Mass spectrometry based metabolomics**

### **1.4.1 Metabolomics**

Metabolomics is defined as ‘the quantitative measurement of time-related multiparametric metabolic response of living systems to pathophysiological stimuli

or genetic modification' (Nicholson *et al.*, 1999). It aims to illustrate and detect the metabolites, which are the final products of the metabolism processes in the cells. The study of metabolomics involves several fields such as biochemistry, analytical chemistry, statistics, and bioinformatics. In the field of toxicology, metabolomics involves the study of system biology, molecular diagnostics, and patho-biochemistry (Griffiths *et al.*, 2010).

Through the previous ten years, there has been a growing interest in the use of metabolomics in the analyses of the biological systems. It is proposed to be an important technology that can aid in better understanding for the biological systems. It studies the complete range and levels of metabolites involved in biological systems reactions. The metabolome includes a wide range of small molecules (<1500 Da) inside the cell such as nucleotides, sugars, and amino acids, fatty acids, and lipids.

Metabolomics has many challenges such as the large number of different chemical compounds inside cells and the possibility of artefacts. It is estimated that there are more than 100,000 metabolites in humans which can vary as a result of the effects of nutrients, drug administration and other physiological factors (Griffiths *et al.*, 2010). Additionally, any compound or even microorganism in the surrounding environment or in the body may affect the metabolome and expand the quantity of metabolites.

Metabolomics offers an important approach to detect the biological markers of toxicity and can aid in constructing models to predict toxic effects (Fiehn, 2002; Wishart, 2007). The application of metabolomics in toxicology analysis aims to 'achieve a comprehensive measurement of the metabolome and how it changes in response to stressors, with biological payoff being an illumination of the relationship

between the perturbations and affected biochemical pathways' (Craig *et al.*, 2006).

The most common approach to conducting metabolomics analysis is to apply mass spectrometry (MS), or nuclear magnetic resonance (NMR). At present, MS metabolomics is the method of choice for biomarker discovery because of its high sensitivity and specificity (Robertson *et al.*, 2005). This thesis will use MS metabolomics.

Since liquid chromatography–electrospray mass spectrometry (LC–ESI-MS) can ionise a wide range of metabolites with little fragmentation, it is preferred by many metabolomic studies. Profiling can be untargeted or targeted. Targeted metabolomics has the advantage of the use of synthetic standards in metabolite analysis allowing quantification of metabolites; it has also been used in many studies. Particular procedures for sample processing (extraction and quenching) are needed since some intracellular metabolites are labile, and it is important to design all the steps of the method of analysis to give the best outcome regardless of these challenges (Bouhifd *et al.*, 2013).

#### **1.4.2 Liquid chromatography-mass spectrometry (LC-MS)**

Liquid chromatography-mass spectrometry (LC-MS) is a combined technique for the separation of different chemicals by liquid chromatography (or high performance liquid chromatography) with the detection technique of mass spectrometry (Leclercq *et al.*, 2009; Lu *et al.*, 2008). Liquid chromatography (see Figure 1.5) is applied to separate the different components of a mixture and mass spectrometry (see Figure 1.6) is applied to detect the structure of each separated component (Dass, 2007).

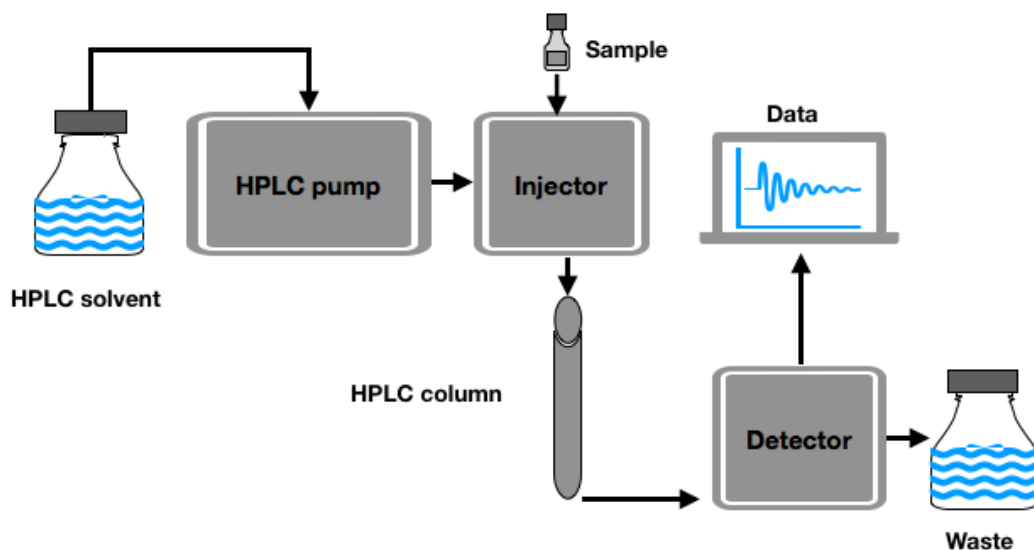


**Figure 1. 5 Scheme of the components of HPLC system with detector.**

LC is a technique for physical separation of a mixture by moving the mixture through two phases (stationary and mobile phases). There are five types of LC chromatographic methods; partition, size-exclusion, adsorption, affinity and ion exchange chromatography. The reverse phase method (partition chromatography) is very widely used. It applies a hydrophobic non polar stationary phase and a polar mobile phase. The mobile phase usually consists of water mixed with a polar solvent such as methanol or acetonitrile. The stationary phase is made of micro meter (3-5  $\mu\text{m}$ ) size silica particles attached to a long chain alkyl moiety (Dass, 2007). After sample injection (10-20  $\mu\text{l}$ ) the sample is mixed with mobile phase and pressured through the stationary phase (packed column). The mixture constituents are separated according to their relative affinity for the mobile and stationary phases (Niessen *et al.*, 2006).

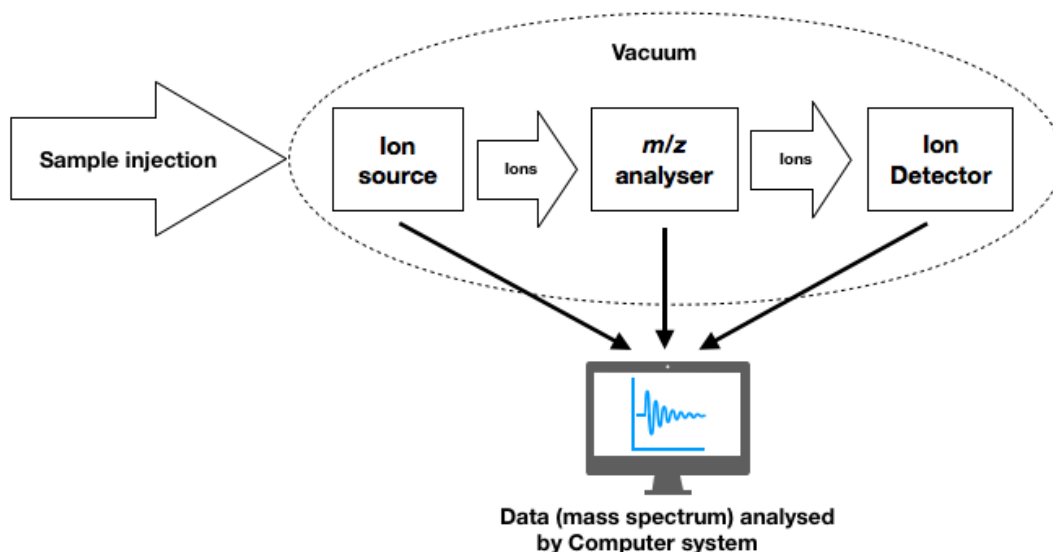


**Figure 1. 6 Mass-spectrometry schematic diagram showing different parts of the detector.**

Mass spectrometry is a detection method for analytes based on the mass to charge ratio of the component ions. The mass spectrometry separation method uses either magnetic or electric fields to control the movement of the ions of the analyte to detect the mass to charge ratio ( $m/z$ ). A mass spectrometer is composed of an ion source,  $m/z$  analyser and ion detector under a vacuum system and attached to a data analyser (see Figure 1.6). The ion source is the part where sample components (came from the LC) are ionised using corona discharge, electric field, photons or laser beams. In an electrospray ionisation ion source, the liquid of uncharged sample molecules will be converted to gaseous ions and sent to the analyser. In a mass to charge analyser, the ions are separated by magnetic or electric fields according to their masses. Then the abundance of each ion is detected by measurement and amplification of the ion current for the mass of each ion in the detector. Finally, the data system will create a mass spectra to be visualised by the users on a computer (Pitt, 2009).

## **1.5 Quantitative real-time polymerase chain reaction (qRT-PCR)**

The polymerase chain reaction (PCR) is defined as a genetic technique that uses certain enzymes and results in the amplification of the amplicons of the complementary DNA (cDNA) or the DNA (Pitt, 2009; Innis *et al.*, 2012). Quantitative real time polymerase reaction (qRT-PCR) is a type of RT-PCR that allows the quantification of the genes of interest expressed after amplification (Higuchi *et al.*, 1992). The constant observation of the amplification of a specific amplicon through the whole PCR process is what we refer to as RT-PCR (Lie and Petropoulos, 1998). RT-PCR procedures can be classified, according to the production of fluorescence, to direct and indirect assays (Holland *et al.*, 1991). When the fluorescence is produced during the primer extension step in the amplification process, the method is called indirect RT-PCR (Kutyavin *et al.*, 2000). The direct RT-PCR method is the process that involves production of fluorescence directly after the reaction between a fluorescent compound and the amplified gene see Figure 1.7 (Tyagi *et al.*, 1998).

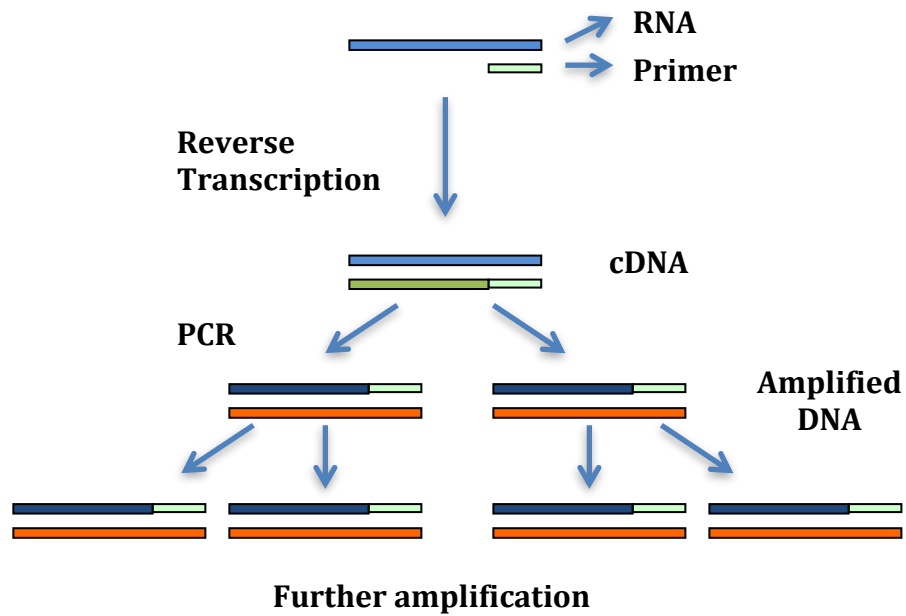


**Figure 1. 7 Simple diagram illustrating the steps of RT-PCR.**

An example of widely used direct method is the SYBR Green dye method, where the fluorescent dye SYBR Green is used. In this method the fluorescence is emitted as a result of DNA binding to the SYBR Green dye (Whitcombe *et al.*, 1999). Fluorescence is measured during the RT-PCR process and a graph is drawn as shown in Figure 1.8.

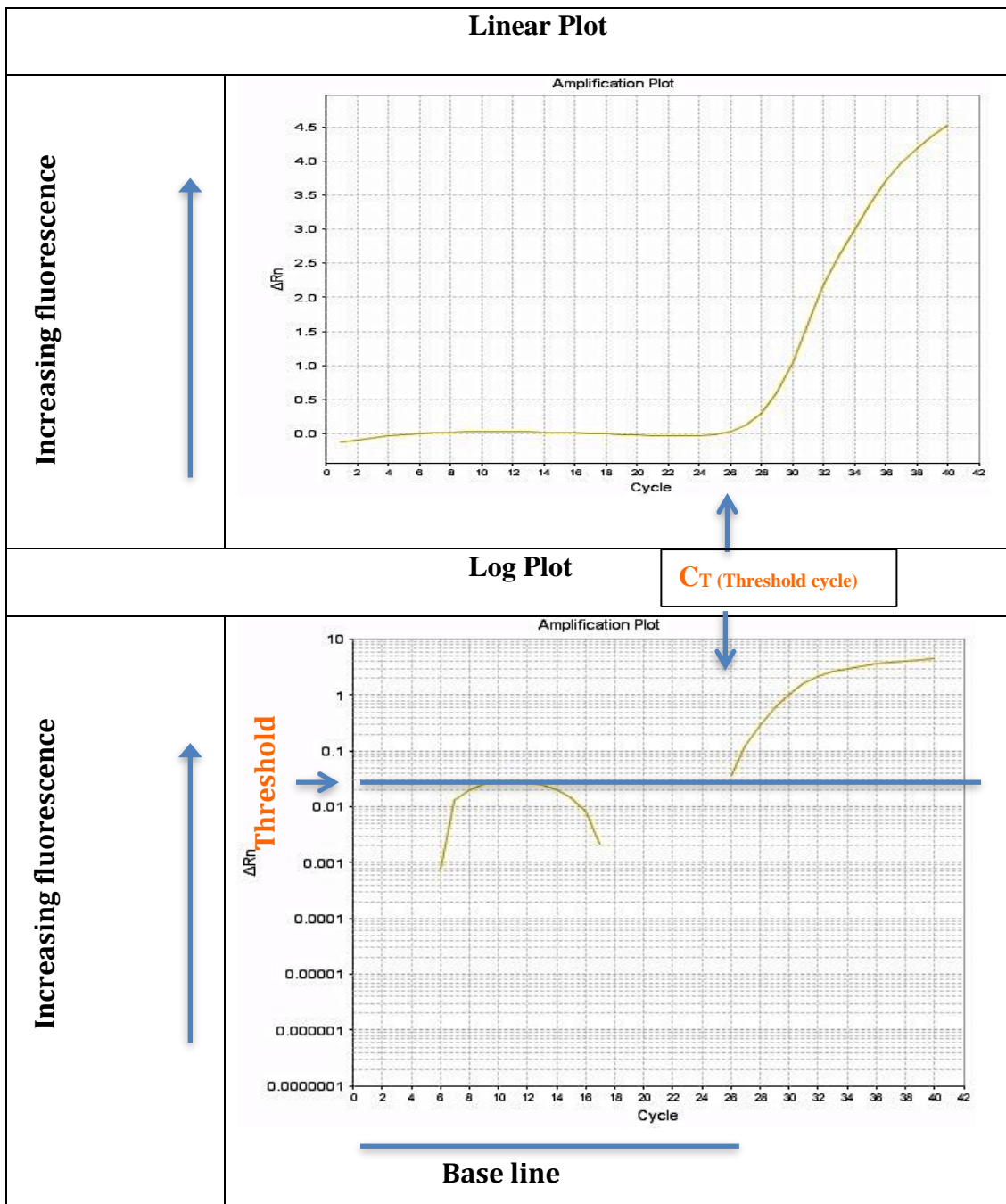


**Figure 1. 8 The linear and log plots of the measured SYBR-Green fluorescence in the RT-PCR process.**

A threshold value is calculated as three to five times the standard deviation above the mean value of the background. Threshold cycle ( $C_T$ ) is detected by identifying the cycle where the fluorescence time point reaches the threshold.  $C_T$  is used for the

quantification of gene expression. The number of copies of the target sequence at the start is reciprocally related to the  $C_T$  value (Bustin *et al.*, 2009).

### **1.6 Reason for the choice of mephedrone and cobalt for analysis**

The goal of this research is to study neurotoxicity in brain by the use of a metabolomic approach, and to find out if the metabolomic approach can be a useful tool to study neurotoxicity. To achieve the goal it was beneficial to search for neurotoxic compounds with different mechanisms of toxicity to apply metabolomic analysis. However, care was taken to choose a toxic compound with little known about its mechanism of action regarding toxicity. Thus, the choice of mephedrone and cobalt was made as they are both considered neurotoxic compounds with little known about their mechanism in terms of toxicity.

### **1.7 The aims of the project**

- Investigation of mephedrone metabolism by hepatic and neuronal cells.
- Evaluation of mephedrone toxicity on neuronal and hepatic cells.
- The study of the intracellular metabolic changes induced by mephedrone.
- Evaluation of cobalt neurotoxicity.
- The study of the intracellular metabolic changes induced by cobalt.
- Evaluation of metabolomics analysis as a tool in neurotoxicity studies.

## **Chapter 2 MATERIALS AND METHODS**

---

## **2.1 Culture of cells**

### **2.1.1 Standard stock solutions and preparation methods**

#### **2.1.1.1 Media**

Complete Dulbecco's Modified Eagle Medium (DMEM) of 500 ml volume (Lonza, catalogue number BE12-604F) was prepared under sterile conditions by the addition of 10% (v/v) sterile Foetal Bovine Serum (FBS) (Biosera), 50 µg/ml streptomycin/50 IU/ml penicillin mixture, and 1% non-essential amino acids (NEAA). Complete DMEM media was used to grow U-373 and Hep G2 cells.

Complete Dulbecco's Modified Eagle Medium: Nutrient Mixture F12 (DMEM/F12) of 500 ml volume (Life Technologies, catalogue number 31331-028) was prepared by the addition of 15% (v/v) sterile FBS, 1:1 of 50 µg/ml streptomycin/50 IU/ml penicillin mixture, and 1% non-essential amino acids (NEAA). Complete DMEM/F12 media was used to grow SH-SY5Y cells.

#### **2.1.1.2 Versene**

Versene was prepared by the addition of 4.5 ml of 0.5% of phenol red, 0.3g of  $\text{KH}_2\text{PO}_4$ , 0.3g of EDTA, 1.73g of anhydrous  $\text{Na}_2\text{HPO}_4$ , 12g of NaCl and 0.3g of KCl to 1.5 L of distilled water. The mixture was then sterilised by autoclaving.

#### **2.1.1.3 Trypsin**

Tris buffered saline (TBS) solution was prepared by the addition of 0.5g of glucose, 0.05g of  $\text{Na}_2\text{HPO}_4$ , 4g of NaCl, 0.19g of KCl, 1.5g of Tris, and 1.5 ml of 0.05% phenol red to 500 ml of distilled water. The pH of the mixture was adjusted to 7.7 by

addition of 0.93 ml of HCl at room temperature. Sterilised trypsin solution was used to make 50 ml of stock solution of 0.25% w/v and stored at -20°C.

#### **2.1.1.4 Mephedrone preparation**

Mephedrone hydrochloride was donated by Dr Oliver Sutcliffe from Manchester Metropolitan University, (4.43 mg) was dissolved in 2% (v/v) acetic acid (0.5 ml) to give 50 mM stock solution of mephedrone, and then diluted in media to obtain the other concentrations. The mephedrone stock solution was stored at -20 °C until the experiments were performed.

#### **2.1.1.5 Cobalt preparation**

5.95 mg of cobalt chloride salt was weighed and dissolved in 5 ml of distilled water to achieve a stock solution with concentration of 5 mM. The solution was then filtered with a 0.04 mm filter to sterilise it. The required concentrations of cobalt were made by the dilution of the stock solution in suitable media.

#### **2.1.2 Cell lines and primary cells**

Human astrocytoma (U373), neuroblastoma (SH-SY5Y), and hepatoma (HepG2) cells were purchased from the European Collection of Cell Cultures (catalogues number 08061901, 94030304, 85011430, respectively). Sprague-Dawley rat liver cells were prepared by Mrs Catherine Henderson under UK Home Office licence. Rats were in bred by the biological procedures unit, University of Strathclyde and we used Sprague-Dawley male rats 200-250 g weight. The work was approved by the University of Strathclyde ethical committee and Animal Welfare and Ethical Review Body (AWERB) and Home Office licence PPL60/4341 is held by Professor M. Helen Grant. Procedure was performed in accordance with Animal Research:

Reporting of In Vivo Experiments (ARRIVE) guidelines and the US National Institute of Health (NIH Publication No. 85-23, revised 1996).

#### **2.1.2.1 Culture of SH-SY5Y and U373 as monolayer cell culture**

Cell lines (SH-SY5Y, U373 and HepG2) were seeded at  $5 \times 10^4$  cells/well in 1 ml media in 24-well plates for metabolism and metabolomics analysis, and in 200  $\mu$ l of medium in a 96-well plate for MTT, NR and LDH assays.

#### **2.1.2.2 Culture of primary rat hepatocyte as monolayer cell culture**

##### 2.1.2.2.1 Isolation of primary rat hepatocytes

Freshly isolated rat hepatocytes were prepared by collagenase perfusion of the livers of male Sprague-Dawley rats by Catherine Henderson (Home Office licence procedure- licence number 60/4341). Primary hepatocytes were isolated from rat liver by collagenase perfusion.

##### 2.1.2.2.2 Method of preparation cell culture and mephedrone treatment

Three 24-well plates were collagen coated with 25- $\mu$ g collagen/cm<sup>2</sup> and stored at – 4°C, 24 hours prior to seeding of cells. Collagen was prepared in-house by acid extraction of rat tail tendons. Hepatocytes were seeded at  $3 \times 10^5$  viable cells/well and incubated at 37°C in 5% CO<sub>2</sub> air. 100  $\mu$ M of mephedrone in medium was added (after 24 hours of seeding the wells) for one row of 6 wells in each plate leaving one row for control (medium without mephedrone on cells). Cell extraction was

performed according to the in-house method (see section 2.1.2.2.3 below) after 6, 24, and 48 hours. Cell extracts were frozen at -80°C until analysed by LC-MS.

#### 2.1.2.2.3 Extraction of cell lysates for metabolomics

Medium was removed from wells and the cells were washed with 0.5 mL of pre-warmed PBS (37°C) twice. A 200 µL volume of pre-cooled extraction solution (50% of methanol, 30% of acetonitrile and 20% water) was added to each well to lyse cells. Cells were scraped off using a small metallic spatula. The extracted cell solution was transferred to 0.5 mL Eppendorf vials. Samples were then shaken at 4°C for 12 minutes. Samples were centrifuged at 0°C and 13000 rpm for 10 minutes. The supernatant was transferred into glass vials and stored at -80°C until analysed with LC-MS.

## 2.2 MTT, NR, LDH and morphology assays

### 2.2.1 Neutral red (NR) assay

The method was obtained from a previously published method (Inoue *et al.*, 2001). NR is a xanthine dye that has the ability to stain lysosomes in live cells. Ability of cells to absorb neutral red will decrease when they start to die. Medium was removed when the incubation with mephedrone was finished, and 100 µl NR solution (0.05 mg/ml of phosphate buffer saline (PBS)) added to each well of a 96-well plate. The plate was incubated at 37° C under 5% CO<sub>2</sub> air for 3 hours. The solution was removed after incubation and wells were washed with 200 µl of PBS. 100 µl destain (mixture of 50 mL of ethanol, 1 mL of glacial acetic acid and 49 mL of distilled

H<sub>2</sub>O) was added to each well and the plate left on the shaker for 30 minutes. The absorbance was then measured at 540 nm by plate reader spectrophotometer (Multiskan GO, Thermo Scientific). NR assay was performed for mephedrone as there was no decrease in the metabolic activity of cells using MTT assay imposing the requirement of an alternative viable assay to confirm the non significant alteration in the viability results. In case of cobalt there was no need for doing other viability assays as MTT have induced significant change in treated samples compared to the relevant controls.

### **2.2.2 Dimethylthiazolyl diphenyltetrazolium bromide (MTT) assay**

3-(4,5-dimethylthiazol-2-yl)-2,5-diphenyltetrazolium bromide (MTT) assay was carried out following the procedure on (Borenfreund and Puerner, 1985). MTT assay is based on the ability of NADPH dependent cellular oxidoreductase enzymes present in the viable cells to reduce the tetrazolium dye (MTT) to formazan (insoluble purple compound). 10 mM of MTT solution was prepared in PBS and filtered through a 0.2 µM filter. A 50 µl volume of the solution was added to each well when the incubation was complete. A 96-well plate was incubated at 37° C in presence of 5% CO<sub>2</sub> air for 4 hours. MTT solution was removed after incubation and 200 µl of DMSO was added to each well. The solution in each well was mixed to give an even colour, and transferred to a 1 ml cuvette. Absorbance was measured at 540 nm by plate reader spectrophotometer (Multiskan GO, Thermo Scientific).

### **2.2.3 Lactate dehydrogenase (LDH) assay**

Lactate dehydrogenase (LDH) assay is based on the ability of LDH to reduce nicotinamide adenine dinucleotide (NAD) to NADH. NADH will reduce the tetrazolium salt 2-(4-iodophenyl)-3-(4-nitrophenyl)-5-phenyl-2H-tetrazolium (INT) to red formazan. Two solutions were prepared. First, to prepare 0.1 M sodium phosphate buffer (NaPi buffer at pH 7.6) we prepared two solutions, Na<sub>2</sub>HPO<sub>4</sub> (14.2 g) was weighed and dissolved in 500 mL of distilled H<sub>2</sub>O to prepare 0.2 M of Na<sub>2</sub>HPO<sub>4</sub>. Another solution was prepared by dissolving 2.4 grams of NaH<sub>2</sub>PO<sub>4</sub> in 100 mL of distilled H<sub>2</sub>O. These two solutions were mixed to give a sodium phosphate buffer, 0.1 M at pH 7.6 (Napi buffer). The second solution was a mixture of 3 mg pyruvic acid and 3 mg of NADH dissolved in 1 mL of NaPi buffer. This was prepared immediately before use due to the low stability of the mixture. For each well measurement, 0.86 mL of 0.1 M sodium phosphate buffer (pH 7.6) and 40 µl of pyruvic acid (3mg in 1ml NaPi buffer)/NADH solution were added to a cuvette (1 ml). Then 100 µl of medium from each well was added. The change in absorbance was recorded at 340 nm by a UV-spectrophotometer (UV-2401PC, Shimadzu) over 60 seconds at room temperature.

### **2.2.4 Morphology**

Cells were imaged after 6 days incubation with and without 100 µM of mephedrone by using a Motic AE31 microscope-20 power dry lenses. Images were stored on a secured USB and on Strathcloud.

### **2.3 Reactive oxygen species (ROS)**

Measurement of ROS activity in cell culture in 24-well plates, was performed by the use of carboxy-H<sub>2</sub>DCFDA dye (Invitrogen, UK C400, Lot number 28351W) as described in a previous study (Mosmann, 1988). Cells were seeded at 5x10<sup>4</sup> cells/ml and incubated at 37°C and 5% CO<sub>2</sub>/air for two days. The cells were then treated with a range of cobalt concentrations (0, 100, 150 and 200 μM) for two periods of time (4 and 24 hours). Then the medium was removed from all wells, and the cells were washed twice with DPBS to remove any traces of media from the wells. Addition of at 200 μl of carboxy-H<sub>2</sub>DCFDA at 25 μM in DPBS followed the washing step. The culture was incubated in the dark at 37°C and 5% CO<sub>2</sub> air for 30 minutes. Cells were washed twice with DPBS after incubation. Cells were examined by microscope (ZOE Fluorescent Cell Imager, BIO RAD, Singapore) and pictures were taken immediately. Finally, triton X-100 (1 ml at 0.1% (v/v)) was added to the wells and they were incubated in the dark for 20 minutes at room temperature. Measurement of the fluorescence was immediately undertaken by a spectrofluorophotometer (RF-5001PC, Shimadzu) at 495nm excitation wavelength and 525 nm emission wavelength in a 1 ml cuvette.

Choice of the concentration range was made to cover the array of concentrations below the LD<sub>50</sub>. The range is far above the clinical level of the compounds as they both only cause toxicity after chronic exposure and will only show an observe effect at higher concentrations. ROS measurement was performed for cobalt treated cells only as there was no previous study that measured ROS in these cell lines. In

contrast, previous work exists for mephedrone ROS production in SH-SY5Y and U-373 cells (den Hollander *et al.*, 2014).

## **2.4 Lowry and western blotting**

### **2.4.1 Sample preparation**

Cells were grown in 25-cm<sup>2</sup> flasks. When cells were ready, the medium was removed and cells were washed twice with DPBS. Following the washing step, 300  $\mu$ l of 0.1 M cold sodium phosphate buffer at pH 7.6 was added to the cells and cells were scraped off by using a cell scraper and transferred to Potter-Elvehjem glass homogeniser tube to be homogenised with seven strokes of a Black and Decker electric drill. The homogenised solution was aliquoted into 50  $\mu$ l aliquots for protein measurement (Lowry) and Western blotting assays.

### **2.4.2 Total protein measurement (Lowry assay)**

All steps were performed according to the method explained by Lowry *et al.*, 1951. The required solutions were as follows.

- a) 0.5 M NaOH.
- b) 1% (v/w) CuSO<sub>4</sub>.
- c) 2% (v/w) NaKtartrate.
- d) 2% (v/w) Na<sub>2</sub>CO<sub>3</sub>.
- e) Folin's (Ciocaltau) reagent (Sigma-Aldrich, USA, Lot number BCBK8133V).

- f) 200  $\mu\text{g/ml}$  of bovine serum albumin (BSA) in 0.5 M of NaOH stored in - 20°C.

The assay was conducted as explained in the following steps. First, solutions A and B were prepared immediately before use. To prepare solution A, 98 ml of  $\text{Na}_2\text{CO}_3$  was added to 1ml of 1%  $\text{CuSO}_4$  and 1ml of 2% NaKtartrate. For solution B, 2 ml of Folins reagent was diluted in 6 ml of d. $\text{H}_2\text{O}$ .

Secondly, the standards were prepared as shown in the following table.

**Table 2. 1 Volumes and materials used to prepare the standards for protein determination.**

Solution	Std-1 (0) $\mu\text{g/ml}$	Std-2 (25) $\mu\text{g/ml}$	Std-3 (50) $\mu\text{g/ml}$	Std-4 (100) $\mu\text{g/ml}$	Std-5 (150) $\mu\text{g/ml}$	Std-6 (200) $\mu\text{g/ml}$
BSA(ml)	0	0.125	0.250	0.500	0.750	1
0.5 M NaOH (ml)	1	0.875	0.750	0.500	0.250	0

After preparation of the standards, 50  $\mu\text{l}$  of each sample was diluted in 950  $\mu\text{l}$  of 0.5 M of NaOH. Later, 5 ml of solution A was added to all standards and samples, then mixed and left for 10 minutes in room temperature. Finally, 0.5 ml of solution B was then added to all standards and the samples and left for 60 minutes before reading the absorbance at 725 nm wavelength against a water blank.

### 2.4.3 Western blotting (WB)

#### 2.4.3.1 Calculations of required volumes for WB

The required volume of Laemli buffer to be added to the sample was calculated using the following equation:

**Equation 2. 1 Equation used to calculate the required volume of Laemli buffer.**

$$C_1V_1=C_2V_2$$

$C_1$  is the concentration of protein obtained from the results of Lowry.  $V_1$  is the sample volume (50  $\mu$ l).  $C_2$  is the desired concentration of protein to be loaded onto the gel, which is in this experiment 1 mg/ml.  $V_2$  is the total volume of the sample and buffer (50  $\mu$ l of sample + Laemli buffer volume). After addition of the calculated volumes, samples inside the lock-tight Eppendorf vials were boiled in hot water for a minute to denature the proteins.

#### 2.4.3.2 Preparation of gel solutions

The stacking and separating buffers were prepared according to the following table.

**Table 2. 2 Stacking and separating gel buffers composition.**

	<b>Stacking gel 0.5 M Tris buffer</b>	<b>Separating gel 1.5 M Tris buffer</b>
<b>Tris</b>	6 g	36.33 g
<b>D.H<sub>2</sub>O</b>	40 ml	–
<b>1M HCl</b>	48 ml	48 ml
<b>pH</b>	6.8	8.8
<b>Final volume</b>	Make up with d.H <sub>2</sub> O to 100 ml	Make up with d.H <sub>2</sub> O to 200 ml

### **2.4.3.3 Preparation of solutions for making gels**

The following solutions were prepared for use to perform the procedure mentioned in section 2.4.3.5.

- a) Laemli buffer (Sigma-Aldrich, USA, Lot number 110M6040)
- b) 10xTris/Glycine/sodium dodecyl sulfate (SDS) buffer (Sigma-Aldrich, USA, Lot number SLBS1582V), which is used to prepare x1 Tris/Glycine/SDS buffer (running buffer) by diluting it in d.H<sub>2</sub>O by a 1:10 dilution factor.
- c) 40% Acrylamide/bis-acrylamide (Sigma-Aldrich, USA, Lot number SLBN8928V).
- d) 1.5% Ammonium persulphate (APS) (Sigma-Aldrich, USA, Lot number MKBV2007V) was made by addition of 1.5 g in 100 ml of d.H<sub>2</sub>O and the solution was stored at -20°C.
- e) Tetramethylethylenediamine (TEMED) (Sigma-Aldrich, USA, BCBQ5821V).

### **2.4.3.4 Making the gels**

The glass sheets were cleaned with 70% ethanol, and were set in the apparatus. They were tested for leaking after assembly. The gels were made according to the following table.

**Table 2. 3 Stacking and resolving gels composition.**

<b>Solutions</b>	<b>4% Stacking gel</b>	<b>10% Resolving gel</b>
<b>40% Acrylamide/bis acr</b>	1 ml	3.75 ml
<b>Stacking gel buffer</b>	2.5 ml	–
<b>Resolving gel buffer</b>	–	3.75 ml
<b>1.5% APS*</b>	0.5 ml	0.75 ml
<b>D.H<sub>2</sub>O</b>	6 ml	6.75 ml
<b>TEMED*</b>	10 $\mu$ l	11.7 $\mu$ l

\*These two ingredients were only added immediately before pouring the gel solution into the set. APS= ammonium persulfate; TEMED= Tetramethylethylenediamine.

#### **2.4.3.5 Procedure steps**

The resolving gel was poured first with addition of a small layer of d.H<sub>2</sub>O added on top to protect the gel from dehydration. After the resolving gel was set, the water layer was removed, the stacking gel poured and the comb inserted. Later, the running buffer was poured inside and outside the tank to the mark. 10  $\mu$ l of each sample and a marker protein standard (Novex<sup>®</sup> Sharp Pre-Stained protein standard, Invitrogen) were loaded in the wells after the stacking gel was set, and the combs removed. The current was started at 32 mAmps and maximum voltage for 15 minutes, and then the voltage was changed to 150 volts and maximum current while the samples bands migrated towards the bottom of the gel. The buffer for transferring the bands in the gel to a membrane was prepared as shown in the following table.

**Table 2. 4 Transfer buffer composition.**

<b>Solution</b>	<b>Transfer buffer</b>
<b>D.H<sub>2</sub>O</b>	1400 ml
<b>Methanol</b>	400 ml
<b>10x Tris/Glycine buffer</b>	200 ml

In addition, the cassette sandwiches were prepared as follows. First, the filter papers and Scotch brite pads were washed with transfer buffer. Gels were put into transfer buffer for 10 minutes. The membranes were soaked in methanol until needed. The sandwich was prepared according to the order in the following diagram.

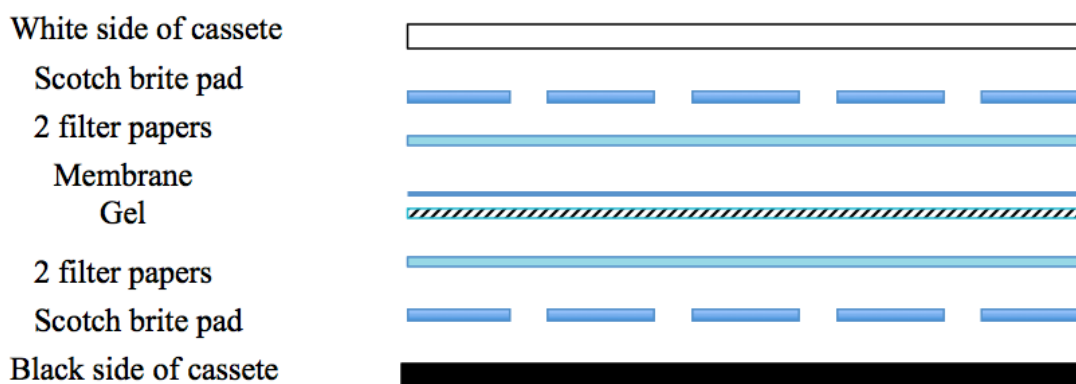


**Figure 2. 1 Order of layers for making the gel/filter sandwich.**

When the cassette was assembled, it was placed in the transfer chamber (Fisherbrand, UK, Model number EB10) and filled with transfer buffer. The current was set to 200 mAmps and voltage to 999 volts and the system run overnight.

Tris buffer saline (TBS) x10 was prepared meanwhile, by adding 24.22 g of 200 mM of Tris and 292.2 g of 5 M NaCl to 1 Litre of d.H<sub>2</sub>O . It was then diluted x10 in

d.H<sub>2</sub>O and the pH was adjusted to 7.4. Tween 20/TBS (TTBS) was prepared by addition of 0.5 ml of Tween 20 to 1 Litre of TBS and adjustment to pH 7.4.

For blocking of proteins, 3% fish gelatine/TTBS was prepared by adding 3 ml of fish gelatine in 42 ml TTBS. For antibody dilution, 1% fish gelatine/TTBS was prepared by diluting 1 ml of fish gelatine in 44 ml of TTBS.

After the cassette was run overnight, the membranes were removed and shaken in 3% fish gelatine/TTBS for 1 hour at 37°C to block other proteins. Later, membranes were removed and washed three times with TTBS for 5 minutes each at room temperature. After washing, 20 µl of the primary antibody of interest was added to 20 ml of 1% of fish gelatine, and the membranes shaken in the solution for 1 hour at 37°C. The membranes were then removed and washed with TTBS three times. After this the membrane was shaken in the secondary antibody solution (2 µl of Ab2 in 20 ml of 1% fish gelatine) at 37°C for 1 hour. The membranes were then washed and shaken twice with TTBS at room temperature for 5 minutes each wash. A third wash was performed in TBS under the same conditions.

Meanwhile, the developing solution was prepared freshly by adding 0.4 ml of each of reagent A and reagent B (AP color reagents, Bio-RAD) to 39.2 ml of developing buffer (Bio-Rad laboratories, USA, Lot number L9701067). The membranes then were soaked and shaken in developing solution for 5 to 10 minutes at room temperature. The membranes were washed by distilled H<sub>2</sub>O, dried, scanned and

stored in between filter papers. GAPDH was used as the control house keeping protein. Pictures were scanned immediately using a Canon scanner (Canon INC, 2009) and stored on a secured USB device. Results were processed using ImageJ software (National Intitute of Health, USA, 2009) to generate peak area from each band and then processed with Excel software (Microsoft, US, 2011).

Antibodies used for detection against target protein are anti-UNG antibody (EPR4371) ab109214, anti-TDG antibody (EPR8774) ab154192, anti-Ogg1 antibody ab135940 from Abcam.com and anti-DNMT1 antibody (VMA00245) from Bio-Rad.com.

## **2.5 DNA and RNA isolation**

DNA and RNA were isolated from U-373 and SH-SY5Y cells according to the procedures in the isolation kit Illustra triplePrep kit (GE Healthcare, UK) for nuclear DNA and total RNA isolation. Cells were grown in 25 cm flasks at  $5 \times 10^4$  seeding density in three replicates for each cobalt concentration and controls. Flasks were left overnight to allow cells to attach to the flask surface. Cobalt at 0, 100, 150 and 200  $\mu\text{M}$  concentrations in medium was added to the cells after removing the old medium. Then the flasks were incubated at  $37^\circ\text{C}$  and 5%  $\text{CO}_2$  air for 72 hours. Flasks were washed with cold DPBS. The cells in the control flasks were treated with 1 ml of lysis buffer (containing 3.5  $\mu\text{l}$  2-mercaptoethanol) from the Illustra triplePrep kit. The other cobalt treated cells were treated with lower volumes of lysis buffer in

accordance with cell loss detected by cell count relative to control samples to avoid dilution of DNA and RNA. The volume was calculated using the following equation.

**Equation 2. 2 Equation of the volume of lysis buffer.**

Volume of lysis buffer added= (MTT result of sample/MTT result of control) x 1 mL

The flasks were agitated until they gave a cloudy solution. Lysates were transferred to Eppendorf tubes to either continue the extraction, or stored at -80°C until ready to extract the nucleic acids. Each lysate was used to isolate DNA and RNA using the procedure of in the Illustra triplePrep kit. Both isolated nucleic acids were stored at -80°C.

## **2.6 DNA digestion**

Isolated DNA samples (20 µg) were incubated overnight in a hydrolysis solution (50 µl) that consisted of 100 mM NaCl, 20 mM Tris pH 7.9, 20 mM MgCl<sub>2</sub>, 80 U/ml alkaline phosphatase, 600 mU/ml phosphodiesterase, 1000 U/ml benzonase, 36 µg/ml EHNA hydrochloride and 2.7 mM deferoxamine. The hydrolysed solution was diluted in acetonitrile by 1:4 dilution factor.

## **2.7 Metabolomics and Metabolism**

Analysis for metabolomics was carried out by Liquid chromatography–mass spectrometry (LC–MS) technology using a Thermo Exactive Orbitrap instrument

(Thermo-Fisher Corporation, Hemel Hempstead, UK) as described in previous research (Kamleh et al, 2009). Detection of negative and positive ions was used in sample analysis. The scanned mass range was 75–1200 m/z. The temperature of the capillary was 250°C, and +4.0 kV spray voltage was used in positive ion and -4.0 kV in negative ion, sheath gas flow was 50 auxiliary gas flow was 17 (arbitrary units). The UltiMate 3000 LC–MS system was run by using Xcalibur Ver. 2.2 (Thermo-Fisher Corporation, Hemel Hempstead, UK). The HPLC method used a binary gradient with an injection volume of 10  $\mu$ L. Solvent A was acetonitrile and solvent B was ammonium carbonate 20 mM; the flow rate was 0.3 mL min<sup>-1</sup>. The column used was a ZIC<sup>®</sup>-pHILIC (150 mm  $\times$  4.6 mm i.d., particle size: 5 $\mu$ m) and was fitted with ZIC<sup>®</sup>-pHILIC guard column (HiChrom Limited, Reading, UK) at room temperature. The gradient program was as shown in table 2.5. Data processing was carried out using Mzmine 2.21 (Pluskal et al, 2010), SIMCA-P software v.14.1 (Umetrics AB, Umeå, Sweden) and Excel (Microsoft, US) software. Compounds were identified to MSI level 2 (matching of elemental composition to an accurate mass to <3 ppm- also considering likely retention times e.g. lipids and fatty acids would not be expected to strongly retain on the ZICpHILIC column) or MSI level 1. Accurate mass plus matching to retention times (to within  $\pm$  0.3 min) of authentic standards run on the ZICpHILIC column (Table 1 appendix 1) (Sumner et al, 2007). Normalisation was not performed during analysis as the cells were counted and the metabolites were normalised by adding equal volume of extraction solution for the same cell number. Positive and negative ion data sets were combined using an in house programmed excel file (examples of negative and positive total ion chromatograms shown in Appendix 1 Figures 1 and 2). Databases used for the

identification of metabolites were KEGG, Hmdb, Metlin and Lipid maps. Multivariate analysis was carried using pareto scaling. The authentic standards were purchased from Sigma Aldrich Chemical Co., Dorset, UK.

**Table 2.5 Gradient program for analysis of each sample showing percentages of A and B mobile phases during the time of the analysis.**

<b>Time (minutes)</b>	<b>A%</b>	<b>B%</b>
0-30	20	80
30-31	80	20
31-37	92	8
37-38	92	8
38-46	20	80
46	20	80

## **2.8 Quantitative Real-time PCR (qRT-PCR)**

### **2.8.1 Materials**

RNA and DNA integrity and quantity were assessed by using a Nanodrop 2000 spectrophotometer (Thermo Scientific, US) before analysis. The complementary DNA (cDNA) was synthesised of 4  $\mu\text{g}$  of RNA by the use of Tetro cDNA Synthesis kit (Bioline Reagents, UK) and Random Hexamer (500  $\text{ng}/\mu\text{L}$ , Bioline Reagents, UK) following the procedure in table 2.7.

## 2.8.2 Method

Oligonucleotide primers shown in table 2.6 were used for the chosen genes. A PowerUp<sup>TM</sup> SYBR<sup>TM</sup> Green Master Mix (Thermo Fisher Scientific, US) and a StepOnePlus<sup>TM</sup> RT-PCR system (Applied Biosystems; UK) were used. Primers were designed by the use of National Center for Biotechnology Information website (Kamleh *et al.*, 2009). The design aimed to yield a length of 100-150 bp amplicon to cover the exons to avoid any amplification of genomic DNA. The designed primers are illustrated in table 2.6.

**Table 2. 6 Primer sets (forward and reverse) designed and used for genes quantification in RT-PCR experiment.**

Gene		Primer sequences (5'->3')	Tm	Amplicon size (bp)
<b>SERT2</b>	Forward	GAA GGT GCA GGA GGC TCA G	60.08	149
	Reverse	CCA AGG TCA GCT CGT CCA G	60.08	
<b>UNG</b>	Forward	ACC TGG ACC CAG ATG TGT GA	60.47	144
	Reverse	ATA AAT GTT CTC CAA ACT GGG CG	59.56	
<b>TDG</b>	Forward	CAT TGT CAT TAT TGG CAT AAA CCC G	59.31	150
	Reverse	CCT GGT AGA GTG TGA TCA TCC AT	59.35	
<b>MLH1</b>	Forward	TTT CGA GGT GAG GCT TTG GC	60.89	149
	Reverse	GTC CCT TGA TTG CCA GCA CA	60.90	
<b>MECP2</b>	Forward	TGA TCA ATC CCC AGG GAA AAG C	60.62	150
	Reverse	TAG GTG GTT TCT GCT CTC GC	59.75	
<b>RPL13A</b>	Forward	ACC TCC TCC TTT TCC AAG CG	59.96	141
	Reverse	GCG TAC GAC CAC CAC CTT C	60.74	
<b>HPRT1</b>	Forward	CTG GAA AGA ATG TCT TGA TTG TGG A	59.53	135
	Reverse	TTC GTG GGG TCC TTT TCA CC	60.18	
<b>B2M</b>	Forward	GTG CTC GCG CTA CTC TCT C	60.30	136
	Reverse	CGG ATG GAT GAA ACC CAG ACA	60.07	

Each sample was run in triplicate for each primer set. First the complementary DNA (cDNA) was synthesised from the RNA by the use of a Tetro cDNA synthesis kit according to the following procedure. Concentration of RNA in each sample was measured by the use of Nanodrop 2000 spectrophotometer (Figures 1 and 2 appendix 2). According to the concentration of the RNA in the sample, 12  $\mu\text{L}$  of sample and RNase free water were prepared to contain 150 ng/ $\mu\text{L}$  of each sample. The remaining 8  $\mu\text{L}$  contained the solutions from the Tetro cDNA Synthesis Kit as shown in table 2.7.

**Table 2. 7 Components of the 8- $\mu\text{L}$  solution mixture to be added to the sample. \*For the RT (-) samples we add 1  $\mu\text{L}$  of Rnase free DEPC-treated water.**

Solution	Volume ( $\mu\text{L}$ )
Primer (Random Hexamer)	1
10 mM dNTP mix	1
5x RT Buffer	4
RiboSafe Rnase Inhibitor	1
Tetro Reverse Transcriptase (200u/ $\mu\text{L}$ )-only into RT (+) samples*	1

Samples were mixed by pipetting after the addition of all solutions. Samples were placed in the DNA Thermal Cycler 480 (Perkin Elmer, US) at 25°C for 10 minutes, then at 45°C for 30 minutes, then at 85°C for 5 minutes. Samples were stored at -20°C until RT-PCR was carried out.

When it was time to conduct the analysis, samples were centrifuged and diluted with a 1 in 5 dilution factor. A MicroAmp® Fast 96-well reaction plate (0.1 mL) and

MicroAmp™ Optical Adhesive Film Kit (Life technologies, US) were used to carry out the reaction steps. For each sample there were two negative controls. One contained water instead of the cDNA sample, and the second contained cDNA but without the reverse transcriptase enzyme. Each sample was run in triplicate and contained the solutions shown in table 2.8.

**Table 2.8 Contents of each sample in the RT-PCR reaction.**

<b>Solution</b>	<b>Volume (μL)</b>
<b>Forward Primer (10 pmol/ml)</b>	1
<b>Reverse Primer (10 pmol/ml)</b>	1
<b>Power Up 2x Master Mix</b>	10
<b>cDNA</b>	1
<b>H<sub>2</sub>O</b>	7

After the addition of all solutions, the plate was sealed by a MicroAmp™ Optical Adhesive Film.

The RT-PCR reactions were run in the fast cycling mode under the conditions in the following table using StepOnePlus™ RT-PCR Instrument and software.

**Table 2.9 Conditions of the RT-PCR experiment.**

<b>Step</b>	<b>Temperature</b>	<b>Duration</b>	<b>Cycles</b>
<b>UDG activation</b>	50°C	2 minutes	Hold
<b>Dual-Lock™ DNA polymerase</b>	95°C	2 minutes	
<b>Denature</b>	95°C	3 seconds	40
<b>Anneal/extend</b>	60°C	30 seconds	

The data was generated as an Excel file from the instrument and stored on an encrypted USB storage device. The data generated were presented as  $C_T$  values. The fold change was calculated according to the following equations.

**Equation 2. 3 Equation of delta threshold cycle of the control sample.**

Control (target gene)  $\Delta C_T$  = mean target gene  $C_T$  for control – mean reference gene  $C_T$  for control

**Equation 2. 4 Equation of delta threshold cycle of the treated sample.**

Treatment X (target gene)  $\Delta C_T$  = mean target gene  $C_T$  for treatment X – mean reference gene  $C_T$  for treatment X

**Equation 2. 5 Equation of delta-delta threshold cycle of the treated sample.**

$\Delta\Delta C_T$  for target gene at treatment X = Treatment X (target gene)  $\Delta C_T$  - Control (target gene)  $\Delta C_T$

**Equation 2. 6 Equation for fold change for treated sample.**

Fold change for treatment X =  $2^{-\Delta\Delta C_T}$  for target gene at treatment X

## 2.9 Statistical methods

For MTT and NR results the mean of 6 replicates and n=3 experiments were calculated by addition of the all absorbance values and divide them by the number of replicates (6). The percentage mean was then calculated for each concentration by dividing the mean of the concentration by the mean of the control and multiply the results by 100. Standard deviation was calculated for each concentration using the following equation.

$$SD = \sqrt{\frac{\sum_{i=1}^N (x_i - \bar{x})^2}{N-1}}$$

For the metabolomic analysis the p values were calculated performing T test in excel according to the following equation.

T test for metabolite x = (average of peak areas of metabolite x in treated samples, average of peak areas of metabolite x in control samples, 2, 3).

Results were analysed by One-way analysis of variance (ANOVA) and Tukey's post hoc honestly significant difference test.

**Chapter 3 THE EFFECT OF COBALT  
ON HUMAN NEUROBLASTOMA  
AND ASTROCYTOMA**

---

### **3.1 Abstract**

The discovery of adverse effects accompanying the release of cobalt ions from metal-on-metal (MoM) hip implants has caused alarm about the systemic complications of cobalt. An increase in circulating cobalt ions resulting from MoM articulations could trigger acute pathological complications (Carvalho and Moreira, 2018). There appear to be a number of important risk factors, both in terms of the implant and the patient, associated with the risk of systemic cobalt toxicity (Ikeda *et al.*, 2010; Munichor *et al.*, 2003).

In the current study, neuroblastoma and astrocytoma cells were treated with a range of cobalt concentrations for different periods in order to investigate the effects of cobalt on the metabolism of human neuronal-derived cells. Proliferative methods combined with western blotting, metabolomics, and real-time PCR were applied in the investigation. Results provided tentative proof of DNA deamination, DNA methylation and glutathione oxidation. It is believed that oxidative stress is the main effect that triggers changes in the other pathways.

## **3.2 Introduction**

### **3.2.1 Cobalt**

Cobalt is a heavy metal that has been widely used in several industries such as manufacture of super alloys, magnets, catalysts, and more recently in the battery industry (lithium-ion cells) (Wroblewski *et al.*, 2004). People who work in such industries are all at risk of high exposure to cobalt. Cobalt is also a vital element for the human body, as it is needed to produce hydroxycobalamin (vitamin B12), which is in fact acquired from the diet. Even though cobalt is important for the body, it is classified as carcinogenic, genotoxic and mutagenic at higher concentrations (Zeng *et al.*, 2015). The normal level of cobalt in human serum was determined to be between 0.33 and 0.4  $\mu\text{g/L}$  using neutron activation analysis (Beyersmann and Hartwig, 1992; Hartwig, 1995). The effects of cobalt were detailed in section 1.1.4 chapter 1.

### **3.2.2 Oxidative stress**

Oxidative stress results from disturbing the balance between the production of reactive oxygen species (ROS) and the availability of antioxidants in the cells (Frieberg *et al.*, 1979; Michel *et al.*, 1991). ROS include several oxygen metabolites such as hydroxyl radicals ( $\text{OH}^{\bullet}$ ), hydrogen peroxide ( $\text{H}_2\text{O}_2$ ) and superoxide anion ( $\text{O}_2^{\bullet-}$ ) (Halliwell, 2007). They are chemical molecules that have a free electron in their outer orbital making them highly reactive and unstable; thus harmful to the cell

(DNA, proteins and lipids) at high concentrations (Thannickal and Fanburg, 2000). ROS are continuously formed endogenously (as a product of aerobic metabolism or as messengers in signal transduction). They can also be formed by exposure to exogenous drugs, radiation and chemicals (Marks, 2005) and can be eliminated by the effect of antioxidants. Antioxidants are compounds that prevent oxidation. They include non-enzymatic antioxidants (e.g., flavanoids, glutathione and ascorbic acid) and enzymatic antioxidants (e.g., glutathione peroxidase, superoxide dismutases). Glutathione peroxidase is an enzyme that acts by the reduction of lipid hydroperoxides to their alcohol analogues and the reduction of hydrogen peroxide to water (Halliwell, 1991), and it is present at low abundance in brain with lower concentrations in neurons than that in microglia and was undetectable in astrocytes and oligodendrocytes (Bhabak and Mugesh, 2010). Superoxide dismutase is an enzyme that catalyses the disproportionation of the oxygen radical  $O_2^-$  into  $O_2$  or  $H_2O_2$  (Power and Blumbergs, 2009), and it is present in the human brain tissues at low concentrations (36-130 Unit/gram of wet brain weight) (Hayyan *et al.*, 2016). Oxidative stress as a result of extracellular compounds intrusion or inflammatory cells occurs in different tissues and is thought to cause many pathological conditions such as diabetes (Marklund, 1984), neurodegenerative diseases (Asmat *et al.*, 2016) and pulmonary fibrosis (Finkel and Holbrook, 2000).

### **3.2.3 DNA methylation**

Gene expression is controlled by epigenetic alterations such as histone modification, noncoding RNAs (miRNAs), and DNA methylation (Cheresh *et al.*, 2013). DNA methylation involves the addition of a methyl group (CH<sub>3</sub>) mainly at the fifth carbon of cytosine, to form 5-methylcytosine, in the cytosine-guanine pair of the CpG dinucleotide (Goldberg *et al.*, 2007).

### **3.2.2 DNA deamination**

Cytosine, occasionally, can be converted to uracil by hydrolytic deamination (see Figure 3.1). This will leave the guanine, initially bound to that cytosine molecule, attached to uracil (uracil is normally not present in DNA only in RNA). In the next replication of this DNA segment in the cell, the guanine in opposite to that uracil molecule would be replaced by adenine because of the similarity of uracil to thymine, and this will change the encoding message of this section of DNA (see Figure 3.2) (Bird, 2002).

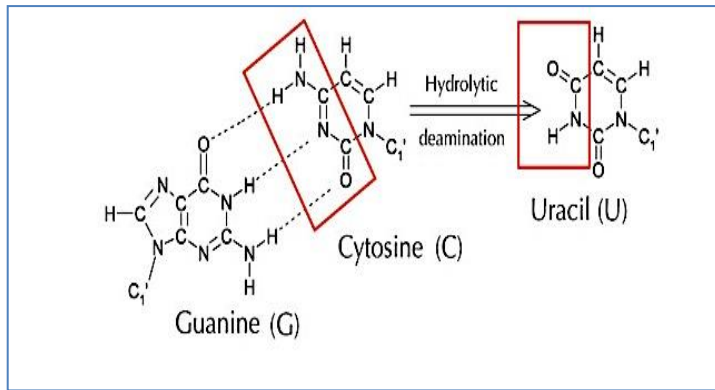


Figure 3. 1 Deamination of Cytosine to Uracil.

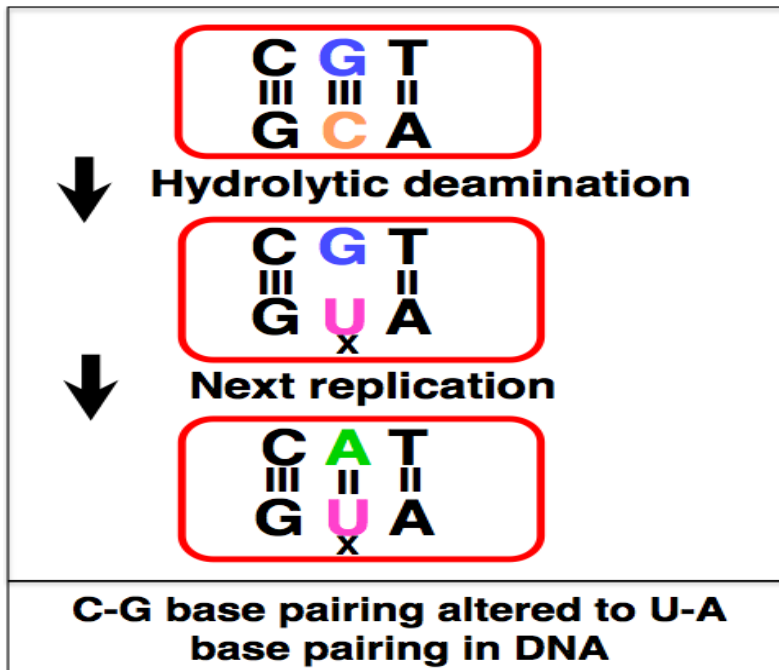
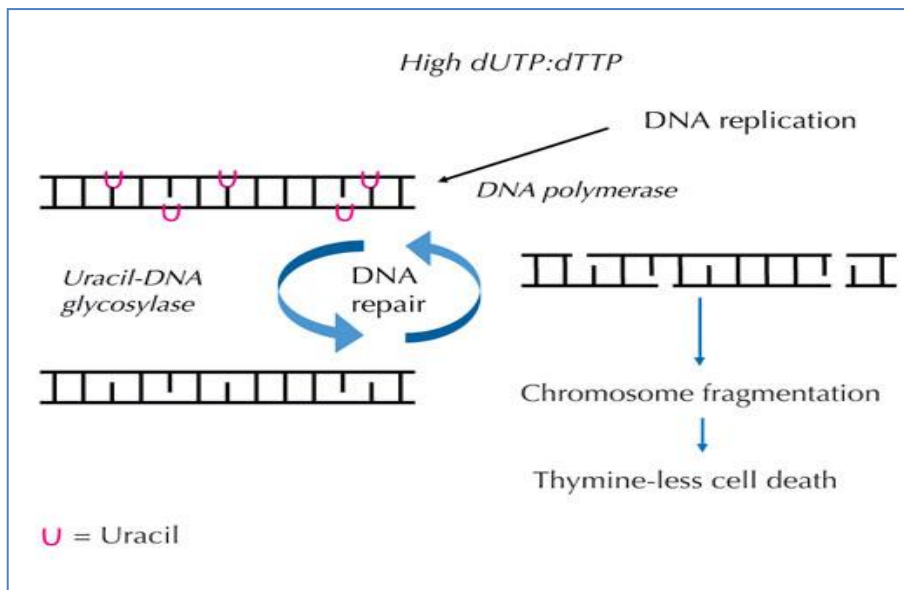


Figure 3. 2 Scheme of the induced change in first and second replication of the deaminated DNA.

Cells have the ability to detect and correct this error before the next replication. There are multiple enzymes involved in this mechanism. Uracil-DNA glycosylases (UNG) is one example of this type of enzymes, it identifies the uracil and removes it from the DNA. Then the other enzymes eliminate and restore the affected part of the DNA, in order to fill the vacant position in the DNA with a newly synthesised cytosine (Kow, 2002).

The aforementioned pathway has a disadvantage of removing both correctly and wrongly situated uracils. Thus, cells have developed another pathway in which a correctly situated uracil (paired with adenine) methylated, converting it to thymine. In this pathway when a uracil is found, it is cut out and fixed, and a methylated uracil (thymine) is added (Krokan *et al.*, 1997).

However, if the ratio of dUTP (deoxyuridine triphosphate – source of uracil) to dTTP (deoxythymidine triphosphate – source of thymine) is raised, more uracil incorporation will be produced by DNA polymerase during the replication and repair processes. Subsequently, uracil-DNA glycosylase will remove uracil residues resulting in breaks in the DNA strand. Additionally, when the repair system introduces uracil, this will lead to an ineffective DNA repair cycle. Finally, at this stage the system will be overloaded and the chromosome will be fragmented, which will eventually cause the death of the cell (see Figure 3.3) (Muha *et al.*, 2009).



**Figure 3. 3 Scheme of the pathway of thymine-less cell death.**

### 3.3 Methods and materials

The materials and methods were described in sections 2.2, 2.3, 2.4, 2.5, 2.6 and 2.7 in Chapter 2.

### 3.4 Results and discussion

#### 3.4.1 Measurement of MTT reduction in neuroblastoma cells in the presence of cobalt

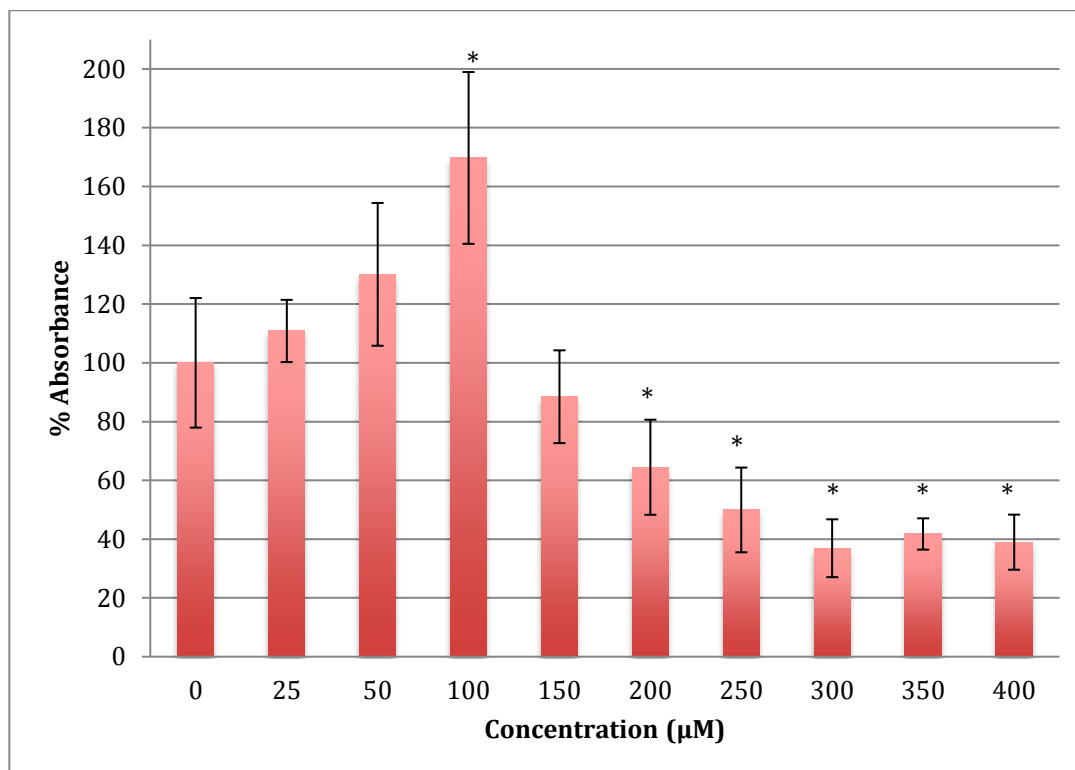


**Figure 3. 4 MTT assay measured in neuroblastoma cells at 24 h. Results are percentage values (Mean  $\pm$  SD, n = 3) where 100% corresponds to control values. SD values correspond to an average of 6 wells plate absorbance reading. Cells treated with cobalt in culture medium throughout the experiment. Data were analysed by One-way ANOVA followed by Tukey test. \* Represents significantly different mean values between treatment and control. P value < 0.05.**

The MTT results showed an increase in the metabolism in SH-SY5Y cells when treated with cobalt at the concentrations 25 and 50 reaching the maximum at 100  $\mu$ M for 24 hours. Beyond this concentration, metabolism fell off with LD<sub>50</sub> being at 254 $\pm$ 17  $\mu$ M of cobalt. The increase in metabolism activity at lower concentrations of cobalt can be explained as a protective response of cells against cobalt as a cytotoxic compound. This effect has been observed several times before in the literature, with

diverse compounds and is referred to as an adaptive response towards cell sensitisation (Békési *et al.*, 2007).

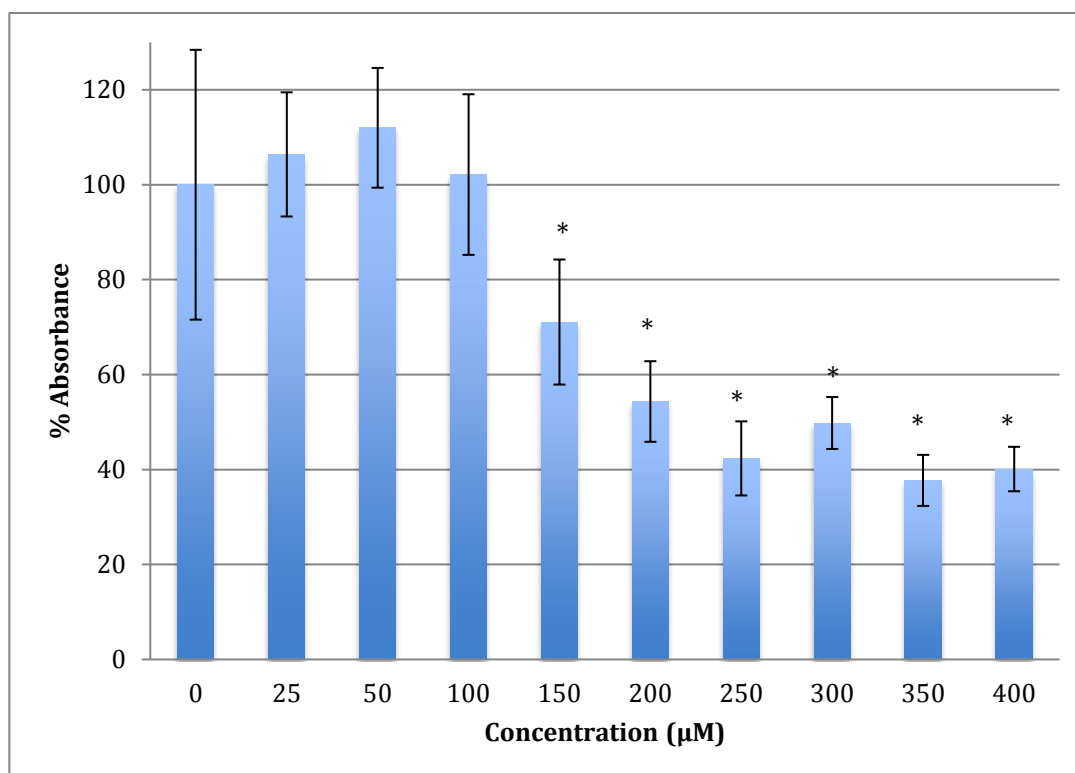


**Figure 3.5 MTT assay measured in neuroblastoma cells at 48 h. Results are percentage values (Mean  $\pm$  SD, n = 3) where 100% corresponds to control values. Cells treated with cobalt in culture medium throughout the experiment. Data were analysed by One-way ANOVA followed by Tukey test. \* Represents significantly different mean values between treatment and control. P value<0.05.**

The time of incubation with cobalt was increased to 48 hours to find out if the effect changed with time. Increasing the time of incubation did change the metabolism, and showed less change in cells treated with lower concentrations of cobalt (25, 50 and 100  $\mu$ M). There were no significant changes in viability between non-treated (control) cells and cells treated with these concentrations. Though, compared to the same concentrations in shorter period of incubation (24 hours) shown in Figure 3.4 there was less increase in metabolism indicating that the cells are on their way to

lower metabolism which is supported by the 72 hours of incubation data (see Figure 3.6). The unchanged metabolism in these low concentrations is also indicator of the ability of the cell to repair and function properly in these concentrations and with this time of incubation (48 hours). However, cells treated with higher concentrations (150-400  $\mu\text{M}$ ) of cobalt showed a significant decrease in viability similar to that seen in the 24 hour incubation. After 48 hours the LD<sub>50</sub> of cobalt was  $220 \pm 15 \mu\text{M}$ . Thus it was proposed that the SH-SY5Y cells could tolerate cobalt treatment up to 100  $\mu\text{M}$  and 48 hours of incubation. Treatment with cobalt at higher concentrations than 100  $\mu\text{M}$  would affect the ability of cells to maintain normal metabolism. The effect of cobalt will be discussed in detail in section 3.4.6.

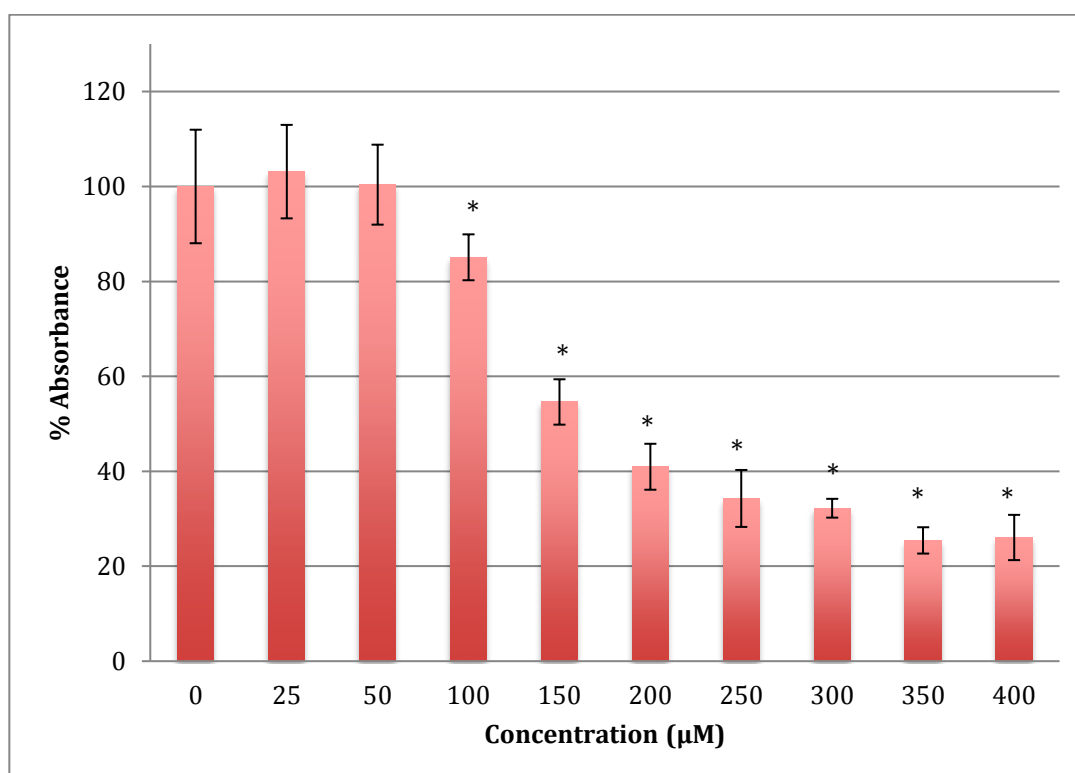


**Figure 3. 6 MTT assay measured in neuroblastoma cells at 72 h. Results are percentage values (Mean  $\pm$  SD, n = 3) where 100% corresponds to control values. Cells treated with cobalt in culture medium throughout the experiment. Data were analysed by One-way ANOVA followed by Tukey test. \* Represents**

**significantly different mean values between treatment and control. P value<0.05.**

After 72 hours of incubation, the cells metabolism could tolerate cobalt treatment only up to 50  $\mu$ M, and the LD<sub>50</sub> of cobalt was 102 $\pm$ 14  $\mu$ M.

It was noteworthy that the SH-SY5Y cells have weakened attachment to the base of the wells, especially at 24 hours and 48 hours. Results showed more differences (higher SD values) between replicates after 24 hours and 48 hours, especially in lower concentrations, compared to the 72 hours of incubations. This can be explained by weaker attachment of these cells in these incubation periods. SH-SY5Y cells are N phenotype neuroblastoma cells which are known to have lower adherence to culture flasks (Zijlstra *et al.*, 2012).

### 3.4.2 Measurement of MTT reduction in astrocytoma cells in the presence of cobalt

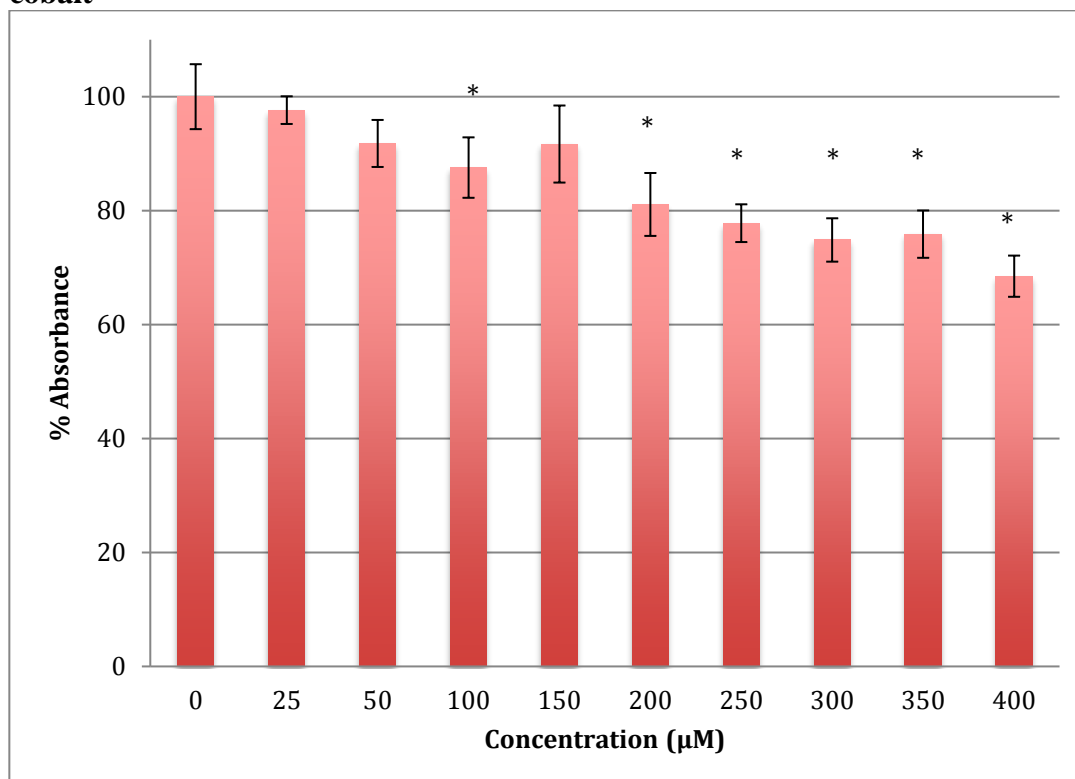


**Figure 3. 7 MTT assay measured in astrocytoma cells at 24 h. Results are percentage values (Mean  $\pm$  SD, n = 3) where 100% corresponds to control values. Cells treated with cobalt in culture medium throughout the experiment. Data were analysed by One-way ANOVA followed by Tukey test. \* Represents significantly different mean values between treatment and control. P value < 0.05.**

The MTT results showed a gradual decrease in the metabolic response of astrocytoma cells when treated with cobalt in a range of 0-400  $\mu\text{M}$  for 24 hours, reaching 68.5% of normal metabolism at the 400  $\mu\text{M}$  cobalt concentration. The calculated  $\text{LD}_{50}$  was  $713 \pm 12$   $\mu\text{M}$  of cobalt. This indicates that cobalt is also a cytotoxic compound to the astrocytoma cells but less so than to SH-SY5Y cells.

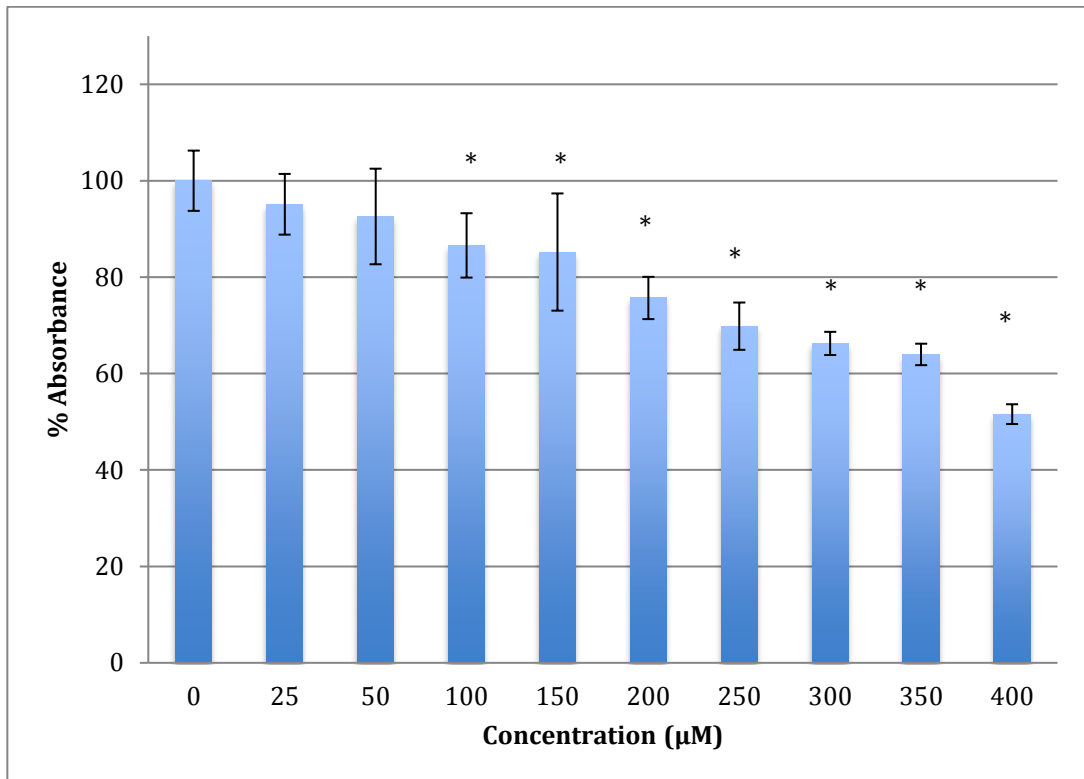


**Figure 3. 8 MTT assay measured in astrocytoma cells at 48 h. Results are percentage values (Mean  $\pm$  SD, n = 3) where 100% corresponds to control values. Cells treated with cobalt in culture medium throughout the experiment. Data were analysed by One-way ANOVA followed by Tukey test. \*Represents significantly different mean values between treatment and control. P value < 0.05.**

After 48 hours of incubation with same range of cobalt concentrations, the degree of decrease was steeper with a lower LD<sub>50</sub> ( $422 \pm 7$  µM of cobalt) than that after a 24 hour incubation. For example, after treatment with 400 µM of cobalt, metabolism of astrocytoma cells maintains only 51.6% viability when compared to non-treated cells. This indicates that cobalt is more harmful to the cells as the incubation period increases.

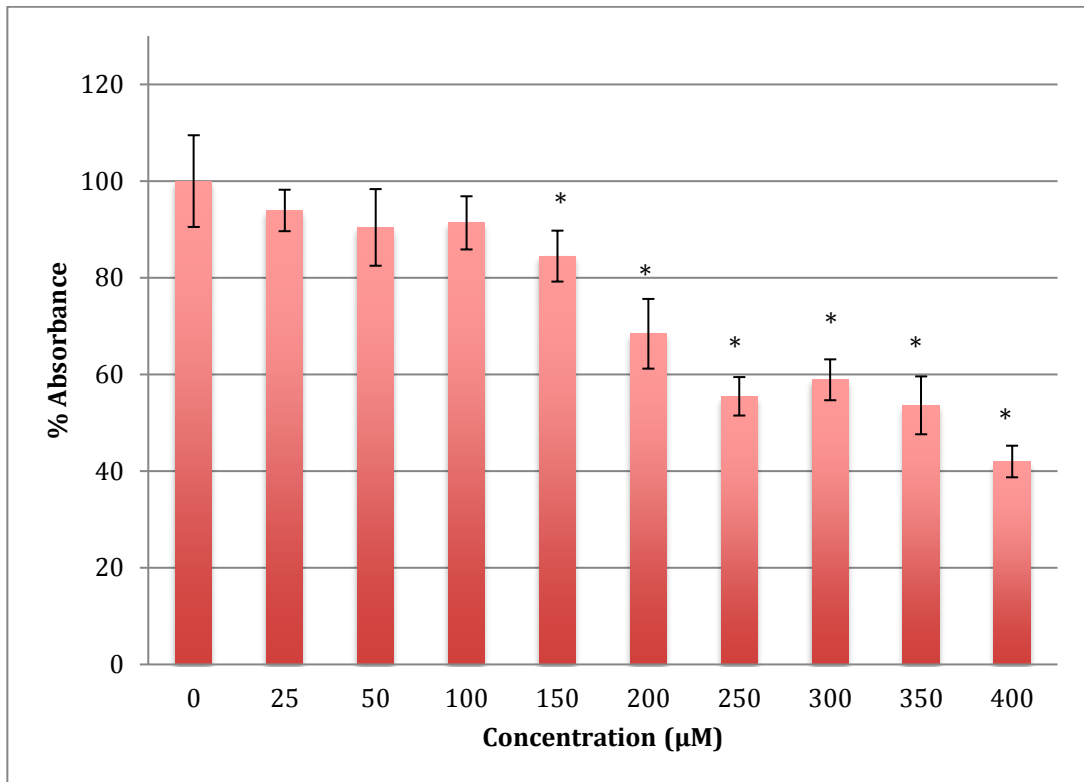


**Figure 3. 9 MTT assay measured in astrocytoma cells at 72 h. Results are percentage values (Mean  $\pm$  SD, n = 3) where 100% corresponds to control values. Cells treated with cobalt in culture medium throughout the experiment. Data were analysed by One-way ANOVA followed by Tukey test. \*Represents significantly different mean values between treatment and control. P value<0.05.**

Similarly, after 72 hours the decline viability was even lower in astrocytoma cells when treated with same range of concentrations of cobalt, reaching 42% viability at 400  $\mu$ M. The calculated LD<sub>50</sub> was 358 $\pm$ 8  $\mu$ M cobalt.

**Table 3. 1 Table summarised the results of calculated LD<sub>50</sub> values derived from MTT results for both cell lines, SH-SY5Y and U-373 cells.**

<b>LD<sub>50</sub></b> / <b>Cell</b>	<b>SH-SY5Y</b>	<b>U-373</b>
<b>24h LD<sub>50</sub></b>	254±17	713±12
<b>48h LD<sub>50</sub></b>	220±15	422±7
<b>72h LD<sub>50</sub></b>	102±14	358±8

MTT results in astrocytoma cells were more precise than in the SH-SY5Y cells, and SD values were smaller due to poor adherence of SH-SY5Y cells as described above in section 3.4.1. However, the degree of damage at higher concentrations of cobalt with all incubation periods was less than that for the SH-SY5Y cells. It is believed that astrocytes (represented here by astrocytoma) as they are located in the brain-blood barrier have a protective role around neurons and have higher antioxidation capacity than neurons (La Quaglia and Manchester, 1996). Additionally, it is known that neurons rely on the astrocyte's metabolic capacity to eradicate oxidative stress (Sagara *et al.*, 1993).

### **3.4.3 ROS detection**

Since many metals have been linked to oxidative stress through production of reactive oxygen species (ROS) (Shih *et al.*, 2003), the production of ROS in neuroblastoma and astrocytoma cells after treatment with a range of cobalt concentrations for 4 and 24 hours was investigated. Oxidative stress resulting from the generation of reactive oxygen species was reported in SH-SY5Y cells after

treatment with mercury (Maxwell and Salnikow, 2004). U-373 cells were also found to generate reactive oxygen species after treatment with copper or zinc (Olivieri *et al.*, 2000).

### 3.4.3.1 ROS measurement in SH-SY5Y cells after treatment with cobalt

The generation of the reactive oxygen species (ROS) in SH-SY5Y cells after treatment with a range of cobalt concentrations (100, 150 and 200  $\mu\text{M}$ ) for 24 hours was measured and compared with untreated controls as shown in Figure 3.10.

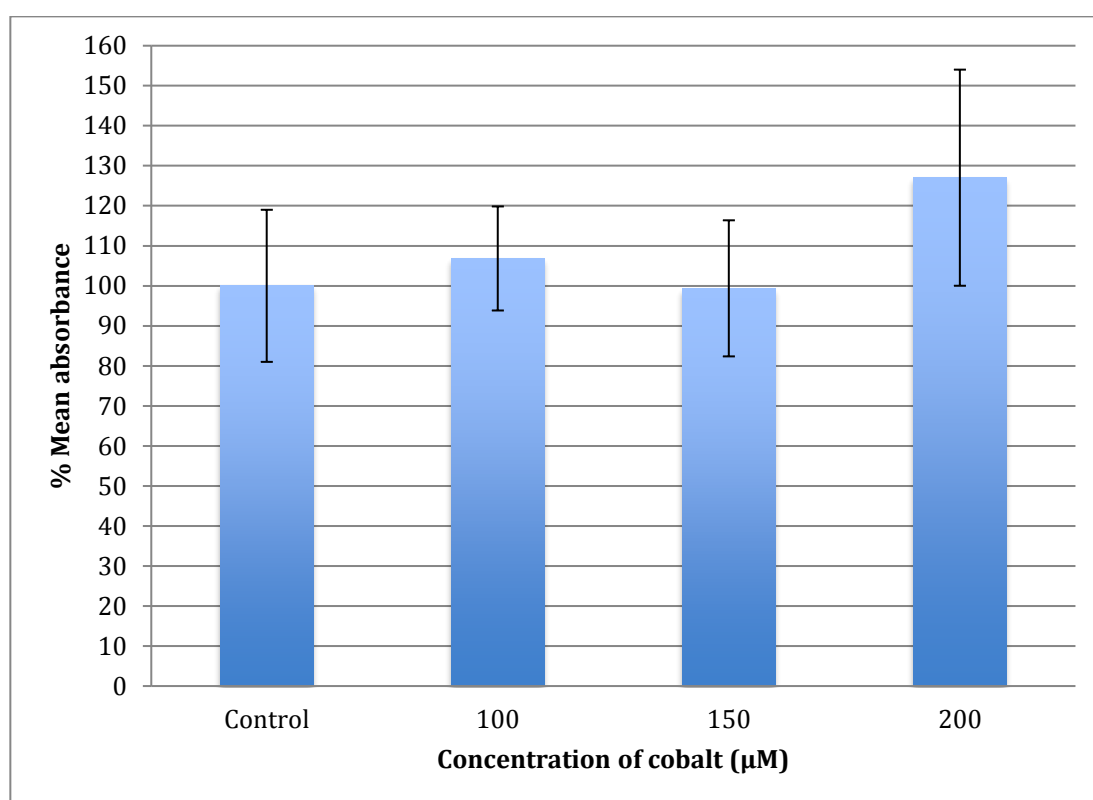


**Figure 3. 10 Measurement of ROS fluorescence intensity in SH-SY5Y cells upon exposure to 100, 150, and 200  $\mu\text{M}$  of cobalt for 24h, using carboxy-H<sub>2</sub>DCFDA to detect ROS at an excitation wavelength of 495 nm and emission wavelength of 525 nm. Data are Mean  $\pm$  SD, n=3, and were analysed by One-way ANOVA (P value <0.3) followed by a Tukey test.**

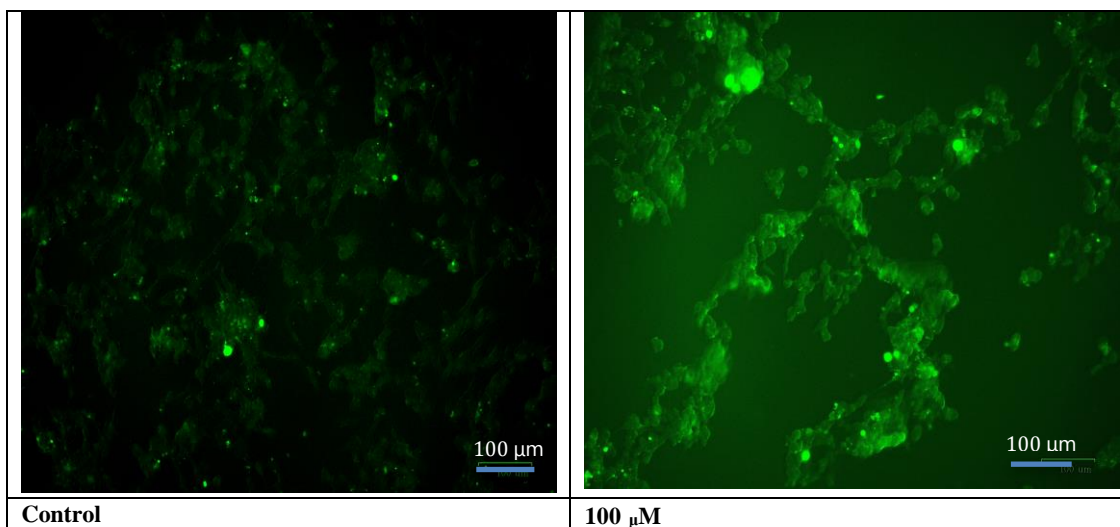


**Figure 3. 11 Images of SH-SY5Y neuroblastoma cells without cobalt treatment (on the top left) and after treatment with 100  $\mu$ M of cobalt (on the top right). Green fluorescence indicates the amount of ROS production in the cells. Pictures were taken by the Motic AE31 microscope-100 power dry lenses.**

Comparing fluorescence measurements of cobalt treated with non-treated SH-SY5Y cells for each incubation period, it was noticed that there was an insignificant increase (with P value=0.3 using One-way ANOVA and Tukey test) in fluorescence in treated cells in comparison with controls after 4 hours incubation with cobalt (data not shown as there were no fluorescence in all concentrations).

On the other hand, there was an increase in the fluorescence measurement of the 200  $\mu$ M treated cells after 24 h in comparison with the relevant controls (Figure 3.10). This is supported by the visual analysis of the dye concentration inside the cells, as the intensity was increased as the concentration of cobalt was increased. However, at the higher doses of cobalt (150 and 200  $\mu$ M), more dead cells were floating in the medium which made the pictures not clear and few cells were still attached to the base of the petri dish. This finding shows that cobalt was increasing ROS production, especially in high doses.

Note: the high standard deviation in the measurements can be explained at least in part by the weakened attachment of SH-SY5Y cells, which leads to detachment of cells after any addition of solutions.

#### **3.4.3.2 ROS measurement in astrocytoma cells after exposure to cobalt for 24 hours**

The U-373 cells were treated with a range of cobalt (100, 150 and 200  $\mu\text{M}$ ) for 24 hours to measure the production of the reactive oxygen species (ROS) in comparison with non-treated cells and the results are shown in Figure 3.12.

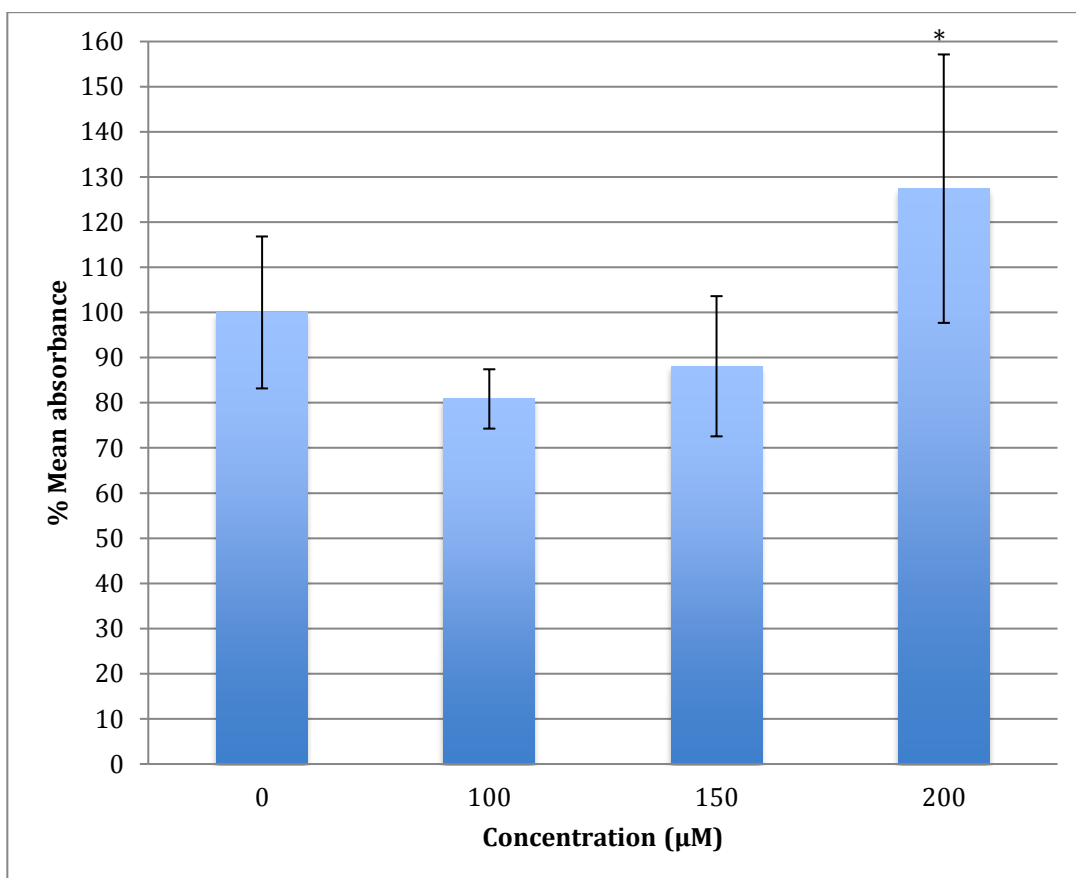


**Figure 3. 12** Measurement of ROS fluorescence intensity in U-373 cells upon exposure to 100, 150, and 200 µM of cobalt for 24h, using carboxy-H<sub>2</sub>DCFDA at an excitation wavelength of 495 nm and emission wavelength of 525 nm for detection. Data are Mean ± SD, n=3 and were analysed by One-way ANOVA (P value<0.005) followed by a Tukey test.

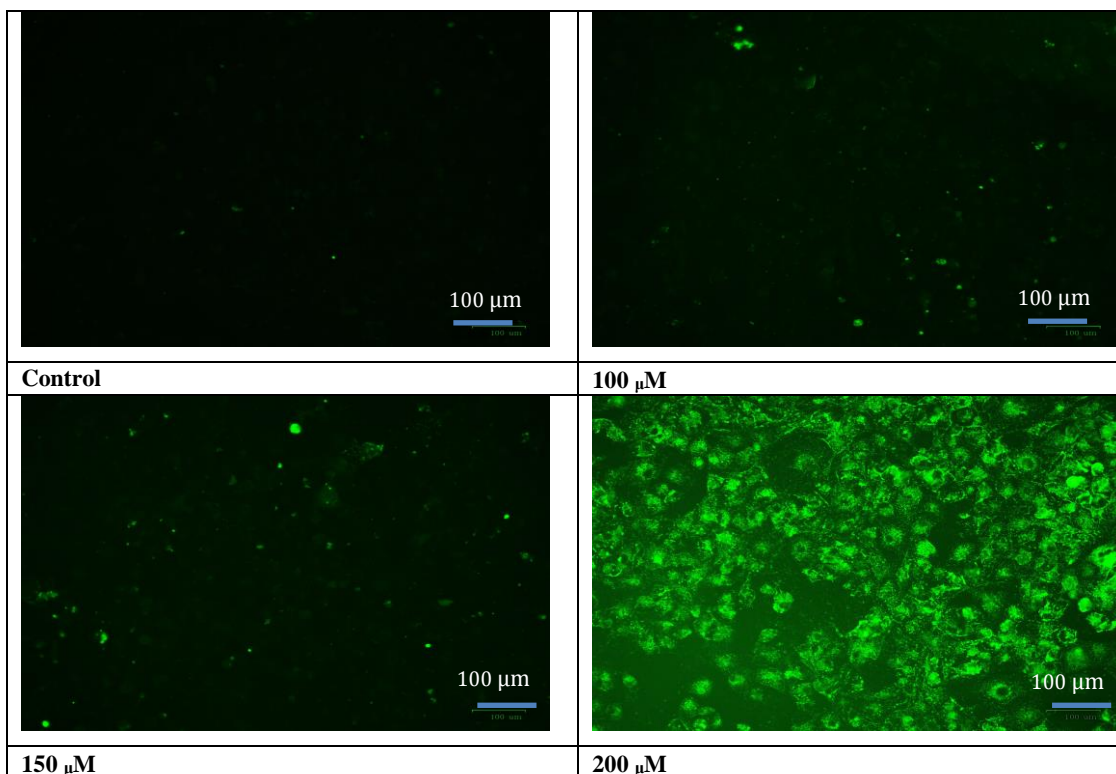


**Figure 3. 13 Images of U-373 astrocytoma cells without cobalt treatment (on the left), and after treatment with 100  $\mu$ M of cobalt for 24 hours (on the top right and the two pictures below). Green fluorescence indicates the amount of ROS production in the cells. Pictures were taken by the Motic AE31 microscope-100 power dry lenses.**

Comparing the fluorescence measurements of cobalt-treated with non-treated U-373 cells for a 24 hour incubation period, it was noticed that there was an significant ( $P$  value $<0.005$ ) rise in fluorescence in the control cells in contrast to a visible increase in fluorescence in the cobalt treated cells at 200  $\mu$ M concentration. This finding indicates that cobalt is inducing ROS at a concentration of 200  $\mu$ M after a 24 hour incubation in the U-373 cells. However, oxidative stress is less obvious  $< 200 \mu$ M.

### 3.4.4 Western blotting (Gels)

#### 3.4.4.1 Western blotting results for neuroblastoma cells

After processing the Western blotting analysis the membranes were scanned and the proteins of interest were identified. Figure 3.14 shows the bands of each protein in the cells exposed to increasing concentrations of cobalt for 72 hours.

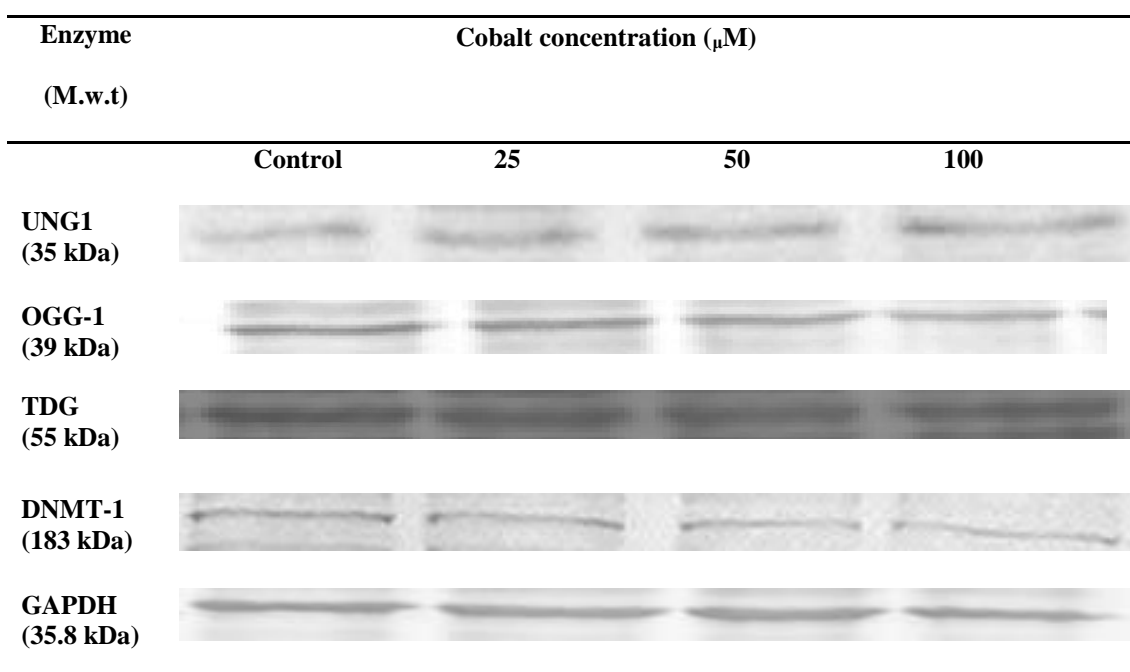


**Figure 3. 14 Expression of UNG1, OGG1, TDG, DNMT and the house keeping glyceraldehyde-3-phosphate dehydrogenase (GAPDH) proteins in SH-SY5Y cell lines after treatment with a range of cobalt concentrations for 72 hours. All lanes were loaded with 10  $\mu$ g total protein.**

Visual analysis indicated that there are only minor changes between control and cobalt treated cells for each enzyme. The replicates showed similar bands with low standard deviation as illustrated in Figure 3.15.

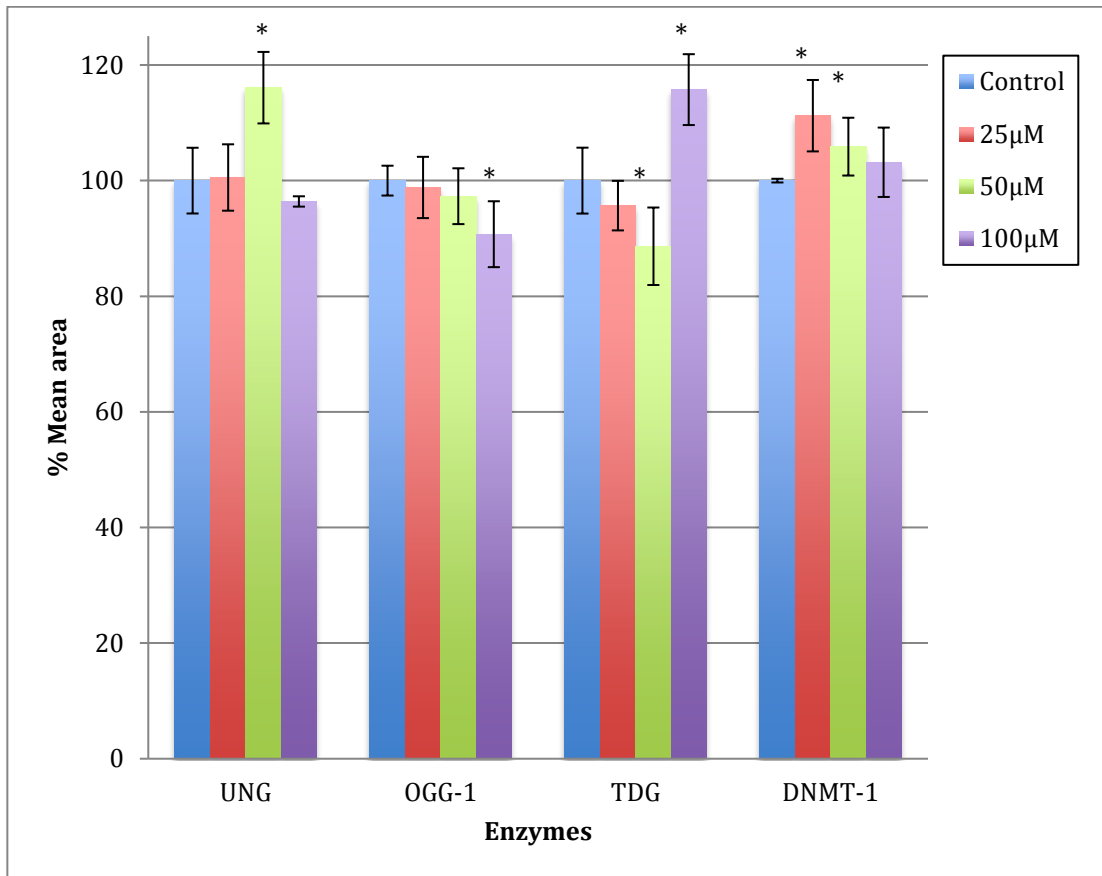


**Figure 3.15** Quantification of the listed proteins in SH-SY5Y cells after treatment with a range of cobalt concentrations for 72 hours. Values generated by the software ImageJ. Values represent percentage mean  $\pm$  SD. Data were analysed by One-way ANOVA followed by Tukey test. n=3. Values represents the ratio of protein expression to the expression of the house keeping protein (GAPDH).\* Represents mean values that are different from control mean value (P value<0.05).

Even though visual analysis did not show any change, optical analysis by ImageJ software showed some small changes as illustrated in Figure 3.15. Those marked with a star represent significant difference from mean with a P value < 0.05. The most noticed change was in uracil DNA glycosylase (UNG) and thymine DNA glycosylase (TDG) enzymes, which have an important role in the base excision repair process.

UNG1 production was increased significantly in the cells treated with 50  $\mu\text{M}$  of cobalt. This indicates that the cells reached their highest ability to recognise and repair/remove the uracil in the G/U mismatch in the DNA of the cells caused by cobalt at this concentration. It is believed that below this concentration cells did not produce higher UNG1 either because damage was low or because the damage caused by lower concentrations may have been fixed earlier than 72 hours.

Production of TDG was increased significantly (reaching 115% compared to controls) in cells treated with 100  $\mu\text{M}$  of cobalt. This indicates that cells reached their maximum repair and removal of thymine from G/T mismatch at this concentration of cobalt.

In case of the enzyme 8-oxoguanine glycosylase (OGG1), it was significantly downregulated by 10% at 100  $\mu\text{M}$  of cobalt compared to relative controls. OGG1 is the enzyme that recognise 8-oxo-deoxyguanine (8-oxo-dG) in the DNA (Olivieri *et al.*, 2000). DNA methyltransferase (DNMT1) has increased at 25 and 50  $\mu\text{M}$  of cobalt by approximately 11% and 6%, respectively. Increase in DNMT1 was associated to an increase in the methylation process (Schärer and Jiricny, 2001).

It should be noted that the changes recorded are small, so although statistically significant, they are unlikely to be biologically significant.

### 3.4.4.2 Western blotting results for astrocytoma

Western blotting for astrocytoma cells was conducted on similar concentrations of cobalt to those used with the neuroblastoma cells. Bands of each protein obtained from scanned membranes are shown in Figure 3.16.

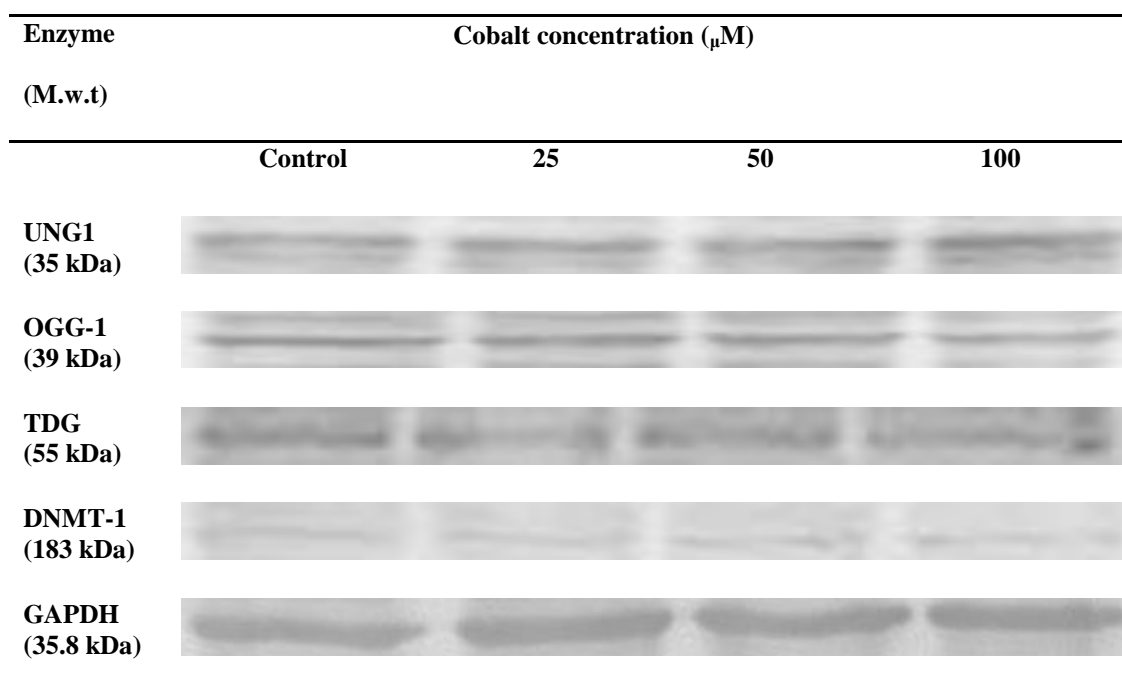


**Figure 3. 16 Expression of UNG1, OGG1, TDG, DNMT and house keeping (GAPDH) proteins in U-373 cells after treatment with a range of cobalt concentrations for 72 hours. All lanes were loaded with 10  $\mu$ g total protein.**

Visual analysis showed small variances between control and cobalt treated cells. Replicates showed reproducible bands with low standard deviations as shown in Figure 3.17.

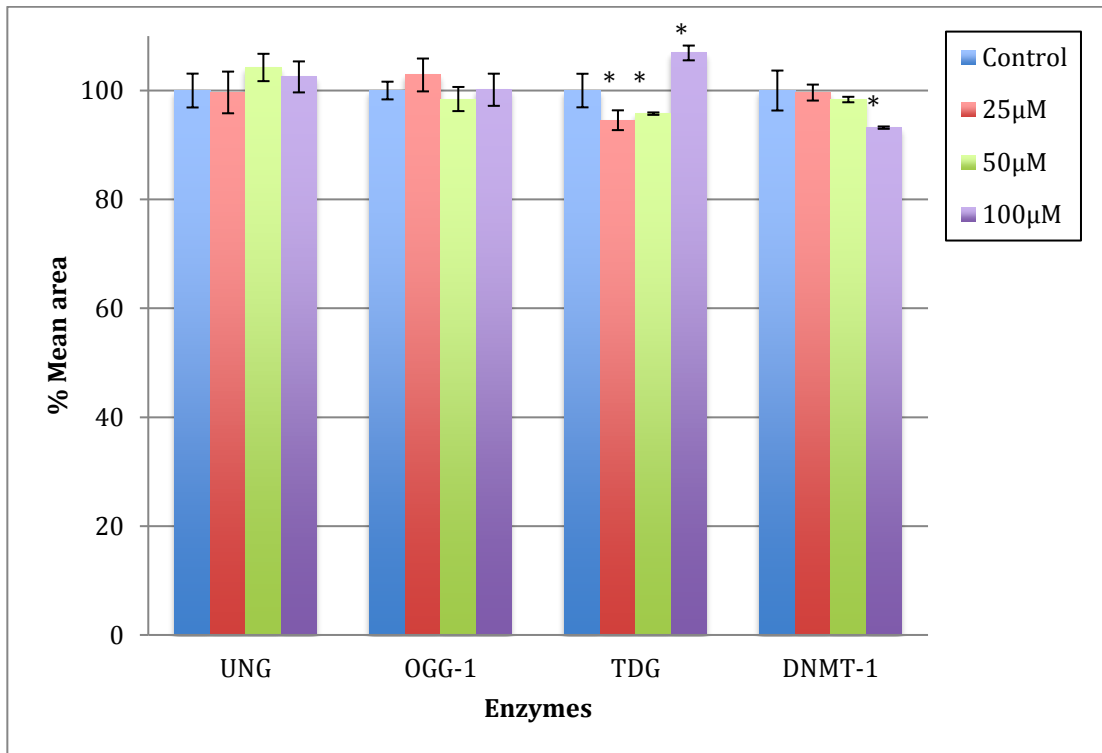


**Figure 3. 17 Quantification of listed proteins in U-373 cells after treatment with a range of cobalt concentrations for 72 hours. Values generated by the software ImageJ. Values represent percentage mean  $\pm$  SD. Data were analysed by One-way ANOVA followed by Tukey test (n=3). Values represent the ratio of protein expression to the expression of the house keeping protein (GAPDH). \* Represents statistically different mean value from control mean value (P value<0.05).**

The results of the western blotting showed no difference in the levels of two enzymes (UNG1 and OGG1), between the different doses of cobalt and the relevant controls. However, TDG increased slightly compared to control at the 100  $\mu$ M dose of cobalt in this experiment. This can be explained by astrocytoma cells starting to remove/repair thymine from a G/T mismatch at this concentration of cobalt.

It was also noticed that the DNMT-1 band slightly decreased at 100  $\mu$ M of cobalt. This could indicate that cells were losing their ability to methylate at this concentration.

However, the change was low and cross reactivity was high (Figures 1-4 appendix 3), and care must be taken in the interpretation of the results.

### **3.4.5 Real-time PCR**

#### **3.4.5.1 Results and discussion for quantitative real-time PCR for the selected genes for neuroblastoma (SH-SY5Y) cells**

Quantitative real-time polymerase reaction (qRT-PCR) was carried out to test for the expression of specific genes after treatment of SH-SY5Y cells with a range of cobalt concentrations for 72 hours. The genes were chosen to investigate if increased gene expression linked to pathways involved in oxidative stress, DNA deamination and DNA methylation could be detected as a result of cobalt treatment. Increased gene expression of Mlh1, SIRT2, MeCP2, UNG1 and TDG was identified with a single peak for each gene in each sample and no peaks in water and negative controls as illustrated in Figures 3.18, 3.19, 3.20 and 3.21.

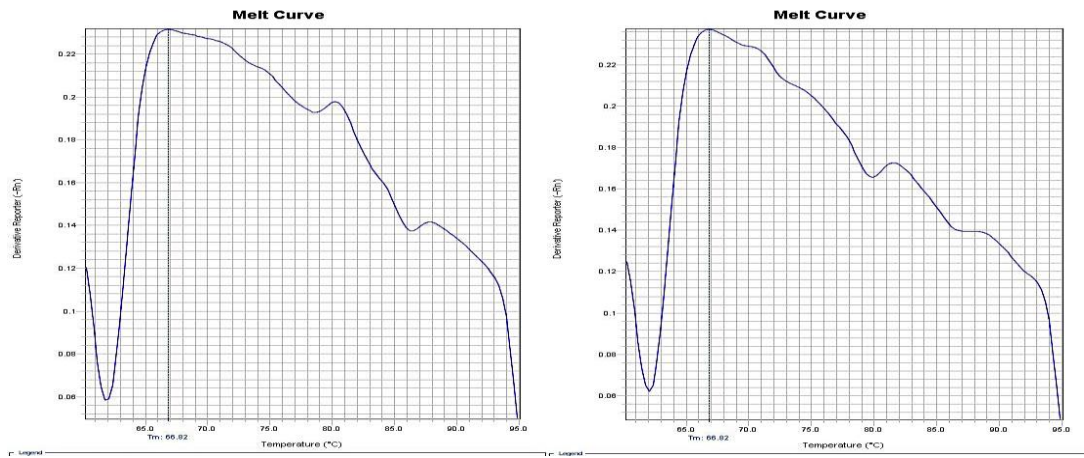


**Figure 3. 18 Melt curve for reference gene ribosomal protein L13A (RPL13A) in water control sample on the left and negative reverse transcriptase control sample on the right.**

Absence of peaks in the water control samples show that the water used has no DNA contamination either from the environment or samples. Similarly, the absence of peaks in the negative reverse transcriptase control samples proved that samples without reverse transcriptase have no residues of genomic DNA in them, which can result from bad extraction of RNA.

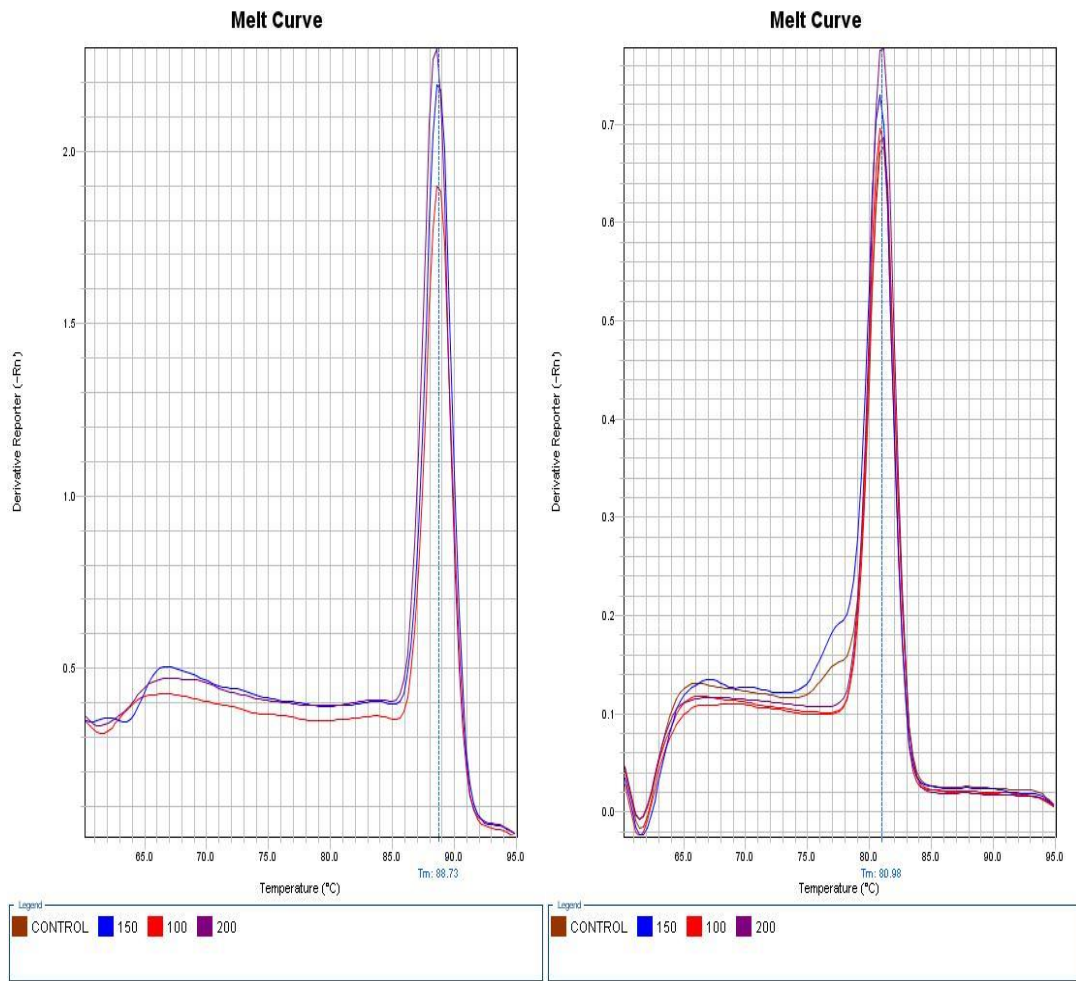


**Figure 3. 19 Melt curve for reference gene (RPL13A) on the left and Mlh1 gene on the right in all samples showing a single reproducible peak for each sample.**

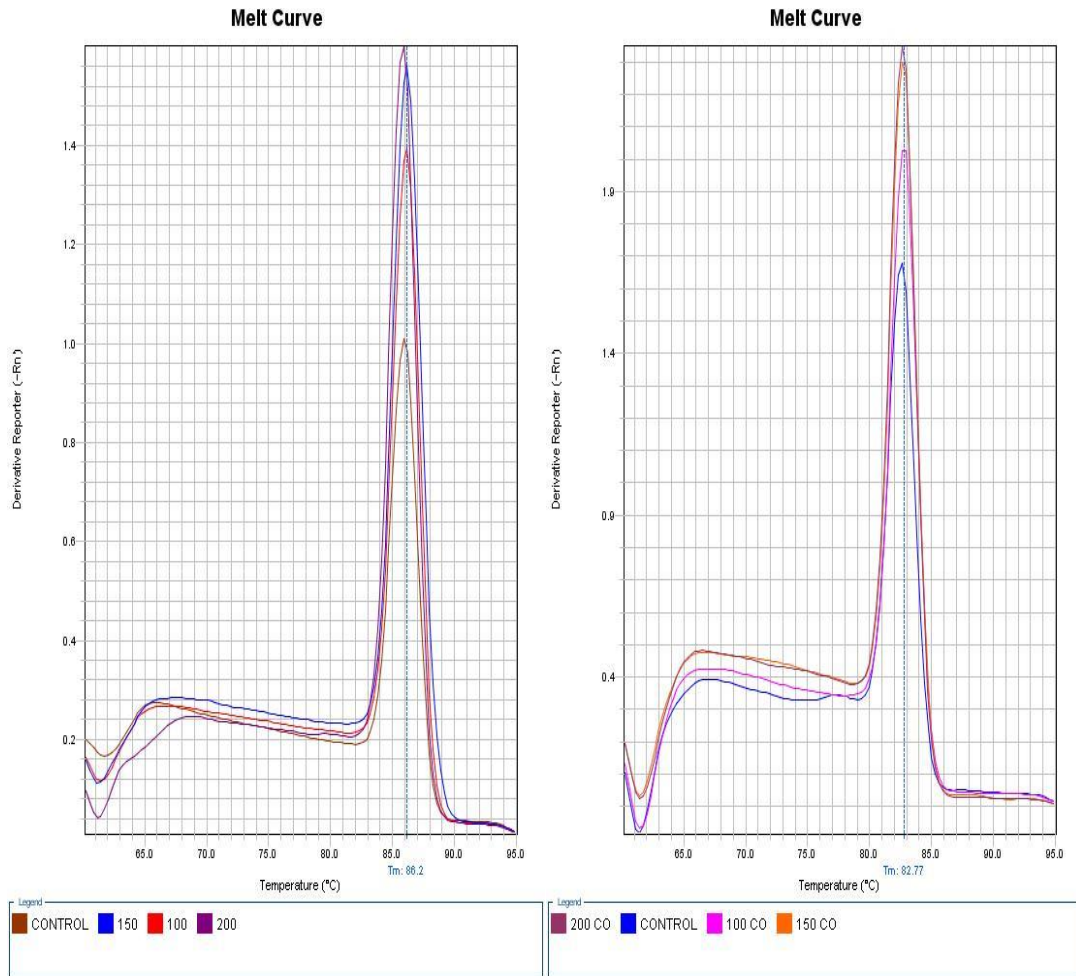


**Figure 3. 20 Melt curve for SIRT2 gene on the left and MeCP2 gene on the right in all samples showing a single reproducible peak for each sample.**

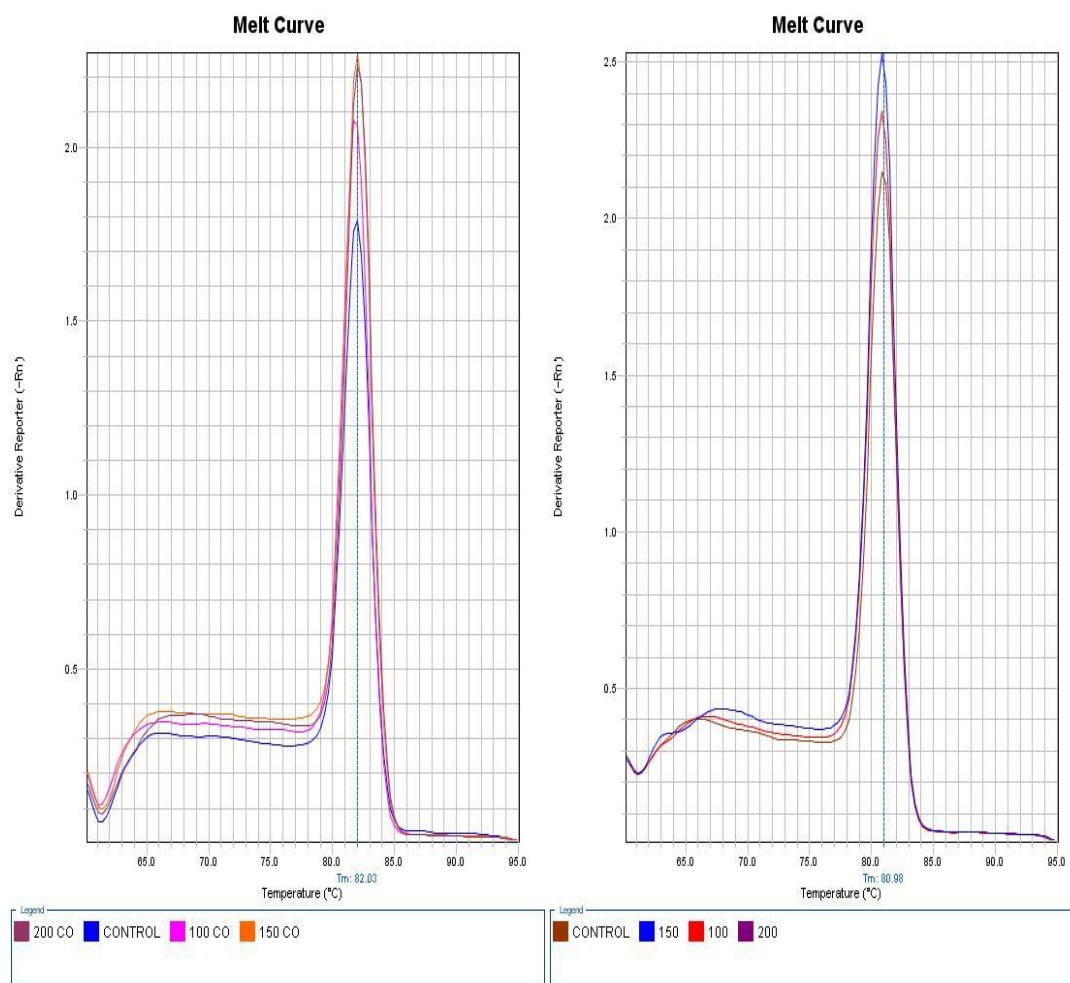


**Figure 3.21 Melt curve for UNG1 gene on the left and TDG gene on the right in all samples showing a single reproducible peak for each sample.**

Quantitative real-time PCR for one reference gene RPL13A and five selected genes; Mlh1, SIRT2, MeCP2, UNG1 and TDG for SH-SY5Y cells after treatment with 25, 50 and 100  $\mu\text{M}$  of cobalt was carried out. The gene expression in each treated sample and the gene expression in non-treated sample (control) are shown in table 3.2 and Figure 3.22. Gene expression values were represented as fold change of the expression of the gene of interest compared to the expression of the reference gene (RPL13A) in the same samples (method detailed in section 2.8 in chapter 2).

**Table 3. 2 Gene transcription fold change in SH-SY5Y cells after treatment with a range of cobalt concentration. Fold change values represented as mean values  $\pm$  (STD).**

Gene		Cobalt concentration ( $\mu$ M)			
		Control	25	50	100
MLH1	Fold change	1 $\pm$ (0.14)	0.79 $\pm$ (0.15)	2.15 $\pm$ (0.11)	4.30 $\pm$ (0.05)
	$\Delta\Delta C_T$	0	0.34	-1.10	-2.11
SIRT2	Fold change	1 $\pm$ (0.26)	2.88 $\pm$ (0.28)	9.87 $\pm$ (0.12)	17.60 $\pm$ (0.09)
	$\Delta\Delta C_T$	0	-1.53	-3.30	-4.14
MeCP2	Fold change	1 $\pm$ (0.23)	2.31 $\pm$ (0.33)	11.04 $\pm$ (0.24)	24.11 $\pm$ (0.14)
	$\Delta\Delta C_T$	0	-1.21	-3.46	-4.59
UNG1	Fold change	1 $\pm$ (0.07)	0.39 $\pm$ (0.02)	1.40 $\pm$ (0.03)	2.34 $\pm$ (0.07)
	$\Delta\Delta C_T$	0	1.37	-0.49	-1.22
TDG	Fold change	1 $\pm$ (0.22)	0.85 $\pm$ (0.19)	1.39 $\pm$ (0.29)	2.13 $\pm$ (0.13)
	$\Delta\Delta C_T$	0	0.24	-0.48	-1.09

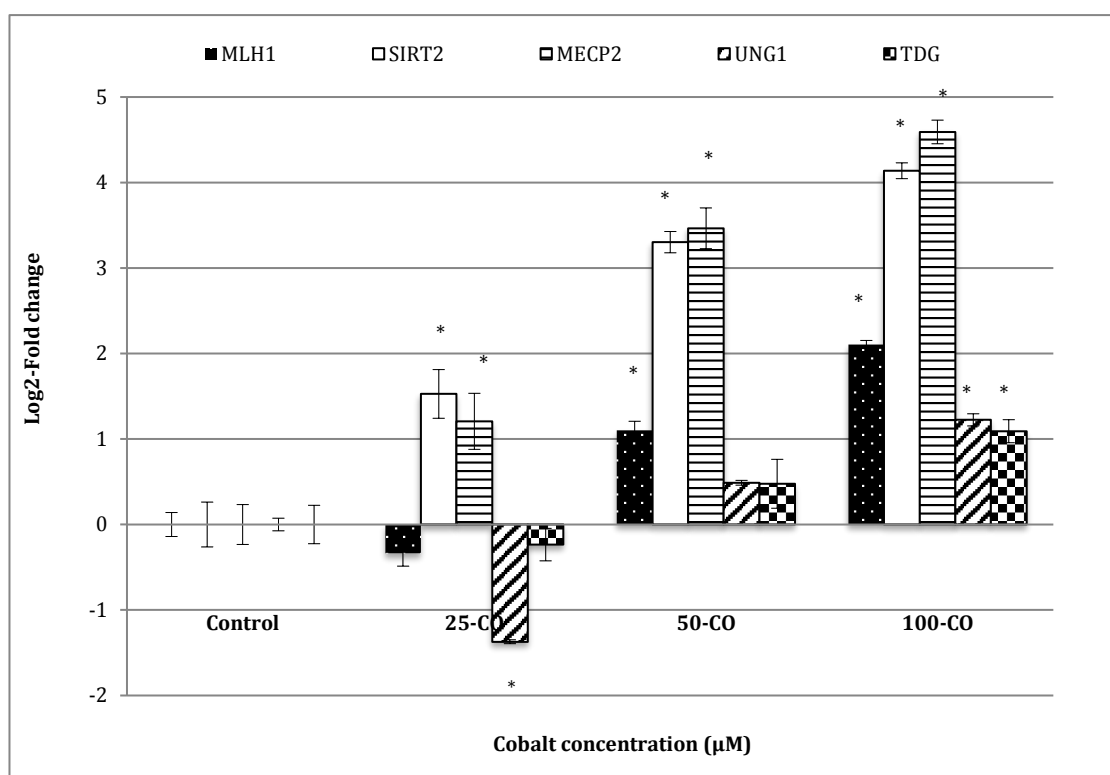


**Figure 3. 22 Gene transcription in a neuroblastoma cell line after treatment with a range of cobalt concentration. Values represent % mean ratio $\pm$ STD. Data were analysed by One-way ANOVA followed by Tukey test (n=3). Mean ratio represents mean value of fold change of gene expression compared to the reference gene.**

The SIRT2 and MeCP2 gene expression was upregulated at 50 and 100  $\mu\text{M}$  of cobalt. All the other genes were less upregulated when the cobalt concentrations were increased.

Sirtuins (SIRT2) play an important role in the regulation of hypoxia inducible factor-1 $\alpha$  (HIF-1 $\alpha$ ). Under hypoxia, SIRT2 is the regulatory gene for HIF-1 $\alpha$  transcription and stability (Lennicke *et al.*, 2015). Upregulation of SIRT2 will lead to reduction in the production of HIF-1 $\alpha$ . In contrast, downregulation of SIRT2 will yield an overexpression of HIF-1 $\alpha$  (Seo *et al.*, 2015). SIRT2 was significantly increased as the cobalt dose was increased (see Figure 3.22). Suggesting that cobalt toxicity is mimicking the conditions produced by hypoxia and that SIRT2 is countering this. Cobalt has been proposed as a treatment for type II diabetes since it promotes the production of HIF1- $\alpha$  which is suppressed by hyperglycemia (Xiao *et al.*, 2013).

Methyl-CpG Binding Protein 2 (MeCP2) is predicted to bind to methylated promoters and silence transcription in SH-SY5Y cells (North and Verdin, 2007). It was also found that MeCP2 was involved in the nickel-induced gpt gene silencing (Yasui *et al.*, 2007). A decrease in MeCP2 levels was associated with the minimisation of the size of neuronal cells (Yan *et al.*, 2003). In our results it was increased gradually as the concentration of cobalt was increased.

Uracil DNA glycosylase gene (UNG1) is the major gene in base excision repair and the first to detect and repair mismatch in DNA. The increase (up to 2 fold at 100  $\mu\text{M}$ ) in UNG1 seen here indicates that base excision repair may play an important role in the defence mechanism of neuroblastoma cells against cobalt toxification.

Mlh1 is one of the mutLgamma (MutL $\gamma$ ) genes (Mlh1 and Mlh3). The MutLgamma endonuclease causes R-loop-dependent CAG fragility. The observation of the upregulation of Mlh1 provides evidence that breakage at expanded CAG repeats occurs due to R-loop formation and reveals a mechanism for CAG repeat instability mediated by cytosine deamination of DNA engaged in R-loops followed by upregulation of other by MutL $\gamma$  (Mlh1/Mlh3) producing cleavage (Armstrong, 2002). The Mlh1 gene was increased by 4 fold at 100  $\mu$ M of cobalt compared to the relevant control.

TDG is responsible for repairing methylation and the conversion of 5-methylcytosine to thymine. Thymine DNA glycosylase (TDG) initiates base excision repair by cleaving the N-glycosidic bond between the sugar and target base (Su and Freudenreich, 2017). This gene was upregulated in the cells by 2 fold at 100  $\mu$ M of cobalt, compared to the control.

#### **3.4.5.2 Results and discussion for quantitative real-time PCR for the selected genes for the Astrocytoma cells (U373)**

Similar to SH-SY5Y cells, the detection of the genes revealed single peaks in all samples, with no peaks in water and negative controls as illustrated in Figures 3.23, 3.24, 3.25 and 3.26.

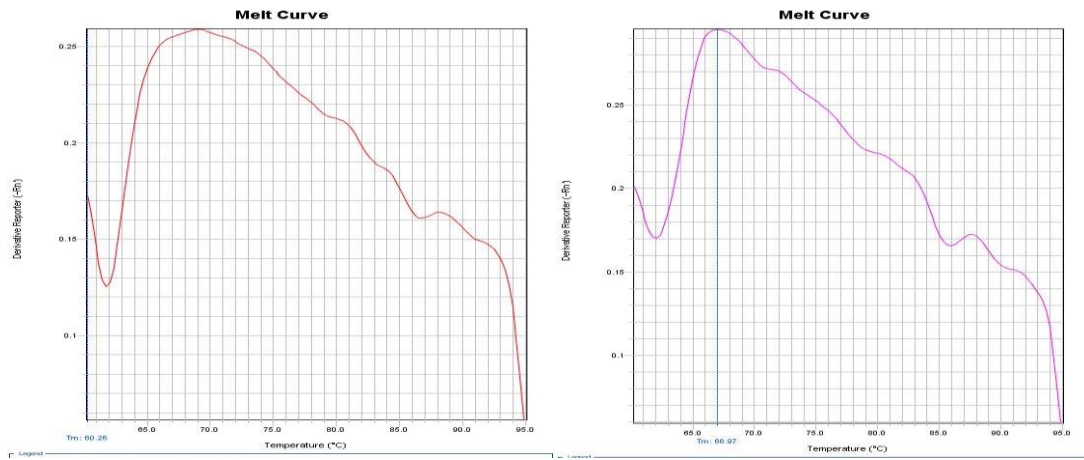


**Figure 3. 23 Melt curve for reference gene (RPL13A) in water control sample on the left and negative reverse transcriptase sample on the right.**

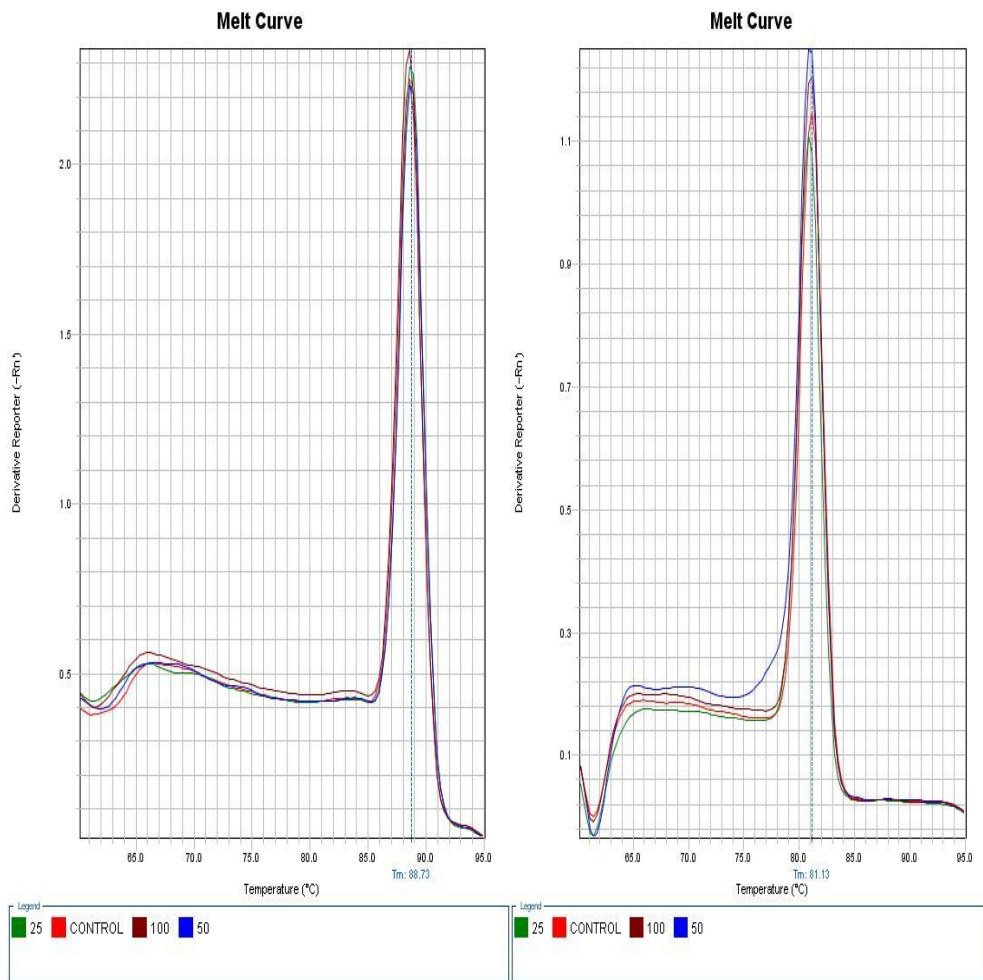


**Figure 3. 24 Melt curve for reference gene (RPL13A) on the left and Mlh1 gene on the right in all samples showing a single reproducible peak for each sample.**

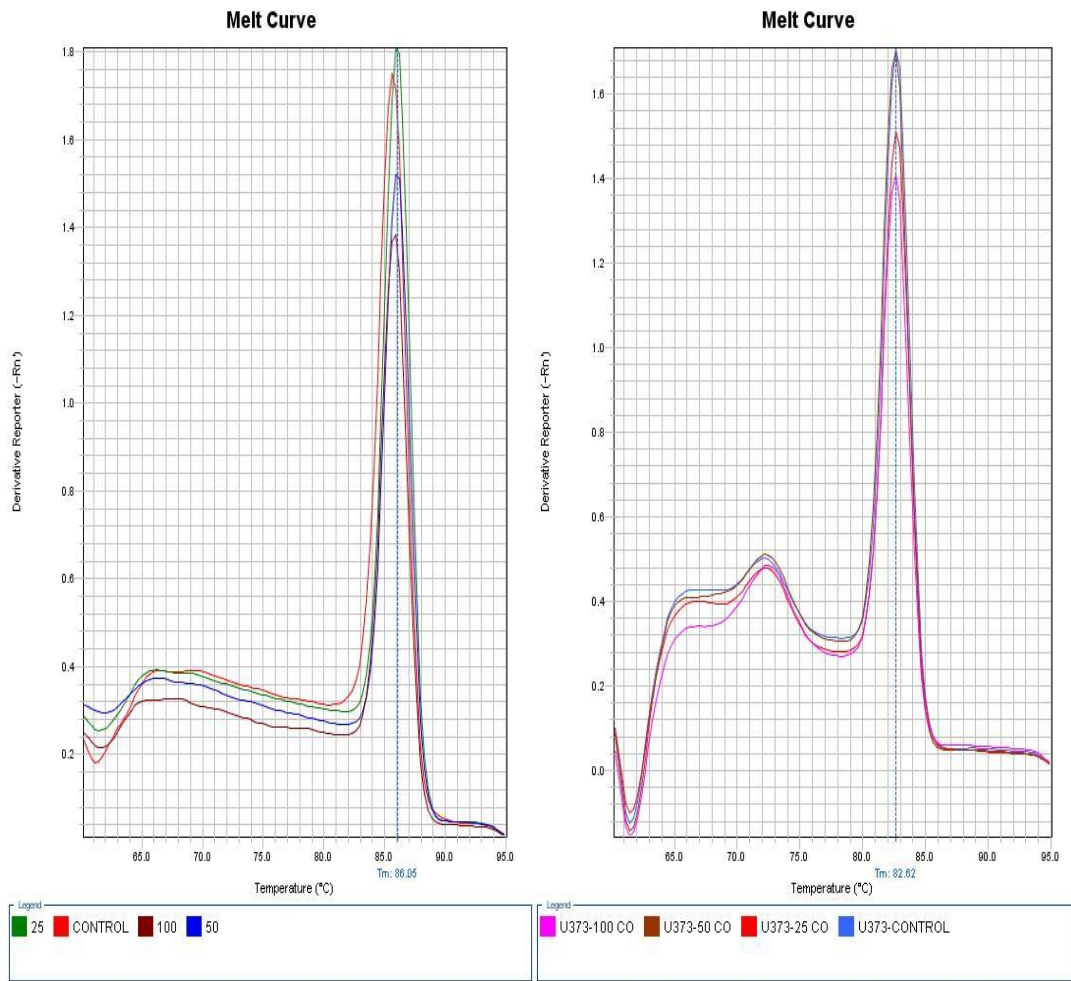


**Figure 3. 25 Melt curve for SIRT2 gene on the left and MeCP2 on the right in all samples showing a single reproducible peak for each sample.**

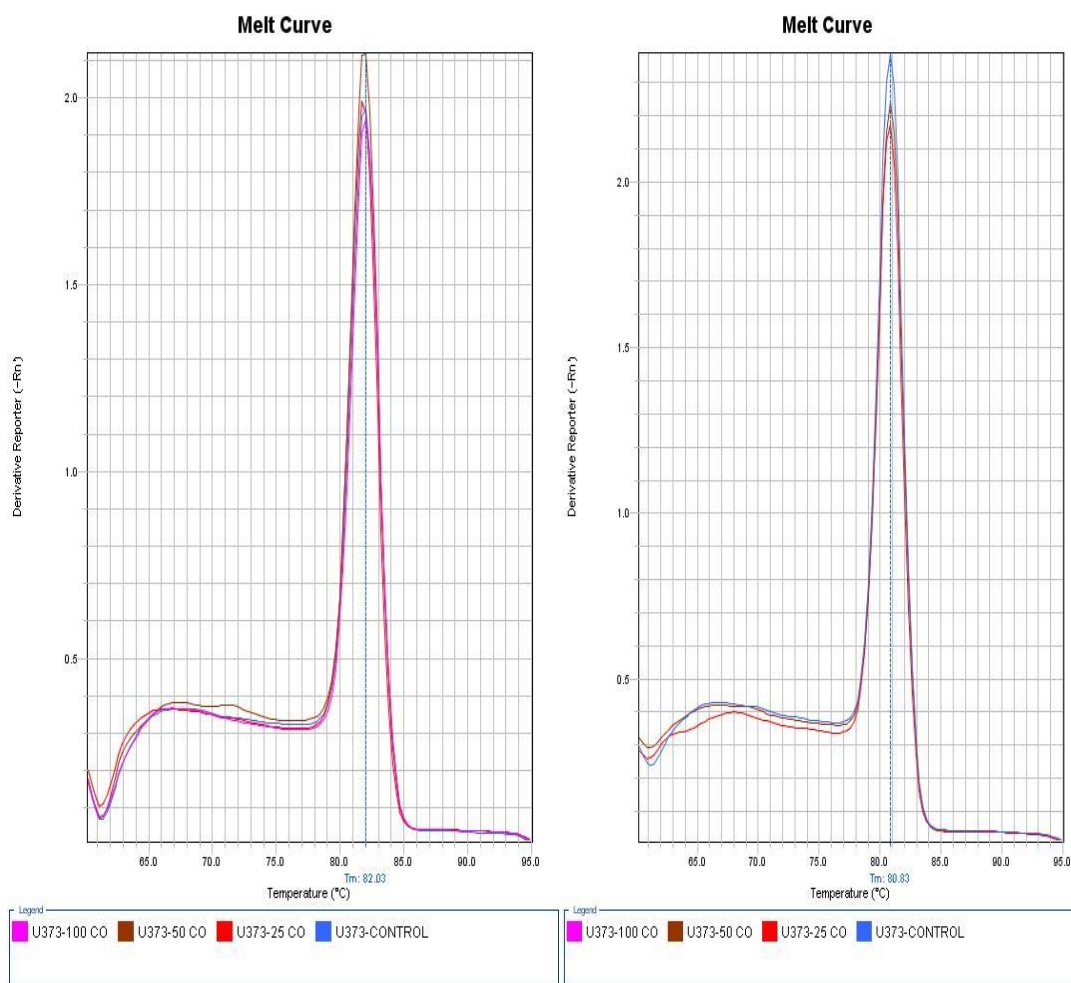


**Figure 3. 26 Melt curve for UNG1 gene on the left and TDG on the right in all samples showing a single reproducible peak for each sample.**

Quantitative real-time PCR was carried out for one reference gene RPL13A and five selected genes; Mlh1, SIRT2, MeCP2, UNG1 and TDG for U-373 cells after treatment with 25, 50 and 100  $\mu$ M of cobalt for 72 hours. Selection of lower cobalt concentrations here was made to avoid the decline of cellular viability shown before in SH-SY5Y cells (see section 3.4.1), causing all genes to be downregulated. The gene expression was compared to the same genes expression in the non-treated cells as shown in table 3.3 and Figure 3.27.

**Table 3. 3 Gene expression exhibited as fold changes in U-373 cells after treatment with a range of cobalt concentrations. Fold change values represented as mean values  $\pm$  (STD).**

Gene		Cobalt concentration ( $\mu$ M)			
		Control	25	50	100
MLH1	Fold change	1 $\pm$ (0.15)	1.67 $\pm$ (0.23)	0.92 $\pm$ (0.18)	7.89 $\pm$ (0.06)
	$\Delta\Delta C_T$	-	-0.74	0.12	-2.98
SIRT2	Fold change	1 $\pm$ (0.27)	2.89 $\pm$ (0.24)	1.13 $\pm$ (0.28)	7.68 $\pm$ (0.28)
	$\Delta\Delta C_T$	-	-1.53	-0.18	-2.94
MeCP2	Fold change	1 $\pm$ (0.19)	1.23 $\pm$ (0.36)	0.37 $\pm$ (0.31)	4.93 $\pm$ (0.36)
	$\Delta\Delta C_T$	-	-0.30	1.45	-2.30
UNG1	Fold change	1 $\pm$ (0.16)	1.27 $\pm$ (0.22)	0.66 $\pm$ (0.04)	5.99 $\pm$ (0.04)
	$\Delta\Delta C_T$	-	-0.35	0.61	-2.58
TDG	Fold change	1 $\pm$ (0.17)	0.86 $\pm$ (0.25)	0.43 $\pm$ (0.05)	3.61 $\pm$ (0.05)
	$\Delta\Delta C_T$	-	0.21	1.23	-1.85

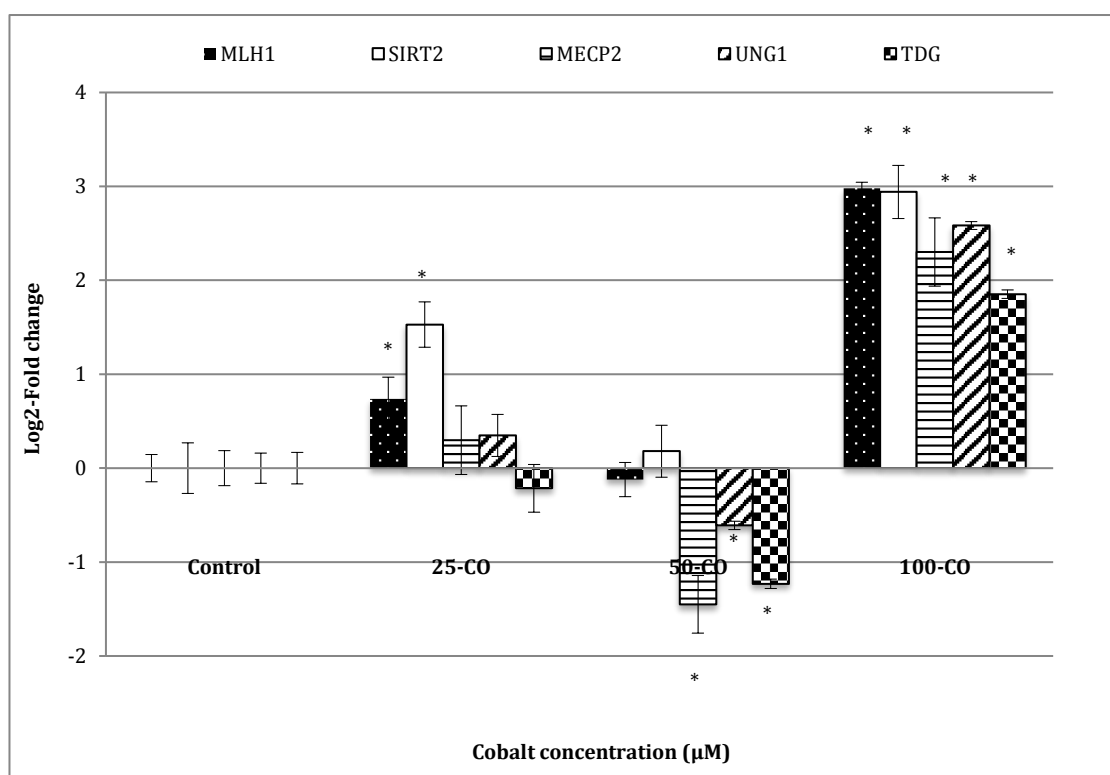


**Figure 3. 27 Expression of genes in astrocytoma cell line after treatment with a range of cobalt concentration for 72 hours. Data were analysed by One-way ANOVA followed by Tukey test (n=3). Mean ratio represents mean value of fold change of gene expression compared to the reference gene.**

There was highly significant upregulation in the production of Mlh1 and SIRT2 genes at 25  $\mu\text{M}$  cobalt, with no significant change in MECP2, UNG1 and TDG genes. Mlh1 and SIRT2 expression decreased at 50  $\mu\text{M}$  to reach same levels in the controls. However, at 100  $\mu\text{M}$  concentration of cobalt all genes were significantly upregulated.

Mlh1 increased at 25 and 100  $\mu\text{M}$ , which is responsible for CAG fragility and repeats as was explained above in section 3.4.5.1. Thus, it is believed that cobalt at 100  $\mu\text{M}$  concentration starts to induce harm to the structure of the nucleic acid.

SIRT2 was significantly increased at 100  $\mu\text{M}$  cobalt in the U-373 cells. An increase of SIRT2 will reduce the production of HIF-1 $\alpha$  (Da *et al.*, 2018) as this suggests that in the case of these cells cobalt is not inducing conditions mimicking hypoxia. Interestingly, this gene was increased in SH-SY5Y cells at all concentrations of cobalt. This provides evidence of the different function and ability of astrocytoma (representing astrocytes) as part of the blood-brain barrier, which protects neuronal cells against any toxification. SIRT2 is an important component in the antioxidant system and one of its functions is activation of the pentose phosphate pathway in order to maintain levels of NADPH which can then be used to recycle GSSG back to GSH. The higher levels of SIRT2 in the astrocytes would be consistent with their improved resistance to cobalt induced oxidative stress. Of all tissues the brain has the highest levels of expression of SIRT2 (Maxwell *et al.*, 2011).

Another increased gene was MeCP2, which was predicted, in previous study (Seo *et al.*, 2015), to bind to methylation promoters and silence transcription in SH-SY5Y cells as described in section 3.4.5.1 above.

UNG1 and TDG were both upregulated. They both play an important role in the base excision repair pathway. The upregulation of these genes might be linked to the improved antioxidant defence of the astrocyte cells. It might be that higher concentrations of cobalt are required to see an effect on the expression of these genes with this cell line.

Comparing the two cell lines reactions to cobalt, they showed a different response to cobalt treatment. Production of genes associated with damage in cell was increased at all concentrations of cobalt in the neuroblastoma cells. However, in astrocytoma cells the increase in gene expression was more abundant only at 100  $\mu$ M of cobalt, indicating that these cells are more resistant to cobalt. This result suggests a different mechanism for defence against cobalt toxicity between the astrocytoma (representing blood-brain barrier) and the neuroblastoma (representing neuronal cells in brain).

### **3.4.6 Metabolomics**

#### **3.4.6.1 Metabolomic results for astrocytoma cells**

Data generated from LC/MS and analysed by MzMine software were processed in Simca-P software in order to visualise the separation between control and treated astrocytoma samples.

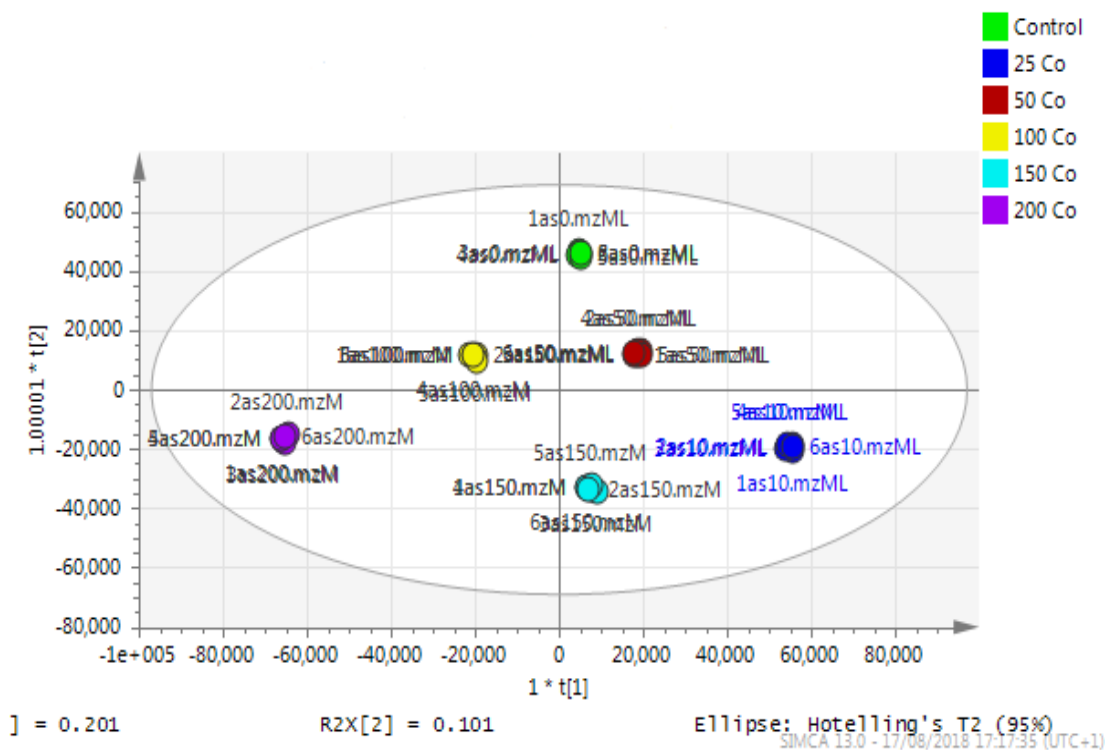


**Figure 3. 28 A PCA-X score plot of the separation between control and cobalt treated U-373 cells after 72 hours of incubation (n=3).**

Astrocytoma cells showed very reproducible data for within sample replicates as there was almost no separation between replicates, and no outliers. The separation was clear between groups (controls and cobalt treated samples).

The overall effect of cobalt on the astrocytes was demonstrated by a clear separation, using the unsupervised method of PCA, between cobalt treated cells and the respective control cells (Figure 3.28). As shown in Figures 3.28, cobalt treated cells were shifted farther from the controls as the dose of cobalt was increased. However, when a deeper analysis of the induced metabolic changes was carried out, it revealed significant changes in multiple metabolites as shown in table 3.1.

Although it might be expected from the upregulation of UNG and TDG1 that there would be evidence of base excision repair in the metabolomics data, there was no evidence for the presence of uracil which would be derived from oxidative damage of cytosine residues. However, there was one candidate marker for DNA excision repair, which was hydroxy thymidine. The data base search had this compound listed as ribosyl imidazole acetate, which is a metabolite of histidine and an isomer of hydroxyl thymidine. Without a standard it is difficult to be completely confident in the identity of this compound. However, there is a tendency for nucleosides to fragment in the source of the instrument losing the sugar portion of the molecule. Thus, evidence of the identity of hydroxy thymidine is provided by a fragment of hydroxy thymidine, hydroxy methyl uracil, which elutes at the same time as the putatively identified hydroxy thymidine as shown in Figure 3.29. It is known that the oxidation of either 5-methylcytosine or thymine will end with the formation of 5-hydroxymethyluracil (Hayes and Knaus, 2013). However, in the current case there is no evidence of the presence of hydroxy methyl uracil other than the fragment formed in the instrument from hydroxymethylthymidine. Hydroxymethylthymidine has not been reported as a DNA excision product.

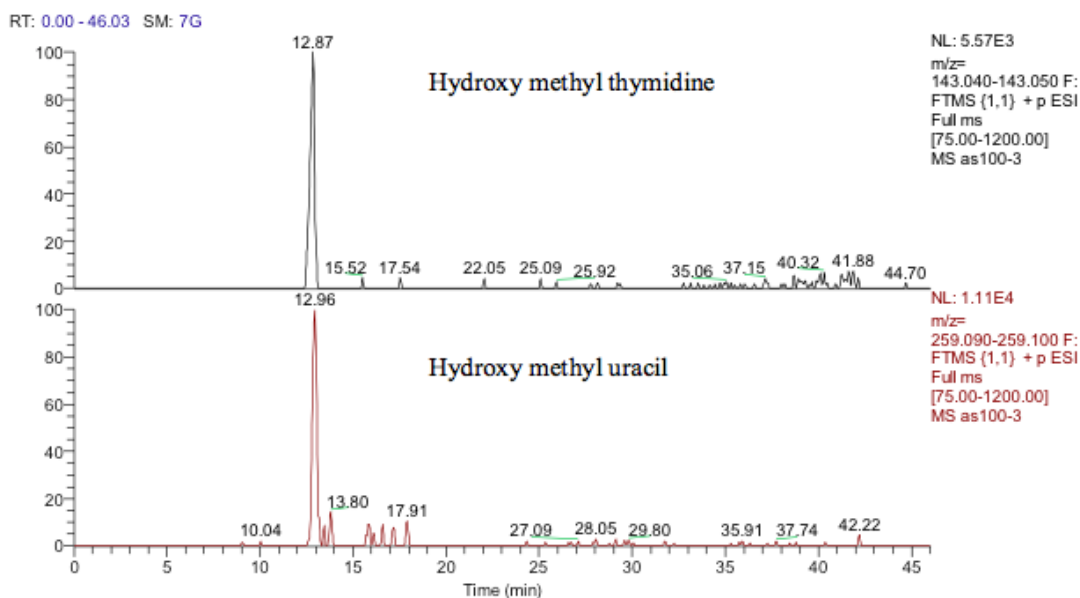


**Figure 3. 29** Extracted ion traces showing hydroxymethyl thymidine and a corresponding extracted ion trace for hydroxymethyl uracil.

5-Methylcytosine can be spontaneously deaminated and this reaction will result in formation of thymine and ammonia, and this deamination is the predominant observed single transmutation. If this mutation was detected in the DNA before the next replication, it would be fixed by the thymine-DNA glycosylase (TDG) enzyme, which detaches thymine in the mismatching of G-T. This creates a basic location in the DNA which will be corrected by AP endonucleases, for example UNG1 (Yonekura *et al.*, 2009). Cytosine can be methylated to 5-Methylcytosine when a methyl group is linked to carbon 5, which will change the structure but not the base pair function (Neddermann *et al.*, 1996). Formation of 5-Methylcytosine is an external genetic alteration caused by DNA methyltransferases (Sassa *et al.*, 2016). 5-methylcytosine was detected in both cell lines in this experiment and an isomer of thymine was also detected but the peak matching thymine, which had changed significantly, had a retention time of 11.4 minutes and thus was an isomer of

thymine. The peak for the thymine standard runs at 7.3 minutes and the peak corresponding to this retention in the samples was not changed by treatment. There were strong effects on guanosine and inosine with both these metabolites being highly elevated by treatment. Inosine is an isomer of deoxyxanthosine, which is a potential oxidation product of deoxyguanosine. However, the retention time of the peak matched that of the inosine standard and in addition there was a clear fragment ion co-eluting corresponding to hypoxanthine (Figure 3.30). The same is the case for guanosine where 5-oxo deoxyguanosine, an important marker of DNA damage, is an isomer of guanosine. However, the compound which was elevated in response to treatment with cobalt was guanosine according to both its retention time and the co-eluting fragment for guanine (Figure 3.30).

One other nucleobase was elevated by treatment which was a methylguanosine. It matches the retention time of 1-methylguanine but in the absence of standards for other positional isomers it is difficult to be confident in its identity. There was a very weak peak, which was elevated in the cells and had a mass corresponding to methylcytidine (Figure 3.31). Its retention time matched that of a standard for methylcytidine. From the elevation of MeCP2 protein resulting from treatment with cobalt, this indirectly suggests increased methylation of DNA and the most likely site to this is the 5 position of cytidine. S-adenosyl methionine (SAM), is the main agent for methylation in biological systems and is elevated in response to cobalt treatment as is S-adenosylhomocysteine which is the product resulting from transfer of a methyl group. Possibly linked to this are elevated levels of trimethyllysine. Trimethyllysine is generated from the degradation of histone proteins, which are methylated by SAM. It has been found that MeCP2 promotes methylation of histone tails which is part of its

gene silencing activity since methylated histones bind more tightly to DNA (Joergenson *et al.*, 2002). Turnover of histones could lead to an increase in the levels of trimethyl lysine. Trimethyllysine is the biosynthetic precursor of trimethylaminobutanoate, which is hydroxylated to form carnitine and both of these compounds are elevated by treatment with cobalt.

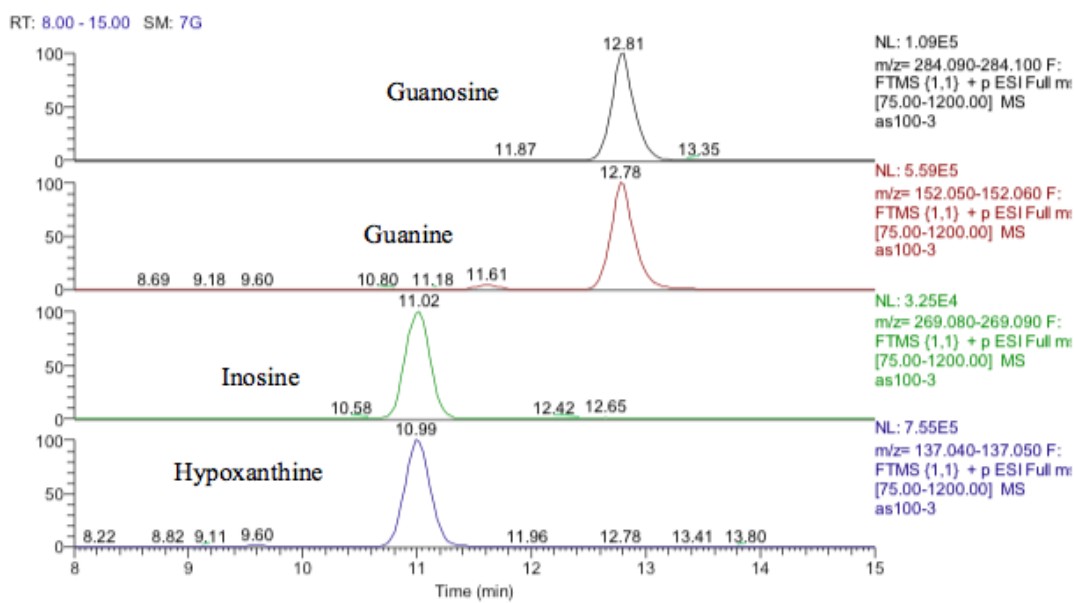


**Figure 3. 30** Extracted ion traces showing guanosine and a corresponding fragment for guanine and inosine and a corresponding fragment for hypoxanthine.

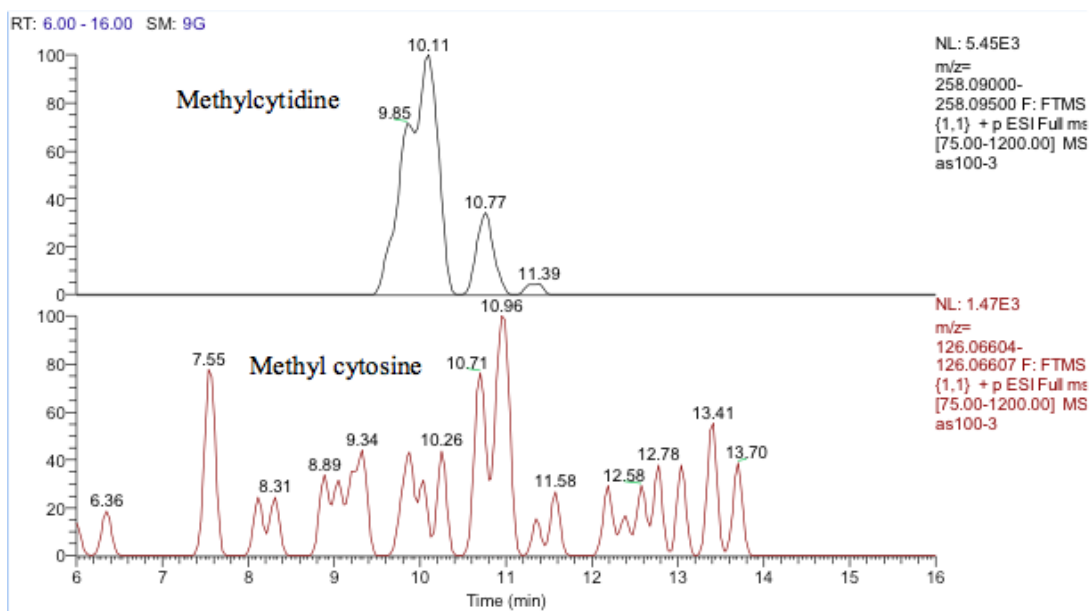


**Figure 3.31** Extracted ion traces showing a weak peak for methylcytidine and a trace showing possibly traces of methyl cytosine.

The astrocytoma cells show marked effects on the nucleosides cytosine and uridine which accumulated increasingly as the dose of cobalt was increased. These are RNA bases rather than DNA bases. The effects on uridine appear to be particularly significant since UDP and UTP are elevated as well as UDP-glucose. Uridine can be readily converted to cytidine and CMP and CTP are also increased by cobalt treatment (Ulus et al, 2006, Yamamoto et al 2011). The increase in UDP-glucose suggests that cobalt may be stimulating glycogen biosynthesis since UDP-glucose is the precursor for glycogen formation. UDP-glucose is formed from UTP and glucose phosphate both of which are increased by cobalt treatment. However, UDP-xylose is also increased and there are non-significant but persistent increases in UDP-N-acetylglucosamine (UNAC) with cobalt dose, linked to this is the accumulation of the N-acetylglucosamine phosphate which is a precursor of UNAC. This suggests there might be some effect on the biosynthesis of glycan chains which are attached to

glycoproteins and this might relate to the observation that the astrocytes lose their ability to adhere to the culture dish following cobalt treatment since glycoproteins are involved in cell adhesion (Lowe, 2003).

CDP-choline and CDP-ethanolamine are both required for phospholipid biosynthesis. There are several phospholipids which are significantly increased in the treated cells and the effect is most marked for the cells treated with 25  $\mu$ M cobalt suggesting that the capacity of the astrocytes to respond to cell membrane damage is greatest at the lowest concentration of cobalt.

The clearest effect of cobalt in astrocytes is in stimulating the anti-oxidant defence system and this might be expected from the observation that SIRT-2 is highly upregulated in the cells. Glutathione disulfide is an oxidised form of the thiol antioxidant glutathione. It is a disulfide formed from two glutathione molecules (Edwards *et al.*, 2017), and can be formed as a result of the reduction of peroxides such as  $H_2O_2$  and ROOH (Meister and Anderson, 1983). Increased glutathione disulfide is considered an important marker for oxidative stress, and has been detected in neurodegenerative diseases (Meister, 1988). Glutathione disulfide was decreased after exposure to lower concentrations of cobalt (at 25 and 50  $\mu$ M) for 72 hours in neuroblastoma cells, but it increased gradually at higher concentrations of cobalt (100, 150 and 200  $\mu$ M). This might be explained by the lower ability of neuroblastoma cells to respond to oxidative stress as indicated by the lower LD<sub>50</sub> value obtained in comparison with astrocytes. However, in astrocytoma cells there was a gradual increase in the level of glutathione disulfide from 2.85 (at 25  $\mu$ M of cobalt) to 9.75 (at 200  $\mu$ M of cobalt). Astrocytoma cells have a better oxidative

defense mechanism than neuroblastoma cells as part of their function as a component of the blood-brain barrier requires (Owen and Butterfield, 2010).

It is clear that the antioxidant defences in the astrocytoma cells are strong since GSH levels are maintained although the GSSG levels also increase markedly. This strong antioxidant defence is related to the increase in SIRT-2 discussed above. The pentose phosphate pathway is upregulated since sedoheptulose phosphate, 6-phosphogluconate and ribose phosphate are increased (Figure 3.32) and diversion of glucose into this pathway provides one of the major routes for converting NADP<sup>+</sup> into NADPH. NADPH is required for recycling GSSG recycling back into GSH via glutathione reductase. There is some evidence for increased glycolysis in response to cobalt treatment since glucose 1-phosphate, glucose 5-phosphate, glyceraldehyde phosphate and fructose biphosphate, which are all in the glycolytic pathway are all increased. This is reflected to some extent in the slightly increased levels of ATP in response to treatment. The use of cobalt to stimulate glycolysis is supported by this data but an increase in glycolysis contradicts the increased levels of SIRT-2 which is supposed to correlate with higher levels of HIF1- $\alpha$  which should promote oxidative phosphorylation and an increase in fatty acid oxidation and the TCA cycle. There is some evidence for increased TCA cycle activity particularly at the higher doses of cobalt since there is a marked increase in the levels of NADH at 150 and 200  $\mu$ M cobalt. In addition, the cobalt treatment elevated the levels of some acyl carnitines and also CoA suggesting increased levels of fatty acid oxidation. A number of partially oxidised fatty acids are elevated by the treatment.

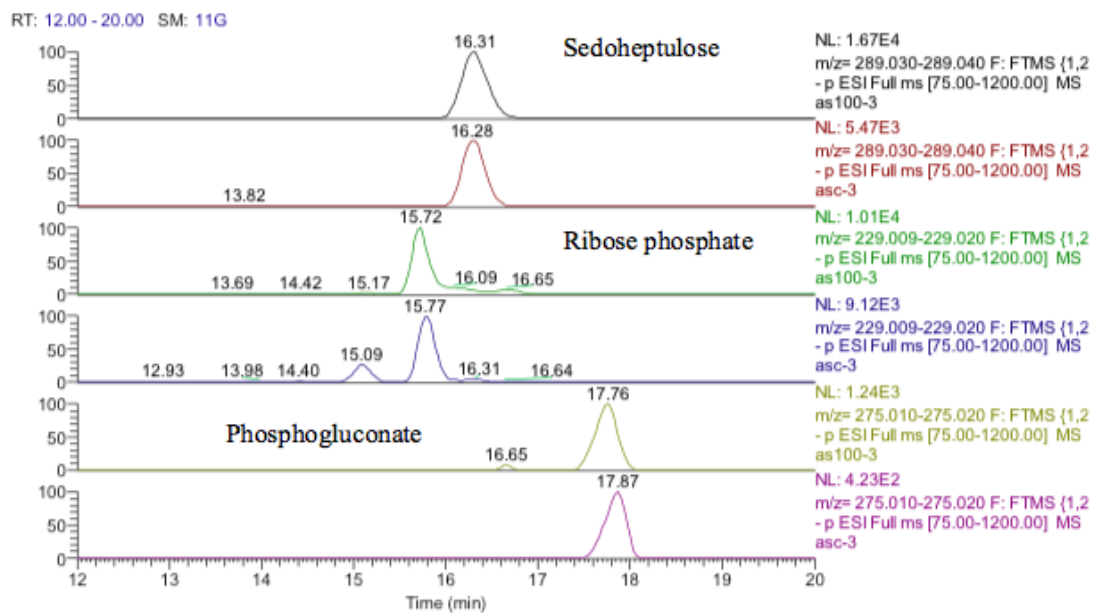


**Figure 3. 32** Extracted ion traces for increased pentose phosphate pathway metabolites, sedoheptulose, ribose phosphate and phosphogluconate.

**Table 3.1 Metabolomic changes in U-373 cells resulting from cobalt treatment.**

m/z	Rt(min)		Metabolite name	Ratio 25	p value	Ratio 50	p value	Ratio 100	p value	Ratio 150	p value	Ratio 200	p value
<b>Purines and Pyrimidines</b>													
112.0505	12.0	C4H5N3O	*Cytosine	1.852	0.002	2.131	0.004	2.069	0.002	1.333	0.109	1.997	0.027
115.0503	14.8	C4H6N2O2	5,6-Dihydrouracil	1.430	0.019	1.336	0.045	1.307	0.049	1.295	0.099	1.593	0.007
166.0721	9.9	C6H7N5O	*3-Methylguanine	2.430	0.034	1.745	0.005	2.458	0.053	1.459	0.077	2.110	0.008
243.062	9.9	C9H12N2O6	*Uridine	4.459	0.033	10.023	0.005	21.015	0.007	0.736	0.444	1.879	0.121
247.0922	15.8	C9H14N2O6	5-6-Dihydrouridine	1.323	0.005	1.300	0.007	1.287	0.009	1.008	0.937	1.133	0.170
259.092	12.9	C10H14N2O6	Hydroxythymidine	8.865	0.000	11.137	0.000	19.143	0.000	15.501	0.001	12.625	0.001
269.0872	11.0	C10H12N4O5	*Inosine	3.779	0.005	5.739	0.011	8.484	0.003	5.006	0.003	10.746	0.012
284.0984	12.8	C10H13N5O5	*Guanosine	2.226	0.016	2.986	0.012	2.079	0.020	1.323	0.259	1.873	0.126
<b>Oxidative stress</b>													
126.0217	14.9	C2H7NO3S	*Taurine	1.371	0.056	1.344	0.059	1.545	0.007	1.165	0.398	1.007	0.968
166.0537	13.2	C5H11NO3S	L-Methionine S-oxide	1.837	0.007	1.825	0.009	2.274	0.008	1.174	0.496	1.815	0.058
229.0114	15.1	C5H11O8P	D-Ribose 5-phosphate	1.032	0.927	1.217	0.004	1.099	0.003	1.157	0.609	1.931	0.190
289.0331	16.3	C7H15O10P	Sedoheptulose 7-phosphate	2.510	0.058	3.535	0.002	4.502	0.001	2.521	0.044	4.606	0.049
380.112	13.3	C13H21N3O8S	(R)-S-Lactoylgutathione	2.695	0.078	1.579	0.409	0.743	0.637	4.622	0.041	9.314	0.027
308.0903	14.3	C10H17N3O6S	*Glutathione	1.251	0.179	1.299	0.196	2.034	0.001	2.390	0.006	2.903	0.004
611.1448	17.4	C20H32N6O12S2	*Glutathione disulfide	2.850	0.042	3.485	0.019	4.888	0.048	4.152	0.020	9.741	0.029
744.0818	16.8	C21H29N7O17P3	*NADP+	1.292	0.078	1.331	0.095	1.540	0.011	1.833	0.011	2.446	0.008
<b>Energy Metabolism</b>													
168.9897	15.2	C3H7O6P	*Glyceraldehyde 3-phosphate	24.175	0.020	38.612	0.009	41.902	0.002	11.556	0.059	85.573	0.027
132.0766	14.8	C4H9N3O2	*Creatine	1.470	0.013	1.382	0.023	1.341	0.030	1.330	0.076	1.646	0.005
173.0207	15.8	C3H9O6P	Sn-Glycerol 3-phosphate	1.405	0.056	1.417	0.056	1.754	0.004	1.275	0.345	1.296	0.261
184.9853	16.8	C3H7O7P	3-Phospho-D-glycerate	4.600	0.097	6.265	0.047	7.848	0.010	1.034	0.924	2.095	0.109

212.0425	15.2	C4H10N3O5P	*Phosphocreatine	0.986	0.954	1.195	0.399	1.658	0.029	1.598	0.121	1.169	0.492
259.0222	17.4	C6H13O9P	*D-Glucose 6-phosphate	2.381	0.047	2.591	0.023	3.199	0.036	1.308	0.416	1.572	0.239
259.0223	16.8	C6H13O9P	*D-Glucose 6-phosphate	1.565	0.092	1.516	0.109	2.232	0.032	1.468	0.276	2.052	0.146
259.0223	16.1	C6H13O9P	*D-Glucose 1-phosphate	1.579	0.028	2.069	0.003	3.368	0.000	1.236	0.200	1.218	0.371
338.9888	18.0	C6H14O12P2	*D-Fructose 1,6-bisphosphate	2.924	0.129	4.183	0.037	6.481	0.010	27.505	0.075	23.177	0.094
428.0357	14.3	C10H15N5O10P2	*ADP	1.075	0.552	1.148	0.412	1.436	0.018	1.132	0.486	1.142	0.338
508.0029	16.7	C10H16N5O13P3	*ATP	1.305	0.113	1.376	0.061	1.541	0.010	1.252	0.279	1.338	0.135
664.1148	14.3	C21H28N7O14P2	*NAD+	1.266	0.124	1.262	0.127	1.553	0.017	1.201	0.322	1.282	0.138
666.1307	13.4	C21H29N7O14P2	*NADH	0.586	1.196	0.852	1.064	0.573	1.184	0.001	5.675	0.019	9.101
768.1211	13.7	C21H36N7O16P3S	*CoA	1.981	0.075	2.496	0.003	2.735	0.002	1.331	0.175	1.543	0.004
810.131	12.4	C23H38N7O17P3S	Acetyl-CoA	0.659	0.169	0.323	0.002	0.615	0.018	1.860	0.000	1.910	0.001
<b>Fatty acid metabolism</b>													
146.1173	13.5	C7H15NO2	4-Trimethylammoniobutanoate	1.454	0.043	1.443	0.056	1.551	0.016	1.292	0.212	1.393	0.159
162.1122	13.4	C7H15NO3	*L-Carnitine	1.375	0.060	1.353	0.094	1.415	0.046	1.179	0.403	1.155	0.487
232.1539	7.2	C11H21NO4	O-Butanoylcarnitine	2.189	0.078	2.400	0.092	2.488	0.010	1.094	0.811	1.496	0.253
260.1856	9.5	C13H25NO4	O-hexanoyl-R-carnitine	1.462	0.055	2.313	0.135	2.433	0.029	1.358	0.140	1.552	0.132
274.2007	7.1	C14H27NO4	Heptanoylcarnitine	1.505	0.126	1.234	0.430	2.017	0.016	1.200	0.510	1.538	0.139
286.2007	5.7	C15H27NO4	2-Octenoylcarnitine	2.063	0.124	0.657	0.348	0.141	0.019	0.924	0.852	1.020	0.970
290.1601	7.3	C13H23NO6	3-Methylglutarylcarnitine	1.006	0.958	1.081	0.415	0.808	0.017	0.917	0.202	0.829	0.023
<b>Nucleobase phosphates</b>													
323.0286	16.3	C9H13N2O9P	*UMP	1.566	0.030	1.653	0.032	1.719	0.005	1.354	0.238	1.847	0.071
324.0583	15.5	C9H14N3O8P	*CMP	1.330	0.136	1.345	0.103	1.622	0.014	1.409	0.174	1.732	0.044
362.0509	19.4	C10H14N5O8P	*GMP	2.835	0.051	3.919	0.006	6.686	0.011	2.957	0.036	4.305	0.037
402.9949	16.6	C9H14N2O12P2	*UDP	1.639	0.278	1.771	0.132	2.275	0.040	1.189	0.659	1.562	0.349
444.0316	17.6	C10H15N5O11P2	GDP	1.361	0.181	1.237	0.261	1.696	0.000	1.430	0.042	1.520	0.045
480.9816	16.1	C10H17N2O14P3	dTTP	1.963	0.036	2.085	0.025	2.393	0.002	1.170	0.708	1.560	0.295

483.9918	18.5	C9H16N3O14P3	*CTP	1.407	0.078	1.481	0.035	1.787	0.003	1.586	0.070	1.367	0.139
484.9758	17.9	C9H15N2O15P3	*UTP	1.484	0.041	1.495	0.034	1.675	0.004	1.417	0.113	1.499	0.094
<b>Tryptophan and nicotinamide metabolism</b>													
123.0555	7.4	C6H6N2O	*Nicotinamide	0.032	2.189	0.001	3.041	0.001	4.230	0.635	1.049	0.149	1.300
138.0547	15.1	C7H7NO2	Anthranilate	1.225	0.163	1.226	0.153	1.415	0.015	1.254	0.203	1.492	0.054
138.0547	12.9	C7H7NO2	Anthranilate	1.982	0.040	2.330	0.006	3.178	0.008	0.928	0.698	1.682	0.047
154.0496	13.3	C7H7NO3	3-Hydroxyanthranilate	1.979	0.000	2.079	0.005	2.132	0.001	0.834	0.315	1.385	0.177
161.1075	10.3	C10H12N2	Tryptamine	1.608	0.030	1.470	0.007	1.892	0.022	1.463	0.057	1.997	0.032
162.0549	7.2	C9H7NO2	Quinoline-3,4-diol	1.192	0.333	0.995	0.984	0.374	0.012	2.679	0.000	2.743	0.000
190.0496	7.1	C10H7NO3	Kynurenate	0.898	0.011	0.853	0.003	0.798	0.001	0.976	0.392	0.910	0.053
205.0967	11.8	C11H12N2O2	*L-Tryptophan	1.525	0.039	1.436	0.052	1.686	0.010	1.567	0.066	2.110	0.029
206.0811	13.2	C11H11NO3	Indolelactate	1.527	0.013	1.465	0.030	1.590	0.009	1.248	0.324	1.908	0.035
<b>Methylation</b>													
189.1597	22.3	C9H20N2O2	*N6,N6,N6-Trimethyl-L-lysine	2.306	0.029	1.593	0.002	1.811	0.007	2.026	0.008	2.924	0.002
385.1279	13.8	C14H20N6O5S	*S-Adenosyl-L-homocysteine	1.624	0.024	1.948	0.011	2.348	0.001	1.157	0.431	1.375	0.177
399.1444	16.6	C15H23N6O5S	*S-Adenosyl-L-methionine	1.153	0.174	1.135	0.255	1.190	0.123	1.402	0.012	1.530	0.006
<b>Sugar Metabolism</b>													
180.0862	15.7	C6H13NO5	D-Glucosamine	1.270	0.198	1.252	0.000	1.943	0.032	1.108	0.047	1.230	0.187
201.0156	12.9	C4H9O7P	D-Erythrose 4-phosphate	1.617	0.014	1.454	0.091	1.729	0.029	1.886	0.056	2.182	0.040
260.0526	11.9	C6H14NO8P	D-Glucosamine 6-phosphate	2.913	0.057	3.388	0.003	4.147	0.004	1.638	0.112	2.693	0.018
261.038	15.2	C6H15O9P	Sorbitol 6-phosphate	1.371	0.305	1.637	0.088	2.696	0.001	2.613	0.034	2.908	0.013
300.049	15.0	C8H16NO9P	N-Acetyl-D-glucosamine 6-phosphate	2.218	0.046	3.184	0.008	4.673	0.005	1.408	0.167	1.885	0.051
308.0989	13.3	C11H19NO9	N-Acetylneuraminate	2.309	0.002	2.485	0.003	2.570	0.000	1.112	0.717	1.543	0.226
535.0372	16.2	C14H22N2O16P2	UDP-D-xylose	1.637	0.022	1.642	0.024	1.860	0.003	1.562	0.115	2.404	0.033
565.0477	16.3	C15H24N2O17P2	*UDP-glucose	2.633	0.015	2.993	0.013	3.207	0.003	1.374	0.363	2.470	0.097
606.074	15.1	C17H27N3O17P2	*UDP-N-acetyl-D-glucosamine	0.408	1.289	0.611	1.180	0.201	1.480	0.111	2.225	0.098	2.155

Amino acids and their metabolites													
104.0709	16.7	C4H9NO2	*4-Aminobutanoate	0.822	0.280	0.800	0.241	0.558	0.001	0.958	0.685	0.753	0.140
104.1071	15.1	C5H13NO	*Choline	1.312	0.134	1.452	0.051	1.911	0.001	1.835	0.017	2.013	0.009
106.0501	10.5	C3H7NO3	L-Serine isomer	1.325	0.114	1.257	0.173	1.403	0.024	1.270	0.183	1.323	0.184
114.055	9.4	C5H7NO2	Pyrraline-5-carboxylate	1.239	0.041	1.275	0.004	1.285	0.014	1.050	0.502	1.047	0.484
116.0707	12.9	C5H9NO2	*L-Proline	1.510	0.019	1.436	0.017	1.603	0.004	1.503	0.045	1.743	0.030
120.0655	7.3	C4H9NO3	L-Threonine isomer	1.842	0.053	4.020	0.040	6.931	0.000	1.350	0.109	1.866	0.006
130.0497	14.6	C5H7NO3	L-1-Pyrraline-3-hydroxy-5-carboxylate	1.216	0.121	1.200	0.182	1.320	0.031	1.287	0.135	1.378	0.099
132.0303	19.4	C4H7NO4	L-Aspartate	1.780	0.031	2.127	0.002	2.535	0.000	1.841	0.031	2.113	0.010
132.1017	11.4	C6H13NO2	* IsoLeucine	1.491	0.030	1.393	0.034	1.530	0.028	1.277	0.186	1.665	0.029
139.05	23.0	C6H6N2O2	Urocanate	0.840	0.035	0.813	0.020	0.691	0.002	0.963	0.377	0.818	0.174
147.0762	15.2	C5H10N2O3	*L-Glutamine	1.132	0.266	1.191	0.105	1.287	0.008	1.200	0.197	1.272	0.041
150.0552	7.9	C8H7NO2	5,6-Dihydroxyindole	1.385	0.024	1.492	0.003	1.365	0.018	1.162	0.156	1.423	0.027
156.0765	15.4	C6H9N3O2	L-Histidine	0.809	0.082	0.703	0.010	0.500	0.001	0.360	0.000	0.390	0.000
156.0766	16.4	C6H9N3O2	L-Histidine	0.726	0.010	0.617	0.002	0.443	0.000	0.464	0.000	0.418	0.000
160.1331	13.5	C8H17NO2	DL-2-Aminooctanoic acid	1.564	0.021	1.444	0.056	1.590	0.047	1.234	0.287	1.262	0.273
166.0858	10.3	C9H11NO2	*L-Phenylalanine	1.527	0.028	1.433	0.039	1.731	0.020	1.402	0.094	1.771	0.027
174.1122	8.1	C8H15NO3	N-Acetyl-L-leucine	1.158	0.499	1.425	0.015	1.436	0.031	1.255	0.099	1.138	0.529
175.0962	4.2	C8H14O4	Suberic acid	1.354	0.044	1.407	0.032	1.324	0.023	1.014	0.914	1.210	0.281
175.1186	26.2	C6H14N4O2	*L-Arginine	1.654	0.004	1.585	0.001	1.841	0.013	0.937	0.635	0.985	0.923
178.0706	13.2	C6H11NO5	4-Hydroxy-4-methylglutamate	2.146	0.005	2.200	0.002	2.906	0.002	1.554	0.233	3.302	0.012
182.0813	13.1	C9H11NO3	*L-Tyrosine	1.557	0.022	1.486	0.031	1.667	0.010	1.219	0.413	1.861	0.029
184.06	13.5	C8H9NO4	4-Pyridoxate	2.154	0.001	1.972	0.006	2.709	0.034	1.441	0.164	1.595	0.110
184.0969	8.4	C9H13NO3	L-Adrenaline	1.361	0.041	1.470	0.011	1.930	0.002	1.471	0.003	1.599	0.000
190.0706	14.0	C7H11NO5	N-Acetyl-L-glutamate	1.657	0.033	2.005	0.005	2.409	0.001	2.456	0.003	3.083	0.006
197.0441	13.3	C9H8O5	3-(3,4-Dihydroxyphenyl)pyruvate	4.084	0.001	4.398	0.004	4.480	0.001	0.783	0.499	1.971	0.218

204.0864	13.1	C8H13NO5	N2-Acetyl-L-aminoadipate	2.159	0.073	2.770	0.003	3.343	0.004	1.247	0.483	2.203	0.051
291.1295	16.8	C10H18N4O6	N-(L-Arginino)succinate	2.501	0.043	2.345	0.051	2.067	0.026	1.105	0.785	1.152	0.750
<b>Fatty Acids</b>													
223.1701	4.2	C14H24O2	Tetradecadienoic acid	1.829	0.023	1.639	0.026	1.596	0.012	0.902	0.548	1.436	0.286
241.2172	4.2	C15H30O2	Pentadecanoic acid	1.511	0.016	1.557	0.024	1.464	0.010	0.932	0.643	1.514	0.173
247.1704	4.1	C16H24O2	Hexadecatetraenoic acid	1.865	0.023	2.131	0.019	2.083	0.012	1.127	0.564	1.615	0.160
265.1811	4.1	C16H26O3	Hydroxyhexadecatrienoic acid	2.086	0.007	2.370	0.013	2.226	0.007	0.532	0.047	1.234	0.513
267.1967	4.1	C16H28O3	Hydroxyhexadecadienoic acid	1.831	0.030	2.231	0.030	1.934	0.034	1.142	0.534	1.522	0.234
299.2021	4.2	C20H28O2	Retinoic Acid	1.980	0.064	2.813	0.041	2.109	0.022	0.947	0.823	1.739	0.159
299.2594	4.0	C18H36O3	Hydroxyoctadecanoic acid	2.718	0.177	2.569	0.105	2.003	0.018	1.118	0.812	2.437	0.256
301.2175	4.1	C20H30O2	Eicosapentaenoic acid	1.798	0.047	2.440	0.026	1.971	0.007	0.870	0.455	1.898	0.160
309.2802	4.1	C20H38O2	Eicosenoic acid	1.712	0.048	1.933	0.020	1.624	0.005	0.699	0.058	1.608	0.250
311.2958	4.1	C20H40O2	Eicosanoic acid	1.746	0.054	2.634	0.016	2.388	0.003	0.957	0.796	1.867	0.118
315.2541	4.1	C18H36O4	Dihydroxyoctadecanoic acid	2.339	0.053	2.622	0.021	2.513	0.005	0.979	0.928	1.387	0.341
317.2125	4.2	C20H30O3	Hydroxy eicosapentaenoic acid	1.888	0.044	2.509	0.052	1.977	0.039	1.003	0.989	1.598	0.242
327.2163	7.3	C18H30O5	Trihydroxylinoleic acid	0.988	0.868	0.888	0.492	0.584	0.001	0.861	0.072	0.854	0.095
333.2802	4.2	C22H38O2	Docosatrienoic acid	1.318	0.170	0.881	0.366	0.633	0.014	0.310	0.000	0.899	0.786
<b>Phospholipid Metabolism</b>													
184.0732	15.0	C5H14NO4P	Choline phosphate	1.288	0.073	1.337	0.063	1.504	0.007	1.599	0.019	1.684	0.020
216.0628	15.8	C5H14NO6P	GPE	1.450	0.057	1.543	0.027	1.741	0.009	1.289	0.302	1.367	0.186
258.1094	14.6	C8H20NO6P	GPC	1.259	0.123	1.250	0.151	1.355	0.042	1.320	0.141	1.333	0.123
383.2189	7.3	C17H35O7P	LGP 14:0	0.881	0.470	0.876	0.425	0.617	0.019	0.794	0.129	0.826	0.200
407.2206	4.8	C19H37O7P	Palmitoylglycerone phosphate	1.384	0.393	0.609	0.073	0.330	0.005	0.626	0.101	0.906	0.796
409.2362	4.2	C19H39O7P	LGP16:0	2.086	0.035	1.472	0.002	1.364	0.007	0.678	0.055	2.156	0.225
438.2993	4.2	C21H46NO6P	LPC 13:2	4.999	0.007	4.592	0.000	7.541	0.000	6.148	0.002	20.121	0.045
447.0672	16.4	C11H20N4O11P2	CDP-ethanolamine	1.706	0.026	1.811	0.018	1.923	0.011	1.620	0.062	1.911	0.065

466.3308	4.2	C23H50NO6P	LPC 15:2	4.428	0.004	4.073	0.001	5.939	0.001	4.403	0.003	15.371	0.047
478.2941	4.7	C23H46NO7P	LPE18:0	0.633	0.219	0.314	0.038	0.205	0.023	0.521	0.115	0.537	0.184
489.1136	15.4	C14H26N4O11P2	CDP-choline	1.358	0.098	1.416	0.046	2.009	0.010	1.819	0.028	2.302	0.007
496.3389	4.8	C24H50NO7P	LPC16:0	0.637	0.108	0.291	0.011	0.293	0.012	1.052	0.832	0.747	0.317
498.2632	4.7	C25H42NO7P	LPE20:5	0.791	0.484	0.319	0.021	0.199	0.011	0.650	0.170	0.453	0.054
500.2786	4.7	C25H44NO7P	LPE20:4	0.549	0.134	0.243	0.024	0.165	0.017	0.552	0.127	0.321	0.035
524.278	4.6	C27H44NO7P	LPE22:6	0.612	0.186	0.325	0.031	0.221	0.019	0.514	0.091	0.306	0.028
526.2945	4.6	C27H46NO7P	LPE22:5	0.491	0.127	0.245	0.036	0.130	0.022	0.377	0.066	0.176	0.026
528.31	4.6	C27H48NO7P	LPE22:4	0.459	0.118	0.237	0.042	0.104	0.024	0.335	0.064	0.155	0.029
616.4719	4.4	C34H68NO6P	SP 16:0	2.019	0.021	1.601	0.005	1.345	0.023	0.306	0.000	0.775	0.439
659.4666	4.2	C43H64O5	GL 40:10	2.591	0.027	2.091	0.018	1.581	0.025	0.628	0.157	1.980	0.239
673.4825	4.2	C37H71O8P	GP 34:1	2.032	0.016	1.723	0.010	1.447	0.027	0.576	0.063	1.812	0.244
687.4982	4.2	C45H68O5	GL 42:10	2.586	0.029	2.047	0.016	1.658	0.010	0.677	0.199	2.553	0.157
716.5246	4.2	C39H76NO8P	PE 32:1	2.445	0.039	1.995	0.012	1.566	0.015	0.424	0.015	1.907	0.337
724.4652	5.1	C36H69NO11S	Sulfogalactosylceramided18	1.410	0.307	2.297	0.026	2.953	0.008	0.940	0.871	0.918	0.806
744.5562	4.2	C41H80NO8P	PE 34:1	2.298	0.022	1.812	0.003	1.536	0.020	0.529	0.048	1.876	0.268
750.5454	4.1	C43H78NO7P	PE 38:5	2.485	0.023	1.775	0.008	1.511	0.047	0.717	0.347	2.847	0.173
752.5598	4.1	C43H80NO7P	PE 38:3 ether	3.928	0.010	2.849	0.001	3.674	0.001	1.736	0.308	12.287	0.083
760.584	4.2	C42H82NO8P	PC34:1	2.026	0.007	1.450	0.016	1.454	0.019	0.583	0.041	1.707	0.287
768.555	4.2	C43H80NO8P	PE38:3	2.585	0.014	1.947	0.001	1.568	0.026	0.625	0.213	2.453	0.207
786.1629	11.6	C27H33N9O15P2	FAD	0.998	0.989	1.047	0.769	1.413	0.040	1.148	0.441	1.388	0.049
788.6157	4.2	C44H86NO8P	PC36:1	2.179	0.005	1.480	0.018	1.608	0.008	0.497	0.087	2.470	0.198
800.6531	20.3	C46H90NO7P	PC38:1 ether	0.998	0.989	0.769	0.197	0.602	0.025	1.121	0.563	1.280	0.281
835.5306	20.8	C43H79O13P	PI34:2	1.127	0.519	0.704	0.140	0.463	0.008	1.089	0.655	1.153	0.596
1009.639	18.9	C50H92N2O18	Ganglioside GA2 (d18:1/12:0)	0.932	0.735	0.676	0.117	0.297	0.004	1.093	0.693	1.217	0.313

#### 3.4.6.2.2 Results and discussion of the metabolomic analysis of the nuclear DNA for astrocytoma cells

It was not clear from the metabolomic profiling of the cell extracts if damage to DNA was a major effect of cobalt treatment. The DNA samples were injected into the LC-MS using the same metabolomics method. The LC-MS data yielded the results shown in table 3.2. Again it is not possible to determine much from these results since apart from deoxyadenosine the typical DNA bases are at low levels in the digest. Deoxy guanosine is present at about 10% of the level of deoxyadenosine, thymidine is absent and deoxycytidine is only present in trace amounts. However, there appears to be methyldeoxycytidine and a large amount of hydroxymethyl deoxycytidine present in both the treated and control cells. The latter compound is isomeric with the RNA base 5-methylcytidine but the standard for 5-methylcytidine runs 5 minutes earlier than the putatively identified hydroxymethyldeoxycytidine. However, such modifications are rare in DNA (Foksinki *et al*, 2017) and it would be unusual to see such a high level of modification of the DNA thus it is possible that the hydroxymethyldeoxycytidine is an RNA base which has been methylated within the ribose portion of the molecule. It is difficult to decide on what this data means particularly since the methyl cytosines are high in the controls as well as the treated cells. Metabolomic profiling of purified DNA has only been carried out rarely and in view of the somewhat unusual findings it would be necessary to repeat this experiment to gain firm conclusions.

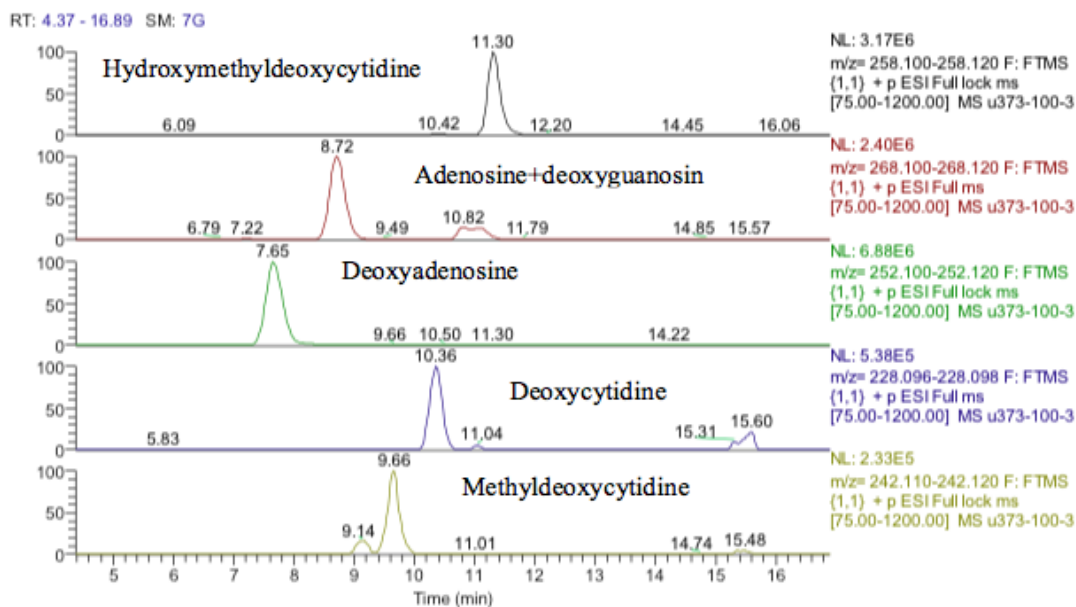


**Figure 3. 33** Extracted ion traces showing hydroxymethyldeoxycytidine, adenosine+deoxyguanosine, deoxyadenosine, deoxycytidine and methyldeoxycytidine.

**Table 3. 2** Metabolomic data derived from LC-MS of the nuclear DNA after separation from astrocytoma treated with cobalt at 25, 50 and 100  $\mu$ M and non-treated for 72 hours. (n=3).

m/z	Rt (min)	Structure	Metabolite name	25/C	p25/C	50/C	p50/C	100/C	p100/C
112.0506	10.3	C <sub>4</sub> H <sub>5</sub> N <sub>3</sub> O	Cytosine	1.388	0.100	1.308	0.144	1.129	0.560
126.0664	9.1	C <sub>5</sub> H <sub>7</sub> N <sub>3</sub> O	5-Methylcytosine	1.305	0.249	1.237	0.245	1.117	0.525
242.1137	9.7	C <sub>10</sub> H <sub>15</sub> N <sub>3</sub> O <sub>4</sub>	5-Methyl-2'-deoxycytidine	1.126	0.064	1.244	0.057	1.087	0.460
244.0929	12.2	C <sub>9</sub> H <sub>13</sub> N <sub>3</sub> O <sub>5</sub>	Cytidine	1.178	0.069	1.195	0.057	1.111	0.452
252.1083	7.7	C <sub>10</sub> H <sub>13</sub> N <sub>5</sub> O <sub>3</sub>	5'-Deoxyadenosine	1.271	0.181	1.173	0.171	1.058	0.722
253.0926	11.9	C <sub>10</sub> H <sub>12</sub> N <sub>4</sub> O <sub>4</sub>	Deoxyinosine	0.799	0.547	0.827	0.399	0.712	0.215
258.1078	11.3	C <sub>10</sub> H <sub>15</sub> N <sub>3</sub> O <sub>5</sub>	5-Methylcytidine	1.090	0.337	1.158	0.077	1.074	0.554
259.0925	14.8	C <sub>10</sub> H <sub>14</sub> N <sub>2</sub> O <sub>6</sub>	Hydroxythymidine	1.104	0.105	0.695	0.379	1.096	0.330
268.1035	11.1	C <sub>10</sub> H <sub>13</sub> N <sub>5</sub> O <sub>4</sub>	Deoxyguanosine	1.250	0.372	1.229	0.174	1.091	0.530
268.1039	8.7	C <sub>10</sub> H <sub>13</sub> N <sub>5</sub> O <sub>4</sub>	Adenosine	1.105	0.331	1.147	0.092	1.050	0.731

### 3.4.6.2 Metabolomics results for the neuroblastoma cells

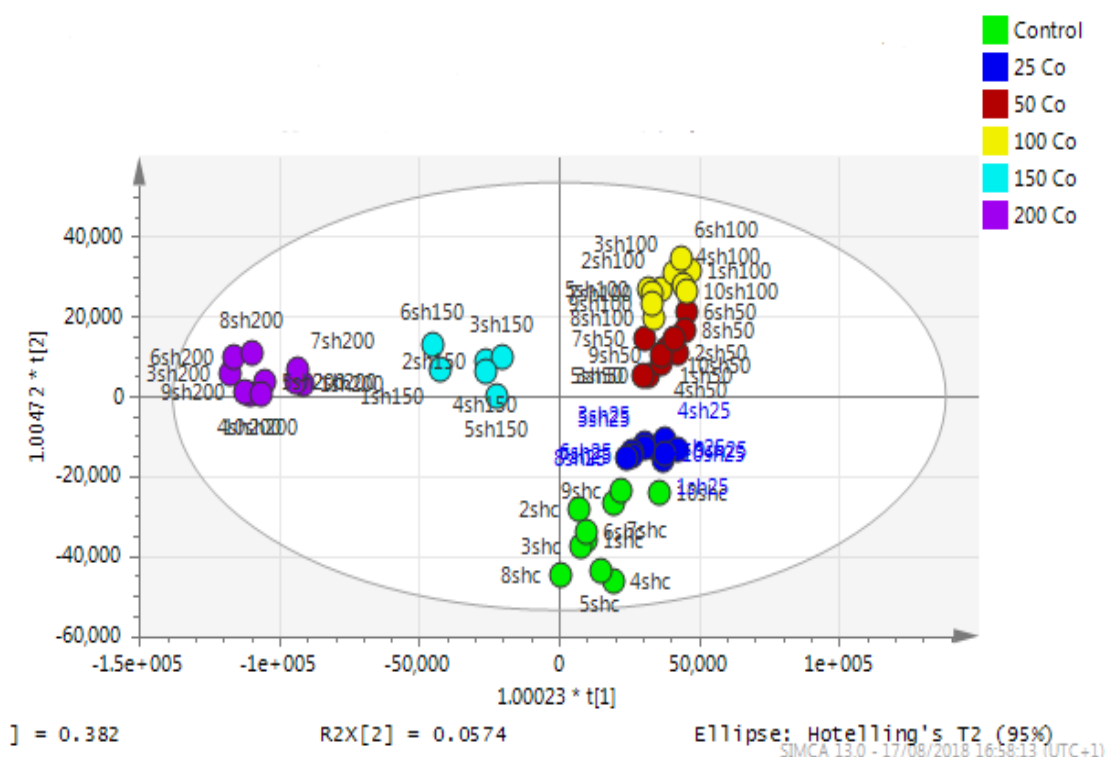


**Figure 3. 34 A PCA-X score plot of the separation between control and cobalt treated SH-SY5Y cells after 72 hours of incubation (n=3).**

Principal component analysis (PCA) showed clear differences between control and cobalt treated samples, and this became wider as the cobalt concentrations were increased. The samples showed some variation within replicates but there were no outliers. Neuroblastoma cells data were analysed using Simca-P to demonstrate geometrical separation and variation between treated and non-treated samples as illustrated in Figure 3.34. Table 3.3 summarises the changes in the metabolome of the neuroblastoma cells resulting from cobalt treatment. The effects on DNA and RNA bases are not as marked as in the case of the astrocytoma cells. The RNA bases uridine, cytosine and adenosine have a tendency to be upregulated but not consistently with dose. Again elevation of uridine and cytosine might be related to the formation of CMP choline and CMP ethanolamine for use in phospholipid

biosynthesis. There is evidence of oxidative stress with glutathione and GSSG being elevated increasingly with cobalt dose. As with the astrocytes there is an effect on glycolysis with ATP being increased markedly with cobalt dose. However, the really huge effect of cobalt is on some selected phospholipids, particularly ether lipids but also some acyl phospholipids. It is always important to check that the raw data reflects the extracted data particularly where changes are very marked and Figure 3.35 shows a control sample where PE 38:3 is absent but is readily seen and in the cobalt treated samples and increases with dose.

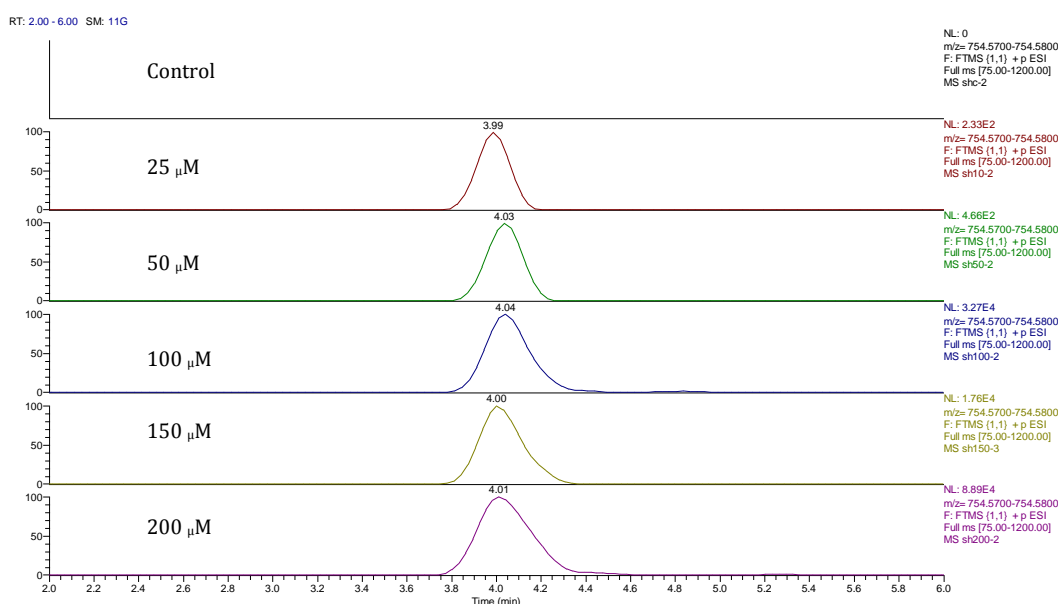


**Figure 3. 35**  
**Extracted ion traces for PE 38:3 ether showing effect of cobalt dose on its levels.**

Similarly Figure 3.36 shows the effect of cobalt dose on the levels of the acyl lipid PC 38:4 which increases about 1000 fold in response to the higher doses of cobalt.

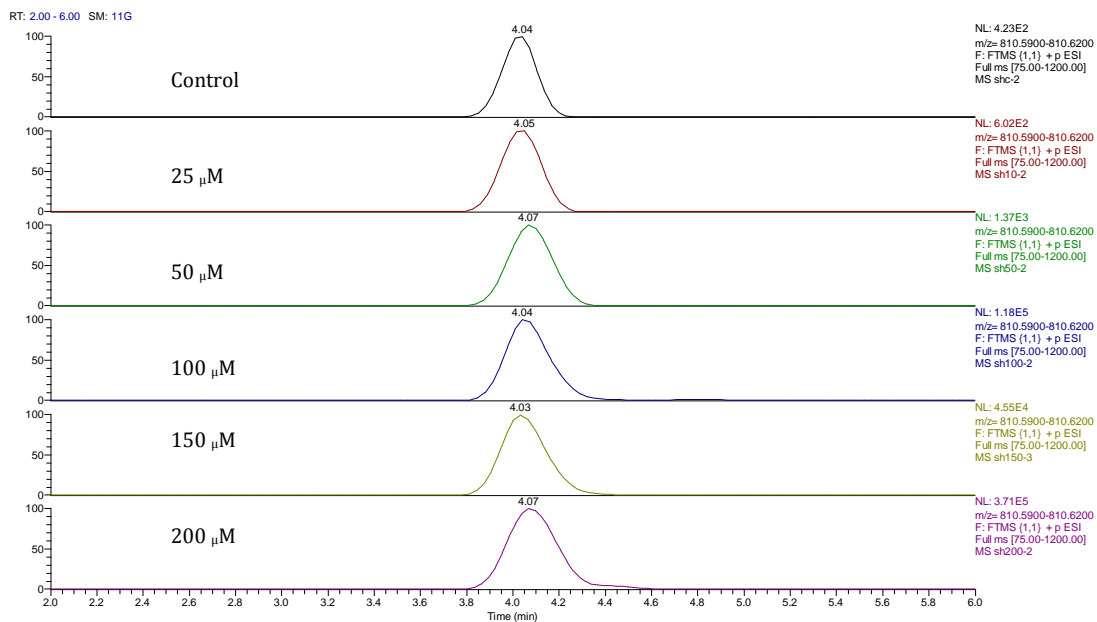


**Figure 3. 36** Extracted ion traces showing the effect of cobalt dose on the levels of PC 38:4.

It is clear the cobalt stimulates major changes in the cell membrane of the SH-SY5Y cells why it should stimulate this type of adaption is not clear.

**Table 3.3 Induced changes in SH-SY5Y cells after treatment with 0-200  $\mu$ M of Co for 72 hours (n=6). All data displayed were statistically significant (P value <0.05) compared with non-treated cells. Values in brackets represent the mean peak area of the metabolite in treated cells; there is no production of this metabolite in controls. \* Retention time from sample matches retention time from standard.**

m/z	Rt	Structure	Metabolite name	25/c	P value	50/c	P value	100/c	P value	150/c	P value	200/c	P value
<b>Nucleotide metabolism</b>													
126.0310	15.8	C4H5N3O2	5-Amino-4-imidazole carboxylate	0.997	0.987	9.832	0.368	0.762	0.032	0.863	0.140	0.571	0.000
129.0659	14.8	C5H8N2O2	5,6-Dihydrothymine	0.898	0.328	0.659	0.006	0.575	0.002	0.689	0.008	0.678	0.011
137.0455	15.3	C5H4N4O	Hypoxanthine	4.831	0.260	5.100	0.198	2.767	0.012	1.969	0.048	2.692	0.032
150.0423	12.3	C5H5N5O	*Guanine	2.157	0.315	1.474	0.192	2.017	0.214	1.155	0.658	2.657	0.012
151.0262	11.3	C5H4N4O2	*Xanthine	3.374	0.121	2.226	0.170	2.336	0.038	1.604	0.009	2.302	0.004
155.0094	10.2	C5H4N2O4	Orotate	0.794	0.051	0.324	0.000	0.415	0.000	0.076	0.000	0.060	0.000
157.0254	11.1	C5H6N2O4	(S)-Dihydroorotate	1.226	0.491	0.653	0.016	1.078	0.467	0.179	0.000	0.175	0.000
157.0367	13.8	C4H6N4O3	*Allantoin	0.939	0.674	1.940	0.015	1.343	0.390	2.330	0.002	2.192	0.003
175.0364	16.6	C5H8N2O5	N-Carbamoyl-L-aspartate	0.395	0.000	0.057	0.000	0.006	0.000	0.007	0.000	0.002	0.000
242.0786	11.9	C9H13N3O5	*Cytidine	2.338	0.086	1.300	0.135	1.155	0.201	0.963	0.635	1.227	0.046
243.0625	9.8	C9H12N2O6	*Uridine	2.922	0.056	1.603	0.171	1.444	0.057	0.707	0.019	0.712	0.006
268.1036	14.3	C10H13N5O4	*Adenosine	3.806	0.244	3.498	0.256	4.562	0.034	1.417	0.083	5.617	0.002
<b>Oxidative stress</b>													
126.0219	14.9	C2H7NO3S	*Taurine	0.833	0.383	0.398	0.000	0.241	0.000	0.206	0.000	0.105	0.000
229.0119	15.6	C5H11O8P	D-Ribose 5-phosphate	3.844	0.009	2.251	0.111	6.988	0.000	3.082	0.019	12.264	0.024
308.0908	15.3	C10H17N3O6S	*Glutathione	0.969	0.792	1.178	0.390	2.364	0.000	3.672	0.000	3.883	0.000
611.1449	17.3	C20H32N6O12S2	*Glutathione disulfide	4.952	0.148	5.064	0.008	4.589	0.004	7.124	0.010	13.580	0.009
<b>Energy metabolism</b>													
96.9697	15.2	H3O4P	Orthophosphate	1.552	0.140	2.347	0.076	6.403	0.001	3.631	0.012	6.057	0.000

130.0620	14.6	C4H9N3O2	*Creatine	1.349	0.317	0.773	0.128	0.690	0.015	0.743	0.011	0.516	0.000
171.0062	14.6	C3H9O6P	Sn-Glycerol 3-phosphate	0.772	0.142	0.402	0.000	0.303	0.000	0.548	0.000	0.565	0.000
176.9359	16.0	H4O7P2	Pyrophosphate	2.383	0.000	3.911	0.007	7.365	0.000	4.994	0.000	6.490	0.000
184.9857	16.7	C3H7O7P	3-Phospho-D-glycerate	1.756	0.094	1.724	0.087	7.521	0.015	3.814	0.009	9.725	0.016
210.0286	15.0	C4H10N3O5P	*Phosphocreatine	0.530	0.006	0.236	<0.001	0.017	0.000	0.374	0.001	0.137	0.000
259.0225	16.8	C6H13O9P	*D-Glucose 6-phosphate	1.930	0.232	2.544	0.013	15.295	0.000	4.871	0.164	19.284	0.019
338.9889	18.3	C6H14O12P2	*D-Fructose 1,6-bisphosphate	1.594	0.052	1.701	0.001	2.166	0.000	2.633	0.000	2.633	0.005
426.0210	16.4	C10H15N5O10P2	*ADP	3.487	0.000	7.161	0.000	6.746	0.000	9.034	0.008	8.423	0.000
505.9888	16.4	C10H16N5O13P3	*ATP	2.183	0.003	4.116	<0.001	6.899	0.000	6.681	<0.001	7.687	0.000
662.1025	14.1	C21H28N7O14P2	*NAD+	0.960	0.568	0.669	0.001	0.399	0.000	1.010	0.910	0.664	0.016
<b>Fatty acid metabolism</b>													
146.1173	14.5	C7H15NO2	4-Trimethylammoniobutanoate	18.695	0.221	16.337	0.012	2.866	0.043	30.222	0.002	3.784	0.002
202.1086	11.1	C9H18NO4	O-Acetylcarnitine	1.749	0.382	0.899	0.767	0.559	0.059	0.572	0.001	0.601	0.002
230.1400	8.8	C11H21NO4	O-Butanoylcarnitine	5.785	0.227	2.215	0.359	0.943	0.898	0.495	0.041	0.320	0.017
400.3422	4.7	C23H45NO4	[FA] O-Palmitoyl-R-carnitine	0.426	0.007	0.109	0.000	0.247	0.000	0.033	0.000	0.098	0.000
<b>Nucleobase phosphate</b>													
321.0489	12.9	C10H15N2O8P	dTMP	90.512	0.249	28.323	0.367	143.645	0.033	7.932	0.424	137.750	0.035
323.0288	15.0	C9H13N2O9P	*UMP	6.404	0.186	2.630	0.288	0.945	0.930	2.376	0.012	3.406	0.013
346.0563	13.7	C10H14N5O7P	*AMP	6.782	0.202	5.130	0.124	1.858	0.457	2.369	0.015	4.065	0.008
347.0401	15.3	C10H13N4O8P	*IMP	26.219	0.235	13.732	0.288	10.659	0.129	4.851	0.000	6.375	0.011
402.0113	16.9	C9H15N3O11P2	CDP	2.644	0.009	3.346	0.000	1.921	0.260	9.075	0.003	17.792	0.000
402.9953	16.3	C9H14N2O12P2	UDP	2.213	0.005	1.853	0.000	1.311	0.408	3.967	0.003	4.518	0.000
442.0175	17.7	C10H15N5O11P2	*GDP	2.570	0.037	2.887	0.001	1.803	0.215	4.082	0.000	6.835	0.001
481.9776	18.2	C9H16N3O14P3	*CTP	1.582	0.036	1.646	0.000	2.835	0.000	5.155	0.004	7.615	0.001
482.9617	17.7	C9H15N2O15P3	UTP	2.168	0.009	2.663	0.000	4.381	0.000	5.118	0.000	5.993	0.000
523.9983	19.4	C10H16N5O14P3	GTP	0.501	0.653	2.765	0.342	91.483	0.012	6.894	0.018	159.827	0.049

<b>Tryptophan and nicotinamide metabolism</b>													
121.0406	8.0	C6H6N2O	*Nicotinamide	1.639	0.263	1.340	0.135	2.595	0.012	1.780	0.002	2.882	0.001
140.0352	26.4	C6H7NO3	2-Aminomuconate semialdehyde	1.293	0.252	1.476	0.145	1.491	0.382	1.101	0.689	2.405	0.029
156.0304	13.5	C6H7NO4	2-Aminomuconate	2.622	0.014	4.696	0.004	5.651	0.057	4.278	0.013	5.236	0.023
164.0354	7.2	C8H7NO3	Formylanthranilate	0.893	0.139	0.733	0.000	0.521	0.000	0.692	0.002	0.509	0.000
223.0723	13.4	C10H12N2O4	3-Hydroxy-L-kynurenine	3.786	0.016	10.217	0.036	16.859	0.017	7.930	0.009	13.692	0.016
235.0727	26.5	C11H12N2O4	L-Formylkynurenine	1.699	0.364	3.820	0.024	6.126	0.001	3.706	0.032	10.235	0.028
<b>Methylation</b>													
102.0549	14.6	C4H7NO2	1-Aminocyclopropane-1-carboxylate	1.457	0.015	0.949	0.759	1.002	0.990	1.856	0.010	2.542	0.006
150.0579	12.6	C5H11NO2S	*L-Methionine	3.235	0.415	0.633	0.617	0.801	0.791	1.302	0.673	3.709	0.023
176.0386	16.1	C6H11NO3S	N-Formyl-L-methionine	0.498	0.012	11.168	0.398	0.089	0.001	0.091	0.001	0.047	0.001
205.1544	19.8	C9H21N2O3	3-Hydroxy-N6,N6,N6-trimethyl-L-lysine	2.492	0.402	0.604	0.701	1.137	0.896	3.173	0.083	15.563	0.001
218.0674	13.8	C8H13NO6	O-Succinyl-L-homoserine	6.059	0.072	6.285	0.003	4.102	0.018	5.734	0.002	3.042	0.032
<b>Sugar metabolism</b>													
117.0193	13.7	C4H6O4	*Succinate	3.223	0.024	7.183	0.000	14.067	0.005	6.857	0.003	12.175	0.012
119.0349	14.0	C4H8O4	D-Erythrose	6.168	0.157	10.283	0.208	5.881	0.015	2.860	0.077	5.066	0.005
179.0563	15.4	C6H12O6	*D-Glucose	1.975	0.006	6.072	0.232	3.680	0.004	2.364	0.023	3.554	0.000
181.0713	27.2	C6H14O6	D-Sorbitol	1.194	0.619	1.568	0.113	2.336	0.008	1.505	0.136	2.843	0.006
229.0119	15.6	C5H11O8P	*D-Ribose 5-phosphate	3.844	0.009	2.251	0.111	6.988	0.000	3.082	0.019	12.264	0.024
258.0388	14.6	C6H14NO8P	D-Glucosamine 6-phosphate	0.624	0.010	0.265	0.000	0.417	0.001	0.703	0.137	0.546	0.004
300.0493	14.8	C8H16NO9P	N-Acetyl-D-glucosamine 6-phosphate	1.602	0.172	1.168	0.228	1.469	0.000	1.546	0.067	2.465	0.008
341.1094	15.6	C12H22O11	*Sucrose	5.284	0.049	5.353	0.252	11.777	0.000	2.826	0.264	11.913	0.005
565.0481	16.2	C15H24N2O17P2	*UDP-glucose	1.060	0.430	0.747	0.037	1.061	0.334	1.762	0.000	1.906	0.000
606.0750	15.0	C17H27N3O17P2	*UDP-N-acetyl-D-glucosamine	1.178	0.366	0.841	0.087	0.968	0.650	1.954	0.000	2.345	0.000
<b>Amino acids and their metabolites</b>													
88.0403	14.9	C3H7NO2	*L-Alanine	0.893	0.500	0.796	0.258	0.973	0.883	1.541	0.044	2.097	0.006

102.0549	14.6	C4H7NO2	1-Aminocyclopropane-1-carboxylate	1.457	0.015	0.949	0.759	1.002	0.990	1.856	0.010	2.542	0.006
102.0558	14.0	C4H9NO2	4-Aminobutanoate	1.210	0.441	0.872	0.508	0.401	0.009	0.815	0.357	0.312	0.004
104.0354	15.1	C3H7NO3	*L-Serine	3.371	0.250	11.944	0.319	0.480	0.006	0.234	0.000	0.183	0.000
110.0273	15.0	C2H7NO2S	Hypotaurine	0.464	0.008	0.226	0.001	0.171	0.001	0.170	0.001	0.130	0.001
112.0403	14.0	C5H7NO2	(S)-1-Pyrroline-5-carboxylate	0.923	0.848	0.674	0.274	0.364	0.043	0.506	0.106	0.267	0.026
116.0706	14.4	C5H9NO2	*L-Proline	2.319	0.200	1.280	0.289	1.596	0.030	2.293	0.010	2.808	0.001
116.0717	12.5	C5H11NO2	*L-Valine	2.544	0.205	1.581	0.200	2.046	0.037	2.588	0.007	4.371	0.002
120.0655	14.4	C4H9NO3	*L-Threonine	1.231	0.284	0.731	0.213	0.772	0.253	1.502	0.053	2.592	0.004
128.0716	27.1	C6H11NO2	L-Pipecolate	0.928	0.814	0.611	0.274	0.153	0.021	0.296	0.043	0.221	0.033
130.0499	15.0	C5H7NO3	L-1-Pyrroline-3-hydroxy-5-carboxylate	1.308	0.040	1.115	0.115	1.220	0.016	1.864	0.000	2.259	0.000
130.0861	12.7	C6H11NO2	L-Pipecolate	5.706	0.294	1.368	0.574	2.226	0.211	4.665	0.001	8.024	0.001
130.0874	11.1	C6H13NO2	*L-Leucine	2.973	0.191	1.675	0.226	1.761	0.024	2.223	0.002	3.672	0.002
131.0825	22.9	C5H12N2O2	L-Ornithine	0.989	0.902	1.373	0.009	4.277	0.017	5.742	0.001	9.623	0.001
132.0304	16.6	C4H7NO4	*L-Aspartate	0.330	0.000	0.169	0.000	0.079	0.000	0.084	0.000	0.113	0.000
132.0304	16.6	C4H7NO4	*L-Aspartate	0.330	0.000	0.169	0.000	0.079	0.000	0.084	0.000	0.113	0.000
133.0610	15.2	C4H8N2O3	*L-Asparagine	1.409	0.184	0.862	0.550	1.041	0.766	1.582	0.002	2.772	0.000
136.0756	13.0	C8H9NO	*2-Phenylacetamide	3.100	0.277	0.970	0.970	0.983	0.981	1.821	0.291	5.453	0.029
137.0356	13.5	C6H6N2O2	Urocanate	0.713	0.444	0.201	0.031	0.118	0.021	0.121	0.021	0.147	0.024
145.0982	24.6	C6H14N2O2	*L-Lysine	2.091	0.108	1.331	0.205	1.981	0.041	1.904	0.003	2.865	0.011
146.1173	14.5	C7H15NO2	4-Trimethylammoniobutanoate	1.722	0.525	0.375	0.009	0.055	0.002	0.604	0.061	0.098	0.002
147.0760	15.0	C5H10N2O3	*L-Glutamine	1.328	0.132	1.192	0.437	1.836	0.001	2.390	0.000	3.699	0.001
156.0764	14.8	C6H9N3O2	*L-Histidine	1.157	0.400	0.630	0.047	0.515	0.017	0.216	0.002	0.302	0.003
161.0921	11.3	C6H12N2O3	D-Alanyl-D-alanine	6.649	0.202	5.298	0.192	2.331	0.581	5.766	0.116	14.809	0.029
164.0718	10.3	C9H11NO2	*L-Phenylalanine	1.404	0.176	1.210	0.095	1.618	0.037	2.399	0.002	3.859	0.001
173.0819	13.7	C8H14O4	Suberic acid	2.944	0.012	6.492	0.015	7.006	0.018	3.997	0.016	6.052	0.040
173.1043	26.2	C6H14N4O2	*L-Arginine	1.953	0.068	0.815	0.464	0.416	0.000	0.087	0.000	0.159	0.000

176.0559	10.9	C6H11NO5	4-Hydroxy-4-methylglutamate	5.410	0.231	3.452	0.212	3.280	0.263	15.466	0.068	50.017	0.003
178.0512	7.5	C9H9NO3	Hippurate	1.331	0.226	1.197	0.454	1.998	0.042	1.195	0.354	1.867	0.046
179.0351	11.3	C9H8O4	3-(4-Hydroxyphenyl)pyruvate	2.099	0.248	1.576	0.290	1.025	0.813	1.421	0.059	1.938	0.000
180.0661	13.0	C9H11NO3	*L-Tyrosine	1.781	0.371	0.930	0.566	1.550	0.151	1.955	0.002	3.569	0.002
202.0725	13.5	C8H13NO5	N2-Acetyl-L-aminoadipate	10.658	0.269	3.903	0.155	10.021	0.036	3.054	0.059	5.954	0.010
202.1086	11.1	C9H18NO4	*O-Acetylcarnitine	1.749	0.382	0.899	0.767	0.559	0.059	0.572	0.001	0.601	0.002
<b>Phospholipid metabolism</b>													
104.1070	19.8	C5H13NO	*Choline	10.267	0.230	1.139	0.907	1.721	0.502	5.950	0.042	20.031	0.006
184.0731	15.1	C5H14NO4P	Choline phosphate	1.152	0.286	0.810	0.229	1.076	0.489	1.697	0.002	1.742	0.002
445.0534	16.2	C11H20N4O11P2	CDP-ethanolamine	2.181	0.324	0.884	0.810	1.769	0.033	2.456	0.069	5.569	0.002
489.1153	15.3	C14H26N4O11P2	CDP-choline	3.875	0.214	2.268	0.406	2.405	0.075	2.445	0.001	5.964	0.000
494.3247	4.8	C24H48NO7P	Lyso PC 16:0	0.795	0.281	6.191	0.018	0.632	0.014	4.619	0.004	0.655	0.027
540.5364	4.0	C34H69NO3	SP 16:0	8.180	0.217	3.521	0.055	58.303	0.024	11.044	0.106	160.65	0.045
556.3057	4.3	C28H48NO8P	PC 20:4	0.385	0.005	0.003	0.000	0.000	0.000	0.000	0.000	0.000	0.000
622.6135	4.0	C40H79NO3	SP 22:0	0.391	0.366	1.430	0.764	98.445	0.010	19.749	0.139	319.91	0.047
650.6456	4.0	C42H83NO3	SP 24:0	0.770	0.737	2.975	0.337	158.34	0.005	28.975	0.105	521.02	0.026
673.4822	4.1	C37H71O8P	GP 34:1	2.202	0.518	4.976	0.239	506.08	0.000	167.16	0.092	735.88	0.007
740.5581	4.0	C42H78NO7P	PC 34:3 ether	<0.001	0.119	0.000	0.119	33.118	0.000	5.191	0.143	59.269	0.009
746.5680	4.0	C41H80NO8P	PE 34:1	1.140	0.724	1.471	0.255	50.110	0.000	6.371	0.080	83.962	0.017
746.6068	4.1	C42H84NO7P	PC 34:0 ether	2.630	0.497	31.645	0.054	2211.4	0.000	232.32	0.058	3573.5	0.017
748.5865	4.1	C41H82NO8P	PE 36:0	0.000	0.363	25.798	0.054	2512.5	0.000	262.11	0.076	4548.6	0.009
750.5433	4.0	C43H76NO7P	PE 38:6 ether	0.842	0.875	4.170	0.164	277.51	0.000	42.203	0.055	363.50	0.020
752.5591	4.0	C43H78NO7P	PE 38:5 ether	0.622	0.537	3.016	0.139	157.35	0.000	26.853	0.058	257.42	0.014
754.5750	4.0	C43H80NO7P	PE 38:3 ether	2.469	0.604	30.704	0.065	2531.3	0.000	449.17	0.052	4229.9	0.010
760.5844	5.2	C42H82NO8P	PC 34:1	0.707	0.500	1.028	0.949	29.491	0.008	5.211	0.134	67.083	0.007
768.5892	4.0	C44H82NO7P	PC 36:3 ether	0.688	0.671	8.604	0.087	767.92	0.000	112.91	0.069	1505.0	0.017

770.5691	4.0	C43H80NO8P	PE 38:3	0.406	0.476	5.596	0.134	462.46	0.000	78.203	0.085	743.57	0.013
774.5989	4.0	C43H84NO8P	PE 38:1	1.992	0.312	1.591	0.378	99.261	0.000	11.662	0.076	181.30	0.020
778.5747	4.0	C45H80NO7P	PE 40:6 ether	0.636	0.552	2.661	0.181	138.43	0.000	20.234	0.048	151.74	0.015
788.5443	3.8	C42H80NO10P	PS 36:1	0.504	0.100	0.761	0.285	30.434	0.003	4.560	0.096	30.130	0.027
794.6059	4.0	C46H84NO7P	PC 38:5 ether	0.442	0.542	6.947	0.142	685.23	0.000	113.49	0.058	1455.5	0.026
796.5855	4.0	C45H82NO8P	PE 40:4	0.583	0.493	2.645	0.196	177.54	0.000	32.480	0.068	306.31	0.008
810.6003	4.0	C46H84NO8P	PC 38:4	0.871	0.875	7.516	0.073	606.63	0.000	92.205	0.078	1126.3	0.017
885.5492	3.8	C47H83O13P	PI 38:4	0.343	0.034	0.566	0.146	22.911	0.007	5.785	0.066	45.801	0.043
<b>Fatty acids</b>													
101.0608	5.3	C5H10O2	Pentanoate	1.726	0.527	0.822	0.527	2.191	0.226	1.660	0.236	3.888	0.006
115.0765	4.9	C6H12O2	Hexanoic acid	1.125	0.623	1.216	0.350	1.695	0.019	3.029	0.005	4.852	0.000
127.0401	4.5	C6H8O3	Oxohexenoic acid	1.262	0.283	0.729	0.036	0.833	0.191	0.997	0.983	1.476	0.042
129.0922	4.7	C7H14O2	heptanoic acid	1.071	0.740	1.019	0.920	1.295	0.147	2.500	0.003	3.846	0.000
141.0921	4.9	C8H14O2	Octenoic acid	0.994	0.978	1.025	0.904	1.311	0.168	1.893	0.007	3.792	0.000
143.1079	4.6	C8H16O2	Octanoic acid	0.888	0.543	1.050	0.790	1.420	0.056	2.484	0.005	4.385	0.001
145.0506	13.5	C6H10O4	Adipate	2.951	0.007	5.326	0.005	7.865	0.016	4.187	0.005	6.135	0.012
145.0870	4.8	C7H14O3	Hydroxy-heptanoic acid	1.289	0.448	1.546	0.056	1.722	0.034	3.787	0.026	7.159	0.000
147.0662	7.7	C6H12O4	Dihydroxy-pentanoic acid	1.842	0.178	1.307	0.340	1.171	0.504	1.706	0.017	2.730	0.000
153.0922	4.6	C9H14O2	Nonadienoic acid	1.328	0.413	1.020	0.913	1.192	0.451	1.490	0.023	2.393	0.001
155.0715	31.8	C8H12O3	Oxooctenoic acid	0.820	0.717	0.906	0.854	0.453	0.181	0.241	0.039	0.261	0.037
157.0870	14.1	C8H14O3	oxo-octanoic acid	0.753	0.176	0.496	0.003	0.246	0.000	0.306	0.000	0.207	0.000
157.1236	4.3	C9H18O2	Nonanoic acid	0.894	0.724	0.836	0.577	0.963	0.897	1.458	0.156	2.683	0.007
159.0662	13.6	C7H12O4	Heptanedioic acid	2.562	0.009	4.639	0.009	7.040	0.022	3.934	0.015	5.878	0.031
171.0663	11.1	C8H12O4	Octanoic acid	1.727	0.033	1.627	0.037	2.240	0.028	7.495	0.029	14.733	0.000
171.1028	14.4	C9H16O3	Oxononanoic acid	1.044	0.876	0.847	0.560	0.581	0.056	0.681	0.156	0.534	0.019
173.0819	13.7	C8H14O4	Suberic acid	2.944	0.012	6.492	0.015	7.006	0.018	3.997	0.016	6.052	0.040

173.1183	4.7	C9H18O3	Hydroxy-nonanoic acid	1.499	0.275	1.530	0.056	1.427	0.190	2.255	0.012	4.040	0.000
175.0972	4.9	C8H16O4	Dihydroxy-octanoic acid	1.288	0.327	1.171	0.205	1.766	0.015	3.862	0.027	7.579	0.000
185.1181	4.8	C10H18O3	Oxodecanoate	1.164	0.607	0.994	0.973	0.978	0.912	1.083	0.672	1.684	0.004
187.1340	4.3	C10H20O3	Hydroxydecanoic acid	1.344	0.269	1.134	0.395	1.062	0.664	1.947	0.046	3.313	0.000
199.0971	4.9	C10H16O4	Decenedioic acid	1.536	0.229	1.405	0.247	1.533	0.126	2.449	0.008	3.783	0.000
199.1340	13.9	C11H20O3	Hydroxyundecenoic acid	0.969	0.903	0.490	0.112	0.053	0.005	0.374	0.033	0.027	0.005
201.1133	4.7	C10H18O4	Decanedioic acid	2.045	0.256	1.389	0.101	1.988	0.015	3.263	0.010	5.501	0.000
201.1497	4.4	C11H22O3	Hydroxy-undecanoic acid	1.140	0.501	1.164	0.485	1.356	0.103	1.785	0.013	3.061	0.000
211.1341	4.3	C12H20O3	Dodecenoic acid	2.117	0.306	1.362	0.245	1.418	0.197	1.527	0.005	2.271	0.000
211.1692	4.5	C13H22O2	Tridecadienoic acid	1.369	0.111	1.038	0.887	1.203	0.381	1.883	0.033	3.176	0.002
213.1498	4.3	C12H22O3	Oxododecanoic acid	1.361	0.406	1.039	0.848	1.051	0.787	1.044	0.802	1.592	0.005
215.1290	4.4	C11H20O4	Undecanedioic acid	1.671	0.265	1.204	0.345	1.288	0.150	1.856	0.010	2.233	0.013
215.1653	4.4	C12H24O3	Hydroxydodecanoic acid	1.938	0.256	1.231	0.356	1.415	0.061	2.312	0.010	3.658	0.000
217.1082	4.9	C10H18O5	Hydroxysebacicacid	1.354	0.253	1.261	0.096	1.455	0.030	2.184	0.015	3.543	0.000
221.0825	4.4	C12H14O4	Dodecatetraenedioic acid	0.863	0.296	0.978	0.853	1.348	0.022	2.299	0.005	3.720	0.004
227.1659	4.2	C13H24O3	Oxo-tridecanoic acid	1.854	0.355	1.238	0.479	1.311	0.329	1.315	0.246	2.004	0.003
229.1448	4.7	C12H22O4	Dodecanedioic acid	2.848	0.200	1.773	0.199	1.550	0.141	1.900	0.002	3.120	0.000
229.1811	4.2	C13H26O3	Hydroxy-tridecanoic acid	2.108	0.309	1.246	0.427	1.352	0.269	1.602	0.026	2.866	0.000
230.1400	8.8	C11H21NO4	O-Butanoylcarnitine	5.785	0.227	2.215	0.359	0.943	0.898	0.495	0.041	0.320	0.017
241.2176	13.3	C15H30O2	Pentadecanoic acid	0.740	0.466	0.405	0.071	0.227	0.029	0.269	0.034	0.227	0.029
243.1604	4.7	C13H24O4	Tridecanedioic acid	4.722	0.196	2.212	0.275	1.310	0.311	1.428	0.136	2.419	0.000
243.1970	4.1	C14H28O3	Hydroxytetradecanoic acid	2.971	0.305	1.484	0.391	1.501	0.285	0.931	0.743	1.663	0.011
245.1398	4.3	C12H22O5	Hydroxydodecanedioicacid	1.589	0.183	1.310	0.160	1.511	0.014	2.194	0.003	3.816	0.000
249.1848	4.3	C16H24O2	Hexadecatetraenoic acid	1.690	0.202	1.050	0.790	0.959	0.803	1.090	0.513	1.352	0.015
257.1764	4.4	C14H26O4	Tetradecanedioic acid	1.441	0.359	1.052	0.832	1.436	0.014	0.888	0.331	1.456	0.004
259.1913	4.4	C14H28O4	Dihydroxy-tetradecanoic acid	9.395	0.224	3.985	0.241	4.400	0.244	2.306	0.105	8.522	0.001

269.2127	3.9	C16H30O3	Oxo-hexadecanoic acid	1.966	0.259	1.975	0.186	2.980	0.043	2.978	0.031	3.415	0.004
273.1714	4.1	C14H26O5	Hydroxytetradecanedioic acid	1.934	0.068	1.517	0.047	3.121	0.000	4.402	0.012	10.418	0.001
273.2058	4.2	C15H28O4	Pentadecanedioic acid	0.670	0.269	0.205	0.009	0.021	0.004	0.029	0.004	0.000	0.004
277.2162	4.3	C18H28O2	Octadecatetraenoic acid	2.725	0.296	1.204	0.606	0.894	0.779	0.669	0.026	0.550	0.009
281.2473	4.2	C18H32O2	Linoleate	1.279	0.579	0.614	0.247	0.445	0.110	0.445	0.109	0.215	0.039
283.2628	4.2	C18H34O2	Oleate	1.557	0.439	0.838	0.342	0.784	0.462	0.490	0.014	0.347	0.003
284.2946	4.5	C18H37NO	Octadecanamide	0.659	0.053	0.700	0.010	0.719	0.007	0.602	0.000	0.664	0.001
285.2073	4.2	C16H30O4	Hexadecanedioic acid	3.392	0.270	1.670	0.364	1.585	0.347	1.032	0.892	1.617	0.029
291.1967	4.1	C18H28O3	oxo-octadecatrienoic acid	0.771	0.150	0.449	0.000	0.245	0.000	0.226	0.000	0.130	0.000
303.2318	4.3	C20H30O2	Eicosapentaenoic acid	1.990	0.257	1.107	0.793	0.993	0.977	0.834	0.221	0.605	0.009
307.2636	4.2	C20H34O2	Eicosatrienoic acid	2.208	0.404	0.607	0.120	0.410	0.014	0.403	0.000	0.139	0.000
313.2373	4.5	C18H32O4	Dihydroxy octadecadienoic acid	3.697	0.312	1.242	0.546	1.186	0.775	0.521	0.008	0.589	0.048
313.2735	4.1	C19H36O3	Oxo-nonadecanoic acid	0.628	0.371	0.077	0.000	0.124	0.000	0.021	0.000	0.059	0.000
323.1870	4.1	C18H28O5	Oxo-octadecatrienoic acid	11.560	0.200	5.573	0.096	8.792	0.061	10.526	0.009	21.092	0.002
327.2183	4.2	C18H32O5	Trihydroxy linoleic acid	7.232	0.253	2.444	0.266	3.558	0.315	1.521	0.271	2.996	0.018
341.1969	3.9	C18H30O6	Tetrahydroxy linolenic acid	18.610	0.166	11.308	0.108	12.328	0.053	13.634	0.015	29.874	0.001
345.2288	4.6	C18H34O6	Tetrahydroxy oleic acid	158.05	0.221	52.668	0.225	51.223	0.291	40.947	0.147	57.100	0.011
351.2162	4.3	C20H30O5	Trihydroxy eicosatetraenoic acid	2.363	0.246	1.295	0.517	1.467	0.250	0.983	0.941	1.922	0.027
353.2340	4.4	C20H34O5	Trihydroxyeicosatrienoic acid	16.607	0.305	8.452	0.287	12.092	0.336	2.781	0.218	4.877	0.034
353.3413	4.4	C23H44O2	Tricosenoic acid	0.689	0.327	1.363	0.101	1.808	0.006	2.189	0.000	2.148	0.000
355.3204	4.4	C22H42O3	oxo-docosanoic acid	1.089	0.661	1.350	0.224	1.881	0.003	1.771	0.042	1.795	0.033
365.1971	4.7	C20H30O6	Tetrahydroxy eicosapentaenoic acid	10.955	0.245	5.343	0.296	2.669	0.424	10.939	0.311	7.601	0.010
365.3422	4.4	C24H44O2	Tetracosadienoic acid	0.872	0.611	0.943	0.788	1.287	0.111	1.187	0.440	1.532	0.026
367.3567	4.4	C24H46O2	Tetracosenoic acid	0.887	0.638	1.102	0.658	1.596	0.017	1.784	0.012	1.687	0.004
400.3422	4.7	C23H45NO4	[FA] O-Palmitoyl-R-carnitine	0.426	0.007	0.109	0.000	0.247	0.000	0.033	0.000	0.098	0.000

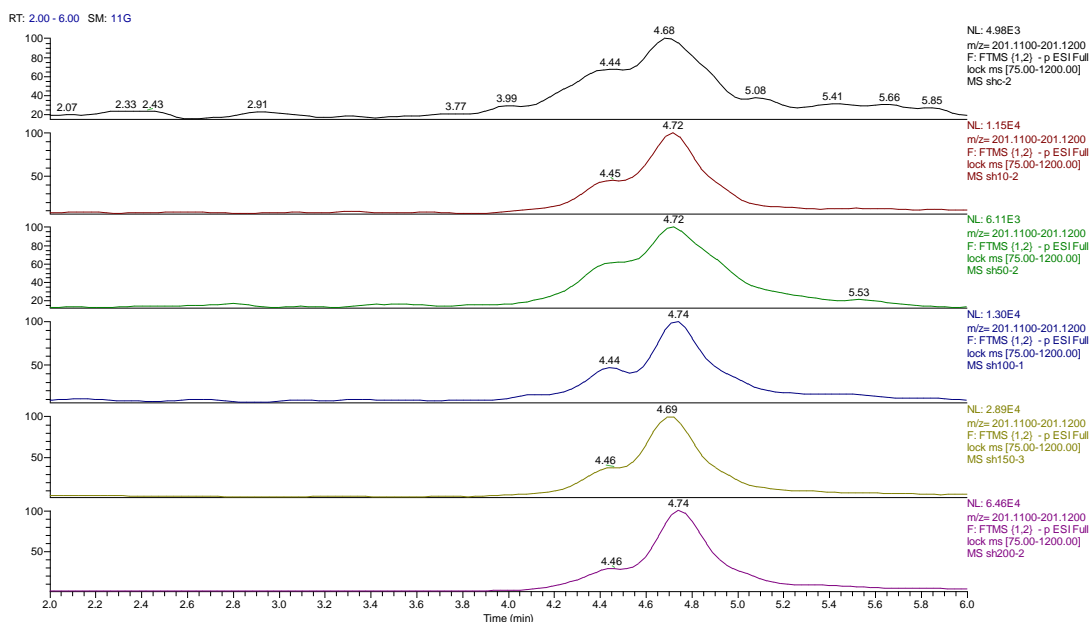


**Figure 3.37** Extracted ion traces for decandioic acid showing the effect of cobalt dose on its levels.

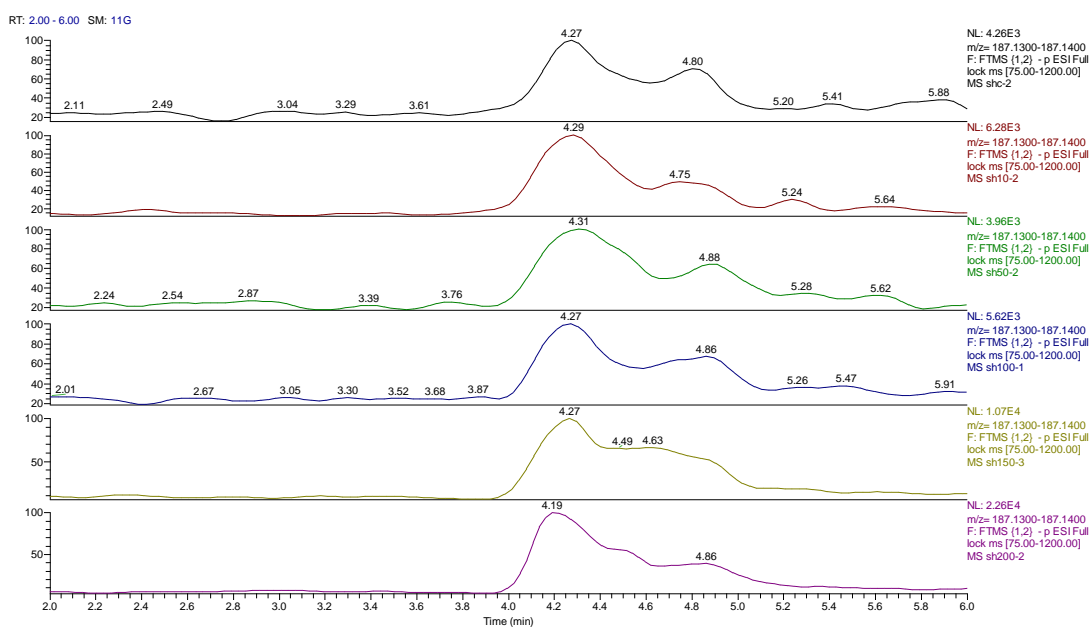


**Figure 3.38** Extracted ion traces for hydroxy decanoic acid showing the effect of cobalt dose on its levels.

In addition to the effect of cobalt on phospholipids it causes a general increase in levels of partially oxidised fatty acids. Many dioic acids are increased by the treatment. Dioic acids are produced by peroxisomal oxidation of long chain fatty

acids via hydroxylation in position 1 of the fatty acid chain (Wanders et al. 2006). Without a suitable standard it is not possible to specify the position of hydroxylation in the current data but many hydroxy fatty acids are also elevated. Figures 3.37 and 3.38 show extracted ion traces for decandioic acid and its corresponding hydroxyl acid. Although the peak shapes are not good the elevation of the two compounds with cobalt dose is clear.

**Table 3. 4 Metabolomic data derived from LC-MS of the nuclear DNA after separation from neuroblastoma treated (25, 50 and 100  $\mu$ M) and non-treated with cobalt for 72 hours. (n=3). \* Mean peak area, as the control sample value was zero. P represents P value for each concentration.**

m/z	Rt (min)	Structure	Metabolite	25/C	P25/C	50/C	P50/C	100/C	P100/C
150.0771	11.2	C <sub>6</sub> H <sub>7</sub> N <sub>5</sub>	Methyladenine	0.65	0.591	0.48	0.412	0.31	0.292
137.0459	9.4	C <sub>5</sub> H <sub>4</sub> N <sub>4</sub> O	Hypoxanthine	0.45	0.003	0.28	0.006	0.17	0.002
269.0876	10.9	C <sub>10</sub> H <sub>12</sub> N <sub>4</sub> O <sub>5</sub>	Inosine	0.65	0.189	0.36	0.074	0.29	0.058
136.0616	8.8	C <sub>5</sub> H <sub>5</sub> N <sub>5</sub>	Adenine	0.54	0.020	0.47	0.018	0.40	0.011
268.1039	8.8	C <sub>10</sub> H <sub>13</sub> N <sub>5</sub> O <sub>4</sub>	Adenosine	0.56	0.002	0.48	0.000	0.40	0.000
252.1087	7.7	C <sub>10</sub> H <sub>13</sub> N <sub>5</sub> O <sub>3</sub>	Deoxyadenosine	0.54	0.013	0.49	0.020	0.36	0.010
251.0791	15.5	C <sub>10</sub> H <sub>12</sub> N <sub>4</sub> O <sub>4</sub>	Deoxyinosine	0.50	0.683	0.59	0.723	0.39	0.605
483.9922	13.7	C <sub>9</sub> H <sub>16</sub> N <sub>3</sub> O <sub>14</sub> P	CTP	4.29	0.043	11.81	0.039	8.87	0.014
244.0931	12.1	C <sub>9</sub> H <sub>13</sub> N <sub>3</sub> O <sub>5</sub>	Cytidine	0.67	0.018	0.45	0.001	0.38	0.000
112.0507	10.5	C <sub>4</sub> H <sub>5</sub> N <sub>3</sub> O	Cytosine	0.52	0.041	0.37	0.032	0.26	0.021
126.0666	9.1	C <sub>5</sub> H <sub>8</sub> N <sub>3</sub> O	3-methylcytosine	0.53	0.004	0.37	0.004	0.27	0.001
331.0445	14.9	C <sub>10</sub> H <sub>11</sub> N <sub>4</sub> O	3',5'-Cyclic IMP	0	0.000	82453 45*	0.418	18211 030*	0.139
127.0502	6.7	C <sub>5</sub> H <sub>6</sub> N <sub>2</sub> O <sub>2</sub>	Thymine	0.57	0.073	0.56	0.083	0.40	0.041
129.0658	11.3	C <sub>5</sub> H <sub>8</sub> N <sub>2</sub> O <sub>2</sub>	5,6-Dihydrothymine	0.82	0.010	0.64	0.022	0.59	0.010
152.0564	11.1	C <sub>5</sub> H <sub>5</sub> N <sub>5</sub> O	Guanine	0.53	0.021	0.37	0.019	0.26	0.014
243.0619	10.0	C <sub>9</sub> H <sub>12</sub> N <sub>2</sub> O <sub>6</sub>	Uridine	5.12	0.114	10.56	0.119	5.75	0.289

From the analysis of the data obtained from the DNA digest the majority of the bases were decreased as the cobalt concentration was increased with the exception of uridine. However, cytidine triphosphate (CTP) was increased significantly by the treatment of cobalt at all concentrations (25, 50 and 100  $\mu$ M) after 72 hours of

incubation. CTP is a substrate used to synthesise RNA (Shih *et al.*, 2003) and it is not clear why CTP was increased here since it should not be a part of DNA and phosphatase treatment used during the isolation should have converted it to cytidine. Overall it is not possible to determine much from these data and it is likely that the digest procedure used failed to properly digest the DNA into its constituent nucleosides.

### **3.5 Conclusion**

Although the biological results using PCR suggested that DNA repair was upregulated when the cell lines were treated with cobalt there was not much evidence in the metabolomics results supporting this. This might be because the levels of DNA modification are very low and thus the metabolites resulting from base excision are not observed in an untargeted screen. In addition, although there were marked increases in gene transcription for the DNA repair enzymes the actual level of the expression of the proteins as judged from Western blotting was not much increased in comparison with controls.

Brain cells are continuously dealing with ROS production resulting from normal functions and they have different ways of defence against ROS and oxidative stress. These ways include antioxidant enzymes, such as glutathione peroxidase, superoxide dismutase and catalase (Agholme *et al.*, 2010; Christensen *et al.*, 2011). There is a clear effect of cobalt treatment on the astrocyte cells where SIRT-2 is upregulated and the antioxidant defence system is also upregulated as judged by increases in pentose phosphate pathway metabolites and glutathione and oxidised glutathione.

This is a much clearer effect than any effects of DNA damage from the cobalt. Amongst the nucleosides uridine is markedly increased and this might be related to its role in producing CMP-choline and CMP-ethanolamine for phospholipid biosynthesis and in the production of sugar conjugates such as UDP-glucose. There are some marked effects on phospholipids with specific phospholipids being elevated. Further work is required to characterise these phospholipids in more detail. The effects of cobalt on the neuroblastoma cells were similar to those on the astrocytes in so far as there were marked effects in increasing glutathione and GSSG. There were no clear effects on DNA bases. Where the neuroblastoma cells differed from the astrocytes was in the strong effect of the cobalt on phospholipids. Several phospholipids were hugely elevated by the treatments suggesting a re-modelling of the cell membrane. Some of the elevated lipids were common between the two cell lines. Again MS<sup>n</sup> experiments with more selective chromatography would be required to fully characterise these lipids. In addition cobalt appeared to stimulate peroxisomal proliferation in the neuroblastoma cells with many dioic acids which are typical markers of peroxisome proliferation being elevated.

### **3.6 Summary of findings**

The main findings of this chapter are:

- 1- The results of the MTT assay have shown that cobalt is toxic to the SH-SY5Y and U-373 cells with more potency on SH-SY5Y cells.
- 2- ROS measurement assay showed an increase in fluorescence in SH-SY5Y cells at 100  $\mu$ M of cobalt and in U-373 cells at 200  $\mu$ M of cobalt.

- 3- Metabolomic analysis of both cell lines (SH-SY5Y and U-373) showed that cobalt is inducing an intracellular change in both cell lines.
- 4- The metabolomic analysis of whole cell extracts showed an increase in metabolites associated with oxidative stress and glutathione oxidation pathways. The evidence for DNA methylation and hydroxy methylation was weaker.
- 5- The metabolomics analysis of the extracted DNA of both cells did not show conclusive changes in the levels of modified DNA. The lack of clear results might be due to the very low levels of this type of modification within DNA, the level of RNA contamination of the DNA sample and also possibly incomplete digestion of the sample.
- 6- The results of the RT-PCR experiment showed an increase in the genes (Mlh1, SERT2, MeCP2, UNG1 and TDG) in both cell lines after treatment with cobalt, and these genes were associated with the aforementioned pathways in both cell lines.

**Chapter 4 MEPHEDRONE  
METABOLISM IN NEURONAL  
CELL LINES, HEPATOCYTOMA  
AND PRIMARY RAT  
HEPATOCTYES, AND THE  
COMPARISON OF MEPHEDRONE  
METABOLISM IN FRESHLY  
ISOLATED HEPATOCTYES WITH  
CULTURED HEPATOCTYES**

---

#### **4.1 Abstract**

Mephedrone used to be called “legal high” which is beta-keto cathinone. Studies of the metabolism of mephedrone have revealed both Phase I and Phase II metabolites (Khreit *et al.*, 2013; Pozo *et al.*, 2015). In the current study three cell lines (HepG2, U373 and SH-SY5Y), hepatocytes and cultured rat hepatocytes were used to investigate the metabolism of mephedrone according to cell type. Cell lines were treated with 100  $\mu$ M of mephedrone for 6 days and primary rat hepatocytes were treated with the same concentration of mephedrone for 24 and 48 hours. The cells were extracted with a cold mixture of methanol:acetonitrile:distilled water (50:30:20) (v/v) before being centrifuged and injected onto the liquid chromatography-mass spectrometry-mass spectrometry (LC-MS<sup>2</sup>). Data were analysed with Xcalibur, Mzmine and Microsoft Excel.

Analysis revealed 14 metabolites in addition to the parent drug across the different cell lines. Mephedrone showed a time dependent metabolism profile. In addition, the abundance of each metabolite showed time dependence relation. Comparison of the metabolism of mephedrone in the cultured hepatocytes in comparison with the freshly isolated hepatocytes showed a different pattern due to impaired metabolism in cultured hepatocytes.

## 4.2 Introduction

### 4.2.1 Mephedrone

Mephedrone (4-methylmethcathinone) is a beta-keto cathinone of the phenethylamine family (NCBI). Mephedrone metabolism and pharmacokinetics have been studied in rats (Valente *et al.*, 2014) and in human cells (Martínez-Clemente *et al.*, 2012; Meyer *et al.*, 2010). Studies conducted *in vitro*, have revealed that CYP2D6 is responsible for oxidation of mephedrone (Pozo *et al.*, 2015; Papaseit *et al.*, 2016).

Mephedrone is characterised by its low bioavailability (Khreit *et al.*, 2013; Pedersen *et al.*, 2013) and fast metabolism (Martínez-Clemente *et al.*, 2013). The metabolic reactions described *in vivo* in humans were; amine group N-demethylation, keto group reduction, tolyl group oxidation, and glucuronidation and succinylation (conjugation) (Pozo *et al.*, 2015). A recent study has identified the following mephedrone metabolites; nor-mephedrone, 1-hydroxymephedrone and 4-hydroxymephedrone, and found that nor-mephedrone was an active metabolite in rats (Pozo *et al.*, 2015). Another more recent study was conducted on six human volunteers, and found that 4-carboxy-mephedrone and nor-mephedrone had the highest concentration in plasma among other metabolites within 2 hours post oral administration (Mayer *et al.*, 2016). The same study had investigated which metabolite has the ability to cross the mouse blood-brain barrier, and found that nor-mephedrone accumulated in the brains of mice 1 hour after of administration (Olesti *et al.*, 2017). This indicates that nor-mephedrone is an active metabolite that can cross the blood-brain barrier and affect the central nervous system (CNS) response in

mice. Additionally, Olesti et al quantified mephedrone metabolites in urine and revealed that 4-carboxy-mephedrone concentrations in urine were 10 times higher than mephedrone concentrations.

A study conducted in freshly isolated rat hepatocytes showed that mephedrone is extensively metabolised (Olesti *et al.*, 2017). Both Phase I and Phase II metabolites were detected and are illustrated below (see Figure 4.1 and table 4.1). In regard of phase II metabolism only glucuronidated metabolites were identified, and no sulphated metabolites were detected.

In this research the metabolism of mephedrone in different cell types was measured to help better understand its effects, and its metabolism by different cells in the body.

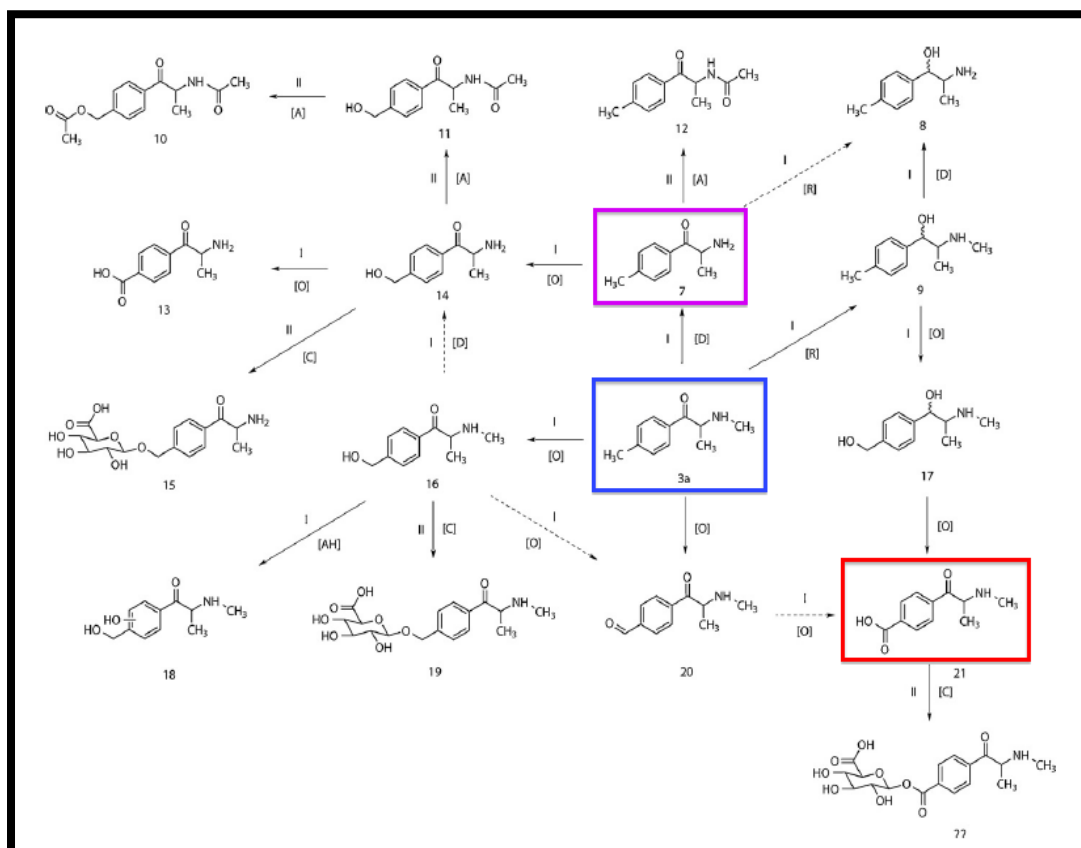


**Figure 4. 1** Possible routes for the Phase I and II metabolism of (±)-mephedrone (4-MMC, 3a) in Sprague-Dawley rat liver hepatocytes. Metabolite numbers correspond to the metabolite data presented in Khreit et al, 2013. Key: [A] = acetylation; [R] = reduction; [D] = demethylation; [O] = oxidation; [C] = conjugation; [AH] = aromatic hydroxylation. 3a in Blue Square is the parent mephedrone. Metabolite number 7 in Purple Square corresponds to nor-mephedrone, which is the most abundant metabolite in freshly isolated rat hepatocytes. Metabolite number 21 in red square correspond to carboxy-mephedrone, which is the most abundant metabolite in the cultured rat hepatocytes.

**Table 4. 1 Relative amounts of metabolites of mephedrone (4-MMC, 3a) formed after incubation with Sprague-Dawley rat liver hepatocytes (n = 3); Histograms represent percentage peak area  $\pm$ SD%. (From Khreit et al, 2013). Numbering system for metabolites corresponds to those in Figure 4.1.**

Treatment	4- MMC	12	10	20	19	15	U	14	9	7	11	8	21	16	18	13	17	22
% Peak area after 30 minutes	58.5	0.057	0.003	0.433	0.239	0.146	4.2	3.23	0.045	23.5	0.015	0.095	3.133	6.17	0.013	0.08	0.018	0.037
% Peak area after 120 minutes	16.03	0.46	0.13	0.989	1.16	1.03	0.7	1.4	0.015	59.4	0.053	0.597	12.9	2.57	0.149	1.81	0.063	0.37

#### 4.2.2 The use of cell lines and primary hepatocytes in metabolism studies

Cultured cell lines are known to express a lower level of cytochrome P450 enzymes compared to primary cells (Khreit *et al.*, 2013). The human liver derived cell line Hep G2 does not provide a good alternative to primary hepatocytes for drug metabolism due to their poor expression of cytochrome P450 (Donato *et al.*, 2008). Hepatocytoma cell lines have been proposed in many previous studies as an *in vitro* model for metabolism and toxicity investigations (Rodríguez-Antona *et al.*, 2002). In a study conducted on the hepatocytoma cell line, Hep G2, it was found that they expressed conjugating enzymes such as UDP-glucuronyltransferase, sulfotransferase and glutathione S-transferase (Donato *et al.*, 2008). However, and as shown in this research, Hep G2 cells did not provide a good alternative to primary hepatocytes in metabolism studies due to low expression of Cytochrome P450s (Donato *et al.*, 1994; Gómez-Lechón *et al.*, 2001).

Liver cells provide the major site for metabolism *in vivo*. They contain the main site for expression and activation of cytochrome P450 enzymes (Rodríguez-Antona *et al.*, 2002). However, neuronal cells were reported to have significant expression of Cytochrome P450 proteins, such as CYP2B6, CYP2E1, CYP1A1, CYP2D6, CYP1A2, CYP19 and CYP46 (Ravindranath and Strobel, 2013). Previous studies showed that the SH-SY5Y cells expressed significant levels of CYP1A1, CYP2B6 and CYP2E1 metabolism related genes (Ferguson and Tyndale, 2011; Dutheil *et al.*, 2009). Astrocytoma cell lines, such as U-373, have been used to represent the blood-brain barrier *in vitro* (Tripathi *et al.*, 2014), and they were used here to investigate whether or not mephedrone can be metabolised by blood-brain barrier cells.

Similarly, the neuroblastoma cell line, SH-SY5Y, was used to represent the neurons in the brain, to see if the neurons can metabolise mephedrone.

### **4.3 Aims and objectives**

This chapter aims to investigate the cultured primary rat hepatocytes as a model for mephedrone metabolism studies. To achieve this aim hepatocytes were cultured in 24-well plates for three different time periods. Another objective was to compare the profile of metabolites produced by cultured hepatocytes with the published profile of metabolites produced by the freshly isolated hepatocytes. The second aim was to investigate the ability of neuronal derived cell lines and hepatoma cells to metabolise mephedrone. To achieve this we investigate the metabolism in SH-SY5Y, U-373 and Hep G2 cells after treatment with mephedrone.

## **4.4 Materials and methods**

### **4.4.1 Materials**

#### **4.4.1.1 Cell lines and primary hepatocytes**

Cell lines (SH-SY5Y, U373, HepG2) were seeded at  $5 \times 10^4$  cells/well in a 24-well plate and incubated for 48 hours, and then treated with  $100 \mu\text{M}$  of mephedrone 6 days after the mephedrone was added the extraction of cells was performed.

Hepatocytes were prepared as described in section 2.1.2.2. Briefly, the cells were seeded at  $3 \times 10^5$  cells/well on a collagen coated (collagen coating density of  $25\text{-}\mu\text{g}$  collagen/ $\text{cm}^2$ ) 24-well plate and treated with  $100 \mu\text{M}$  of mephedrone after 24 hours from seeding the wells. Extraction was performed after 24 and 48 hours of incubation with and without  $100 \mu\text{M}$  of mephedrone at  $37^\circ\text{C}$  in an atmosphere of 95%  $\text{O}_2$  and 5%  $\text{CO}_2$ .

#### **4.4.1.2 Mephedrone**

Mephedrone was prepared at  $100 \mu\text{M}$  by dilution in medium, from the stock solution described in 2.1.1.4. Cell lines and hepatocytes were treated with mephedrone solution 48 and 24 hours, respectively, after seeding the 24-well plates.

## **4.4.2 Methods**

### **4.4.2.1 Extraction of cells**

Cells were extracted after incubation with mephedrone with 200  $\mu$ L of a precooled extraction solution made of 50% of methanol, 30% of acetonitrile and 20% distilled water. Cells were then scraped, transferred into Eppendorf vials and centrifuged before being injected in the LC-MS.

### **4.4.2.2 Method used for LC-MS analysis**

As described in chapter 2 section 2.7.

### **4.4.2.3 Statistical analysis**

Peak area % of each metabolite was calculated by dividing each metabolite peak area by the sum of all peak areas of the other metabolites and expressed the result as percentage.

## 4.5 Results and discussion

### 4.5.1 Comparison of mephedrone metabolism in freshly isolated hepatocyte with cultured hepatocytes

**Table 4. 2 Identified metabolites in cultured hepatocytes after 100  $\mu$ M mephedrone treatment for 6, 24 and 48 hours (n=6). In each case mephedrone was present without the times indicated, without a medium change. \* Metabolites are numbered in accordance with Khreit et al, 2013. \*\* ND stands for not detected. Data represent percentage peak area and relative standard deviation (RSD).**

Metabolite	Structure	M/z	M.Wt	Rt (min)	% Peak area					
					6 h	RSD	24 h	RSD	48 h	RSD
Mephedrone	C11H15NO	178.123	177.115	6.4	63	9.6	66.7	17.9	71.94	29.4
Nor-mephedrone (7*)	C10H13NO	164.107	163.0998	5.9	3.16	15.9	11.15	6.5	12.15	16.5
Dihydro-nor-mephedrone (8*)	C10H15NO	166.123	165.1153	15.9	ND**	-	0.17	20.9	0.28	12
4-hydroxymethyl-cathinone (14*)	C10H13NO <sub>2</sub>	180.1019	179.095	5.1	0.17	8.7	0.15	9.9	0.15	5
Dihydro-mephedrone (9*)	C11H17NO	180.138	179.131	5.5	0.29	20.5	0.42	16.2	0.46	27
Aldehyde (20*)	C11H13NO <sub>2</sub>	192.102	191.095	4.6	0.21	25.1	0.34	18.1	0.15	7.6
Hydroxytolyl-mephedrone (U*)	C11H15NO <sub>2</sub>	194.1177	193.1103	8.5	2.92	13.6	4.45	10.3	4.99	16.7
Acetyl metabolite (12*)	C12H15NO <sub>2</sub>	206.1177	205.1103	4.4	0.16	12.13	0.16	10.45	0.20	14
4-carboxy-mephedrone (21*)	C11H13NO <sub>3</sub>	208.097	207.0895	5.1	25.63	29.7	15.12	9.5	8.4	7.2
4-carboxy-dihydro-mephedrone (18*)	C11H15NO <sub>3</sub>	210.112	209.105	4.7	0.49	26.5	0.25	16.2	0.18	7.3
10*	C14H19NO <sub>4</sub>	266.139	265.131	14.4	ND**	-	0.02	21.7	0.02	10.5
11*	C12H15NO <sub>3</sub>	222.1125	221.105	4.9	0.76	29.4	ND**	-	0.39	4.8

<b>13*</b>	C10H11NO3	194.082	193.074	4.9	ND**	-	0.16	6.6	ND**	-
<b>15*</b>	C16H23NO8	358.149	357.142	7.4	3.20	20.6	0.75	11.2	0.71	13.8
<b>19*</b>	C17H24NO8	370.149	369.143	5.1	0.27	15.3	0.13	14.8	0.10	13.7

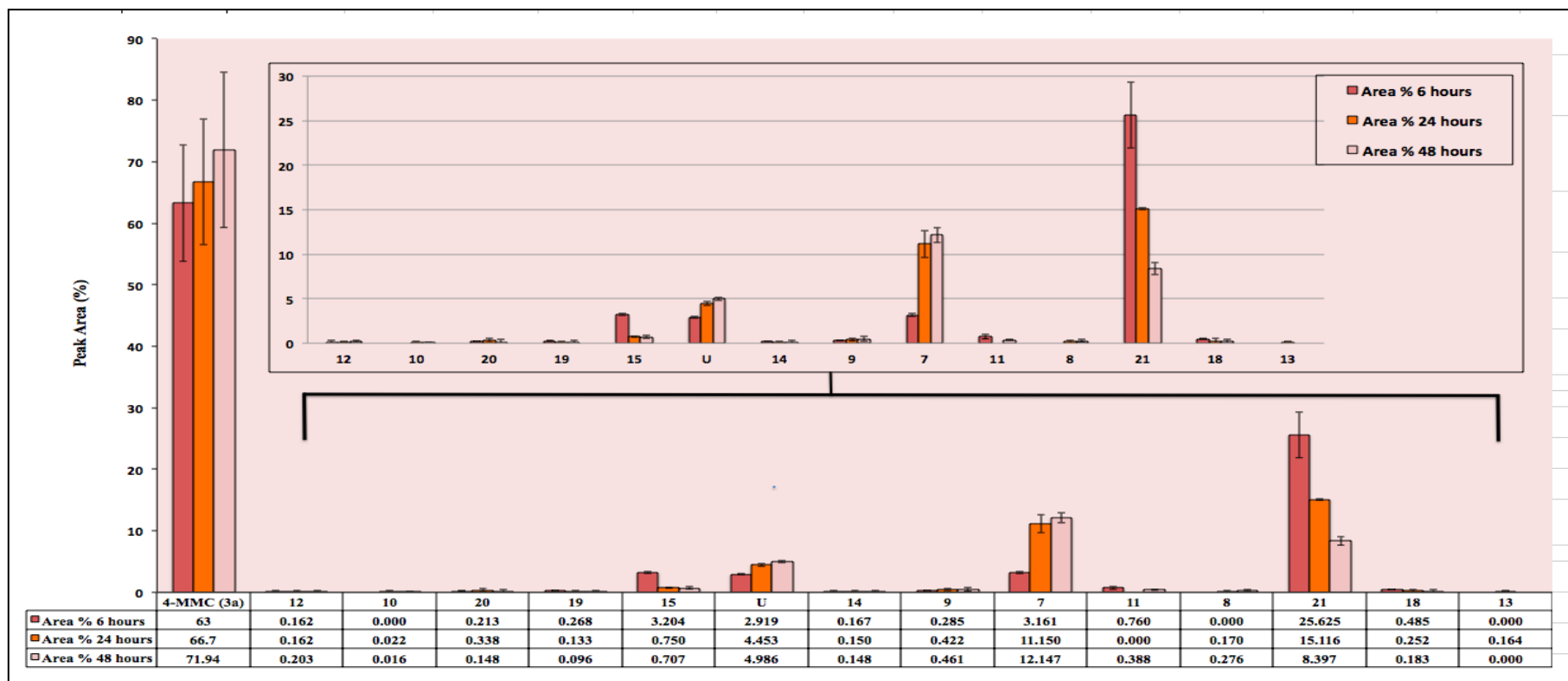


**Figure 4. 2** Relative amounts of metabolites of mephedrone (4-MMC, 3a) formed after incubation with cultured Sprague-Dawley rat liver hepatocytes (n = 3 rats); Histograms represent percentage peak area  $\pm$ SD%.

The data (see Figure 4.2) showed that metabolism of mephedrone in cultured hepatocytes was time dependent. For 6 and 24 hour incubation the most abundant metabolite was carboxy-mephedrone (metabolite number 21 in Figure 4.2), but after 48 hours incubation nor-mephedrone (metabolite number 7 in Figure 4.2) was formed to the largest extent. Nor-mephedrone and hydroxytolyl-mephedrone (metabolite U in Figure 4.2) formation increased as the incubation time increased, while carboxy-mephedrone showed the opposite pattern. Metabolite number 15 was highest in amount after a 6 hour incubation and then it dropped and stabilised at both time periods (6, 24 and 48 hours), suggesting further metabolism may have occurred, or that this was an intermediate metabolite.

Comparison of mephedrone metabolism by cultured rat hepatocytes with the published findings in freshly isolated rat hepatocytes showed that the metabolism pattern was different. The most abundant metabolite in freshly isolated hepatocytes after incubation with mephedrone for 30 and 120 minutes was nor-mephedrone (Toimela *et al.*, 2004). In contrast, carboxy-mephedrone was the most abundant metabolite in the cultured hepatocytes after incubation with mephedrone for 6 and 24 hours. This can be explained by the impairment of the CYP 450 enzyme system in the cultured hepatocytes. Pedersen *et al.* reported that the cytochrome P450 2D6 (CYP2D6) gene is the major enzyme responsible for metabolising mephedrone during *in vitro* Phase I metabolism (Khreit *et al.*, 2013).

All the metabolites identified in the freshly isolated hepatocytes incubations (120 minutes) were also detected in the cultured hepatocyte experiment, with the exception of metabolites number 17 and 22 (see Figure 4.2 and table 4.1).

Interestingly, similar to previous research finding (Pedersen *et al.*, 2013), metabolite 19 (mephedrone glucuronide) was identified.

This work has shown that cultured hepatocytes can metabolise mephedrone up to 48 hours producing a wide range of metabolites, but the rate of metabolism is slower than in freshly isolated hepatocytes and fewer metabolites are formed compared with freshly isolated hepatocytes probably as a result of CYP 450 enzyme system impairment.

Even though, the metabolism of mephedrone has been studied widely, only a few studies were conducted using cell systems (Khreit *et al.*, 2013). The majority of other articles studied urine or blood samples derived from human or rats (Pedersen *et al.*, 2013; Khreit *et al.*, 2013). Khreit et al have studied the metabolism *in vitro* in freshly isolated primary rat hepatocytes for short period of time (120 minutes). The current research studied the *in vitro* metabolism in the same cells for longer periods (6 h, 24 h and 48 h) in primary culture in collagen-coated plates. Despite the report of impaired metabolism described in literature (Meyer *et al.*, 2010; Pozo *et al.*, 2015; Linhart *et al.*, 2016), almost all the metabolites described in the previous research were detected in the current study, albeit at much lower levels. Additionally, it was shown that mephedrone metabolism *in vitro* was time dependent and the amount and number of metabolites detected changed according to the time point at which the cells were analysed.

## 4.5.2 Metabolism of mephedrone in neuroblastoma, astrocytoma and hepatocytoma

### 4.5.2.1 Metabolism in Human Astrocytoma Cells (U373)

**Table 4. 3 Metabolites identified in U373 cells after 100  $\mu$ M mephedrone treatment for 6 days (n=6). \* The number is related to the numbering order in previous study (Donato et al., 2008) and described in table 4.1. % peak represents the percentage of the amount of the metabolite relative to the sum of all metabolites detected.**

Metabolite	Structure	M/z	M.Wt	Rt (min)	% Peak area
Mephedrone	C11H15NO	178.123	177.115	6.39	98.3
Dihydro-mephedrone	C11H17NO	180.138	179.131	5.45	0.6
Hydroxytolyl-mephedrone	C11H15NO <sub>2</sub>	194.1177	193.1103	8.51	1.098
20* Aldehyde	C11H13NO <sub>2</sub>	192.1019	191.095	4.58	0.002

U-373 cells showed a low ability to metabolise mephedrone compared to the primary hepatocytes, as shown in tables 4.2 and 4.3, but they had a higher metabolic capacity than that either Hep G2 or SH-SY5Y cells.

Interestingly, it was noticed that a glycine-conjugated metabolite was detected to (% peak area of 0.002). Formation of a phase II metabolite means that astrocytoma cells have the ability to form molecules such as glycine in an attempt to eliminate toxic compounds. This is explained as a defensive mechanism of the glial cells (such as astrocytes), which form the first line of defence (blood-brain barrier) to protect the neurons. This finding is consistent with the previous research findings, which were conducted on the effect of toxic compounds (such as tert-butylhydroquinone and dimethyl fumarate) on astrocytes (Khreit *et al.*, 2013). In addition, another study investigated the effect of phenytoin on the CYP in astrocytes and found that astrocytes had the ability to degrade phenytoin to detoxify it before reaching the

neurons (Murphy *et al.*, 2001). Astrocytes were able to biotransform phenytoin as they have higher, compared to neuronal cells, expression of cytochrome P450, which act as a defensive chemical system to eliminate harmful substances (Meyer *et al.*, 2001).

#### 4.5.2.2 Metabolism in Human Neuroblastoma (SH-SY5Y)

**Table 4. 4 Identified metabolites in SH-SY5Y cells after 100  $\mu$ M mephedrone treatment for 6 days (n=6). % peak represents the percentage of the amount of the metabolite relative to the sum of all metabolites detected. All peaks are significant with p value <0.05.**

Metabolite	Structure	M/z	M.Wt	Rt (min)	% Peak area
<b>Mephedrone</b>	C11H15NO	178.123	177.115	7.67	89.3
<b>4-hydroxymethyl-cathinone</b>	C10H13NO2	180.102	179.095	5.31	10.7

The SH-SY5Y showed a weaker ability than the U-373 cells to metabolise mephedrone, since there was only one metabolite (4-hydroxymethyl-cathinone) detected as shown in table 4.4. It is noteworthy to illustrate that eventhough SH-SY5Y represent a good *in vitro* model for primary neuronal cells, they have lower expression of CYP2D6 which has an important protective role against neurotoxins (Mann and Tyndale, 2010). This fact can be responsible for the weak metabolism, as expected being a neuronal cells, observed in this research.

#### 4.5.2.3 Metabolism in Human hepatocytoma (Hep G2)

**Table 4. 5 Metabolites identified in Hep G2 after 100  $\mu$ M mephedrone treatment for 6 days (n=6). %peak area represents the percentage of the peak area of the metabolite relative to the sum of total peak areas of all metabolites detected.**

Metabolite	Structure	M/z	M.Wt	Rt (min)	% Peak area
<b>Mephedrone</b>	C11H15NO	178.123	177.115	7.67	99.95
<b>4-carboxy-mephedrone</b>	C11H13NO3	208.097	207.089	5.15	0.05

Hep G2 cells produced only one (phase I) metabolite, which is 4-carboxymephedrone (table 4.5). Interestingly, this metabolite was one of the most abundant metabolites produced by primary hepatocytes (see table 4.2 in section 4.5.1). The low metabolism activity observed here was expected as HepG2 cells were found to be poor model for *in vitro* metabolism in several studies (Dai *et al*, 1993; Chen and Cederbaum, 1998). This is explained by the lower expression of CYP2E1, which has an important role in metabolism (Cederbaum *et al*, 2001).

Overall, the low number and level of secondary metabolites seen in U-373, SH-SY5Y and HepG2 cells is an indicator that any effect observed after treatment with mephedrone is probably related to the parent drug (mephedrone).

#### **4.6 Conclusion**

In conclusion, cultured primary rat hepatocytes showed they were a good system for producing metabolites for mephedrone, especially after longer incubation periods. In addition, the metabolism profile changed with time in culture as a result of impaired metabolism in the cultured hepatocytes compared to freshly isolated hepatocytes. Metabolism of mephedrone has been shown to be time dependent, and the 48 hours metabolism profile was the closest to the *in vivo* metabolism profile. The research has also confirmed the ability of hepatic, glial and neuronal cell lines to metabolise mephedrone and it gave a profile for each cell type. Although the amounts of metabolites formed were very small apart from neuroblastoma cell line where substantial amount of 4-hydroxy methyl cathinone was formed.

The findings of this chapter can be summarised in the following points:

- 1- The culture of the primary rat hepatocytes proved to be acceptable method for metabolism studies for mephedrone, with consideration of the weaker metabolism and changed profile according to the duration of incubation.
- 2- Hepatoma (Hep G2) cells showed very weak metabolism of mephedrone compared to primary hepatocytes.
- 3- Neuronal derived SH-SY5Y cells have shown weaker metabolism of mephedrone with less number of metabolites produced compared to astrocytoma (U-373) cells.

**Chapter 5 MEPHEDRONE EFFECTS  
ON HUMAN NEUROBLASTOMA  
AND ASTROCYTOMA CELLS**

---

## **5.1 Abstract**

Mephedrone is an illegal drug that is used recreationally. Few studies have been conducted to investigate the mechanisms by which mephedrone is harming the cell. In this research we investigated the effect of mephedrone using toxicology coupled with LC-MS/MS based metabolomics in the two CNS derived cell lines, hepatocytoma cell line and in primary rat hepatocytes. A concentration of 100  $\mu\text{M}$  of mephedrone was used in the metabolomic analysis, because at this concentration mephedrone had induced several intracellular changes. Major pathways detected were oxidative stress, altered metabolism of neurotransmitters and glutathione oxidation.

## **5.2 Introduction**

### **5.2.1 Mephedrone effect on CNS**

Mephedrone was found to block the reuptake of dopamine and serotonin in rat brain (Baumann *et al.*, 2012; Hadlock *et al.*, 2011), and increased rat locomotor activity (Motbey *et al.*, 2012) and to induce euphoria and stimulate sexual abilities in rats (Kehr *et al.*, 2011). Den Hollander suggested that mephedrone is acting by oxidative stress in SH-SY5Y cells (den Hollander *et al.*, 2014).

### **5.2.2 Mephedrone stability**

Mephedrone stability in comparison to other cathinones has been investigated in limited studies (Johnson and Botch-Jones, 2013; Sørensen, 2011; Tsujikawa *et al.*, 2012; Maskell *et al.*, 2013; Busardò *et al.*, 2015). It showed a weaker stability (degraded by 75% in day 4 and was not detected in days 7 and 14 in blood samples) compared to 3,4-methylenedioxypropylamphetamine (MDPV), N-benzylpiperazine (BZP) and 1-[3-(trifluoromethyl)phenyl]piperazine (TFMPP) when stored at room temperature (+22°C) for different periods of incubation (1, 2, 4, 7 and 8 days) in different matrices (blood, plasma and urine) (Johnson and Botch-Jones, 2013). In the same study mephedrone was significantly degraded at longer periods (7 and 8 days). This previous finding and the fact that, in this research, mephedrone was incubated in the medium at 37°C for up to 7 days should be taken in consideration when interpreting the results in longer incubations.

### **5.3 Aims and objectives**

The primary aim of this section of the research was to study the toxicity and effect of mephedrone directly on human neuroblastoma and astrocytoma as representative cells to human brain cells. This approach was used to investigate the direct effect of mephedrone on brain when drug users take mephedrone directly (by inhalation). A secondary aim of this section of the research was to investigate the effect of mephedrone on liver by the use of cultured rat primary hepatocytes.

### **5.4 Materials and methods**

All materials and methods were described in chapter 2 sections 2.1.1.4, 2.1.2.2.3, 2.1.2.2.4 and 2.2.

## 5.5 Results and discussion

### 5.5.1 The effects of mephedrone on viability measured by MTT, NR and LDH viability assays

#### 5.5.1.1 MTT assay

To study the effect of mephedrone on cells metabolic activity, MTT assay was performed on both cell lines (neuroblastoma and astrocytoma) after treatment with a range of concentrations of mephedrone for 48 hours see Figure 5.1.

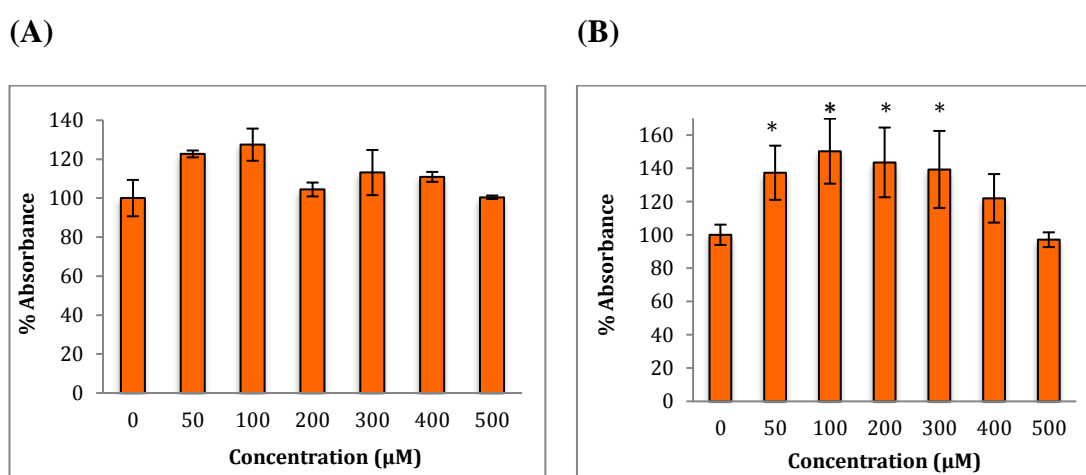


**Figure 5. 1 MTT assay measured in (A) SH-SY5Y cells and in (B) U-373 cells after 48 h. Results are percentage values (Mean  $\pm$  SD, n = 6) where 100% corresponds to control values. Cells treated with mephedrone in culture medium throughout the experiment. Data were analysed using one-way ANOVA followed by Tukey test. \* Data were significantly different from their relevant control P value <0.05.**

The MTT assay has shown that mephedrone at low concentration (100  $\mu$ M) raised metabolism up to 127% and 150% in SH-SY5Y and U-373 cells, respectively. This is thought to be an adaptive response in response to mephedrone-induced stress on the cells similar to that observed with exposure to other substances (e.g. Chromium) in previous studies (Zijlstra *et al.*, 2012; Posada *et al.*, 2015). Thereafter the activity drops again to reach levels around 100%.

### 5.5.1.2 NR assay

Both cell lines (neuroblastoma and astrocytoma) were treated with a range of concentrations of mephedrone for 48 hours, and NR assay was performed on the cells to see the effect on the cell count see Figure 5.2 below.

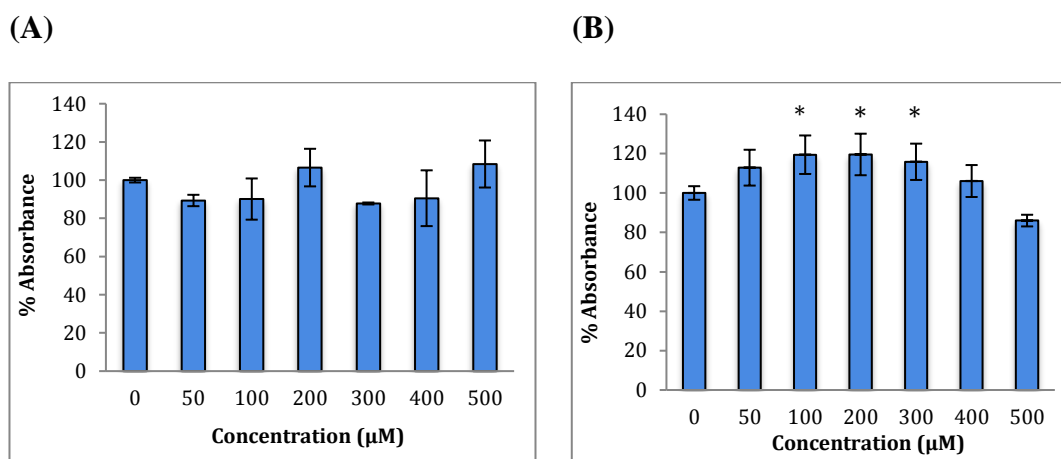


**Figure 5. 2 Neutral red assay measured in (A) SH-SY5Y cells and in (B) U-373 cells after 48 h. Results are percentage values (Mean ± SD, n=6) where 100% corresponds to control values. Cells treated with mephedrone in culture medium throughout the experiment. Data were analysed using one-way ANOVA plus Tukey test. \* data were significantly different from their relevant control P value <0.05.**

The NR assay showed no significant effect of mephedrone, over a range of concentrations, on the growth rate of SH-SY5Y as shown in Figure 5.2. For the U-373 cells there was gradual increase in cell number as we increased the concentration of mephedrone up to 300 µM. Cell growth started to decline at the 400 µM and 500 µM concentrations of mephedrone.

In conclusion, it is suggested that SH-SY5Y and U-373 cells, in a protective response, began to enhance protein levels when some substances are added. In the MTT assay, both cell types increased metabolic activity after mephedrone treatment. The SH-SY5Y cells have not shown any increase in NR assay in the 100 µM wells.

In contrast, in the U-373, the increased activity was observed at both assays (NR and MTT), with higher increase in the metabolism activity. This can be explained by the additional protection ability of U-373 to increase cell numbers, as they represent astrocytes, which play a role in protecting neuronal cells.

### 5.5.1.3 LDH assay

LDH assay results of neuroblastoma and astrocytoma cells after treatment with 100  $\mu$ M of mephedrone for 6 days are shown in table 5.1.

**Table 5. 1 LDH release 6 days after treatment of SH-SY5Y and U-373 cells with 100  $\mu$ M mephedrone (n=3). Data represent absorbance  $\pm$  standard error.**

SH-SY5Y	Treatment	LDH activity (nmol/ml/min) $\pm$ STD
	100 $\mu$ M of mephedrone	5.98 $\pm$ (0.01)
Control	5.74 $\pm$ (0.006)	
U-373	Treatment	LDH activity (nmol/ml/min) $\pm$ STD
	100 $\mu$ M of mephedrone	4.01 $\pm$ (0.01)
Control	4.00 $\pm$ (0.007)	

From the results in the table 5.1 we can conclude that there were no significant differences in LDH activity between the 100  $\mu$ M mephedrone treated and the non-treated cells in either cell type.

LDH release measurement is a good indicator of cellular damage and the integrity of cell membrane. Though, since the results showed no significant increase in both cell types, we can conclude that mephedrone at this concentration and time of exposure did not have a strong impact on the integrity of the cell membrane in these cells.

### 5.5.1.4 Morphology

The visual examination by microscope for both cell types (neuroblastoma and astrocytoma) before and after treatment with 100  $\mu$ M of mephedrone for 6 days, is shown in Figure 5.3.

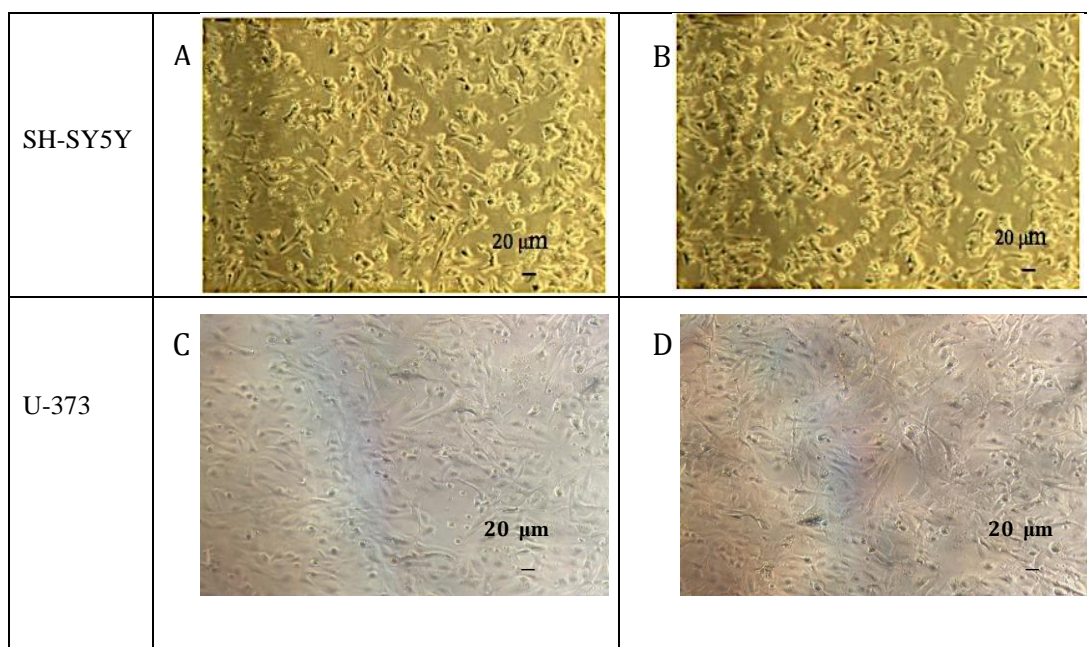


**Figure 5. 3 Morphology of SH-SY5Y (A and B) and U373 (C and D) cells after 6 days incubation without mephedrone treatment (A and C), and with mephedrone (B and D). Pictures were taken by the Motic AE31 microscope-20 power dry lenses.**

Examination of the morphology (see Figure 5.3) for both cell types showed no sign of abnormal proliferation after treatment with 100  $\mu$ M mephedrone.

We can conclude from the morphology examination that there was no significant change in the shape of the cells as a result of mephedrone treatment at this concentration and time of exposure in SH-SY5Y and U-373 cells.

## 5.5.2 Metabolomics in all cell types in-vitro

The metabolomic analysis showed significant changes in metabolites inside both cell types after mephedrone treatment as shown in Figures 5.4 and 5.5 and tables 5.2 and 5.3.

### 5.5.2.1 Effect of mephedrone on the metabolomes of SH-SY5Y neuroblastoma cells

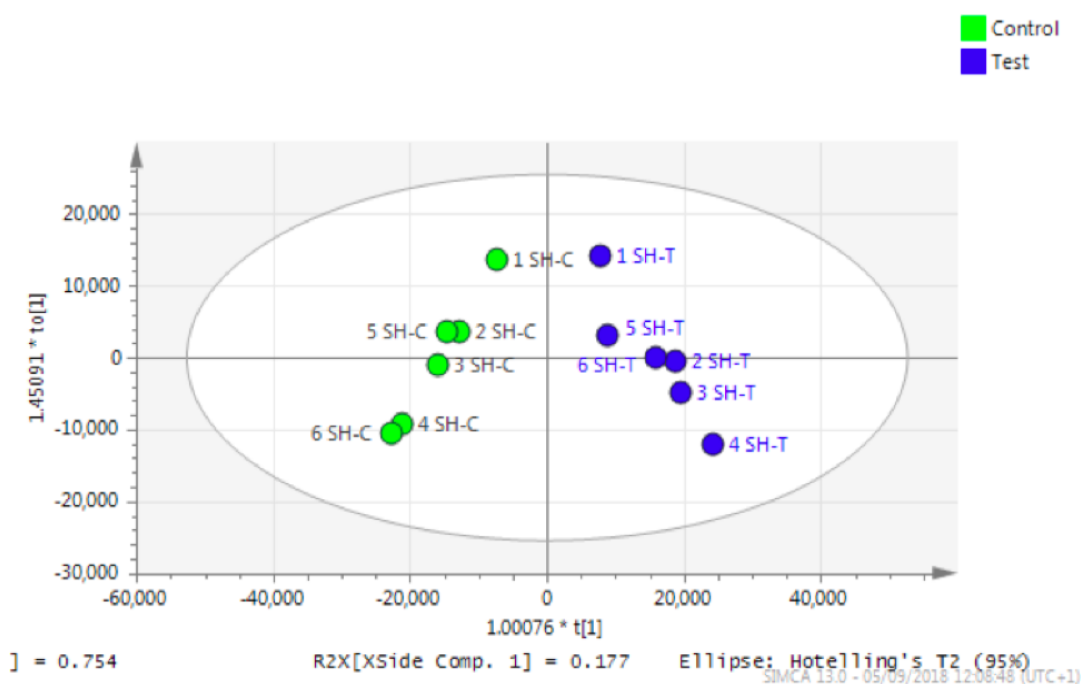
The metabolomic analysis results of neuroblastoma cells after treatment with 100  $\mu$ M of mephedrone for 6 days are shown in table 5.2.

**Table 5. 2 Metabolomic results of SH-SY5Y cell line after incubation with 100  $\mu$ M mephedrone for 6 days (n=6). Values indicate ratio of (treated/non-treated) peak areas of metabolites. \* Mean peak area of samples treated with mephedrone only as mean peak area value of control samples was zero.**

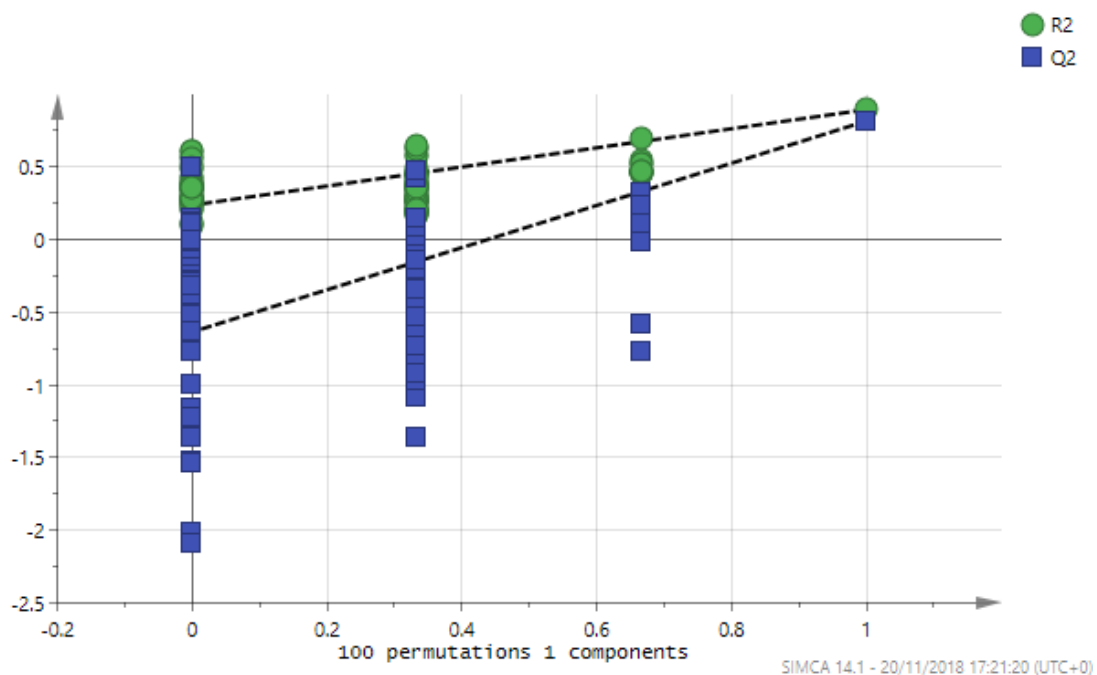
Rt (min)	M.Wt	Structure	Metabolite name	Meph/c	P- value
15.1	119.05824	C4H9NO3	L-Threonine	1.27	0.038
10.5	122.04801	C6H6N2O	Nicotinamide	1.35	0.045
17.9	130.02661	C5H6O4	Mesaconate	1.98	0.044
15.5	129.04259	C5H7NO3	Oxoproline	2.01	0.039
11.6	131.09463	C6H13NO2	L-Leucine	1.53	0.041
15.6	146.06914	C5H10N2O3	L-Glutamine	1.65	0.005
15.6	148.07356	C6H12O4	Methyl,hydroxymethyl,hydroxy-pentanoic acid	1.40	0.020
12.1	149.05105	C5H11NO2S	*L-Methionine	1.49	0.043
21.2	155.06948	C6H9N3O2	L-Histidine	1.44	0.046
16.5	158.06914	C6H10N2O3	4-Methylene-L-glutamine	1.33	0.038
12.3	204.08988	C11H12N2O2	L-Tryptophan	1.43	0.040
10.3	217.13141	C10H19NO4	O-Propanoylcarnitine	1.36	0.018
4.5	222.08921	C12H14O4	Dodecatetraenedioic acid	0.46	0.035
4.4	244.16746	C13H24O4	Tridecanedioic acid	2.07	0.008
23.2	264.10448	C12H17N4OS	Thiamine	1.90	0.041
5.1	287.28243	C17H37NO2	Heptadecaspinganine	0.02	0.037
4.3	351.31373	C22H41NO2	Eicosadienoyl-ethanolamine	1.47	0.025
4.3	353.32938	C22H43NO2	Eicosaenoyl)-ethanolamine	2.29	0.015
17.3	426.08791	C13H22N4O8S2	S-glutathionyl-L-cysteine	- (130050)*	0.027

Table 5.2 shows ratio (mephedrone treated cells/non-treated cells) for the most significant changed metabolites after treatment of SH-SY5Y neuroblastoma cells with mephedrone.

Separation between the control and test groups is shown in Figure 5.4.



**Figure 5. 4 OPLS-DA score plot of neuroblastoma (SH-SY5Y) treated with mephedrone (blue) and non-treated (green). Test stands for treated samples and control stands for non-treated samples.**



**Figure 5. 5** Permutation analysis of the OPLSDA model for mephedrone treated and non-treated astrocytoma cells. Validation of the model was performed with 100 permutation tests.  $R_2$  represent the goodness of the fit and  $Q_2$  represent the predictive capability.

**Table 5. 3** CVANOVA statistics for the OPLS-DA model for astrocytoma cells treated and non-treated with mephedrone.

	SS	DF	MS	F	P-value	SD
<b>Total correlation</b>	11	11	1			1
<b>Regression</b>	8.96	4	2.24	7.697	0.0105	1.497
<b>Residual</b>	2.038	7	0.29			0.54

Orthogonal partial least squares-discriminant analysis (OPLS-DA) score plot exhibited in Figure 5.4 shows that there was a geometrical separation between treated and non-treated samples. It can be concluded that treatment with mephedrone has produced significant changes in the metabolome of the treated samples compared with the metabolome of the non-treated samples. The changes were further investigated to identify which metabolites were mostly affected and to what extent their amounts were altered, by the following metabolic analysis.

In SH-SY5Y mephedrone treated cells, there was a large increase in cysteine glutathione disulfide, which is produced as a result of oxidative stress. Oxidation of glutathione results in formation of mixed disulfides with protein thiol groups, and initiating reversible S-glutathionylation. S-glutathionylation is vital to transfer signals of oxidants (Lim *et al.*, 2003), by uncoupling the enzyme endothelial nitric oxide synthase (eNOS) to adjust it to produce  $O_2^{\bullet-}$  instead of NO (La Quaglia and Manchester, 1996).

Overall the impression is that there is no strong pattern of effect of mephedrone on the SH-SY5Y cells. This can be explained by either that the mephedrone is targeting a specific type of cells other than neuroblastoma or that this concentration of mephedrone is not able to cause a potent effect on this cell line. The metabolite alterations are in a random selection of metabolites, which do not fall in any particular pathway and the fold changes are generally small.

It is also noteworthy to mention that these cell lines (SH-SY5Y) lose their dopaminergic abilities after 20 passages (Biedler *et al.*, 1978), and the analysis was performed at 35 and above passages, which makes these cells less representative of neuronal cells. The rise in the metabolism seen in the MTT results (Figure 5.1) at this concentration can be explained as a possible increase in specific proteins that are not detectable by metabolomics analysis.

### 5.5.2.2 Effect of mephedrone on the metabolomes of U-373 astrocytes

Figure 5.6 shows a PCA model of the control and mephedrone treated astrocytes. The pooled samples although not in the centre are quite well clustered showing technical stability.

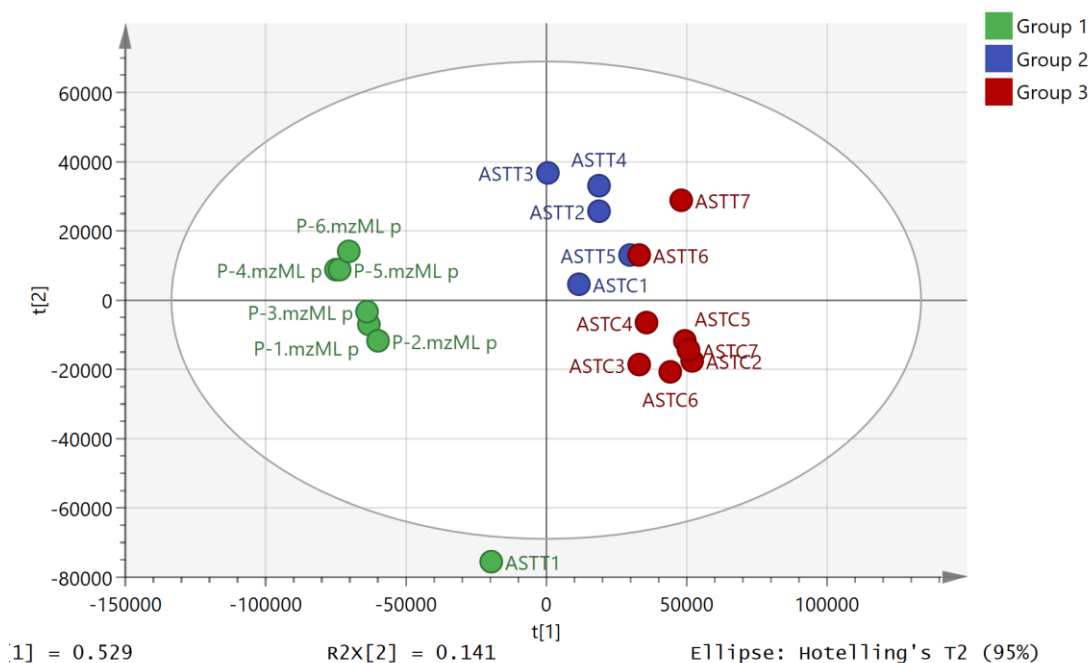


**Figure 5. 6 PCA model of the control (brown), mephedrone treated (blue) astrocytes and pooled samples (green).**

One outlying sample was excluded leading to a PCA model with hierarchical cluster analysis in which there was partial separation between control and treated samples (Figure 5.6).

Using an OPLSDA model it was possible to separate the treated and control samples (Figure 5.7) and the model was valid according to the cross-validation test (Figure 5.8)

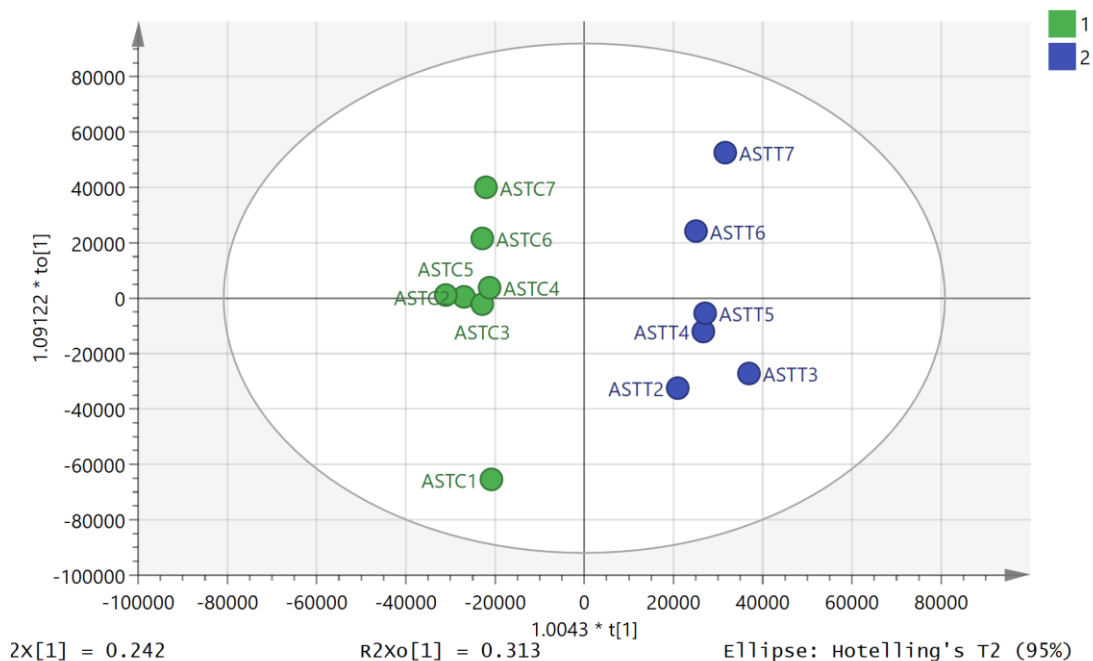


**Figure 5.7 OPLS-DA score plot of astrocytoma (U-373) treated with mephedrone (blue) and non-treated (green) without pooled samples. C represents the control (non-treated) samples, and T represents the test (treated) samples.**

Omitting the pooled samples from the model allowed a better separation for treated and control samples using an OPLS-DA model as shown in Figure 5.7.

The model was validated by the validation test with 100 permutations as shown in Figure 5.8.

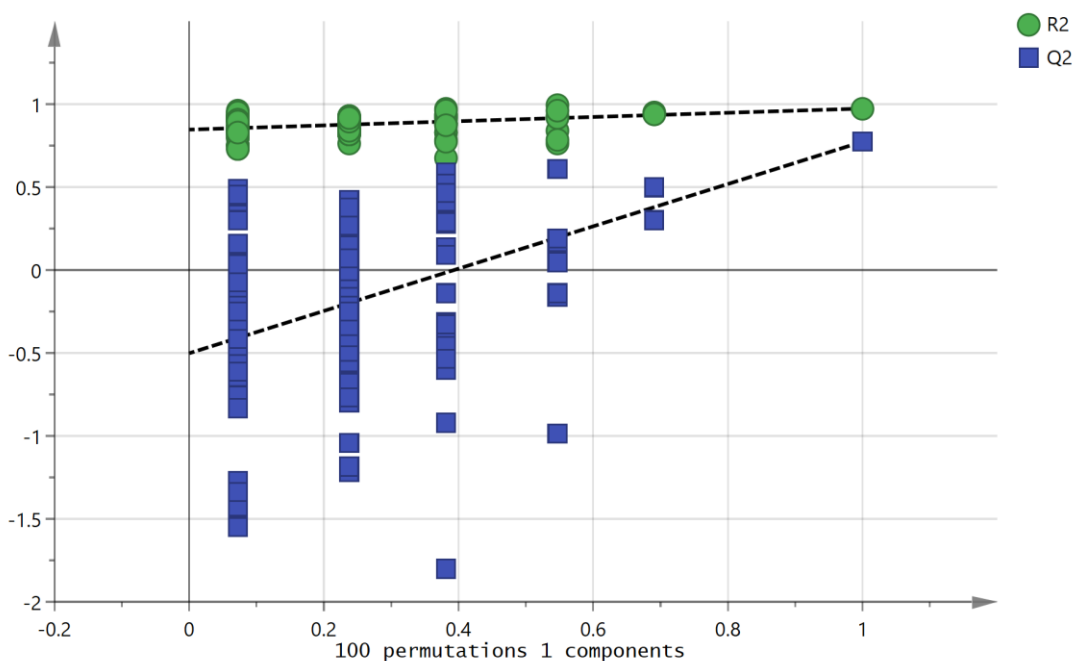


**Figure 5.8** Permutation analysis of the OPLS-DA model for mephedrone treated and non-treated astrocytoma cells. Validation of the model was performed with 100 permutation tests.  $R_2$  represent the goodness of the fit and  $Q_2$  represent the predictive capability.

**Table 5. 4** CVANOVA of the OPLS-DA model for mephedrone treated and non-treated astrocytoma.

	SS	DF	MS	F	P-value	SD
<b>Total correlation</b>	11	11	1			1
<b>Regression</b>	10.098	4	2.52	19.59	0.0007	1.59
<b>Residual</b>	0.902	7	0.129			0.36

Metabolomic analysis results of astrocytoma cells after treatment with 100  $\mu$ M of mephedrone for 6 days, is shown in table 5.5.

Separation between astrocytoma samples and between control and test groups is shown in Figure 5.6.

OPLS-DA score plot exhibited in Figure 5.7 shows that there was greater separation, than that for neuroblastoma, between treated and non-treated samples. It can be concluded that treatment with mephedrone has produced significant change in the metabolome of treated astrocytoma samples compared with the metabolome of the

non-treated astrocytoma samples. The effects in this cell line are much clearer than in the neuroblastoma cells. The illustration of the exact change in metabolites and their amounts was explained in the heat map shown in Figure 5.9. Although there is quite a lot of variability within the sample sets, thus, in contrast to the neuroblastoma cells mephedrone treatment has a clear impact on the metabolome of the astrocyte cells. There is a widespread effect on lipids most of which are decreased in the cells by the treatment. This can be seen in the heatmap (Figure 5.9) where even some very abundant lipids are changed. Since most of the metabolites affected are decreased it is important to check that there is not some bias in the treatment and in table 5.6 it can be seen that some important intracellular metabolites such as glutathione and ATP are no different between treatment and control. An example of this can also be seen in Figure 5.10. So for instance if there was general toxic reaction producing cell lysis one might expect ATP and glutathione to be largely lost from the samples since they do not occur in the cell medium.

m/z	Rt(min)	metabolite	astro-c1	astro-c2	astro-c3	astro-c4	astro-c5	astro-c6	astro-t1	astro-t2	astro-t3	astro-t4	astro-t5	astro-t6	Ratio	P-Value
786.6021	4.1	PC 36:2													0.051	0.013
500.2781	4.7	LPE 20:4													1.251	0.417
496.3398	4.8	LPC 16:0													0.810	0.350
808.5863	4.1	PC 38:5													0.050	0.018
478.2937	4.7	LPE 18:1													0.699	0.299
298.2741	4.3	Sphingadienine													0.679	0.251
300.2897	6.1	Dehydrosphinganine													0.281	0.003
524.3714	4.7	LPC18:0													0.529	0.040
806.5698	4.1	PC 38:6													0.053	0.007
435.2515	4.8	LPA 18:1													0.771	0.162
599.3201	4.3	LPI 18:0													0.630	0.141
704.5216	4.2	PC 30:1													0.097	0.004
524.2992	4.2	LPS 18:0													0.550	0.073
438.2982	4.7	LPE 16:0 ether													0.492	0.018
544.3398	4.7	LPC 20:4													1.659	0.025
526.2941	4.6	LPE 22:5													1.037	0.890
409.236	4.8	LGP 16:0													0.800	0.369
464.3141	4.6	LPE 18:1 ether													0.327	0.004
746.5695	4.1	PE 36:1													0.128	0.025
528.3089	4.6	LPE 22:5													1.035	0.892
466.3295	4.6	LPE 18:0 ether													0.370	0.003
838.5599	3.8	PS 40:5													0.132	0.002
528.3094	4.6	LPE 22:4													1.124	0.754

794.6071	4.1	PC 38:5 ether													0.049	0.018
819.5171	3.6	PG 40:7													0.132	0.001
772.5859	4.1	PE 38:2													0.047	0.018
452.2783	4.8	LPE 16:0													0.792	0.568
766.5764	4.1	LPC 36:4 ether													0.042	0.028
508.376	4.7	LPC 18:1													0.609	0.039
480.3446	4.7	LPC 16:1													0.668	0.058
571.2883	4.4	LPI 16:0													0.934	0.720
832.5862	4.1	PC 40:7													0.030	0.011
500.2782	7.4	LPE 20:4													0.846	0.705
509.288	3.9	LPG 18:0													0.818	0.211
522.2833	4.3	LPS 18:0													0.767	0.181
834.6015	4.1	PC 40:6													0.020	0.015
750.5451	4.1	PE 38:5 ether													0.220	0.049
754.5394	4.1	PC 34:4													0.101	0.007
768.5916	4.1	PC 36:3 ether													0.048	0.025
482.3604	4.9	LPC 16:2													0.938	0.742
468.3086	5.0	LPC 14:0													1.067	0.787
616.4706	4.4	PG 16:0													0.202	0.002
671.4654	4.1	PG 34:2													0.083	0.002
716.5581	4.2	PC 32:1 ether													0.045	0.008
746.6072	4.2	PC 34:0 ether													0.158	0.023
813.6856	4.3	SM 42:2													6.277	0.238
508.3397	4.7	LPE 20:0													0.698	0.204
417.2412	4.2	LPA 18:1 ether													0.130	0.001
788.543	4.0	PS 36:2													0.813	0.717

729.5913	4.3	SM 36:2	Yellow	Light Green	Light Green	Yellow	Yellow	Yellow	Blue	Blue	Blue	Blue	Blue	Blue	0.054	0.003
748.5264	4.0	PE 38:7	Yellow	Blue	Blue	Light Green	Yellow	Light Green	Blue	Light Green	Blue	Blue	Blue	Blue	0.094	0.034
457.236	4.7	LPG 20:4	Light Green	1.616	0.035											
570.3561	4.6	LPC 22:5	Light Green	1.314	0.060											
716.5236	4.1	PE 34:2	Yellow	Light Green	Light Green	Yellow	Yellow	Yellow	Blue	Blue	Blue	Blue	Blue	Blue	0.070	0.004
766.5371	4.1	PE 38:5	Yellow	Light Green	Light Green	Yellow	Light Green	Light Green	Blue	Blue	Blue	Blue	Blue	Blue	0.108	0.015
532.3399	4.6	LPE 22:3	Blue	Light Green	Light Green	Blue	Yellow	Yellow	Blue	Blue	Blue	Light Green	Light Green	Light Green	0.485	0.111
699.4953	4.1	PG 36:2	Yellow	Light Green	Light Green	Yellow	Yellow	Yellow	Blue	Blue	Blue	Blue	Blue	Blue	0.111	0.005
550.3869	4.6	LPC 20:1	Light Green	Blue	Blue	Blue	Light Green	Light Green	Light Green	0.485	0.018					
774.5992	4.1	PE 38:1	Yellow	Blue	Blue	Light Green	Light Green	Light Green	Blue	Light Green	Blue	Blue	Blue	Blue	0.108	0.040
770.5685	4.1	PE 38:3	Yellow	Blue	Blue	Yellow	Light Green	Light Green	Blue	Blue	Blue	Blue	Blue	Blue	0.092	0.031
730.539	4.2	PC 32:1	Light Green	Light Green	Light Green	Light Green	Yellow	Yellow	Blue	Blue	Blue	Blue	Blue	Blue	0.095	0.001
794.5705	4.1	PE 40:5	Yellow	Blue	Blue	Yellow	Light Green	Light Green	Blue	Blue	Blue	Blue	Blue	Blue	0.088	0.045
433.2359	4.8	LPA 18:2	Light Green	0.969	0.821											
756.5535	4.1	PC 34:2	Light Green	Blue	Blue	Blue	Blue	Blue	Blue	0.079	0.002					
747.5173	3.8	PG 34:1	Yellow	Blue	Blue	Light Green	Light Green	Light Green	Blue	Blue	Blue	Blue	Blue	Blue	0.139	0.034

**Figure 5. 9 Lipids in astrocytes sorted by abundance before and after treatment with mephedrone. Red = 30% of maximum value, yellow=2% of maximum value and blue= 0. SM=sphingomyelin, CER=ceramide.**

**Table 5. 5 Non-lipid metabolite changes in U-373 astrocytes following treatment with 100  $\mu$ M mephedrone for 6 days (n=6). Values indicate ratio of metabolites compared with controls (average of mephedrone treated peak area/control peak area).**

M/z	Rt (min)	Structure	Metabolite	Ratio	P-Value
316.248	4.1	C17H33NO4	O-decanoyl-R-carnitine	0.836	0.044
311.294	4.2	C20H38O2	Eicosenoic acid	1.737	0.033
155.107	4.8	C9H14O2	Nonadienoic acid	0.561	0.004
353.231	4.4	C20H32O5	Trihydroxy eicosatetraenoic acid	1.999	0.038
365.342	3.8	C24H46O2	Tetracosenoic acid	0.305	0.032
173.117	4.9	C9H16O3	Oxononanoic acid	0.555	0.001
283.192	4.3	C16H28O4	Dihydroxy hexdecadienoic acid	1.511	0.016
337.311	3.9	C22H42O2	Docosenoic acid	0.487	0.031
309.28	3.9	C20H38O2	Eicosenoic acid	0.548	0.046
282.279	5.6	C18H35NO	Octadecenamide	0.387	0.021
145.014	15.6	C5H6O5	2-Oxoglutarate	0.407	0.027
162.076	11.4	C6H11NO4	L-2-Aminoadipate	1.633	0
258.038	14.8	C6H14NO8P	D-Glucosamine 6-phosphate	1.62	0.035
190.051	11.3	C10H9NO3	5-Hydroxyindoleacetate	0.665	0.04
206.081	13.6	C11H11NO3	Indolelactate	0.763	0.031
402.011	17.3	C9H15N3O11P2	CDP	0.479	0.048
503.162	17.5	C18H32O16	Glycogen	1.905	0.037
665.214	18.2	C24H42O21	Glycogen	3.03	0.044
133.061	15.8	C4H8N2O3	L-Asparagine	0.555	0.013
336.14	16.4	C12H21N3O8	N4-(Acetyl-beta-D-glucosaminy)asparagine	0.482	0.001
368.999	18.6	C7H16O13P2	D-Sedoheptulose 1,7-bisphosphate	0.5	0.032
664.117	13.7	C21H29N7O14P2	NADH	0.553	0.03
123.055	7.5	C6H6N2O	Nicotinamide	1.442	0.005
162.113	13.8	C7H15NO3	L-Carnitine	0.6	0.039
230.139	5.1	C11H19NO4	Butenylcarnitine	0.828	0.035
248.149	7.4	C11H21NO5	Hydroxybutyrylcarnitine	0.687	0.023
229.144	5.1	C12H22O4	Dodecanedioic acid	1.332	0.045
216.063	16.1	C5H14NO6P	Sn-glycero-3-Phosphoethanolamine	0.652	0.049

**Table 5.6 Major intracellular metabolites in astrocytoma cells that are not affected by mephedrone treatment.**

<b>M/z</b>	<b>Rt (min)</b>	<b>Structure</b>	<b>Metabolite name</b>	<b>Ratio</b>	<b>P-Value</b>
232.1545	9.1	C11H21NO4	O-Butanoylcarnitine	1.001	0.994
118.0863	13.0	C5H11NO2	L-Valine	0.995	0.962
88.04019	15.3	C3H7NO2	L-Alanine	1.009	0.955
579.0266	19.1	C15H22N2O18P2	UDP-glucuronate	0.988	0.948
132.1019	11.5	C6H13NO2	Leucine	0.983	0.900
189.1599	23.1	C9H20N2O2	N6,N6,N6-Trimethyl-L-lysine	1.018	0.893
130.0621	15.2	C4H9N3O2	Creatine	1.050	0.868
402.9948	15.3	C9H14N2O12P2	UDP	0.953	0.814
608.0888	15.3	C17H27N3O17P2	UDP-N-acetyl-D-glucosamine	0.958	0.806
104.107	21.1	C5H13NO	Choline	1.071	0.806
124.0394	7.6	C6H5NO2	Nicotinate	0.953	0.805
282.0843	13.1	C10H13N5O5	Guanosine	1.046	0.801
147.1128	25.2	C6H14N2O2	L-Lysine	0.930	0.785
523.9981	19.4	C10H16N5O14P3	GTP	0.958	0.777
133.0142	16.1	C4H6O5	(S)-Malate	1.051	0.777
505.9881	16.7	C10H16N5O13P3	ATP	0.881	0.285
482.9611	18.0	C9H15N2O15P3	UTP	0.711	0.345
308.091	14.6	C18H13NO4	Glutathione	0.897	0.616

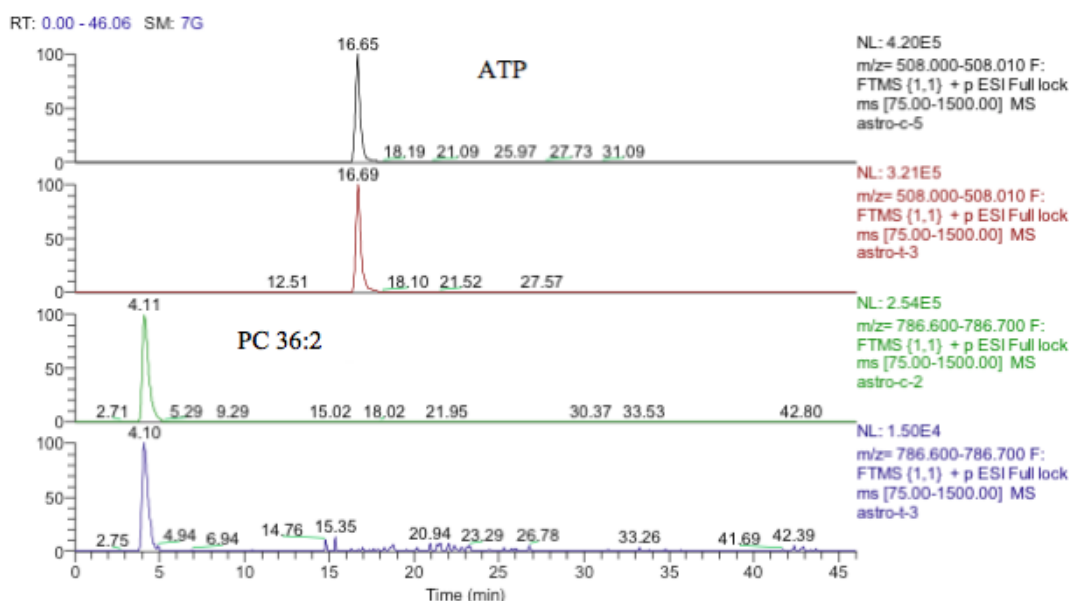


**Figure 5. 10** Extracted ion traces showing similar levels of ATP in treated and untreated extracts but a large reduction of the amount of a major cellular lipid (PC 36:2) in treated astrocytoma cells.

Some of the most marked effects on the astrocytes are on ether lipids which are not particularly abundant in cells but have important effects on membrane fluidity (Lohner, 1996) and protective effects toward myelin against oxidative stress. Some of the ether lipids (LPE 18:1 ether, PC 38:5 ether, LPC 36:4 ether, PC 36:3 ether and PC 32:1 ether) in the cells are almost completely depleted. Mice and human patients with deficiency in ether lipids developed problems in myelination in CNS (da Silva *et al.*, 2012). Thus, it is proposed here that mephedrone could affect myelination in astrocytoma cells.

Several PC and PE lipids: PE 34:1, PC 38:2, LPC 18:2, PC 36:2, PC 28:0, PC 30:0, PC 30:1, PC 30:2, PC 32:1, PC 32:2, PC 32:3, PC 32:4, PC 34:1, PC 38:5 and PC 40:7 and PC ether lipids: PC 36:3 ether, PC 32:0, PC 32:1 ether, PC 36:3 ether, PC 38:3 ether and PC 40:5 ether were all decreased. Glycerophospholipids are the main component of the cellular membrane (Hannun and Obeid, 2002). It is believed that cells change the cell membrane as a defensive reaction when attacked by

extracellular toxic compounds (Montealegre *et al.*, 2014). Glycerophosphocholines control the balance between the solute concentration inside and outside the cell (Hannun and Obeid, 2002). A previous study showed that PC levels were decreased in mouse brain after treatment with antidepressant drugs (paroxetine and maprotiline) (Lee *et al.*, 2009). In another study, a decrease in glycerophospholipids was associated with oxidative stress and changes in the lipid membrane in the cell (Kahle *et al.*, 2015). It is believed that oxidative stress has affected the cellular membrane composition in mephedrone treated cells. Interestingly, oxidative stress as a result of chronic unpredictable stress was shown to disturb the phospholipids levels in mouse brain (Faria *et al.*, 2014). In another study conducted on the hippocampus of rat prefrontal cortex, 4 weeks of chronic unpredictable stress caused significant decrease in PE levels (Oliveira *et al.*, 2016). Oxidative stress causes lipid peroxidation which leads to alteration in lipid balance, which was related with neurological disorders (Black, 2002). Oxidation of lipids causes destabilisation of membrane of the cell and then cell death (Tyurin *et al.*, 2009). This finding suggest that mephedrone may be reducing glycerophosphocholine by oxidative stress as the effects of mephedrone were previously related to oxidative stress (den Hollander *et al.*, 2014).

Other altered membrane lipids include glycerophospholipids (PG) phosphatidylserines (PS) and sphingomyelins (SM) which all decreased. All these lipids are parts of cellular membrane, thus decrease in these lipids is a sign of membrane damage. Several lyso phospholipids were altered. As lyso phospholipids are known to have a neuroprotective role (Casado and Ascher, 1998) and any decrease will have an impact on the protective ability of neurons.

In addition, several sphingomyelins are affected by the treatment. Sphingomyelin 36:2 has decreased and it is a type of sphingolipid located in the myelin sheath of the membrane which covers the axon of the nerve cell.

Three sphingamines decreased and they have a role in blocking esterification of low-density lipoprotein of cholesterol to yield accumulation of unesterified cholesterol in perinuclear vesicles (Deguchi *et al.*, 2004). Sphingamines are an effective signaling lipid or lipid messenger that are attached to target protein receptor, which will facilitate the function of the lipid on particular responses of the cell (Hannun and Obeid, 2008). We can conclude that a decrease in sphingamines will affect lipid signalling in the cell.

Nine fatty acids were affected (table 5.5), two increased and seven decreased. Astrocytes (represented by astrocytoma cells) are responsible for transferring fatty acids from plasma to the brain (Spector, 1988; Magret *et al.*, 1996) and they are the only cells in the brain that can oxidise fatty acids and actually prefer them as their fuel (Magret *et al.*, 1996). Any malfunction in astrocytes will lead to a disturbance in fatty acids levels in the brain and any decrease in fatty acids levels will lead to a decrease in astrocytes function. Mephedrone may cause a disturbance in the fatty acid levels in astrocytoma. Since, astrocytes provide other brain cells with glucose and ketone bodies through their ability to oxidise fatty acids (Flynn and Wecker, 1987), thus any effect on them will lead to decrease in energy supply for other brain cells.

Three carnitine metabolites were decreased which are l-carnitine, butenylcarnitine and hydroxybutyrylcarnitine. Carnitines have a very important role in providing cells with energy and they are vital for metabolism of fatty acids (Olpin, 2005).

Menaquinol-8 or vitamin K2 has decreased which has a role in regulating blood clotting. Vitamin K vitamins have the same methylated naphthoquinone ring structure, and differ only in the type of the side aliphatic chain linked at site 3 (Shearer and Newman, 2014).

Two glycogens are increased by the treatment. Glycogen is the main storage product of glucose in human cells. Glycogen is located in granular structures in the cytosol (Zderic *et al.*, 2004). It is proposed that cells have produced more glycogen in order to compensate for the loss in energy supply in the face of membrane damage. In the brain glycogen is found predominantly in the astrocytes where it acts as an energy source to protect the brain from hypoglycemia (Walls *et al.*, 2009).

Other metabolites associated with glutamate metabolism such as 2-oxoglutarate, 1-2-aminoadipate and d-glucosamine 6-phosphate were altered. The oxidised glutamate (oxoglutarate) was decreased by 60% and the others were increased. Aminoadipate was upregulated and it is an antagonist for glutamate excitatory effect and is a metabolite of lysine (Wu *et al.*, 1995). Glutamate is an important neurotransmitter and responsible for fast excitation effect in the brain (Smith, 2000). L-Asparagine was decreased and it is a metabolite of glutamate (Avramis and Panosyan, 2005). However, we cannot conclude any effect on glutamate, as its level was not altered significantly.

Two metabolites related to the tryptophan and serotonin pathway were decreased. 5-Hydroxyindoleacetate is a metabolite of the neurotransmitter serotonin (Owens and Nemeroff, 1994). Indolelactate was also decreased which is a metabolite of tryptophan, the precursor for serotonin and melatonin (Morita *et al.*, 1990). However, we could not detect serotonin or tryptophan in our method.

Nicotinamide and NADH were also altered with significant p values. NADH was decreased and nicotinamide was increased. Nicotinamide plays an important role in the protection of neurons (Fricker *et al.*, 2018) as the pretreatment with nicotinamide reversed hypoxia in hippocampus of rats (Shetty *et al.*, 2014). Thus, we conclude that in one of its defence mechanisms, astrocytoma cells produced nicotinamide to protect themselves and neuronal cells against oxidative stress caused by mephedrone treatment.

Overall, the major pathway affected was the lipids pathway particularly cell membrane lipids. This finding can open the way to understand the effect of mephedrone on the brain particularly the brain-barrier (astrocytes). Affecting the astrocytes as an important part of the brain barrier will affect the neurons as the astrocytes known to have protective role towards the neuronal cells. However, mephedrone was not a strong cytotoxic at this concentration and eventhough it has induced changes in the CNS cell metabolome, these are not responsible for its toxicity in the body as cell numbers were not reduced as shown in the results of NR assay (see section 5.5.1.2 Figure 5.2).

The metabolomic analysis has proved that there was a change in the metabolism of SH-SY5Y and U373 cells after treatment with mephedrone at 100  $\mu$ M, which was consistent with MTT assay findings. Both cell types metabolomic results proposed a rise in glutamine concentration after treatment with mephedrone. The appearance of cysteineglutathione disulfide in SH-SY5Y after treatment with mephedrone suggests

an oxidative stress occurs. The effect of mephedrone was much more marked on the U373 cells.

## 5.6 Conclusion

From the analysis of different cell types, it is clear that although mephedrone did not kill or decrease the growth of cells; it did marked intracellular metabolic changes. It is believed that even small change in brain cell homeostasis can lead to neurological disease (Budzynska *et al.*, 2015; López-Arnau *et al.*, 2015).

Findings of this chapter can be summarised as following:

A) For SH-SY5Y, less change occurs compared to other cells and there was no clear pattern of metabolic disruption resulting from mephedrone treatment

B) For U-373, the main pathways affected were:

1- Marked effect (decrease) on the level of ether lipids which have important effects on membrane fluidity.

2- Cellular membrane damage showed by the decrease in the levels of the majority of membrane lipids.

3- Energy storage and metabolism pathway due to an increase in glycogen production.

4- U-373 cell tend to increase nicotinamide level as a protection response against mephedrone.

## **Chapter 6 SUMMARY AND FUTURE WORK**

---

## **6.1 Summary of results of the cobalt study**

The main findings related to cobalt experiments (chapter 3) in SH-SY5Y and U-373 cell lines are summarised here and suggestions for future research are presented in the following sections.

### **6.1.1 Assessment of the toxicity of cobalt**

Toxicity was assessed by the MTT assay and by detection of ROS by fluorescence microscopy at three different time points (24, 48 and 72 hours) for SH-SY5Y neuroblastoma cells and U-373 astrocytoma cells. The data showed different sensitivities to the effects of cobalt for each cell type. The reduction of MTT as incubation time and dose are increased was clear in both cell lines, however, U-373 cells showed better resistance to cobalt than SH-SY5Y cells. It is speculated that the resistance of U-373 cells *in vitro* reflects their *in vivo* role in the brain. They are better equipped to protect themselves against toxicity, and in doing so protect the neuronal cells from toxic insults.

ROS assay results showed an increase in the generation of the reactive oxygen species, measured by the fluorescence of carboxy-H<sub>2</sub>DCFDA dye, in SH-SY5Y cells after treatment with 100  $\mu$ M of cobalt. Similarly, ROS increased in U-373 cells after treatment with 200  $\mu$ M of cobalt. This supported the MTT results and the suggestion that U-373 cells have better resistance towards cobalt compared with SH-SY5Y

cells. These results provide evidence of an oxidative stress mechanism of action for cobalt toxicity.

### **6.1.2 Summary of the western blotting results for specific enzymes**

Results of western blotting for the enzymes uracil DNA glycosylase (UNG1), thymine DNA glycosylase (TDG), 8-oxoguanine glycosylase (OGG1) and DNA methyltransferase (DNMT1) in SH-SY5Y cells after treatment with 50  $\mu\text{M}$  of cobalt for 72 hours revealed a significant increase in the levels of UNG1 compared to non-treated cells. Another enzyme which was increased is TDG at 100  $\mu\text{M}$  of cobalt. The enzyme OGG1 was decreased after exposure to 100  $\mu\text{M}$  of cobalt. DNMT1 was increased at both concentrations 25 and 50  $\mu\text{M}$  of cobalt. In contrast, U-373 cells after treatment with a similar range of cobalt (25, 50 and 100  $\mu\text{M}$ ) have shown a significant increase in the TDG level and a significant slight decrease in DNMT1 level at 100  $\mu\text{M}$  of cobalt.

However, considering the high cross reactivity and the low levels of the changes detected it is necessary to take care in the interpretation of the results of this experiment.

### **6.1.3 Summary of the results of real-time polymerase chain reaction experiment**

Quantitative real-time PCR for SIRT2, MeCP2, UNG1 and TDG genes in SH-SY5Y cells showed a gradual increase in all genes compared with the reference gene and control cells as the concentration of cobalt was increased up to 100  $\mu\text{M}$ . In U-373

cells, there was increase in the levels of all genes at 100  $\mu$ M of cobalt. The genes UNG1 and TDG are associated with base excision repair (Yonekura *et al.*, 2009; Da *et al.*, 2018), which supports our finding in this pathway. Mlh1 has a role in the R-loop-dependent CAG fragility, which is responsible for DNA strand breakage. SIRT2 plays an important role in antioxidation and hypoxia (Seo *et al.*, 2015). MeCP2 gene increased as a defensive mechanism initiated to combat methylation in the cell (Yan *et al.*, 2003).

#### **6.1.4 Evaluation of cobalt effect on neuronal cells by metabolomic analysis**

The metabolomic analysis of SH-SY5Y and U-373 cells after treatment with a range of cobalt (25, 50, 100, 150 and 200  $\mu$ M) revealed multiple altered metabolites. The detection of increased levels of glutathione disulfide (the oxidised form of glutathione) suggested that cobalt was acting through glutathione oxidation in both cell lines. There were marked alterations in several lipids and increases in CMP-ethanolamine and CMP-choline which are required for lipid biosynthesis. Although the transcription of genes enzymes required for DNA repair was upregulated the increase was not supported by protein expression data as judged from Western blotting or from metabolite changes. Isolation and digestion of DNA followed by analysis of the digested bases did not indicate increases in the elevation of markers such as deoxyuridine, thymidine, or methyl deoxy cytidine.

### 6.2.5 Suggestions for future work on cobalt

The metabolomics results for cobalt require some clarification. The production of oxidative stress was clear enough. However, the effects on DNA and RNA bases was less clear. There was one particular marker which appeared to be hydroxythymidine. This marker yielded a fragment which confirmed that it contained hydroxymethyl uracil. However, further characterisation of this marker by MS<sup>n</sup> experiments is required. The following experiments should be carried out:

- 1- Characterisation of the lipids altered by cobalt treatment by using MS<sup>n</sup> methods and more selective chromatography.
- 2- Metabolomic analysis for the effect of cobalt treatment on primary rat brain tissue and compare it with the effect of cobalt treatment on neuronal cell lines.
- 3- Performing untargeted shotgun proteomics for similar cell lines and primary brain cells after treatment with cobalt to study the effect on proteins and compare it with the metabolomics data.
- 4- The use of metabolomics to compare the effect of cobalt chloride, cobalt hard metal and cobalt/tungsten carbide mixture (used in alloys) and compare the response of cells toward these different forms of cobalt.
- 5- Isolation of the mitochondria, evaluate its content of H<sub>2</sub>O<sub>2</sub> and examine it by metabolomics and other approaches to investigate the effect on mitochondria separately and to investigate our hypothesis that cobalt is causing more harm to mitochondria due to its high H<sub>2</sub>O<sub>2</sub> content.

6- Isolation of mitochondrial DNA and examination of the bases in it by microarray or metabolomic approaches to detect what specific damage occurs after cobalt treatment.

## **6.1 Summary of results of the mephedrone study**

A summary of the main findings for the two chapters covering mephedrone metabolism and mephedrone effects on cells (4 and 5, respectively) are presented here.

### **6.1.1 Metabolism of mephedrone in cultured primary rat hepatocytes**

In the culture of primary hepatocytes, the metabolism pattern of mephedrone is different according to the time of incubation. It was noticed that the extent of metabolism decreases with time as a result of impaired metabolism activity: mephedrone metabolism in cultured rat hepatocytes is time and dose dependent. Carboxy-mephedrone was the most abundant metabolite at 6 and 24 hours incubation periods, whereas nor-mephedrone was the most abundant after the 48 hours incubation period.

The hepatic derived cell line HepG2, showed very weak metabolism of mephedrone and proved not to be not good alternative model to primary hepatocytes. Similarly, the neuronal derived cell lines U-373 and SH-SY5Y, showed low mephedrone metabolism with slightly improved metabolism, in matter of number of metabolites produced, in U-373 cells compared to SH-SY5Y cells. HepG2 cells produced a

single metabolite (4-carboxy-mephedrone) with very low relative abundance (0.05%). SH-SY5Y neuroblastoma cells produced a single metabolite as well (4-hydroxymethyl-cathinone) with 10% relative abundance. Finally, U-373 astrocytoma cells produced three metabolites (dihydro-mephedrone, hydroxytolyl-mephedrone and glycine conjugated mephedrone) with low abundance (0.6, 1.1 and 0.002%, respectively). All results observed after incubation of cell lines with 100  $\mu$ M over 6 days.

### **6.1.2 Assessment of the toxicity of mephedrone**

The use of multiple assays (NR, MTT, LDH and metabolomics) to assess the effect of mephedrone has revealed many findings which are presented here. Results of the NR and MTT assays showed no significant effect on cell number or metabolism of SH-SY5Y cells (after exposure to a range of concentrations of mephedrone) with the exception of increased metabolic activity at 100  $\mu$ M concentration of mephedrone after 72 hours of incubation. In contrast, U-373 cells showed an increase in both cell number and metabolism at a 100  $\mu$ M concentration and higher at similar incubation time. Results of the LDH assay showed no change between treated and non-treated SH-SY5Y and U-373 cells after treatment with 100  $\mu$ M of mephedrone for 72 hours. These results combined showed that mephedrone has limited effect on the metabolism and growth of SH-SY5Y and U-373 cells. However, the increased metabolism in both of the cell lines at 100  $\mu$ M of mephedrone for longer period of time (6 days) was studied using metabolomic analysis to further investigate intracellular change induced by mephedrone at this specific concentration.

### **6.1.3 Evaluation of mephedrone effect on neuronal cells by metabolomic analysis**

Metabolomic analysis of human SH-SY5Y and U-373 cells after treatment with 100  $\mu\text{M}$  of mephedrone (for 6 days incubation) was studied in comparison with appropriate control cells. The metabolomic analysis showed multiple alterations in intracellular metabolites.

The resultant effects on cells can be classified according to the pathways affected into four categories. First, oxidative stress was apparent in all cell types characterised by the production of cysteine-glutathione. The second pathway is associated with phenylalanine and tryptophan metabolism, and the third affected pathway is the metabolism of glucose. The fourth and most affected group of compounds was lipids particularly ether, lyso and other membrane lipids.

Even though, there was no effect on the cell proliferation of SH-SY5Y and U-373 cells as the results of NR, MTT and LDH assays suggested, there was an intracellular effect after the treatment with 100  $\mu\text{M}$  of mephedrone. However, for the SH-SY5Y cell line the effects were minor. It is believed that even small change in the brain cells homeostasis can lead to neurological disease (Laposa and Cleaver, 2001).

However, there are limitations to extend our results to primary human neuronal cells since cell lines are cancer cells and can act in a different way to stressors (Agholme *et al.*, 2010). In addition the relatively low concentration and long period of incubation of mephedrone can cause the drug to be evaporated by time of analysis, which can reduce the effect and allow cells to restore their healthy status. Thus,

quantification of mephedrone in samples at time of analysis was necessary to confirm that the effect is directly caused by the drug. Moreover, since the most prominent effect was on lipid and the fact that the metabolomic method was more selective to polar compounds, which led to weak retainment of lipids. Thus, more clear picture of the effect on lipid can be achieved with non polar selective metabolomic method. The major limitation of the work reported in this thesis is the extrapolation from cells cultured in a petridish to cells living in the in vivo environment in the brain and furthermore to the effects in the whole human body.

#### **6.1.4 Suggestions for future work on mephedrone**

To better understand mephedrone effects on the brain it is recommended to further investigate its effects. According to our results we suggest the following approaches to consider in the future studies.

- 1- The highest priority would be to further investigate the apparent effect of mephedrone in altering the lipid profile of the astrocyte cells. This is an unusual observation since the effects are far reaching. Thus the reproducibility of this effect should be studied and MS<sup>2</sup> methods with more selective chromatography should be used to provide more extensive characterisation of the lipids altered by the mephedrone treatment.
- 2- Metabolomic analysis of mephedrone treated primary rat brain cells for specific parts of the brain individually. This will help in the investigation of the effects on normal brain cells.

- 3- Investigation of mephedrone effect on diabetic rats (see section 5.5.2 for mephedrone effect on glucose) to see if mephedrone can cause more harm to diabetic rats compared to healthy rats.
- 4- Examination of oxidative stress related to the production of reactive oxygen species in cell lines and primary cells after treatment with mephedrone at different concentrations and exposures.
- 5- More in depth study of the relation between the ability of mephedrone to react with cysteine and the effect of this reaction on the glutathione concentration in the cell.
- 6- The application of western blotting for the detection of enzymes related to oxidative stress and glucose metabolism to identify the enzymes highly affected by mephedrone treatment.
- 7- The use of genomics (RT-PCR) and proteomics to confirm the results explored in this research.
- 8- Investigation of the benefit of antioxidants to reduce the effect of mephedrone on cells.

## 7 References

Agholme, L., Lindström, T., Kågedal, K., Marcusson, J. and Hallbeck, M. (2010) 'An in vitro model for neuroscience: differentiation of SH-SY5Y cells into cells with morphological and biochemical characteristics of mature neurons', *Journal of Alzheimer's disease*, 20(4), pp. 1069-1082.

Alexander, C. S. (1969) 'Cobalt and the heart', *Annals of Internal Medicine*, 70(2), pp. 411-3.

Alexander, C. S. (1972) 'Cobalt-beer cardiomyopathy. A clinical and pathologic study of twenty-eight cases', *The American Journal of Medicine*, 53(4), pp. 395-417.

Ameline, A., Dumestre-Toulet, V., Raul, J.-S. and Kintz, P. (2018) 'Abuse of 3-MMC and forensic aspects: About 4 cases and review of the literature', *Toxicologie Analytique et Clinique*.

Anard, D., Kirsch-Volders, M., Elhajouji, A., Belpaeme, K. and Lison, D. (1997) 'In vitro genotoxic effects of hard metal particles assessed by alkaline single cell gel and elution assays', *Carcinogenesis*, 18(1), pp. 177-84.

Angoa-Pérez, M., Kane, M. J., Herrera-Mundo, N., Francescutti, D. M. and Kuhn, D. M. (2014) 'Effects of combined treatment with mephedrone and methamphetamine or 3, 4-methylenedioxymethamphetamine on serotonin nerve endings of the hippocampus', *Life sciences*, 97(1), pp. 31-36.

Angoa - Pérez, M., Kane, M. J., Briggs, D. I., Francescutti, D. M., Sykes, C. E., Shah, M. M., Thomas, D. M. and Kuhn, D. M. (2013) 'Mephedrone does not damage dopamine nerve endings of the striatum, but enhances the neurotoxicity of methamphetamine, amphetamine, and MDMA', *Journal of neurochemistry*, 125(1), pp. 102-110.

Angoa - Pérez, M., Kane, M. J., Francescutti, D. M., Sykes, K. E., Shah, M. M., Mohammed, A. M., Thomas, D. M. and Kuhn, D. M. (2012) 'Mephedrone, an abused psychoactive component of 'bath salts' and methamphetamine congener, does not cause neurotoxicity to dopamine nerve endings of the striatum', *Journal of neurochemistry*, 120(6), pp. 1097-1107.

Apostoli, P. (1999) 'The role of element speciation in environmental and occupational medicine', *Fresenius' journal of analytical chemistry*, 363(5-6), pp. 499-504.

Armstrong, D. D. (2002) 'Neuropathology of Rett syndrome', *Mental retardation and developmental disabilities research reviews*, 8(2), pp. 72-6.

Asmat, U., Abad, K. and Ismail, K. (2016) 'Diabetes mellitus and oxidative stress-A concise review', *Saudi Pharmaceutical Journal*, 24(5), pp. 547-553.

ATSDR (2004) Toxicological profile for cobalt. Available at: <https://http://www.atsdr.cdc.gov/ToxProfiles/tp.asp?id=373&tid=64> 2017).

Avramis, V. I. and Panosyan, E. H. (2005) 'Pharmacokinetic/pharmacodynamic relationships of asparaginase formulations: the past, the present and recommendations for the future', *Clinical Pharmacokinetics*, 44(4), pp. 367-93.

Badylak, S. F., Freytes, D. O. and Gilbert, T. W. (2009) 'Extracellular matrix as a biological scaffold material: structure and function', *Acta biomaterialia*, 5(1), pp. 1-13.

Bae, O. N. and Lee, J. Y. (2016) 'Shedding New Lights with the Breakthrough Ideas to Understand Current Trends in Modern Toxicology', *Toxicological Research*, 32(1), pp. 1-3.

Barborik, M. and Dusek, J. (1972) 'Cardiomyopathy accompanying industrial cobalt exposure', *British Heart Journal*, 34(1), pp. 113.

Barceloux, D. G. (1999) 'Cobalt', *Journal of Toxicology. Clinical Toxicology*, 37(2), pp. 201-6.

Bar-Or, David, Edward Lau, and James V. Winkler. (2000) 'A novel assay for cobalt-albumin binding and its potential as a marker for myocardial ischemia—a preliminary report'. *The Journal of emergency medicine*, 19(4), pp. 311-15.

Baumann, M. H., Ayestas, M. A., Partilla, J. S., Sink, J. R., Shulgin, A. T., Daley, P. F., Brandt, S. D., Rothman, R. B., Ruoho, A. E. and Cozzi, N. V. (2012) 'The designer methcathinone analogs, mephedrone and methylone, are substrates for monoamine transporters in brain tissue', *Neuropsychopharmacology*, 37(5), pp. 1192-203.

Beyersmann, D. and Hartwig, A. (1992) 'The genetic toxicology of cobalt', *Toxicology and Applied Pharmacology*, 115(1), pp. 137-45.

Bhabak, K. P. and Mugesh, G. (2010) 'Functional mimics of glutathione peroxidase: bioinspired synthetic antioxidants', *Accounts of Chemical Research*, 43(11), pp. 1408-19.

Biedler, J. L., Roffler-Tarlov, S., Schachner, M. and Freedman, L. S. (1978) 'Multiple neurotransmitter synthesis by human neuroblastoma cell lines and clones', *Cancer Research*, 38(11 Pt 1), pp. 3751-7.

- Bird, A. (2002) 'DNA methylation patterns and epigenetic memory', *Genes and Development*, 16(1), pp. 6-21.
- Black, P. H. (2002) 'Stress and the inflammatory response: a review of neurogenic inflammation', *Brain, Behavior, and Immunity*, 16(6), pp. 622-53.
- Bonenfant, J. L., Auger, C., Miller, G., Chenard, J. and Roy, P. E. (1969) 'Québec beer-drinkers' myocardiosis: pathological aspects', *Annals of the New York Academy of Sciences*, 156(1), pp. 577-82.
- Borenfreund, E. and Puerner, J. A. (1985) 'Toxicity determined in vitro by morphological alterations and neutral red absorption', *Toxicology Letters*, 24(2-3), pp. 119-24.
- Bouhifd, M., Hartung, T., Hogberg, H. T., Kleensang, A. and Zhao, L. (2013) 'Review: toxicometabolomics', *Journal of Applied Toxicology*, 33(12), pp. 1365-83.
- Bourg, W. J., Nation, J. R. and Clark, D. E. (1985) 'The effects of chronic cobalt exposure on passive-avoidance performance in the adult rat', *Bulletin of the Psychonomic Society*, 23(6), pp. 527-530.
- Brandt, S. D., Sumnall, H. R., Measham, F. and Cole, J. (2010) 'Analyses of second-generation 'legal highs' in the UK: initial findings', *Drug Testing and Analysis*, 2(8), pp. 377-82.
- Brunt, T. M., Poortman, A., Niesink, R. J. and van den Brink, W. (2011) 'Instability of the ecstasy market and a new kid on the block: mephedrone', *Journal of Psychopharmacology*, 25(11), pp. 1543-7.
- Bucher, J. (1991) 'NTP technical report on the toxicity studies of Cobalt Sulfate Heptahydrate in F344/N Rats and B6C3F1 Mice (Inhalation Studies)(CAS No. 10026-24-1)', *Toxicity report series*, 5, pp. 1-38.
- Bucher, J. R., Elwell, M. R., Thompson, M. B., Chou, B. J., Renne, R. and Ragan, H. A. (1990) 'Inhalation toxicity studies of cobalt sulfate in F344/N rats and B6C3F1 mice', *Fundamental and Applied Toxicology*, 15(2), pp. 357-72.
- Bucher, J. R., Hailey, J. R., Roycroft, J. R., Haseman, J. K., Sills, R. C., Grumbein, S. L., Mellick, P. W. and Chou, B. J. (1999) 'Inhalation toxicity and carcinogenicity studies of cobalt sulfate', *Toxicological Sciences*, 49(1), pp. 56-67.
- Budzynska, B., Boguszewska-Czubara, A., Kruk-Slomka, M., Kurzepa, J. and Biala, G. (2015) 'Mephedrone and Nicotine: Oxidative Stress and Behavioral Interactions in Animal Models', *Neurochemical research*, 40(5), pp. 1083-1093.
- Bunn, H. F., Gu, J., Huang, L. E., Park, J.-W. and Zhu, H. (1998) 'Erythropoietin: a model system for studying oxygen-dependent gene regulation', *Journal of Experimental Biology*, 201(8), pp. 1197-1201.

Busardò, F. P., Kyriakou, C., Tittarelli, R., Mannocchi, G., Pantano, F., Santurro, A., Zaami, S. and Baglìo, G. (2015) 'Assessment of the stability of mephedrone in ante-mortem and post-mortem blood specimens', *Forensic Science International*, 256, pp. 28-37.

Bustin, S. A., Benes, V., Garson, J. A., Hellemans, J., Huggett, J., Kubista, M., Mueller, R., Nolan, T., Pfaffl, M. W., Shipley, G. L., Vandesompele, J. and Wittwer, C. T. (2009) 'The MIQE guidelines: minimum information for publication of quantitative real-time PCR experiments', *Clinical Chemistry*, 55(4), pp. 611-22.

Békési, A., Pukáncsik, M., Muha, V., Zagyva, I., Leveles, I., Hunyadi-Gulyás, E., Klement, E., Medzihradzky, K. F., Kele, Z., Erdei, A., Felföldi, F., Kónya, E. and Vértessy, B. G. (2007) 'A novel fruitfly protein under developmental control degrades uracil-DNA', *Biochemical and Biophysical Research Communications*, 355(3), pp. 643-8.

Camilleri, A., Johnston, M. R., Brennan, M., Davis, S. and Caldicott, D. G. (2010) 'Chemical analysis of four capsules containing the controlled substance analogues 4-methylmethcathinone, 2-fluoromethamphetamine, alpha-phthalimidopropiophenone and N-ethylcathinone', *Forensic Science International*, 197(1-3), pp. 59-66.

Cao, J., Vecoli, C., Neglia, D., Tavazzi, B., Lazzarino, G., Novelli, M., Masiello, P., Paolocci, N., Puri, N., L'Abbate, A. and Abraham, N.G. (2012) 'Cobalt-protoporphyrin improves heart function by blunting oxidative stress and restoring NO synthase equilibrium in an animal model of experimental diabetes'. *Frontiers in Physiology*, 3, p.160.

Carvalho, C. and Moreira, P. I. (2018) 'Oxidative Stress: A Major Player in Cerebrovascular Alterations Associated to Neurodegenerative Events', *Frontiers in physiology*, 9, pp. 806.

Casado, M. and Ascher, P. (1998) 'Opposite modulation of NMDA receptors by lysophospholipids and arachidonic acid: common features with mechanosensitivity', *The Journal of Physiology*, 513 ( Pt 2), pp. 317-30.

Cederbaum, A.I., Wu, D., Mari, M. and Bai, J., 2001. CYP2E1-dependent toxicity and oxidative stress in HepG2 cells. *Free Radical Biology and Medicine*, 31(12), pp.1539-1543.

Cezar, G. G., Quam, J. A., Smith, A. M., Rosa, G. J., Piekarczyk, M. S., Brown, J. F., Gage, F. H. and Muotri, A. R. (2007) 'Identification of small molecules from human embryonic stem cells using metabolomics', *Stem Cells and Development*, 16(6), pp. 869-82.

Chen, Q.; Cederbaum, A. I. (1998) 'Cytotoxicity and apoptosis produced by cytochrome P450 2E1 in HepG2 cells'. *Molecular Pharmacology*, 53, pp. 638 – 48.

Cheresh, P., Kim, S. J., Tulasiram, S. and Kamp, D. W. (2013) 'Oxidative stress and pulmonary fibrosis', *Biochimica et Biophysica Acta*, 1832(7), pp. 1028-40.

Christensen, J., Steain, M., Slobedman, B. and Abendroth, A. (2011) 'Differentiated neuroblastoma cells provide a highly efficient model for studies of productive varicella-zoster virus infection of neuronal cells', *Journal of Virology*, 85(16), pp. 8436-42.

Christova, T. Y., Duridanova, D. B. and Setchenska, M. S. (2002) 'Enhanced heme oxygenase activity increases the antioxidant defense capacity of guinea pig liver upon acute cobalt chloride loading: comparison with rat liver', *Comparative Biochemistry and Physiology. Toxicology & Pharmacology*, 131(2), pp. 177-84.

Ciudad-Roberts, A., Duarte-Castells, L., Camarasa, J., Pubill, D. and Escubedo, E. (2016) 'The combination of ethanol with mephedrone increases the signs of neurotoxicity and impairs neurogenesis and learning in adolescent CD-1 mice', *Toxicology and Applied Pharmacology*, 293, pp. 10-20.

Craig, A., Sidaway, J., Holmes, E., Orton, T., Jackson, D., Rowlinson, R., Nickson, J., Tonge, R., Wilson, I. and Nicholson, J. (2006) 'Systems toxicology: integrated genomic, proteomic and metabolomic analysis of methapyrilene induced hepatotoxicity in the rat', *Journal of Proteome Research*, 5(7), pp. 1586-601.

Da, L. T., Shi, Y., Ning, G. and Yu, J. (2018) 'Dynamics of the excised base release in thymine DNA glycosylase during DNA repair process', *Nucleic Acids Research*, 46(2), pp. 568-581.

da Silva, T. F., Sousa, V. F., Malheiro, A. R. and Brites, P. (2012) 'The importance of ether-phospholipids: a view from the perspective of mouse models', *Biochimica et Biophysica Acta*, 1822(9), pp. 1501-8.

Dai, Y.; Rashba-Step, J.; Cederbaum, A. I. (1993) 'Stable transfection of human cytochrome P4502E1 in HepG2 cells: characterization of catalytic activities and production of reactive oxygen intermediates'. *Biochemistry* 32, pp. 6928-37.

Dargan, P. and Wood, D. (2011) 'Annex 1 to the risk assessment report: technical report on mephedrone', Available from: Prepared by Dr. Paul Dargan and Dr. David Wood, Guy's and St Thomas' NHS Foundation Trust, London, UKEMCDDA contract CT, 10.

Dargan, P. I., Albert, S. and Wood, D. M. (2010a) 'Mephedrone use and associated adverse effects in school and college/university students before the UK legislation change', *Quarterly Journal of Medicine*, 103(11), pp. 875-9.

Dargan, P. I., Albert, S. and Wood, D. M. (2010b) 'Mephedrone use and associated adverse effects in school and college/university students before the UK legislation change'.

Dargan, P. I., Sedefov, R., Gallegos, A. and Wood, D. M. (2011) 'The pharmacology and toxicology of the synthetic cathinone mephedrone (4-methylmethcathinone)', *Drug Testing and Analysis*, 3(7-8), pp. 454-63.

Dass, C. (2007) *Fundamentals of contemporary mass spectrometry*. John Wiley & Sons.

Davey, Z., Corazza, O., Schifano, F. and Deluca, P. (2010) 'Mass-information: mephedrone, myths, and the new generation of legal highs', *Drugs and Alcohol Today*, 10(3), pp. 24-28.

Davis, J. E. and Fields, J. P. (1958) 'Experimental production of polycythemia in humans by administration of cobalt chloride', *Proceedings of the Society for Experimental Biology and Medicine*, 99(2), pp. 493-5.

Deguchi, H., Yegneswaran, S. and Griffin, J. H. (2004) 'Sphingolipids as bioactive regulators of thrombin generation', *The Journal of Biological Chemistry*, 279(13), pp. 12036-42.

den Hollander, B., Rozov, S., Linden, A.-M., Uusi-Oukari, M., Ojanperä, I. and Korpi, E. R. (2013) 'Long-term cognitive and neurochemical effects of “bath salt” designer drugs methylone and mephedrone', *Pharmacology Biochemistry and Behavior*, 103(3), pp. 501-509.

den Hollander, B., Sundström, M., Pelander, A., Ojanperä, I., Mervaala, E., Korpi, E. R. and Kankuri, E. (2014) 'Keto amphetamine toxicity-focus on the redox reactivity of the cathinone designer drug mephedrone', *Toxicological Sciences*, 141(1), pp. 120-31.

Dick, D. and Torrance, C. (2015) EMCDDA | 2011 Annual report online version: New drugs and emerging trends Follow-up on mephedrone. Available at: <http://www.emcdda.europa.eu/online/annual-report/2011/new-drugs-and-trends/3> - bibRef1.

Dickson, A. J., Vorce, S. P., Levine, B. and Past, M. R. (2010) 'Multiple-drug toxicity caused by the coadministration of 4-methylmethcathinone (mephedrone) and heroin', *Journal of Analytical Toxicology*, 34(3), pp. 162-8.

Domingo, J. L. and Llobet, J. M. (1984) 'Treatment of acute cobalt intoxication in rats with L-methionine', *Revista Española de Fisiología*, 40(4), pp. 443-8.

Domingo, J. L., Llobet, J. M. and Bernat, R. (1984) 'A study of the effects of cobalt administered orally to rats', *Archivos de Farmacología y Toxicología*, 10(1), pp. 13-20.

Donato, M. T., Castell, J. V. and Gómez-Lechón, M. J. (1994) 'Cytochrome P450 activities in pure and co-cultured rat hepatocytes. Effects of model inducers', *In Vitro Cellular and Developmental Biology. Animal*, 30A(12), pp. 825-32.

Donato, M. T., Lahoz, A., Castell, J. V. and Gómez-Lechón, M. J. (2008) 'Cell lines: a tool for in vitro drug metabolism studies', *Current Drug Metabolism*, 9(1), pp. 1-11.

Dragon, P. I. and Wood, D. M. (2010) Technical Report on Mephedrone [http://www.emcdda.europa.eu/attachements.cfm/att\\_116646\\_EN\\_TDA\\_K11001ENC\\_WEB-OPTIMISED\\_FILE.pdf](http://www.emcdda.europa.eu/attachements.cfm/att_116646_EN_TDA_K11001ENC_WEB-OPTIMISED_FILE.pdf): Guy's and St Thomas' NHS Foundation Trust, London, UK.

Dutheil, F., Dauchy, S., Diry, M., Sazdovitch, V., Cloarec, O., Mellottée, L., Bièche, I., Ingelman-Sundberg, M., Flinois, J. P., de Waziers, I., Beaune, P., Declèves, X., Duyckaerts, C. and Lorient, M. A. (2009) 'Xenobiotic-metabolizing enzymes and transporters in the normal human brain: regional and cellular mapping as a basis for putative roles in cerebral function', *Drug Metabolism and Disposition*, 37(7), pp. 1528-38.

Edwards, J. R., Yarychivska, O., Boulard, M. and Bestor, T. H. (2017) 'DNA methylation and DNA methyltransferases', *Epigenetics Chromatin*, 10, pp. 23.

Elliott, N. T. and Yuan, F. (2011) 'A review of three-dimensional in vitro tissue models for drug discovery and transport studies', *Journal of Pharmaceutical Sciences*, 100(1), pp. 59-74.

Eshleman, A. J., Wolfrum, K. M., Hatfield, M. G., Johnson, R. A., Murphy, K. V. and Janowsky, A. (2013) 'Substituted methcathinones differ in transporter and receptor interactions', *Biochemical Pharmacology*, 85(12), pp. 1803-15.

Faria, R., Santana, M. M., Aveleira, C. A., Simões, C., Maciel, E., Melo, T., Santinha, D., Oliveira, M. M., Peixoto, F., Domingues, P., Cavadas, C. and Domingues, M. R. (2014) 'Alterations in phospholipidomic profile in the brain of mouse model of depression induced by chronic unpredictable stress', *Neuroscience*, 273, pp. 1-11.

Feed, E. (2009) 'Scientific Opinion on the use of cobalt compounds as additives in animal nutrition', *European Food Safety Authority Journal*, 7(12), pp. 1383.

Ferguson, C. S. and Tyndale, R. F. (2011) 'Cytochrome P450 enzymes in the brain: emerging evidence of biological significance', *Trends in Pharmacological Sciences*, 32(12), pp. 708-14.

Festa, M. D., Anderson, H. L., Dowdy, R. P. and Eilersieck, M. R. (1985) 'Effect of zinc intake on copper excretion and retention in men', *The American Journal of Clinical Nutrition*, 41(2), pp. 285-92.

Fiehn, O. (2002) 'Metabolomics--the link between genotypes and phenotypes', *Plant Molecular Biology*, 48(1-2), pp. 155-71.

- Finkel, T. and Holbrook, N. J. (2000) 'Oxidants, oxidative stress and the biology of ageing', *Nature*, 408(6809), pp. 239-47.
- Flynn, C. J. and Wecker, L. (1987) 'Concomitant increases in the levels of choline and free fatty acids in rat brain: evidence supporting the seizure-induced hydrolysis of phosphatidylcholine', *Journal of Neurochemistry*, 48(4), pp. 1178-84.
- Fricker, R. A., Green, E. L., Jenkins, S. I. and Griffin, S. M. (2018) 'The Influence of Nicotinamide on Health and Disease in the Central Nervous System', *International Journal of Tryptophan Research*, 11, pp. 1178646918776658.
- Friberg, L., Nordberg, G., Vouk, V. and II Elsevier Science Publ., A. (1979) 'Handbook on the toxicology of metals'.
- Gallo, M. A. and Doull, J. (1996) 'History and scope of toxicology', Cassarett and Doull's Toxicology. The Basic Science of Poisons (Klassen CD, ed). 5th ed. New York: McGraw-Hill, pp. 3-11.
- Gardner, F. H. (1953) 'The use of cobaltous chloride in the anemia associated with chronic renal disease', *Journal of Laboratory and Clinical Medicine*, 41(1), pp. 56-64.
- Ghodse, A. H., Corkery, J., Claridge, H., Goodair, C. and Schifano, F. (2013) Drug-related deaths in the UK: annual report 2012. International Centre for Drug Policy.
- Gibbons, S. and Zloh, M. (2010) 'An analysis of the 'legal high' mephedrone', *Bioorganic and Medicinal Chemistry Letters*, 20(14), pp. 4135-9.
- Goldberg, A. D., Allis, C. D. and Bernstein, E. (2007) 'Epigenetics: a landscape takes shape', *Cell*, 128(4), pp. 635-8.
- Goldoni, M., Catalani, S., De Palma, G., Manini, P., Acampa, O., Corradi, M., Bergonzi, R., Apostoli, P. and Mutti, A. (2004) 'Exhaled breath condensate as a suitable matrix to assess lung dose and effects in workers exposed to cobalt and tungsten', *Environmental Health Perspectives*, 112(13), pp. 1293-8.
- Gossel, T. A. (1994) Principles of clinical toxicology. CRC Press.
- Govender, R., De Greef, J., Delpont, R., Vermaak, W.J.H. and Becker, P.J., 2008. Biological variation of ischaemia-modified albumin in healthy subjects. *Cardiovascular journal of Africa*, 19(3), p.141.
- Griffiths, W. J., Koal, T., Wang, Y., Kohl, M., Enot, D. P. and Deigner, H. P. (2010) 'Targeted metabolomics for biomarker discovery', *Angewandte Chemie International Edition in English*, 49(32), pp. 5426-45.
- Gustavsson, D. and Escher, C. (2009) 'Mephedrone-Internet drug which seems to have come and stay. Fatal cases in Sweden have drawn attention to previously unknown substance', *Läkartidningen*, 106(43), pp. 2769.

Gómez-Lechón, M. J., Ponsoda, X., Bort, R. and Castell, J. V. (2001) 'The use of cultured hepatocytes to investigate the metabolism of drugs and mechanisms of drug hepatotoxicity', *Alternatives to Laboratory Animals*, 29(3), pp. 225-31.

Hadlock, G. C., Webb, K. M., McFadden, L. M., Chu, P. W., Ellis, J. D., Allen, S. C., Andrenyak, D. M., Vieira-Brock, P. L., German, C. L., Conrad, K. M., Hoonakker, A. J., Gibb, J. W., Wilkins, D. G., Hanson, G. R. and Fleckenstein, A. E. (2011) '4-Methylmethcathinone (mephedrone): neuropharmacological effects of a designer stimulant of abuse', *Journal of Pharmacology and Experimental Therapeutics*, 339(2), pp. 530-6.

Haga, Y., Clyne, N., Hatori, N., Hoffman-Bang, C., Pehrsson, S. and Ryden, L. (1996) 'Impaired myocardial function following chronic cobalt exposure in an isolated rat heart model', *Trace Elements and Electrocytes*, 13(2), pp. 69-74.

Halliwell, B. (1991) 'Drug antioxidant effects. A basis for drug selection?', *Drugs*, 42(4), pp. 569-605.

Halliwell, B. (2007) 'Cellular responses to oxidative stress: adaptation, damage, repair, senescence and death', *Free radicals in biology and medicine*, pp. 187-267.

Halliwell, B. and Gutteridge, J. M. (1990) 'Role of free radicals and catalytic metal ions in human disease: an overview', *Methods Enzymol*, 186, pp. 1-85.

Hamilton-Koch, W., Snyder, R. D. and Lavelle, J. M. (1986) 'Metal-induced DNA damage and repair in human diploid fibroblasts and Chinese hamster ovary cells', *Chemico-Biological Interactions*, 59(1), pp. 17-28.

Hannemann, F., Hartmann, A., Schmitt, J., Lützner, J., Seidler, A., Campbell, P., Delaunay, C. P., Drexler, H., Ettema, H. B., García-Cimbrelo, E., Huberti, H., Knahr, K., Kunze, J., Langton, D. J., Lauer, W., Learmonth, I., Lohmann, C. H., Morlock, M., Wimmer, M. A., Zagra, L. and Günther, K. P. (2013) 'European multidisciplinary consensus statement on the use and monitoring of metal-on-metal bearings for total hip replacement and hip resurfacing', *Orthopaedics & Traumatology: Surgery & Research*, 99(3), pp. 263-71.

Hannun, Y. A. and Obeid, L. M. (2002) 'The Ceramide-centric universe of lipid-mediated cell regulation: stress encounters of the lipid kind', *The Journal of Biological Chemistry*, 277(29), pp. 25847-50.

Hannun, Y. A. and Obeid, L. M. (2008) 'Principles of bioactive lipid signalling: lessons from sphingolipids', *Nature Reviews Molecular Cell Biology*, 9(2), pp. 139-50.

Hartwig, A. (1995) 'Current aspects in metal genotoxicity', *Biometals*, 8(1), pp. 3-11.

Hartwig, A., Snyder, R. D., Schlepegrell, R. and Beyersmann, D. (1991) 'Modulation by Co(II) of UV-induced DNA repair, mutagenesis and sister-chromatid exchanges in mammalian cells', *Mutation Research*, 248(1), pp. 177-85.

Hayes, P. and Knaus, U. G. (2013) 'Balancing reactive oxygen species in the epigenome: NADPH oxidases as target and perpetrator', *Antioxidants and Redox Signaling*, 18(15), pp. 1937-45.

Hayyan, M., Hashim, M. A. and AlNashef, I. M. (2016) 'Superoxide Ion: Generation and Chemical Implications', *Chemical Reviews*, 116(5), pp. 3029-85.

Higuchi, R., Dollinger, G., Walsh, P. S. and Griffith, R. (1992) 'Simultaneous amplification and detection of specific DNA sequences', *Biotechnology (N Y)*, 10(4), pp. 413-7.

Hoet, P. H., Roesems, G., Demedts, M. G. and Nemery, B. (2002) 'Activation of the hexose monophosphate shunt in rat type II pneumocytes as an early marker of oxidative stress caused by cobalt particles', *Archives of Toxicology*, 76(1), pp. 1-7.

Hogstedt, C. and Alexandersson, R. 'Mortality among hard-metal workers in Sweden'. *Scandinavian Journal of Work Environment & Health*. 41A, SF-00250 Helsinki, Finland, 177-178.

Holland, P. M., Abramson, R. D., Watson, R. and Gelfand, D. H. (1991) 'Detection of specific polymerase chain reaction product by utilizing the 5'----3' exonuclease activity of *Thermus aquaticus* DNA polymerase', *Proceedings of the National Academy of Sciences of the United States of America*, 88(16), pp. 7276-80.

Humans, I. (2006) 'Cobalt in hard metals and cobalt sulfate, gallium arsenide, indium phosphide and vanadium pentoxide', *IARC Monographs on the Evaluation of Carcinogenic Risks to Humans*, 86, pp. 1-294.

IARC, I. (1991) 'Chlorinated drinking-water; chlorination by-products; some other halogenated compounds; cobalt and cobalt compounds. International Agency for Research on Cancer (IARC) Working Group, Lyon, 12-19 June 1990', *IARC Monographs on the Evaluation of Carcinogenic Risks to Humans*, 52, pp. 1-544.

Ikeda, T., Takahashi, K., Kabata, T., Sakagoshi, D., Tomita, K. and Yamada, M. (2010) 'Polyneuropathy caused by cobalt-chromium metallosis after total hip replacement', *Muscle Nerve*, 42(1), pp. 140-3.

Innis, M. A., Gelfand, D. H., Sninsky, J. J. and White, T. J. (2012) *PCR protocols: a guide to methods and applications*. Academic press.

Inoue, H., Yokota, H., Makino, T., Yuasa, A. and Kato, S. (2001) 'Bisphenol a glucuronide, a major metabolite in rat bile after liver perfusion', *Drug Metabolism and Disposition*, 29(8), pp. 1084-7.

- Ivancsits, S., Diem, E., Pilger, A. and Rüdiger, H. W. (2002) 'Induction of 8-hydroxy-2'-deoxyguanosine by cobalt(II) and hydrogen peroxide in vitro', *Journal of Toxicology and Environmental Health. Part A*, 65(9), pp. 665-76.
- Jaishankar, M., Tseten, T., Anbalagan, N., Mathew, B. B. and Beeregowda, K. N. (2014) 'Toxicity, mechanism and health effects of some heavy metals', *Interdisciplinary Toxicology*, 7(2), pp. 60-72.
- James, D., Adams, R. D., Spears, R., Cooper, G., Lupton, D. J., Thompson, J. P., Thomas, S. H. and Service, N. P. I. (2011) 'Clinical characteristics of mephedrone toxicity reported to the U.K. National Poisons Information Service', *Emergency Medicine Journal*, 28(8), pp. 686-9.
- Johnson, R. D. and Botch-Jones, S. R. (2013) 'The stability of four designer drugs: MDPV, mephedrone, BZP and TFMP in three biological matrices under various storage conditions', *Journal of Analytical Toxicology*, 37(2), pp. 51-5.
- Jordan, C., Whitman, R. D., Harbut, M. and Tanner, B. (1990) 'Memory deficits in workers suffering from hard metal disease', *Toxicology Letters*, 54(2-3), pp. 241-3.
- Justice, B. A., Badr, N. A. and Felder, R. A. (2009) '3D cell culture opens new dimensions in cell-based assays', *Drug Discovery Today*, 14(1-2), pp. 102-7.
- Kahle, M., Schäfer, A., Seelig, A., Schultheiß, J., Wu, M., Aichler, M., Leonhardt, J., Rathkolb, B., Rozman, J., Sarioglu, H., Hauck, S. M., Ueffing, M., Wolf, E., Kastenmueller, G., Adamski, J., Walch, A., Hrabé de Angelis, M. and Neschen, S. (2015) 'High fat diet-induced modifications in membrane lipid and mitochondrial-membrane protein signatures precede the development of hepatic insulin resistance in mice', *Molecular Metabolism*, 4(1), pp. 39-50.
- Kamleh, M. A., Dow, J. A. and Watson, D. G. (2009) 'Applications of mass spectrometry in metabolomic studies of animal model and invertebrate systems', *Briefings in Functional Genomics and Proteomics*, 8(1), pp. 28-48.
- Kasprzak, K. (1996) 'Oxidative DNA damage in metal-induced carcinogenesis', *Toxicology of metals*, 18, pp. 299.
- Kasten, U., Mullenders, L. H. and Hartwig, A. (1997) 'Cobalt(II) inhibits the incision and the polymerization step of nucleotide excision repair in human fibroblasts', *Mutation Research*, 383(1), pp. 81-9.
- Keegan, G., Learmonth, I. and Case, C. (2008) 'A systematic comparison of the actual, potential, and theoretical health effects of cobalt and chromium exposures from industry and surgical implants', *Critical reviews in toxicology*, 38(8), pp. 645-674.
- Kehr, J., Ichinose, F., Yoshitake, S., Gojny, M., Sievertsson, T., Nyberg, F. and Yoshitake, T. (2011) 'Mephedrone, compared with MDMA (ecstasy) and

amphetamine, rapidly increases both dopamine and 5-HT levels in nucleus accumbens of awake rats', *British Journal of Pharmacology*, 164(8), pp. 1949-58.

Kellett, C. E. (1946) 'The history of medicine', *Medical World*, 64, pp. 330-4.

Khreit, O. I., Grant, M. H., Zhang, T., Henderson, C., Watson, D. G. and Sutcliffe, O. B. (2013) 'Elucidation of the Phase I and Phase II metabolic pathways of ( $\pm$ )-4'-methylmethcathinone (4-MMC) and ( $\pm$ )-4'-(trifluoromethyl)methcathinone (4-TFMMC) in rat liver hepatocytes using LC-MS and LC-MS<sup>2</sup>', *Journal of Pharmaceutical and Biomedical Analysis*, 72, pp. 177-85.

Kim, J., Gherasim, C. and Banerjee, R. (2008) 'Decyanation of vitamin B12 by a trafficking chaperone', *Proceedings of the National Academy of Sciences of the United States of America*, 105(38), pp. 14551-4.

Klaassen, C. D. and Casarett, L. J. (2001) *Casarett and Doull's toxicology : the basic science of poisons*. 6th edn. New York ; London: McGraw-Hill Medical Pub. Division.

Kleinstreuer, N. C., Smith, A. M., West, P. R., Conard, K. R., Fontaine, B. R., Weir-Hauptman, A. M., Palmer, J. A., Knudsen, T. B., Dix, D. J., Donley, E. L. and Cezar, G. G. (2011) 'Identifying developmental toxicity pathways for a subset of ToxCast chemicals using human embryonic stem cells and metabolomics', *Toxicology and Applied Pharmacology*, 257(1), pp. 111-21.

Kow, Y. W. (2002) 'Repair of deaminated bases in DNA', *Free Radical Biology and Medicine*, 33(7), pp. 886-93.

Krasovskii, G. and Fridlyand, S. (1971) 'Experimental data for the validation of the maximum permissible concentration of cobalt in water bodies', *Hygiene and Sanitary*, 26, pp. 277-279.

Krokan, H. E., Standal, R. and Slupphaug, G. (1997) 'DNA glycosylases in the base excision repair of DNA', *The Biochemical Journal*, 325 ( Pt 1), pp. 1-16.

Kutyavin, I. V., Afonina, I. A., Mills, A., Gorn, V. V., Lukhtanov, E. A., Belousov, E. S., Singer, M. J., Walburger, D. K., Likhov, S. G., Gall, A. A., Dempsy, R., Reed, M. W., Meyer, R. B. and Hedgpeth, J. (2000) '3'-minor groove binder-DNA probes increase sequence specificity at PCR extension temperatures', *Nucleic Acids Research*, 28(2), pp. 655-61.

L'Abbate, A., Neglia, D., Vecoli, C., Novelli, M., Ottaviano, V., Baldi, S., Barsacchi, R., Paolicchi, A., Masiello, P., Drummond, G.S. and McClung, J.A. (2007) 'Beneficial effect of heme oxygenase-1 expression on myocardial ischemia-reperfusion involves an increase in adiponectin in mildly diabetic rats'. *American Journal of Physiology-Heart and Circulatory Physiology*.

- La Quaglia, M. P. and Manchester, K. M. (1996) 'A comparative analysis of neuroblastic and substrate-adherent human neuroblastoma cell lines', *Journal of Pediatric Surgery*, 31(2), pp. 315-8.
- Laposa, R. and Cleaver, J. (2001) 'DNA repair on the brain', *Proceedings of the National Academy of Sciences*, 98(23), pp. 12860-12862.
- Lasfargues, G., Lardot, C., Delos, M., Lauwerys, R. and Lison, D. (1995) 'The delayed lung responses to single and repeated intratracheal administration of pure cobalt and hard metal powder in the rat', *Environmental Research*, 69(2), pp. 108-21.
- Lasfargues, G., Wild, P., Moulin, J. J., Hammon, B., Rosmorduc, B., Rondeau du Noyer, C., Lavandier, M. and Moline, J. (1994) 'Lung cancer mortality in a French cohort of hard-metal workers', *American Journal of Industrial Medicine*, 26(5), pp. 585-95.
- Lasnitzki, I. (1958) 'Observations on the effects of condensates from cigarette smoke on human foetal lung in vitro', *British Journal of Cancer*, 12(4), pp. 547-52.
- Lasnitzki, I. and Lucy, J. A. (1961) 'Amino acid metabolism and arginase activity in mouse prostate glands grown in vitro with and without 20-methylcholanthrene', *Experimental Cell Research*, 24, pp. 379-92.
- Leclercq, L., Cuyckens, F., Mannens, G. S., de Vries, R., Timmerman, P. and Evans, D. C. (2009) 'Which human metabolites have we MIST? Retrospective analysis, practical aspects, and perspectives for metabolite identification and quantification in pharmaceutical development', *Chemical Research in Toxicology*, 22(2), pp. 280-93.
- Lee, L. H., Shui, G., Farooqui, A. A., Wenk, M. R., Tan, C. H. and Ong, W. Y. (2009) 'Lipidomic analyses of the mouse brain after antidepressant treatment: evidence for endogenous release of long-chain fatty acids?', *The International Journal of Neuropsychopharmacology*, 12(7), pp. 953-64.
- Lennicke, C., Rahn, J., Lichtenfels, R., Wessjohann, L. A. and Seliger, B. (2015) 'Hydrogen peroxide - production, fate and role in redox signaling of tumor cells', *Cell Communication and Signaling*, 13, pp. 39.
- Licht, A., Oliver, M. and Rachmilewitz, E. A. (1972) 'Optic atrophy following treatment with cobalt chloride in a patient with pancytopenia and hypercellular marrow', *Israel Journal of Medical Sciences*, 8(1), pp. 61-6.
- Lie, Y. S. and Petropoulos, C. J. (1998) 'Advances in quantitative PCR technology: 5' nuclease assays', *Current Opinion in Biotechnology*, 9(1), pp. 43-8.
- Lim, A., Prokaeva, T., McComb, M. E., Connors, L. H., Skinner, M. and Costello, C. E. (2003) 'Identification of S-sulfonation and S-thiolation of a novel transthyretin Phe33Cys variant from a patient diagnosed with familial transthyretin amyloidosis', *Protein Science*, 12(8), pp. 1775-85.

Linhart, I., Himl, M., Židková, M., Balíková, M., Lhotková, E. and Páleníček, T. (2016) 'Metabolic profile of mephedrone: Identification of nor-mephedrone conjugates with dicarboxylic acids as a new type of xenobiotic phase II metabolites', *Toxicology Letters*, 240(1), pp. 114-21.

Lison, D., Carbonnelle, P., Mollo, L., Lauwerys, R. and Fubini, B. (1995) 'Physicochemical mechanism of the interaction between cobalt metal and carbide particles to generate toxic activated oxygen species', *Chemical Research in Toxicology*, 8(4), pp. 600-6.

Lison, D., De Boeck, M., Verougstraete, V. and Kirsch-Volders, M. (2001) 'Update on the genotoxicity and carcinogenicity of cobalt compounds', *Occupational and Environmental Medicine*, 58(10), pp. 619-25.

Lloyd, D. R., Phillips, D. H. and Carmichael, P. L. (1997) 'Generation of putative intrastrand cross-links and strand breaks in DNA by transition metal ion-mediated oxygen radical attack', *Chemical Research in Toxicology*, 10(4), pp. 393-400.

Lohner, K. (1996) 'Is the high propensity of ethanolamine plasmalogens to form non-lamellar lipid structures manifested in the properties of biomembranes?', *Chemistry and Physics of Lipids*, 81(2), pp. 167-84.

Lombardi, A. V., Barrack, R. L., Berend, K. R., Cuckler, J. M., Jacobs, J. J., Mont, M. A. and Schmalzried, T. P. (2012) 'The Hip Society: algorithmic approach to diagnosis and management of metal-on-metal arthroplasty', *The Journal of Bone and Joint Surgery. British volume*, 94(11 Suppl A), pp. 14-8.

Lu, W., Bennett, B. D. and Rabinowitz, J. D. (2008) 'Analytical strategies for LC-MS-based targeted metabolomics', *Journal of chromatography. B, Analytical Technologies in the Biomedical and Life Sciences*, 871(2), pp. 236-42.

López-Arnau, R., Martínez-Clemente, J., Pubill, D., Escubedo, E. and Camarasa, J. (2012) 'Comparative neuropharmacology of three psychostimulant cathinone derivatives: butylone, mephedrone and methylone', *British Journal of Pharmacology*, 167(2), pp. 407-20.

López-Arnau, R., Martínez-Clemente, J., Rodrigo, T., Pubill, D., Camarasa, J. and Escubedo, E. (2015) 'Neuronal changes and oxidative stress in adolescent rats after repeated exposure to mephedrone', *Toxicology and Applied Pharmacology*, 286(1), pp. 27-35.

Magret, V., Elkhail, L., Nazih-Sanderson, F., Martin, F., Bourre, J. M., Fruchart, J. C. and Delbart, C. (1996) 'Entry of polyunsaturated fatty acids into the brain: evidence that high-density lipoprotein-induced methylation of phosphatidylethanolamine and phospholipase A2 are involved', *The Biochemical Journal*, 316 ( Pt 3), pp. 805-11.

- Malard, V., Berenguer, F., Prat, O., Ruat, S., Steinmetz, G. and Quemeneur, E. (2007) 'Global gene expression profiling in human lung cells exposed to cobalt', *Biomedical Central Genomics*, 8, pp. 147.
- Mann, A. and Tyndale, R.F., 2010. Cytochrome P450 2D6 enzyme neuroprotects against 1-methyl-4-phenylpyridinium toxicity in SH-SY5Y neuronal cells. *European Journal of Neuroscience*, 31(7), pp.1185-1193.
- Marklund, S. L. (1984) 'Extracellular superoxide dismutase in human tissues and human cell lines', *The Journal of Clinical Investigation*, 74(4), pp. 1398-403.
- Marks, A. (2005) *Marks' basic medical biochemistry: a clinical approach* Philadelphia: Lippincott Williams & Wilkins.
- Martínez-Clemente, J., Escubedo, E., Pubill, D. and Camarasa, J. (2012) 'Interaction of mephedrone with dopamine and serotonin targets in rats', *European Neuropsychopharmacology*, 22(3), pp. 231-6.
- Martínez-Clemente, J., López-Arnau, R., Carbó, M., Pubill, D., Camarasa, J. and Escubedo, E. (2013) 'Mephedrone pharmacokinetics after intravenous and oral administration in rats: relation to pharmacodynamics', *Psychopharmacology (Berl)*, 229(2), pp. 295-306.
- Maskell, P. D., Seetohul, L. N., Livingstone, A. C., Cockburn, A. K., Preece, J. and Pounder, D. J. (2013) 'Stability of 3,4-methylenedioxymethamphetamine (MDMA), 4-methylmethcathinone (mephedrone) and 3-trifluoromethylphenylpiperazine (3-TFMPP) in formalin solution', *Journal of Analytical Toxicology*, 37(7), pp. 440-6.
- Mathur, N., Pandey, G. and Jain, G. (2010) 'Male reproductive toxicity of some selected metals: A review', *Journal of biological sciences*, 10(5), pp. 396-404.
- Maxwell, M. M., Tomkinson, E. M., Nobles, J., Wizeman, J. W., Amore, A. M., Quinti, L., Chopra, V., Hersch, S. M. and Kazantsev, A. G. (2011) 'The Sirtuin 2 microtubule deacetylase is an abundant neuronal protein that accumulates in the aging CNS', *Human Molecular Genetics*, 20(20), pp. 3986-96.
- Maxwell, P. and Salnikow, K. (2004) 'HIF-1: an oxygen and metal responsive transcription factor', *Cancer Biology and Therapy*, 3(1), pp. 29-35.
- Mayer, F. P., Wimmer, L., Dillon-Carter, O., Partilla, J. S., Burchardt, N. V., Mihovilovic, M. D., Baumann, M. H. and Sitte, H. H. (2016) 'Phase I metabolites of mephedrone display biological activity as substrates at monoamine transporters', *British Journal of Pharmacology*, 173(17), pp. 2657-68.
- Measham, F., Moore, K., Newcombe, R. and Smith, Z. n. (2013) 'Tweaking, bombing, dabbing and stockpiling: the emergence of mephedrone and the perversity of prohibition', <http://dx.doi.org/10.5042/daat.2010.0123>.

Meecham, H. M. and Humphrey, P. (1991) 'Industrial exposure to cobalt causing optic atrophy and nerve deafness: a case report', *Journal of Neurology, Neurosurgery, and Psychiatry*, 54(4), pp. 374-5.

Meister, A. (1988) 'Glutathione metabolism and its selective modification', *The Journal of Biological Chemistry*, 263(33), pp. 17205-8.

Meister, A. and Anderson, M. E. (1983) 'Glutathione', *Annual Reviews of Biochemistry*, 52, pp. 711-60.

Meng, H., Cao, J., Kang, J., Ying, X., Ji, J., Reynolds, W. and Rampe, D. (2012) 'Mephedrone, a new designer drug of abuse, produces acute hemodynamic effects in the rat', *Toxicology Letters*, 208(1), pp. 62-8.

Meyer, M. R., Wilhelm, J., Peters, F. T. and Maurer, H. H. (2010) 'Beta-keto amphetamines: studies on the metabolism of the designer drug mephedrone and toxicological detection of mephedrone, butylone, and methylone in urine using gas chromatography-mass spectrometry', *Analytical and Bioanalytical Chemistry*, 397(3), pp. 1225-33.

Meyer, R. P., Knoth, R., Schiltz, E. and Volk, B. (2001) 'Possible function of astrocyte cytochrome P450 in control of xenobiotic phenytoin in the brain: in vitro studies on murine astrocyte primary cultures', *Experimental Neurology*, 167(2), pp. 376-84.

Michel, R., Nolte, M., Reich, M. and Löer3. (1991) 'Systemic effects of implanted prostheses made of cobalt-chromium alloys', 110(2), pp. 61-74.

Mohiuddin, S. M., Taskar, P. K., Rheault, M., Roy, P. E., Chenard, J. and Morin, Y. (1970) 'Experimental cobalt cardiomyopathy', *American Heart Journal*, 80(4), pp. 532-43.

Montealegre, C., Verardo, V., Luisa Marina, M. and Caboni, M. F. (2014) 'Analysis of glycerophospho- and sphingolipids by CE', *Electrophoresis*, 35(6), pp. 779-92.

Morin, Y. and Daniel, P. (1967) 'Quebec beer-drinkers' cardiomyopathy: etiological considerations', *Canadian Medical Association Journal*, 97(15), pp. 926-8.

Morin, Y., Têtu, A. and Mercier, G. (1971) 'Cobalt cardiomyopathy: clinical aspects', *British Heart Journal*, 33, pp. Suppl:175-8.

Morita, I., Kawamoto, M., Hattori, M., Eguchi, K., Sekiba, K. and Yoshida, H. (1990) 'Determination of tryptophan and its metabolites in human plasma and serum by high-performance liquid chromatography with automated sample clean-up system', *Journal of Chromatography*, 526(2), pp. 367-74.

- Morvan D, Demidem A. (2007) 'Metabolomics by proton nuclear magnetic resonance spectroscopy of the response to chloroethylnitrosourea reveals drug efficacy and tumor adaptive metabolic pathways'. *Cancer*. 67, pp. 2150–59.
- Mosmann, T. R. (1988) 'Directional release of lymphokines from T cells', *Immunology Today*, 9(10), pp. 306-7.
- Motbey, C. P., Hunt, G. E., Bowen, M. T., Artiss, S. and McGregor, I. S. (2012) 'Mephedrone (4-methylmethcathinone, 'meow'): acute behavioural effects and distribution of Fos expression in adolescent rats', *Addiction Biology*, 17(2), pp. 409-22.
- Moulin, J. J., Wild, P., Mur, J. M., Fournier-Betz, M. and Mercier-Gallay, M. (1993) 'A mortality study of cobalt production workers: an extension of the follow-up', *American Journal of Industrial Medicine*, 23(2), pp. 281-8.
- Moulin, J. J., Wild, P., Romazini, S., Lasfargues, G., Peltier, A., Bozec, C., Deguerry, P., Pellet, F. and Perdrix, A. (1998) 'Lung cancer risk in hard-metal workers', *American Journal of Epidemiology*, 148(3), pp. 241-8.
- Muha, V., Zagyva, I., Venkei, Z., Szabad, J. and Vértessy, B. G. (2009) 'Nuclear localization signal-dependent and -independent movements of *Drosophila melanogaster* dUTPase isoforms during nuclear cleavage', *Biochemical and Biophysical Research Communications*, 381(2), pp. 271-5.
- Munichor, M., Cohen, H., Volpin, G., Kerner, H. and Iancu, T. C. (2003) 'Chromium-induced lymph node histiocytic proliferation after hip replacement. A case report', *Acta Cytologica*, 47(2), pp. 270-4.
- Mur, J., Moulin, J., Charruyer - Seinerra, M. and Lafitte, J. (1987) 'A cohort mortality study among cobalt and sodium workers in an electrochemical plant', *American Journal of Industrial Medicine*, 11(1), pp. 75-81.
- Murdock, H. R. (1959) 'Studies on the pharmacology of cobalt chloride', *Journal of the American Pharmaceutical Association*, 48(3), pp. 140-2.
- Murphy, T. H., Yu, J., Ng, R., Johnson, D. A., Shen, H., Honey, C. R. and Johnson, J. A. (2001) 'Preferential expression of antioxidant response element mediated gene expression in astrocytes', *Journal of Neurochemistry*, 76(6), pp. 1670-8.
- Mutafova-Yambolieva, V., Staneva-Stoytcheva, D., Lasova, L. and Radomirov, R. (1994) 'Effects of cobalt or nickel on the sympathetically mediated contractile responses in rat-isolated vas deferens', *Pharmacology*, 48(2), pp. 100-110.
- Nackerdien, Z., Kasprzak, K. S., Rao, G., Halliwell, B. and Dizdaroglu, M. (1991) 'Nickel (II)-and cobalt (II)-dependent damage by hydrogen peroxide to the DNA bases in isolated human chromatin', *Cancer research*, 51(21), pp. 5837-5842.

Nation, J. R., Bourgeois, A. E., Clark, D. E. and Hare, M. F. (1983) 'The effects of chronic cobalt exposure on behavior and metallothionein levels in the adult rat', *Neurobehavioral Toxicology and Teratology*, 5(1), pp. 9-15.

NCBI <https://http://www.ncbi.nlm.nih.gov>: National Library of Medicine. Available at: <https://http://www.ncbi.nlm.nih.gov> 2018).

Neddermann, P., Gallinari, P., Lettieri, T., Schmid, D., Truong, O., Hsuan, J. J., Wiebauer, K. and Jiricny, J. (1996) 'Cloning and expression of human G/T mismatch-specific thymine-DNA glycosylase', *The Journal of Biological Chemistry*, 271(22), pp. 12767-74.

Nicholson, J. K., Lindon, J. C. and Holmes, E. (1999) 'Metabonomics': understanding the metabolic responses of living systems to pathophysiological stimuli via multivariate statistical analysis of biological NMR spectroscopic data', *Xenobiotica*, 29(11), pp. 1181-9.

Nicholson, P. J., Quinn, M. J. and Dodd, J. D. (2010) 'Headshop heartache: acute mephedrone 'meow' myocarditis', *Heart*, 96(24), pp. 2051-2.

Niessen, W. M., Manini, P. and Andreoli, R. (2006) 'Matrix effects in quantitative pesticide analysis using liquid chromatography-mass spectrometry', *Mass Spectrometry Reviews*, 25(6), pp. 881-99.

North, B. J. and Verdin, E. (2007) 'Mitotic regulation of SIRT2 by cyclin-dependent kinase 1-dependent phosphorylation', *The Journal of Biological Chemistry*, 282(27), pp. 19546-55.

Olesti, E., Farré, M., Papaseit, E., Krotonoulas, A., Pujadas, M., de la Torre, R. and Pozo, Ó. (2017) 'Pharmacokinetics of Mephedrone and Its Metabolites in Human by LC-MS/MS', *American Association of Pharmaceutical Scientists Journal*, 19(6), pp. 1767-1778.

Oliveira, T. G., Chan, R. B., Bravo, F. V., Miranda, A., Silva, R. R., Zhou, B., Marques, F., Pinto, V., Cerqueira, J. J., Di Paolo, G. and Sousa, N. (2016) 'The impact of chronic stress on the rat brain lipidome', *Molecular Psychiatry*, 21(1), pp. 80-8.

Olivieri, G., Brack, C., Müller-Spahn, F., Stähelin, H. B., Herrmann, M., Renard, P., Brockhaus, M. and Hock, C. (2000) 'Mercury induces cell cytotoxicity and oxidative stress and increases beta-amyloid secretion and tau phosphorylation in SHSY5Y neuroblastoma cells', *Journal of Neurochemistry*, 74(1), pp. 231-6.

Olpin, S. E. (2005) 'Fatty acid oxidation defects as a cause of neuromyopathic disease in infants and adults', *Clinical Laboratory*, 51(5-6), pp. 289-306.

Owen, J. B. and Butterfield, D. A. (2010) 'Measurement of oxidized/reduced glutathione ratio', *Methods in Molecular Biology*, 648, pp. 269-77.

- Owens, M. J. and Nemeroff, C. B. (1994) 'Role of serotonin in the pathophysiology of depression: focus on the serotonin transporter', *Clinical Chemistry*, 40(2), pp. 288-95.
- Palmer, J. A., Smith, A. M., Egnash, L. A., Colwell, M. R., Donley, E. L. R., Kirchner, F. R. and Burrier, R. E. (2017) 'A human induced pluripotent stem cell-based in vitro assay predicts developmental toxicity through a retinoic acid receptor-mediated pathway for a series of related retinoid analogues', *Reproductive Toxicology*, 73, pp. 350-361.
- Palmer, J. A., Smith, A. M., Egnash, L. A., Conard, K. R., West, P. R., Burrier, R. E., Donley, E. L. and Kirchner, F. R. (2013) 'Establishment and assessment of a new human embryonic stem cell-based biomarker assay for developmental toxicity screening', *Birth Defects Research. Part B, Developmental and Reproductive Toxicology*, 98(4), pp. 343-63.
- Pampaloni, F., Reynaud, E. G. and Stelzer, E. H. (2007) 'The third dimension bridges the gap between cell culture and live tissue', *Nature Reviews. Molecular Cell Biology*, 8(10), pp. 839-45.
- Papaseit, E., Pérez-Mañá, C., Mateus, J. A., Pujadas, M., Fonseca, F., Torrens, M., Olesti, E., de la Torre, R. and Farré, M. (2016) 'Human Pharmacology of Mephedrone in Comparison with MDMA', *Neuropsychopharmacology*, 41(11), pp. 2704-13.
- Paustenbach, D. J., Tvermoes, B. E., Unice, K. M., Finley, B. L. and Kerger, B. D. (2013) 'A review of the health hazards posed by cobalt', *Critical Reviews in Toxicology*, 43(4), pp. 316-62.
- Pedersen, A. J., Reitzel, L. A., Johansen, S. S. and Linnet, K. (2013) 'In vitro metabolism studies on mephedrone and analysis of forensic cases', *Drug Testing and Analysis*, 5(6), pp. 430-8.
- Pitt, J. J. (2009) 'Principles and applications of liquid chromatography-mass spectrometry in clinical biochemistry', *The Clinical Biochemistry Reviews*, 30(1), pp. 19-34.
- Posada, O. M., Tate, R. J. and Grant, M. H. (2015) 'Effects of CoCr metal wear debris generated from metal-on-metal hip implants and Co ions on human monocyte-like U937 cells', *Toxicology In Vitro*, 29(2), pp. 271-80.
- Poth, L. S., O'Connell, B. P., McDermott, J. L. and Dluzen, D. E. (2012) 'Nomifensine alters sex differences in striatal dopaminergic function', *Synapse*, 66(8), pp. 686-93.
- Power, J. H. and Blumbergs, P. C. (2009) 'Cellular glutathione peroxidase in human brain: cellular distribution, and its potential role in the degradation of Lewy bodies in

Parkinson's disease and dementia with Lewy bodies', *Acta Neuropathologica*, 117(1), pp. 63-73.

Pozo, Ó., Ibáñez, M., Sancho, J. V., Lahoz-Beneytez, J., Farré, M., Papaseit, E., de la Torre, R. and Hernández, F. (2015) 'Mass spectrometric evaluation of mephedrone in vivo human metabolism: identification of phase I and phase II metabolites, including a novel succinyl conjugate', *Drug Metabolism and Disposition*, 43(2), pp. 248-57.

Pu, C., Fisher, J. E., Cappon, G. D. and Vorhees, C. V. (1994) 'The effects of amfonelic acid, a dopamine uptake inhibitor, on methamphetamine-induced dopaminergic terminal degeneration and astrocytic response in rat striatum', *Brain Research*, 649(1-2), pp. 217-24.

Ramsey, J., Dargan, P. I., Smyllie, M., Davies, S., Button, J., Holt, D. W. and Wood, D. M. (2010) 'Buying 'legal' recreational drugs does not mean that you are not breaking the law', *QJM: An International Journal of Medicine*, 103(10), pp. 777-83.

Ravindranath, V. and Strobel, H. W. (2013) 'Cytochrome P450-mediated metabolism in brain: functional roles and their implications', *Expert opinion on drug metabolism and toxicology*, 9(5), pp. 551-8.

Robertson, D.G., 2005. *Metabonomics in toxicology: a review*. *Toxicological sciences*, 85(2), pp.809-822.

Robertson, D. G., Lindon, J. C., Nicholson, J. K. and Holmes, E. (2005) *Metabonomics in toxicity assessment*. Taylor & Francis Boca Raton, FL.

Robison, S. H., Cantoni, O. and Costa, M. (1982) 'Strand breakage and decreased molecular weight of DNA induced by specific metal compounds', *Carcinogenesis*, 3(6), pp. 657-62.

Rodríguez-Antona, C., Donato, M. T., Boobis, A., Edwards, R. J., Watts, P. S., Castell, J. V. and Gómez-Lechón, M. J. (2002) 'Cytochrome P450 expression in human hepatocytes and hepatoma cell lines: molecular mechanisms that determine lower expression in cultured cells', *Xenobiotica*, 32(6), pp. 505-20.

Romagnoli, P., Labhardt, A. M. and Sinigaglia, F. (1991) 'Selective interaction of Ni with an MHC-bound peptide', *European Molecular Biology Organization Journal*, 10(6), pp. 1303-6.

Ruokonen, E. L., Linnainmaa, M., Seuri, M., Juhakoski, P. and Söderström, K. O. (1996) 'A fatal case of hard-metal disease', *Scandinavian Journal of Work, Environment and Health*, 22(1), pp. 62-5.

Sadler, P.J., Tucker, A. and Viles, J.H. (1994) 'Involvement of a lysine residue in the N-terminal Ni<sup>2+</sup> and Cu<sup>2+</sup> binding site of serum albumins: Comparison with Co<sup>2+</sup>, Cd<sup>2+</sup> and Al<sup>3+</sup>'. *European Journal of Biochemistry*, 220(1), pp.193-200.

- Sagara, J. I., Miura, K. and Bannai, S. (1993) 'Maintenance of neuronal glutathione by glial cells', *Journal of Neurochemistry*, 61(5), pp. 1672-6.
- Sammler, E. M., Foley, P. L., Lauder, G. D., Wilson, S. J., Goudie, A. R. and O'Riordan, J. I. (2010) 'A harmless high?', *Lancet*, 376(9742), pp. 742.
- Sarkar, B. (1995) 'Metal replacement in DNA-binding zinc finger proteins and its relevance to mutagenicity and carcinogenicity through free radical generation', *Nutrition*, 11(5 Suppl), pp. 646-9.
- Sassa, A., Kanemaru, Y., Kamoshita, N., Honma, M. and Yasui, M. (2016) 'Mutagenic consequences of cytosine alterations site-specifically embedded in the human genome', *Genes and Environment*, 38(1), pp. 17.
- Sauni, R., Oksa, P., Uitti, J., Linna, A., Kerttula, R. and Pukkala, E. (2017) 'Cancer incidence among Finnish male cobalt production workers in 1969–2013: a cohort study'. *Biomedcentral cancer*, 17(1), p.340.
- Schifano, F., Albanese, A., Fergus, S., L. Stair, J., Deluca, P., Corazza, O., Davey, Z., Corkery, J., Siemann, H., Scherbaum, N., 'Farre', M., Torrens, M., Demetrovics, Z. and Ghodse, A. H. (2015) 'Mephedrone (4-methylmethcathinone; 'meow meow'): chemical, pharmacolog', *Psychopharmacology*, 214(3), pp. 593-02.
- Schifano, F., Albanese, A., Fergus, S., Stair, J. L., Deluca, P., Corazza, O., Davey, Z., Corkery, J., Siemann, H., Scherbaum, N., Farre', M., Torrens, M., Demetrovics, Z., Ghodse, A. H., Mapping, P. W. and Groups, R. R. (2011) 'Mephedrone (4-methylmethcathinone; 'meow meow'): chemical, pharmacological and clinical issues', *Psychopharmacology (Berl)*, 214(3), pp. 593-602.
- Schärer, O. D. and Jiricny, J. (2001) 'Recent progress in the biology, chemistry and structural biology of DNA glycosylases', *Bioessays*, 23(3), pp. 270-81.
- Schnackenberg, L.K., Sun, J. and Beger, R.D., 2009. *Metabolomics in systems toxicology: Towards personalized medicine*. General, Applied and Systems Toxicology.
- Seo, K. S., Park, J. H., Heo, J. Y., Jing, K., Han, J., Min, K. N., Kim, C., Koh, G. Y., Lim, K., Kang, G. Y., Uee Lee, J., Yim, Y. H., Shong, M., Kwak, T. H. and Kweon, G. R. (2015) 'SIRT2 regulates tumour hypoxia response by promoting HIF-1 $\alpha$  hydroxylation', *Oncogene*, 34(11), pp. 1354-62.
- Shearer, M. J. and Newman, P. (2014) 'Recent trends in the metabolism and cell biology of vitamin K with special reference to vitamin K cycling and MK-4 biosynthesis', *Journal of Lipid Research*, 55(3), pp. 345-62.

Shetty, P. K., Galeffi, F. and Turner, D. A. (2014) 'Nicotinamide pre-treatment ameliorates NAD(H) hyperoxidation and improves neuronal function after severe hypoxia', *Neurobiology of Disease*, 62, pp. 469-78.

Shih, A. Y., Johnson, D. A., Wong, G., Kraft, A. D., Jiang, L., Erb, H., Johnson, J. A. and Murphy, T. H. (2003) 'Coordinate regulation of glutathione biosynthesis and release by Nrf2-expressing glia potently protects neurons from oxidative stress', *The Journal of Neuroscience*, 23(8), pp. 3394-406.

Simonsen, L. O., Harbak, H. and Bennekou, P. (2012) 'Cobalt metabolism and toxicology--a brief update', *The Science of the Total Environment*, 432, pp. 210-5.

Singh, P. and Junnarkar, A. (1991) 'Behavioural and toxic profile of some essential trace metal salts in mice and rats', *Indian Journal of Pharmacology*, 23(3), pp. 153.

Smith, Q. R. (2000) 'Transport of glutamate and other amino acids at the blood-brain barrier', *The Journal of Nutrition*, 130(4S Suppl), pp. 1016S-22S.

Smith, T.A.D. (2005) 'Human serum transferrin cobalt complex: stability and cellular uptake of cobalt'. *Bioorganic & medicinal chemistry*, 13(14), pp.4576-4579.

Spector, R. (1988) 'Fatty acid transport through the blood-brain barrier', *Journal of Neurochemistry*, 50(2), pp. 639-43.

Speijers, G. J., Krajnc, E. I., Berkvens, J. M. and van Logten, M. J. (1982) 'Acute oral toxicity of inorganic cobalt compounds in rats', *Food and Chemical Toxicology*, 20(3), pp. 311-4.

Stillman, M. J., Shaw, C. F. and Suzuki, K. T. (1992) *Metallothionein: Synthesis, structure, and properties of metallothioneins, phytochelatins, and metal-thiolate complexes*. Wiley-VCH.

Su, X. A. and Freudenreich, C. H. (2017) 'Cytosine deamination and base excision repair cause R-loop-induced CAG repeat fragility and instability in', *Proceedings of the National Academy of Sciences of the United States of America*, 114(40), pp. E8392-E8401.

Sullivan, J. F., Egan, J. D. and George, R. P. (1969) 'A distinctive myocardial pathology occurring in Omaha, Nebraska: clinical aspects', *Annals of the New York Academy of Sciences*, 156(1), pp. 526-43.

Szpunar, J. (2000) 'Bio-inorganic speciation analysis by hyphenated techniques', *Analyst*, 125(5), pp. 963-88.

Sørensen, L. K. (2011) 'Determination of cathinones and related ephedrines in forensic whole-blood samples by liquid-chromatography-electrospray tandem mass spectrometry', *Journal of Chromatography. B, Analytical Technologies in the Biomedical and Life Sciences*, 879(11-12), pp. 727-36.

Thannickal, V. J. and Fanburg, B. L. (2000) 'Reactive oxygen species in cell signaling', *American Journal of Physiology. Lung Cellular and Molecular Physiology*, 279(6), pp. L1005-28.

Toimela, T., Mäenpää, H., Mannerström, M. and Tähti, H. (2004) 'Development of an in vitro blood–brain barrier model—cytotoxicity of mercury and aluminum', *Toxicology and Applied Pharmacology*, 195(1), pp. 73-82.

Torrance, H. and Cooper, G. (2010) 'The detection of mephedrone (4-methylmethcathinone) in 4 fatalities in Scotland', *Forensic Science International*, 202(1-3), pp. e62-3.

Tripathi, V. K., Kumar, V., Singh, A. K., Kashyap, M. P., Jahan, S., Pandey, A., Alam, S., Khan, F., Khanna, V. K., Yadav, S., Lohani, M. and Pant, A. B. (2014) 'Monocrotophos induces the expression and activity of xenobiotic metabolizing enzymes in pre-sensitized cultured human brain cells', *Public Library of Science One*, 9(3), pp. e91946.

Tsujikawa, K., Mikuma, T., Kuwayama, K., Miyaguchi, H., Kanamori, T., Iwata, Y. T. and Inoue, H. (2012) 'Degradation pathways of 4-methylmethcathinone in alkaline solution and stability of methcathinone analogs in various pH solutions', *Forensic Science International*, 220(1-3), pp. 103-10.

Tvermoes, B.E., Paustenbach, D.J., Kerger, B.D., Finley, B.L. and Unice, K.M. (2015) 'Review of cobalt toxicokinetics following oral dosing: Implications for health risk assessments and metal-on-metal hip implant patients'. *Critical reviews in toxicology*, 45(5), pp.367-387.

Tyagi, S., Bratu, D. P. and Kramer, F. R. (1998) 'Multicolor molecular beacons for allele discrimination', *Nature Biotechnology*, 16(1), pp. 49-53.

Tyurin, V. A., Tyurina, Y. Y., Jung, M. Y., Tungekar, M. A., Wasserloos, K. J., Bayir, H., Greenberger, J. S., Kochanek, P. M., Shvedova, A. A., Pitt, B. and Kagan, V. E. (2009) 'Mass-spectrometric analysis of hydroperoxy- and hydroxy-derivatives of cardiolipin and phosphatidylserine in cells and tissues induced by pro-apoptotic and pro-inflammatory stimuli', *Journal of Chromatography. B, Analytical Technologies in the Biomedical and Life Sciences*, 877(26), pp. 2863-72.

Unice, K.M., Monnot, A.D., Gaffney, S.H., Tvermoes, B.E., Thuett, K.A., Paustenbach, D.J. and Finley, B.L. (2012) 'Inorganic cobalt supplementation: Prediction of cobalt levels in whole blood and urine using a biokinetic model'. *Food and chemical toxicology*, 50(7), pp.2456-2461.

Valente, M. J., Guedes de Pinho, P., de Lourdes Bastos, M., Carvalho, F. and Carvalho, M. (2014) 'Khat and synthetic cathinones: a review', *Archives of Toxicology*, 88(1), pp. 15-45.

- Vardakou, I., Pistos, C. and Spiliopoulou, C. (2011) 'Drugs for youth via Internet and the example of mephedrone', *Toxicology Letters*, 201(3), pp. 191-5.
- Vassilev, P. P., Venkova, K., Pencheva, N. and Staneva-Stoytcheva, D. (1993) 'Changes in the contractile responses to carbachol and in the inhibitory effects of verapamil and nitrendipine on isolated smooth muscle preparations from rats subchronically exposed to Co<sup>2+</sup> and Ni<sup>2+</sup>', *Archives of Toxicology*, 67(5), pp. 330-7.
- West, P. R., Weir, A. M., Smith, A. M., Donley, E. L. and Cezar, G. G. (2010) 'Predicting human developmental toxicity of pharmaceuticals using human embryonic stem cells and metabolomics', *Toxicology and Applied Pharmacology*, 247(1), pp. 18-27.
- Whitcombe, D., Theaker, J., Guy, S. P., Brown, T. and Little, S. (1999) 'Detection of PCR products using self-probing amplicons and fluorescence', *Nature Biotechnology*, 17(8), pp. 804-7.
- Wild, P., Perdrix, A., Romazini, S., Moulin, J.-J. and Pellet, F. (2000) 'Lung cancer mortality in a site producing hard metals', *Occupational and Environmental Medicine*, 57(8), pp. 568-573.
- Winstock, A., Mitcheson, L. and Marsden, J. (2010) 'Mephedrone: still available and twice the price', *Lancet*, 376(9752), pp. 1537.
- Winstock, A., Mitcheson, L., Ramsey, J., Davies, S., Puchnarewicz, M. and Marsden, J. (2011a) 'Mephedrone: use, subjective effects and health risks', *Addiction*, 106(11), pp. 1991-6.
- Winstock, A. R., Mitcheson, L. R., Deluca, P., Davey, Z., Corazza, O. and Schifano, F. (2011b) 'Mephedrone, new kid for the chop?', *Addiction*, 106(1), pp. 154-61.
- Wishart, D. S. (2007) 'Human Metabolome Database: completing the 'human parts list'', *Pharmacogenomics*, 8(7), pp. 683-6.
- Wood, D. M., Davies, S., Greene, S. L., Button, J., Holt, D. W., Ramsey, J. and Dargan, P. I. (2010) 'Case series of individuals with analytically confirmed acute mephedrone toxicity', *Clinical Toxicology (Philadelphia)*, 48(9), pp. 924-7.
- Wood, D. M., Sedefov, R., Cunningham, A. and Dargan, P. I. (2015) 'Prevalence of use and acute toxicity associated with the use of NBOMe drugs', *Clinical Toxicology (Philadelphia)*, 53(2), pp. 85-92.
- Wroblewski, B. M., Siney, P. D. and Fleming, P. A. (2004) 'Wear of the cup in the Charnley LFA in the young patient', *The Journal of Bone and Joint Surgery. British Volume*, 86(4), pp. 498-503.

Wu, H. Q., Ungerstedt, U. and Schwarcz, R. (1995) 'L-alpha-amino adipic acid as a regulator of kynurenic acid production in the hippocampus: a microdialysis study in freely moving rats', *European Journal of Pharmacology*, 281(1), pp. 55-61.

Wu, K. (1984) '[Ancient medical classic - the Papyrus Ebers] (Chi)', *Zhonghua Yi Shi Za Zhi*, 14(2), pp. 107-11.

Xue, W., Cai, L., Tan, Y., Thistlethwaite, P., Kang, Y.J., Li, X. and Feng, W. (2010) 'Cardiac-specific overexpression of HIF-1 $\alpha$  prevents deterioration of glycolytic pathway and cardiac remodeling in streptozotocin-induced diabetic mice'. *The American journal of pathology*, 177(1), pp.97-105.

Yan, Y., Kluz, T., Zhang, P., Chen, H. B. and Costa, M. (2003) 'Analysis of specific lysine histone H3 and H4 acetylation and methylation status in clones of cells with a gene silenced by nickel exposure', *Toxicology and Applied Pharmacology*, 190(3), pp. 272-7.

Yasui, D. H., Peddada, S., Bieda, M. C., Vallero, R. O., Hogart, A., Nagarajan, R. P., Thatcher, K. N., Farnham, P. J. and Lasalle, J. M. (2007) 'Integrated epigenomic analyses of neuronal MeCP2 reveal a role for long-range interaction with active genes', *Proceedings of the National Academy of Sciences of the United States of America*, 104(49), pp. 19416-21.

Yonekura, S., Nakamura, N., Yonei, S. and Zhang-Akiyama, Q. M. (2009) 'Generation, biological consequences and repair mechanisms of cytosine deamination in DNA', *Journal of Radiation Research*, 50(1), pp. 19-26.

Zanetti, G. and Fubini, B. (1997) 'Surface interaction between metallic cobalt and tungsten carbide particles as a primary cause of hard metal lung disease', *Journal of Materials Chemistry*, 7(8), pp. 1647-1654.

Zderic, T. W., Schenk, S., Davidson, C. J., Byerley, L. O. and Coyle, E. F. (2004) 'Manipulation of dietary carbohydrate and muscle glycogen affects glucose uptake during exercise when fat oxidation is impaired by beta-adrenergic blockade', *American Journal of Physiology. Endocrinology and Metabolism*, 287(6), pp. E1195-201.

Zeng, X., Li, J. and Shen, B. (2015) 'Novel approach to recover cobalt and lithium from spent lithium-ion battery using oxalic acid', *Journal of Hazardous Materials*, 295, pp. 112-8.

Zhang, C. G., Cai, W. Q., Li, Y., Huang, W. Q. and Su, H. C. (1998) 'Quantitative analysis of calcitonin gene-related peptide- and neuropeptide Y-immunoreactive nerve fibers in mesenteric blood vessels of rats irradiated with cobalt-60 gamma rays', *Radiation Research*, 149(1), pp. 19-26.

Zijlstra, W. P., Bulstra, S. K., van Raay, J. J., van Leeuwen, B. M. and Kuijer, R. (2012) 'Cobalt and chromium ions reduce human osteoblast-like cell activity in vitro,

reduce the OPG to RANKL ratio, and induce oxidative stress', *Journal of Orthopaedic Research*, 30(5), pp. 740-7.

# 8 Appendices

## Appendix 1

**Table 1** Authentic standards run on a ZICpHILIC column with an acetonitrile/20 mM ammonium carbonate gradient.

Compound Name	m/z	mode	RT min
Glycine	76.0394	+	16.2
Sarcosine	90.0551	+	14.3
L-Alanine	90.0552	+	15.1
B-Alanine	90.0552	+	15.7
L-Homoserine Lactone	102.0550	+	7.2
Malonate	103.0020	+	17.1
3-hydroxy-butyrate	103.0390	-	16.4
γ-Aminobutyric acid	104.0700	+	15.8
Choline(+)	105.1100	+	20.5
L-Serine	106.0500	+	16.3
L-cytosine	112.0500	+	12.4
Histamine	112.0870	+	27.8
Uracil	113.0350	+	8.6
Creatinine	114.0540	+	10.1
DL-Valine	116.0700		12.7
L-Proline	116.0700	+	12.9
Succinic acid	117.0180		16.5
Methylmalonate	117.0180	-	16.2
L-Homoserine	118.0500	-	15.4
Indole	118.0650	+	6.1
Betaine	118.0860	+	11.3
L-Valine	118.0860	+	12.7
L-Norvaline	118.0860	+	12.2
L-Homoserine	120.0650	+	15.5
Threonine	120.0660	+	15.0
Isonicotinic acid	122.0240	-	7.3
Cysteine	122.0270	+	8.5
Nicotinamide	123.0550	+	7.2
taurine	124.0073	-	15.1
methylcytosine	126.0622	+	11.1
Imidazole acetate	127.0502	+	12.0
2-Pyrrolidone-5-carboxylic acid	128.0340	-	11.0
Citraconate	129.0180	-	13.6
Dihydrothymine	129.0660	+	8.3
5-Oxoproline	130.0490	+	15.1
2-Pyrrolidone-5-carboxylic acid	130.0490	+	11.2
Cis-4-Hydroxy-D-Proline	132.0650	+	15.4
aminolevulinate	132.0650	+	14.0
L-Threonic acid	132.0650	-	11.1
Creatine	132.0760	+	15.0
L-isoleucine	132.1010	+	11.3

Leucine	132.1020	+	10.8
(L)-Malate	133.0130	-	17.4
L-asparagine	133.0610	+	15.9
L- Ornithine	133.0970	+	23.3
Aspartate	134.0320	+	15.5
L-Homocysteine	134.0460	-	13.5
S-Methyl-L-cysteine	136.0420	+	12.3
adenine	136.0618	+	10.0
Hypoxanthine	137.0450	+	10.3
1-Methylnicotinamide	137.0700	+	5.4
2-Imino-1-imidazolidine acetic acid	144.0760	+	14.1
Ketoglutaric acid	145.0143	-	16.2
2-phenyl-Imidazole	145.0750	+	5.7
O-Acetyl-L-serine	146.0450	-	11.5
Spermidine	146.1650	+	14.2
Citramalate	147.0290	-	16.1
D-2-Hydroxyglutaric acid	147.0300	-	11.9
D-Galactono-14-lactone	147.0300	-	13.4
Trans-Cinnamic acid	147.0440	-	4.8
L-Lysine	147.1120	+	24.8
L-Methionine	148.0430	-	11.7
B-Glutamic acid	148.0590	+	15.0
Ribose	149.0460	-	11.9
L-Arabinose	149.0460	-	11.1
7-Methyladenine	150.0760	+	8.5
Triethanolamine (GPL)	150.1120	+	9.3
Xylitol	151.0250	-	13.1
Xanthine	151.0250	-	12.2
2-phenylglycin	152.0530	+	11.5
Guanine	152.0560	+	12.6
L-Histidine	154.0610	-	ND
N-Acetylhistamine	154.0650	+	7.3
Dopamine	154.0860	+	26.0
L-Histidine	156.0760	+	14.4
Allantoin	159.0510	+	14.9
Hydroxyectoine	159.0750	+	15.0
Indole-3-carboxylate	160.0390	-	7.3
methyl-L-lysine	161.1280	+	23.5
L-2-Amino adipic acid	162.0750	+	15.7
Tryptophanol	162.0910	+	4.7
Carnitine	162.1110	+	13.4
4-Coumarate	163.0390	+	8.8
Rhamnose	163.0390	-	11.4
3-(2-Hydroxyphenyl) propanoic acid	165.0540	+	13.4
1-Methylguanine	166.0710	+	9.5
Pyridoxal	168.0660	+	7.9
Phenylephrine	168.0680	+	10.7
3-Methyl-L-histidine	168.0770	-	13.3
Dihydroxyacetonephosphate	168.9900	-	17.9
Urate	169.0350	-	13.6
Pyridoxamine	169.0970	+	ND
L-Cysteic acid	170.0110	+	16.9
Pyridoxine	170.0800	+	8.1
N(pi)-Methyl-L-histidine	170.0800	+	7.9
6-Hydroxydopamine (Oxidopamine)	170.0800	+	7.9
L-Noradrenaline	170.0810	+	25.7

3-Methyl-L-histidine	170.0910	+	13.2
Sn-Glycerol 3-phosphate	171.0110	-	7.1
Gallate	171.0290	+	4.9
Dimethyl-L-lysine	173.1290	-	21.4
3-Indol acetate	174.0440	-	11.9
Ascorbate	175.0240	-	17.5
D-Isoascorbic acid	175.0240	-	10.9
D-Glucuronolactone	175.0430	-	15.8
N-Acetyl-L-ornithine	175.1070	+	15.4
L-Arginine	175.1180	+	26.5
N-Acetyl-L-aspartate	176.0550	+	15.8
indole-3-acetic acid	176.070	+	9.4
L-Citrulline	176.1020	+	16.3
L-Gulonic gamma-lactone	177.0400	-	13.3
Hippuric acid	178.0500	-	7.4
N-formyl-L-methionine	178.0530	-	7.5
D-Glucosamine	178.0710	-	14.1
Caffeate	179.0450	-	12.7
Myo-Inositol	179.0550		17.8
D-Glucose	179.0550	-	15.2
Galactose	179.0550	-	15.5
D-Mannose	179.0550	-	14.5
fructose	179.0550	-	14.0
Paraxanthine	181.0710	+	6.1
Mannitol	181.0710	-	14.5
D-sorbitol	181.0720		14.4
L-Tyrosine	182.0810	+	13.4
L-Adrenaline	184.0820	+	12.0
3-phosphoglycerate	184.9850	-	18.1
N-acetyl-L-glutamine	187.0710	-	11.2
N <sup>6</sup> -Acetyl-L-Lysine	187.1080	-	15.2
Kynurenic acid	188.0350	-	7.4
N-Acetyl-L-glutamate	188.0560	+	15.2
N-acetyl-L-glutamine	189.0860	+	11.2
Homo-arginine	189.1340	+	26.7
Homo-arginine	189.1340	+	26.8
N <sup>6</sup> - trimethyl-L-lysine	189.1590	+	22.1
5-Hydroxyindoleacetate	190.0500	-	10.8
Isocitrate	191.0190	-	18.8
Citrate	191.0190	-	18.9
D(-)-quinic acid	191.0550	-	13.6
D-Galacturonate	193.0350	-	17.5
D-Glucuronate	193.0350	-	17.4
D-Gluconic acid	195.0500	-	15.1
L-Tryptophan	203.0820	-	11.8
Diethyl 2-oxoglutarate	203.0910	+	4.0
Xanthurenic acid	204.0300	-	12.4
DL-Indole-3-lactic acid	204.0660	-	8.4
Indole-3-lactic acid	204.0690	-	8.4
O-Acetylcarnitine	204.1210	+	10.7
D-panthenol	204.1240	-	7.2
Lipoate	205.0160	-	4.6
L-Tryptophan	205.0960	+	11.9
Xanthurenic acid	206.0440	+	12.4
D-panthenol	206.1380	+	7.2
3-phenylpropionylglycine	208.0790	+	13.2

Mucic acid	209.0300	-	18.6
L-Kynurenine	209.0910	+	11.0
Galactarate	209.0930	-	15.2
2-Methyl-3(3,4-dihydroxy-phenyl)alanine	210.0770	-	15.2
Phosphocreatine	212.0430	-	16.1
2-Methyl-3(3,4-dihydroxy-phenyl)alanine	212.0900	+	15.2
2-deoxyribose-5-phosphate	213.0170	-	15.2
5-hydroxy-L-tryptophan	219.0770	-	15.2
Pantothenate	220.1160	+	9.1
5-hydroxy-L-tryptophan	221.0910	+	15.2
N-Acetyl-D-mannosamine	222.0910	+	4.1
N-Acetyl-D-Glucosamine	222.0970	+	12.0
Cystathionine	223.0740	+	17.7
2-Deoxycytidine	226.0830	-	10.4
L-Carnosine	227.1130	+	16.0
2-Deoxycytidine	228.0960	+	10.6
D-Xylulose 5-phosphate	229.0120	-	16.7
D-Ribose 5-phosphate	229.0120	-	16.6
Deoxy-uridine	229.0800	+	8.2
Melatonin	231.1140	-	4.6
Melatonin	233.1280	+	4.7
Dihydrobiopterin	240.1080	+	12.7
L-Cystine	241.0300	+	17.0
Cytidine	242.0780	-	12.1
Cytidine	242.0920	+	12.1
Uridine	243.0620	-	10.0
Biotin	243.0810	-	9.1
Uridine	245.0760	+	10.0
2-O-Methyluridine	257.0780	-	8.4
5-methyluridine	257.0780	-	8.4
3-O-Methyluridine	257.0780	-	7.2
D-Glucosamine 6-Phosphate	258.0390	-	17.2
5-methylcytidine	258.0960	-	10.7
glucose 1 phosphate	259.0230	-	16.8
Glucose 6-phosphate	259.0230	-	17.9
Galactose 1 phosphate	259.0230	-	16.8
D-Fructose-1-phosphate	259.0230	-	16.9
fructose 6 phosphate	259.0230	-	16.9
Phosphoenolpyruvate	259.0230	-	19.0
D-Mannose 1- phosphate	259.0230	-	17.1
3-O-Methyluridine	259.0900	+	7.2
5-methyluridine	259.0920	+	8.3
Thiamine (+)	265.1110	+	20.8
Thiamine (+)	266.1150	+	20.8
Inosine	267.0730	-	11.1
Adenosine	268.1030	+	8.7
Inosine	269.0870	+	11.0
6-phosphogluconic acid	275.0180	-	18.4
6-Phospho-D-gluconate	275.0180	-	18.4
L-Saccharopine	275.1250	-	16.2
Guanosine	282.0840	-	12.9
Xanthosine	283.0680	-	13.1
Guanosine	284.0980	-	12.9
7-Methylguanosine	298.0960	+	9.6
5'-Methylthioadenosine	298.1130	+	13.3
N-Acetyl-D-glucosamine 6-phosphate	300.0490	-	15.9

Cytidine 2':3'-cyclic monophosphate	306.0470	+	13.1
Glutathione	308.0900	+	15.2
N-Acetylneuraminic acid	308.1000	-	14.1
N-Acetylneuraminic acid	310.1120	+	14.1
CMP	322.0450	-	16.7
UMP	323.0290	-	16.0
CMP	324.0580	+	16.7
UMP	325.0420	+	16.0
2-Deoxyadenosinemonophosphate	330.0610	-	13.2
2- Deoxyadenosine 5-monophosphate	332.0740	+	13.1
beta-D-Fructose-1,6-bisphosphate	338.9890	-	18.8
D-(+)-Trehalose	341.1090		16.4
Sucrose	341.1090	-	15.5
Maltose	341.1090	-	16.5
AMP	346.0560	-	14.3
IMP	347.0400	-	16.3
IMP	349.0350	+	16.3
inosine-5-monophosphate	349.0530	+	16.3
GMP	362.0510	-	17.7
GMP	364.0640	+	17.7
Lithocholic acid	375.2900	-	4.0
Riboflavin	377.1440	+	8.2
Lactoglutathione	378.0980	-	14.0
S-Adenosyl-L-homocysteine	385.1270	+	13.5
Deoxycholic acid	391.2850	-	4.4
Chenodeoxycholic acid	391.2860	-	4.5
S-Adenosyl-L-methionine	399.1430	-	16.3
CDP	402.0140	-	18.2
UDP	402.9960	-	17.7
CDP	404.0250	+	18.2
Cholate	407.2800	-	7.2
ADP	426.0230	-	14.5
GDP	442.0180	-	19.5
Glycodeoxycholate	448.3070	-	4.4
Glycocholic acid	464.3010	-	4.6
Glycocholic acid	464.3010	-	4.8
Glycocholic acid	466.3130	+	4.8
CTP	481.9780	-	18.5
CTP	483.9900	+	18.5
ATP	505.9900	-	17.1
ATP	508.0010	+	17.1
Taurocholate (bile)	514.2840	-	7.2
Taurocholate (D.P)	516.2980	+	7.2
GTP	521.9840	-	22.4
Bilirubin	583.2570	-	3.8
UDP-N-acetyl-D-glucosamine	606.0760	-	16.1
L-Glutathione oxidized	611.1460	-	17.5
L-Glutathione oxidized	613.1570	+	17.5
NAD+	664.1140	+	14.5
NADP+	744.0800	+	17.7
NADPH	744.0860	-	18.4
NADPH	746.0960	+	18.4
CoA	768.1227	+	14.3
FAD	786.1620	+	11.9

**Figure 1** Example of negative ion total ion chromatogram (TIC).

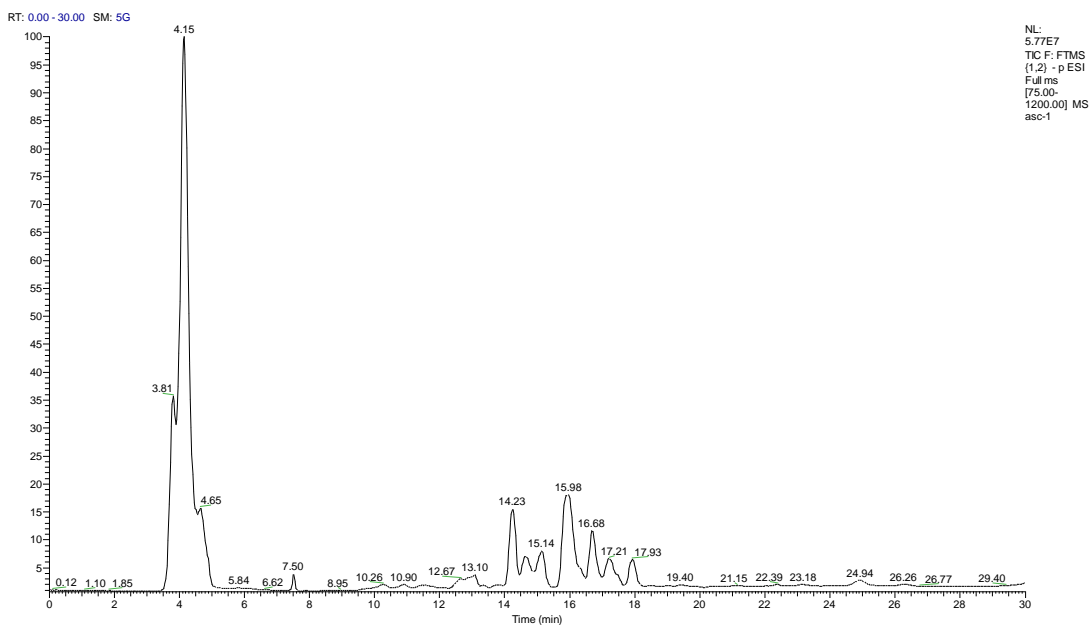
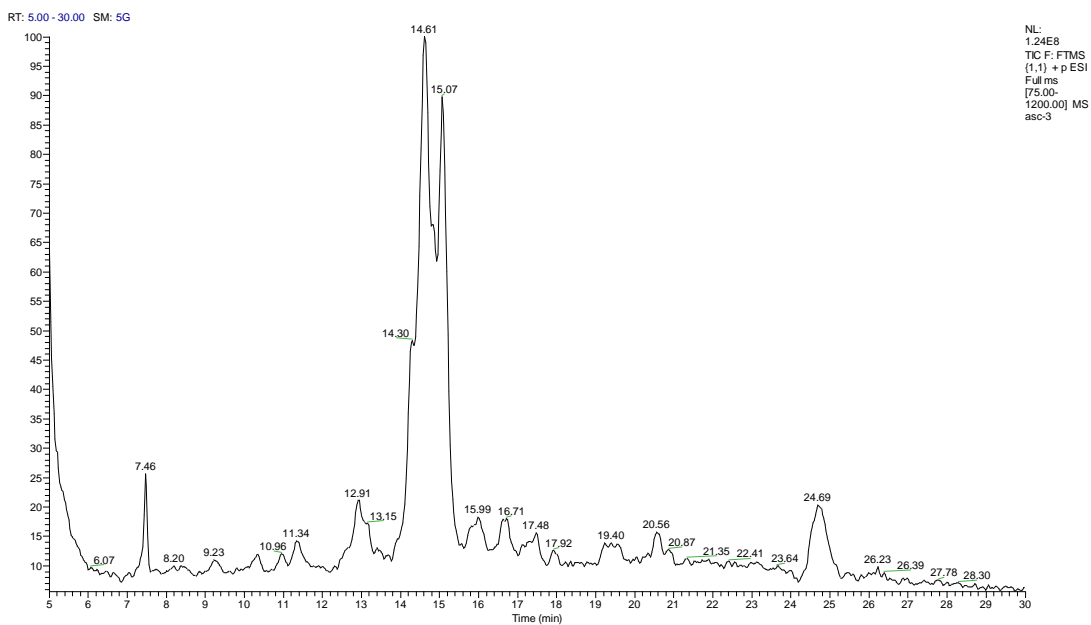


**Figure 2** Example of positive ion TIC.



## Appendix 2

**Figure 1** RNA quality and concentration derived from Nanodrop 2000 spectrophotometer.

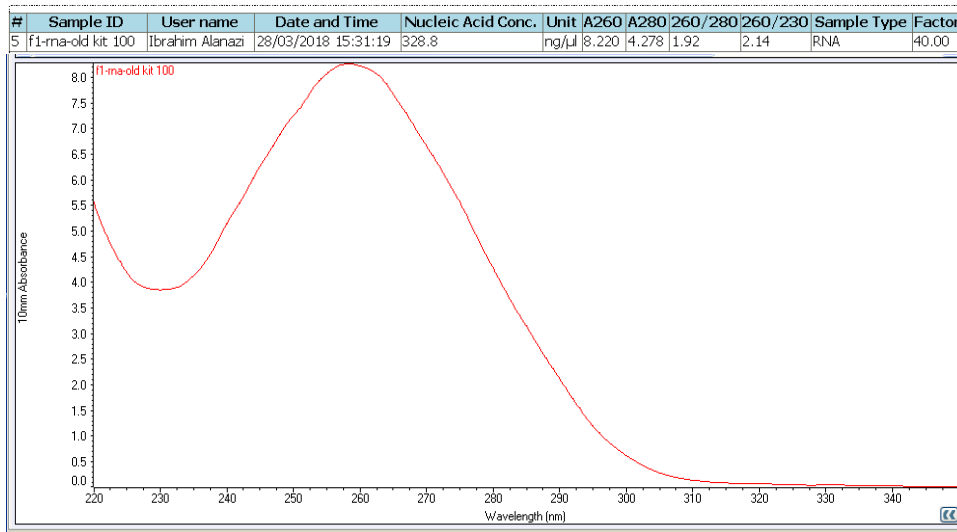
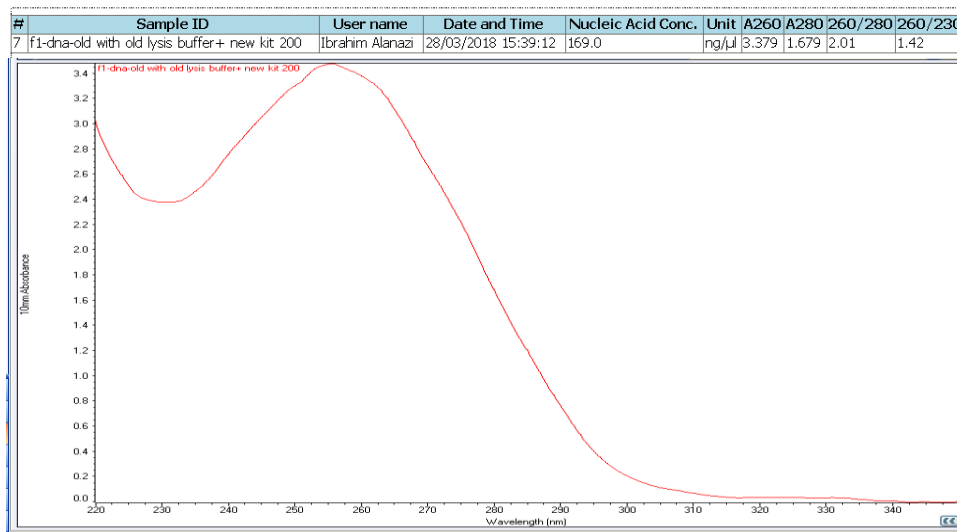


**Figure 2** DNA quality and concentration obtained from Nanodrop 2000 spectrophotometer.



### Appendix 3

**Figure 1** The photograph of the membrane used to develop the UNG protein.

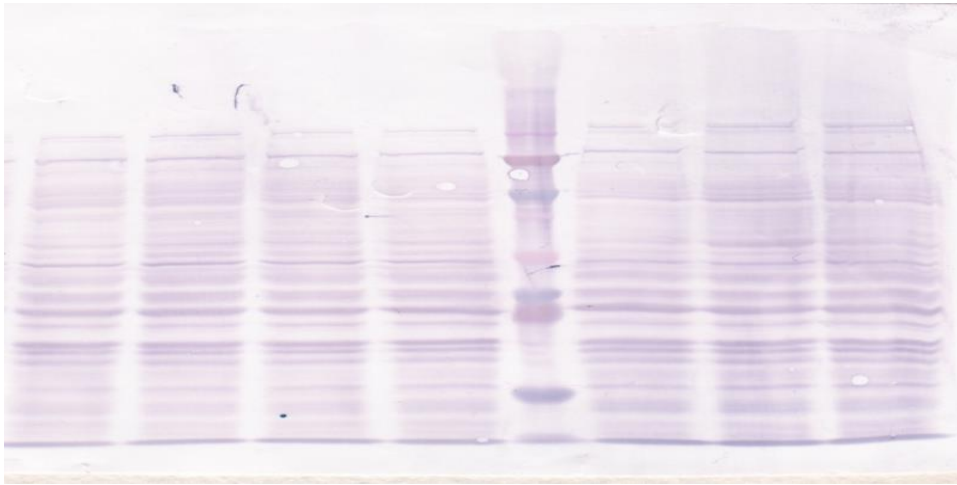


**Figure 2** The photograph of the membrane used to develop the TDG protein.

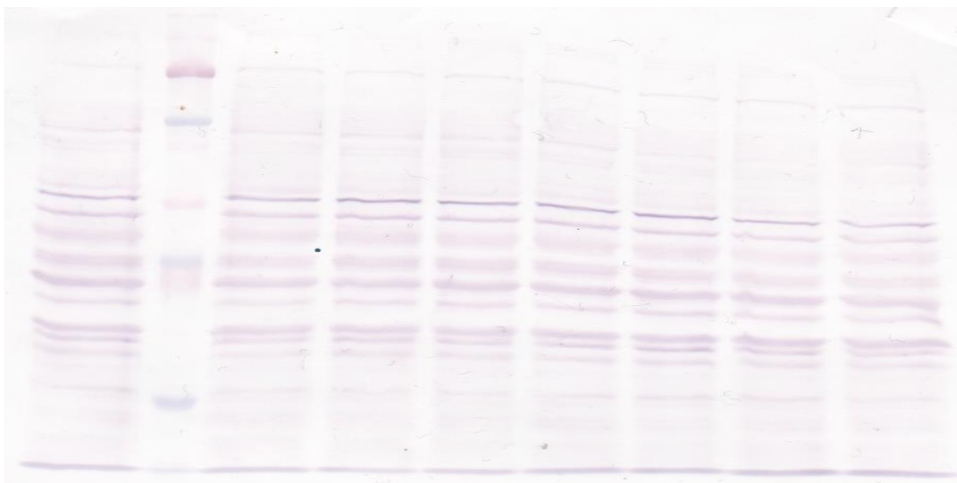


**Figure 3** The photograph of the membrane used to develop the DNMT1 protein.

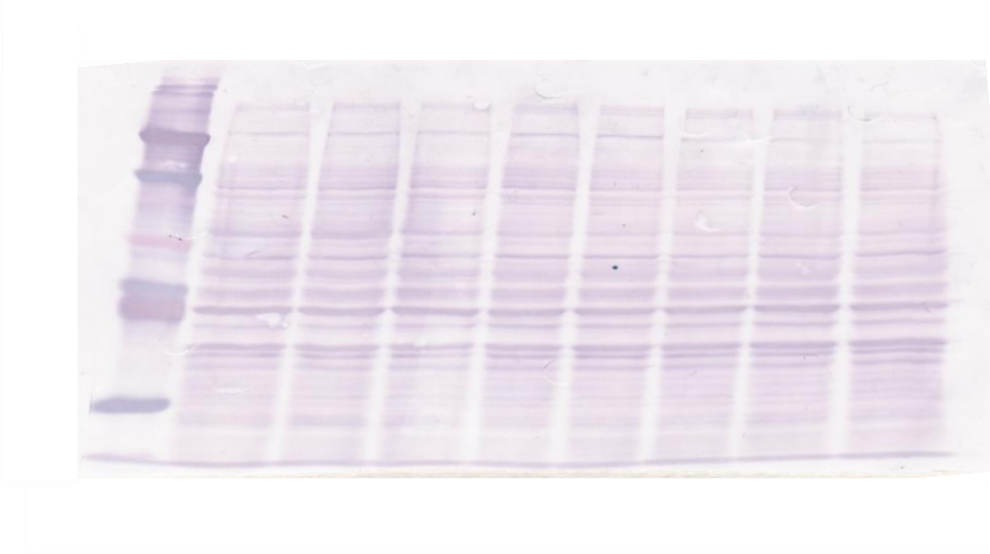


**Figure 4** The photograph of the membrane used to develop the OGG1 protein.

